Modified Quasi-Orthogonal Space-Time Block Coding in Distributed Wireless Networks

by

Mustafa Abdelaziz Manna

A thesis submitted in partial fulfilment of the requirements for the award of the degree of Doctor of Philosophy (PhD)

July 2014

Advanced Signal Processing Group,
School of Electronic, Electrical and System Engineering,
Loughborough University, Loughborough,
Leicestershire, UK, LE11 3TU

I dedicate this thesis to the spirit of my leader, the spirit of my brother, my parents, my wife, my son, my brothers and sisters.

Abstract

Cooperative networks have developed as a useful technique that can achieve the same advantage as multi-input and multi-output (MIMO) wireless systems such as spatial diversity, whilst resolving the difficulties of co-located multiple antennas at individual nodes and avoiding the effect of path-loss and shadowing. Spatial diversity in cooperative networks is known as cooperative diversity, and can enhance system reliability without sacrificing the scarce bandwidth resource or consuming more transmit power. It enables single-antenna terminals in a wireless relay network to share their antennas to form a virtual antenna array on the basis of their distributed locations. However, there remain technical challenges to maximize the benefit of cooperative communications, e.g. data rate, asynchronous transmission and outage.

In this thesis, therefore, firstly, a modified distributed quasi-orthogonal space-time block coding (M-D-QO-STBC) scheme with increased code gain distance (CGD) for one-way and two-way amplify-and-forward wireless relay networks is proposed. This modified code is designed from set partitioning a larger codebook formed from two quasi-orthogonal space time block codes with different signal rotations then the subcodes are combined and pruned to arrive at the modified codebook with the desired rate in order to increase the CGD. Moreover, for higher rate codes the code distance is maximized by using a genetic algorithm to search for the optimum rotation matrix. This scheme has very good performance and significant coding gain over existing

codes such as the open-loop and closed-loop QO-STBC schemes.

In addition, the topic of outage probability analysis in the context of multi-relay selection from N available relay nodes for one-way amplify-and-forward cooperative relay networks is considered together with the best relay selection, the N^{th} relay selection and best four relay selection in two-way amplify-and-forward cooperative relay networks. The relay selection is performed either on the basis of a max-min strategy or one based on maximizing exact end-to-end signal-to-noise ratio.

Furthermore, in this thesis, robust schemes for cooperative relays based on the M-D-QO-STBC scheme for both one-way and two-way asynchronous cooperative relay networks are considered to overcome the issue of a synchronism in wireless cooperative relay networks. In particular, an orthogonal frequency division multiplexing (OFDM) data structure is employed with cyclic prefix (CP) insertion at the source in the one-way cooperative relay network and at the two terminal nodes in the two-way cooperative network to combat the effects of time asynchronism. As such, this technique can effectively cope with the effects of timing errors.

Finally, outage probability performance of a proposed amplify-and-forward cooperative cognitive relay network is evaluated and the cognitive relays are assumed to exploit an overlay approach. A closed form expression for the outage probability for multi-relay selection cooperation over Rayleigh frequency flat fading channels is derived for perfect and imperfect spectrum acquisitions. Furthermore, the M-QO-STBC scheme is also proposed for use in wireless cognitive relay networks. MATLAB and Maple software based simulations are employed throughout the thesis to support the analytical results and assess the performance of new algorithms and methods.

Contents

Dedication ii

Abstract iii

Acknowledgements xiii

List of Acronyms xiv

List of Symbols xvi

List of Figures xix

List of Tables xx

1 INTRODUCTION 1

1.1 General 1

1.2 Cooperative relay networks 4

1.3 Orthogonal frequency division multiplexing 7

1.4 Cognitive radio 8

1.5 Motivation of the proposed research work 12

1.5.1 Aims and objectives 13

1.6 Organisation of the thesis 14

2 RELATED LITERATURE REVIEW 17

2.1 Point-to-point space-time block coding 17

2.1.1 Alamouti scheme 19

2.1.2 Quasi-orthogonal space-time block codes 22
2.1.2.1 Pairwise decoding 25
2.1.2.2 Rotated quasi-orthogonal space-time block coding 26
2.1.2.3 Closed-loop quasi-orthogonal space-time block coding 29
2.1.3 Simulations 30
2.2 Distributed space-time block coding 32
2.2.1 Wireless relay network for distributed space-time block coding 33
2.2.1.1 Complex-orthogonal designs 36
2.2.1.2 Quasi-orthogonal designs 38
2.2.1.3 The general distributed linear dispersion code 38
2.2.1.4 Random orthogonal designs 40
2.2.2 Simulations 42
2.3 Modified quasi-orthogonal space-time block codes 43
2.3.1 Set partitioning 43
2.4 Summary 48

3 MODIFIED DISTRIBUTED QUASI-ORTHOGONAL SPACE-TIME BLOCK CODES FOR ONE-WAY AND TWO-WAY TRANSMISSION 49
3.1 Introduction 50
3.2 Modified distributed quasi-orthogonal space-time block codes for one-way wireless relay networks 51
3.2.1 System model 51
3.2.2 Modified code design for one-way transmission 54
3.2.3 Code gain distance 56

3.3 Distributed closed-loop quasi-orthogonal STBC for one-way transmission 57
3.4 Simulation results 61
3.5 Modified distributed quasi-orthogonal space-time block coding for two-way wireless relay networks 62
3.5.1 System model 63
3.5.2 Modified code design for two-way design 66
3.6 Simulation results 68
3.7 Summary 70

4 OUTAGE PROBABILITY AND RELAY SELECTION ANALYSIS IN ONE-WAY AND TWO-WAY RELAY NETWORKS 71

4.1 Introduction 71
4.2 Outage probability for four relay selection in one-way relay networks 72
4.2.1 System model for a one-way cooperative relay network 73
4.2.2 Four relay selection and outage probability analysis in one-way relay networks 76
4.2.3 Simulation results for the proposed one-way cooperative relay network 80
4.3 Outage probability for relay selection in two-way relay networks 81
4.3.1 System model for two-way cooperative relay network 82
4.3.2 Relay selection scheme in two-way wireless relay networks 84
4.3.3 The outage probability analysis in two-way wireless relay networks 85
4.3.4 The CDF and PDF of the exact SNR in two-way wireless relay networks 86

4.3.5 The best relay selection in two-way wireless relay networks 87
4.3.6 The best Nth relay selection in two-way wireless relay networks 88
4.3.7 Simulation results for the proposed two-way wireless relay network 89
4.3.7.1 Simulation analysis for the best relay selection 90
4.3.7.2 Simulation analysis for the N^{th} best relay selection 91
4.4 Summary 92

5 OFDM-BASED MODIFIED QUASI-ORTHOGONAL SPACE-TIME SCHEME FOR USE IN ONE-WAY AND TWO-WAY ASYNCHRONOUS COOPERATIVE NETWORKS 93
5.1 Introduction 94
5.2 System model for one-way asynchronous cooperative relay network 95
5.2.1 Source node processing 96
5.2.2 Relay nodes processing 97
5.2.3 Destination node processing 98
5.2.4 Relay selection technique 100
5.2.5 Simulation results 101
5.3 Two-way asynchronous cooperative relay network using M-QO-STBC 103
5.3.1 System model 103
5.3.2 Transmission process at terminals 104
5.3.3 Transmission process at relay nodes 105
5.3.4 Information extraction process at the terminal nodes 106
5.3.5 Relay selection technique 110

5.3.6 Simulation results 111
5.4 Summary 112

6 OUTAGE PROBABILITY ANALYSIS OF A COGNITIVE RELAY NETWORK WITH FOUR RELAY SELECTION 114
6.1 Introduction 115
6.2 Overview of the proposed system 118
6.3 The outage probability analysis 120
6.3.1 Outage probability analysis of the two-relay scheme 121
6.3.2 Outage probability analysis of the three-relay scheme 122
6.3.3 Outage probability analysis of selecting four relays from M relays 123
6.4 The outage probability analysis when spectrum acquisition is imperfect 126
6.5 The quasi-orthogonal code structure for the availability of two, three and four cognitive relays 127
6.5.1 Modified distributed quasi-orthogonal STBC 128
6.6 Simulation results 130
6.7 Summary 136

7 CONCLUSIONS AND FUTURE WORK 137
7.1 Conclusions 137
7.2 Future work 142

Appendix 145

Statement of Originality

The contributions of this thesis are concerned with modified distributed quasi-orthogonal space-time block coding in one-way and two-way cooperative wireless relay systems and mainly in the improvement of diversity, code gain distance and transmission rate together with outage probability analysis in the context of single and multi-relay selection. The novelty of the contributions are supported by the following international journal and conference papers:

In Chapter 3, a modified distributed quasi-orthogonal space-time block coding (M-D-QO-STBC) scheme with increased code gain distance (CGD) for one-way and two-way amplify-and-forward wireless relay networks is proposed. The M-D-QO-STBC scheme has very good performance and significant coding gain over existing codes such as open-loop and closed-loop D-QO-STBC schemes. The results have been published in:

- M. A. Manna and J. A. Chambers., "Distributed Quasi-Orthogonal Type Space-Time Block Coding with Maximal Distance Property for Wireless Relay Networks," IEEE 18th International Conference on Software, Telecommunications and Computer Networks (SoftCOM), pp. 351-354, 2010.

- M. A. Manna, F. Abdurahman and J. A Chambers., "Quasi-Orthogonal Type Space-Time Block Codes for Using Cooperative Wireless Networks," IEEE UKIWCWS Conference, pp.1-4, 2010.

- M. A. Manna, F. Abdurahman and J. A Chambers., "Distributed Quasi-Orthogonal Type Space-Time Block Coding with maximum distance property For Two-Way Wireless Relay Networks," Wireless Communications and Mobile Computing Conference (IWCMC), 2011 7th International Conference., pp. 1704-1707, 2011.

In Chapter 4, new analytical expressions for the PDF, and CDF of end-to-end SNR are derived together with closed form expressions and integral forms for outage probability for one-way and two-way amplify-and-forward relay networks over flat Rayleigh fading channels. In the case of a one-way relay network a closed form expression for the outage probability for four relay selection is derived whereas, for two-way relay networks, the outage probability analyses for the best, the best N^{th} and the best four relay selection from a set of N available relays are presented. These works have been presented in:

- M. A. Manna, G. Chen and J. A Chambers.,"Outage Probability for Four Relay Selection in Wireless Relay Networks," IEEE 20th International Conference on Software, Telecommunications and Computer Networks (SoftCOM), pp. 1-4, 2012.

- M. A. Manna and J. A. Chambers "Exact Outage Probability of Best, N^{th} Best and Four Best Relay Selection for Two-Way Wireless Relay Networks," 2014.

In Chapter 5, a robust scheme for cooperative relays based on the M-D-QO-STBC scheme for one-way asynchronous cooperative relay networks with relay selection is considered. The proposed scheme exploits cooperative communication OFDM-based transmission to mitigate timing errors between relay nodes. This technique mitigate the effects of timing errors and the results have been published in:

- M. A. Manna, W. Qaja and J. A Chambers., "OFDM-based Modified

Quasi-Orthogonal Space-Time Scheme for Use in Asynchronous Cooperative Networks with Relay Selection," Telecommunications (ICT), 2013 20th International Conference on, pp 1-4, 2013

In Chapter 6, outage probability analysis for a cognitive amplify-and-forward relay network with multi-relay selection is presented. The novelty of this work is supported by the following fall journal publication:

- M. A. Manna, G. Chen and J. A Chambers., "Outage Probability Analysis of a Cognitive Relay Network with Four Relay Selection and End-to-End Performance with Modified Quasi-Orthogonal Space-Time Coding," Communications, IET, vol.8, no.2, pp. 233-241, 2014.

Acknowledgements

Praise be to Allah (God), the most gracious and the most merciful, without his blessing and guidance my accomplishments would never have been possible. Then I would like to express my gratitude to my supervisor Prof. Jonathon A. Chambers for his inspiration, advice, and guidance without which this thesis would not have been possible. Throughout my doctoral work, he helped me to improve my analytical thinking and assisted me with technical writing. For all of the help, I am greatly thankful.

I extend many thanks to all the members of the Advanced Signal Processing Group (ASPG), Loughborough University, for creating a friendly environment during my research studies in the Laboratory.

Most importantly, I would like to thank my parents, to whom this thesis is dedicated, for their never-ending, unconditional, loving support, and for the constant encouragement during my studies. I also owe my loving thanks to my wife and my lovely son Almutassim Billah. I am grateful to my sisters and brothers and my friends and all my extended family for their encouragement and enthusiasm.

Mustafa Abdelaziz Manna

List of Symbols

Scalar variables are denoted by plain lower-case letters, (e.g., x), vectors by bold-face lower-case letters, (e.g., $\mathbf{x}$), and matrices by upper-case bold-face letters, (e.g., $\mathbf{X}$). Some frequently used notations are as follows:

$(.)^H$	Hermitian conjugate operator
$(.)^*$	Conjugate operator
$(.)^T$	Transpose operator
$\|.\|$	Absolute value of a complex number
$\mathbf{R}e(.)$	Real part of a complex number
$\mathbf{I}m(.)$	Imaginary part of a complex number
$E\{.\}$	Statistical expectation
$\|\|.\|\|$	Euclidean norm
$arg\ \ a_1...a_n$	Argument of $a_1...a_n$
N	Total number of available relays
$DFT(.)$	Discrete Fourier Transform operator
$FFT(.)$	Fast Fourier Transform operator
$IFFT(.)$	Inverse Fast Fourier Transform operator
$IDFT(.)$	Inverse Discrete Fourier Transform operator

$\circ$	The Hadamard product
$\zeta(.)$	Time-reversal operator
$CN(0, N_0)$	Circularly symmetric complex Gaussian distribution with zero mean and N_0 is noise variance
$max(.)$	Maximum value
$min(.)$	Minimum value
$argmax$	The argument which maximizes the expression
$argmin$	The argument which minimizes the expression
$K(0, .)$	Modified Bessel function of the first order
$K(1, .)$	Modified Bessel function of the second order
T_x	Number of transmit antennas
R_x	Number of receiver antennas
T_s	Symbol duration
A_i	Space-time coding matrix that is used at the relays
B_i	Space-time coding matrix that is used at the relays
Δ	The Grammian matrix
$\mathbb{S}$ *and* $\mathbb{T}$	Quasi-orthogonal codebooks with different rotations
τ	Timing misalignments between relay nodes
$\bar{\gamma}_c$	The average signal-to-noise ratio
α	Threshold value

List of Figures

1.1 MIMO wireless communication system diagram. 2

1.2 Ergodic capacity of MIMO channel H as a function of SNR and for different antenna dimensions. 3

1.3 Coverage extension and service reliability proposed by cooperative relay network. 6

1.4 Basic block diagram of the conventional OFDM system, exploiting the IFFT and FFT.. 7

1.5 Overlay approach of cognitive radio. 10

1.6 Underlay approach of cognitive radio. 10

2.1 Transmitter diversity for Alamouti space-time block coding. 19

2.2 Receiver with two antennas for Alamouti space-time block coding. 21

2.3 Four transmit and one receive antenna system. 23

2.4 Performance of the Alamouti code using QPSK constellation. 30

2.5 Performance of the non rotated, rotated and closed-loop QO-STBCs using QPSK constellation. 31

2.6 Wireless relay network with one transmitter node T_x, one receiver node R_x and R_N relay nodes. 34

2.7 End-to-end CWER performance of relay networks with QPSK signal. 42

2.8 Set Partitioning Tree for BPSK. 44

2.9 Subsets created by the combination of 0 and L/2. 45
2.10 Subtree of set partitioning for QPSK based on Figure 2.9. 46
2.11 Subtree of set partitioning for QPSK after switching some of the subsets. 46

3.1 Two hop one-way wireless four relay network. 52
3.2 The proposed distributed one-way closed-loop QO-STBC system for four relay nodes with feedback to two nodes. 58
3.3 End-to-end CWER performance of relay networks with BPSK symbols 61
3.4 End-to-end CWER performance of relay networks with QPSK symbols 63
3.5 Basic structure of two-way wireless four-relay network where channels from the terminals to the relay nodes (solid) and from the relay nodes to the terminals (dashed). 64
3.6 Performance comparison of two-way wireless four relay network with BPSK modulation. 68
3.7 Performance comparison of two-way wireless four relay network with QPSK modulation. 69

4.1 Two-hop one-way wireless relay network with N available relays and four selected relays for end-to-end transmission. 74
4.2 The theoretical and the simulation results of the outage probability performance of the best four relay selection; the simulation results are shown in points and the theoretical results as line style, where the SNR=5 dB. 80
4.3 (a) shows a system model of two-way wireless relay network selecting the best single relay whereas (b) shows a system model of two-way wireless relay network selecting the best four relays 83

4.4 *Integration region to determine overall outage probability.* 87

4.5 The theoretical and the simulation results of the outage probability performance of the best relay selection, the simulation results are shown in points and the theoretical results as line style, where the SNR=10 dB. 90

4.6 The theoretical and the simulation results of the outage probability performance of the best N^{th} relay selection, the simulation results are shown in points and the theoretical results as line style, where the SNR=10dB. 91

5.1 A one-way asynchronous cooperative relay network constituting of source, destination and N two-antenna relay nodes. Asynchronism is modeled by the delays τ_{i1}, τ_{i2} for $i = 2, ..., N$. 96

5.2 CP-removal based on relay one (two antennas) synchronization. 98

5.3 Performance of OFDM-based M-D-QO-STBC for one-way asynchronous cooperative relay network with relay selection technique using QPSK signal. 102

5.4 A two-way asynchronous cooperative relay network consisting of two terminal nodes and N relay nodes. 104

5.5 Performance of OFDM-based M-D-QO-STBC for two-way asynchronous cooperative relay network with relay selection technique using QPSK signal. 112

6.1 A half-duplex cognitive relay network with source node (S), a set of M clusters each consisting of a cognitive relay node (R_m) and a licensed node (shown inside broken circles) and a destination node (D). 118

6.2 The theoretical and the simulation results of the outage probability performance of two, three and four relay network. 130

6.3 The theoretical and the simulation results of the outage probability performance based on selection cooperation versus SNR in dB. 131

6.4 The theoretical results of the outage probability performance when spectrum acquisition is imperfect (Pd=.95) for two, three and four cognitive relay network. 132

6.5 The theoretical and the simulation results of the outage probability performance for four relay cognitive network for different values of Pd. 133

6.6 The CWER performance comparison of M-D-QO STBCs when there are two, three and four operational cognitive relays in the cognitive relay network for QPSK signal. 134

6.7 The performance comparison of M-D-QO STBCs and conventional D-QO STBCs in cognitive relay network and the performance of the system when the number of the active relays increases with QPSK modulation. 134

6.8 Performance comparison of cognitive relay network for the M-D-QO-STBCs when the availability of the cognitive relays changes randomly from two to four, two to five, two to seven and two to nine relays for QPSK signal. 135

A.1 The domain of γ. 146

List of Tables

2.1 Set Partitioning for BPSK. 45

2.2 The combinations between 0 and 2. 45

2.3 Set Partitioning for QPSK. 47

Chapter 1

INTRODUCTION

1.1 General

Demands for capacity in wireless communications, driven by cellular mobile, Internet and multimedia services have been rapidly increasing worldwide. On the other hand, the available radio spectrum is limited and the communication capacity needs cannot be met without a significant increase in communication spectral efficiency. Advances in coding, such as turbo [1] and low density parity check codes [2] and [3] made it feasible to approach the Shannon capacity limit [4] in systems with a single antenna link. Significant further advances in spectral efficiency are available through increasing the number of antennas at both the transmitter and the receiver [5] and [6]. By using multiple antennas at both ends of a point-to-point communication link a multi-input multi-output (MIMO) system can be formed, which can potentially combat multipath fading propagation effects and increase the channel capacity as compared with a conventional single-input single-output (SISO) system. This is already happening in 802.11x systems wireless fidelity (WiFi), 802.16x worldwide interoperability for microwave access (WiMax) and is a major focus for 4G and long term evolution (LTE) cellular systems. A MIMO system is a wireless communication system with multiple transmitting and receiving antenna elements. MIMO signaling commonly operates by spreading the information across both space and time. Signal processing in time is the natural dimension of digital communication data.

Spatial processing is possible through the use of multiple spatially distributed antennas. MIMO spatial processing takes advantage of multipath propagation, which is a key feature of a wireless channel. Multipath fading is one of the main problems in wireless transmission. However, MIMO effectively takes advantage of random fading [7] and [8], and when available, multipath delay spread [9], for improving the quality of wireless communication. This improved performance requires no extra spectrum, but demands added hardware and complexity. Figure 1.1 illustrates a MIMO system with T_x

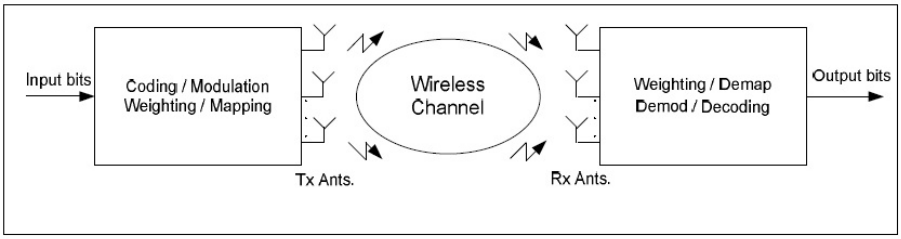

Figure 1.1. MIMO wireless communication system diagram.

transmit antennas and R_x receive antennas. The MIMO transmitter potentially includes error control coding as well as a complex modulation symbol mapper. After frequency demodulation to radio frequency (RF), filtering and amplification, the signals are transmitted through the wireless channel. The signal is captured by multiple receive antennas on the receive side. The receiver performs demodulation and demapping to recover the message. The coding method and antenna mapping algorithm may vary due to several considerations such as channel estimation and complexity. Perfect channel state information will be assumed to be available; further discussion of channel estimation and complexity can be found in [10] and [11]. For T_x transmit and R_x receive antennas, in the case of a MIMO flat fading channel, the ergodic capacity of the MIMO channel is given by [12] and [13]

$$C_{MIMO} = E_H\{log_2(det(I_{R_x} + \frac{\rho}{T_x} HH^*))\} \tag{1.1.1}$$

where E_H is the statistical expectation operator with respect to H, I_{R_x} is the identity matrix of size R_x, ρ is the SNR at any receive antenna, H is the $T_x \times R_x$ channel matrix, $det(.)$ denotes the determinant of a matrix and $(.)^*$ transpose-conjugate. Foschini [12] and Telatar [13] both demonstrated that the capacity in (1.1.1) grows linearly with $m = min(T_x, R_x)$. Figure 1.2 shows the ergodic capacity of a MIMO flat fading wireless link with an equal number of T_x transmitter and R_x receiver antennas. As it is shown in the figure, the ergodic capacity increases with SNR and also with T_x and R_x. The potential of MIMO is clearly seen at 20dB SNR, when the ergodic capacity for a 1×1 link is increased eight fold when using an 8×8 link. Therefore, when the channels between all antennas are uncorrelated, MIMO can offer increase in capacity proportional to $\min(T_x, R_x)$, i.e, increased transmission data rates or capacity for the same bandwidth and without any additional power expenditure [1]. To improve link performance the diversity gain of a

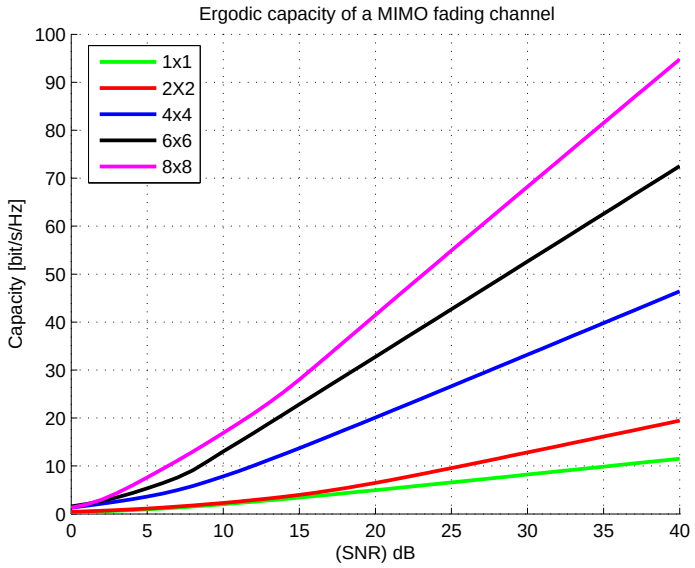

Figure 1.2. Ergodic capacity of MIMO channel H as a function of SNR and for different antenna dimensions.

MIMO system can be exploited. Under the assumption of enough spacing between antenna elements and under a rich multipath condition, it can be

shown that a space time communication system can be designed to provide diversity gain, which is equal to the product of number of transmit and receiver antennas, where the diversity gain $G_d = T_x \times R_x$ [14]. In a MIMO channel the diversity gain G_d in terms of error probability is given by

$$G_d = -\lim_{SNR\to\infty} \frac{log(P_e(SNR))}{log(SNR)} \tag{1.1.2}$$

where P_e denotes the average probability of error at average SNR over the randomness of the channel, the noise, and the data transmission. The diversity gain G_d can be defined as the slope of the error probability curve in terms of received SNR on a log-log scale. In other words, the diversity gain G_d describes how fast the probability of error decreases asymptotically with increasing SNR. Evidently, the higher the diversity order, the more reliable the wireless communication system will be. Coding across space and time is generally necessary to exploit the potential spatial diversity available within MIMO systems in cooperative relay networks to achieve a higher reliability, higher spectral efficiency and higher performance gain. Implementing multiple antennas at the transmitter and/or the receiver is practically difficult due to the cost and size. Therefore, a new communication paradigm was designed [15] to overcome this difficulty. In the next section, a brief introduction to cooperative relay networks will be presented.

1.2 Cooperative relay networks

Cooperative networks have developed as a useful technique that can achieve the same advantage as MIMO wireless systems whilst resolving the difficulties of co-located multiple antennas at individual nodes and avoiding the effect of path-loss and shadowing [16], [17] and [18]. Therefore, it has recently been considered in different wireless system standards such as WiMAX standards (IEEE 802.16j and IEEE 802.16m) [19] and WiFi standards (IEEE

802.11s and IEEE 802.11n) [20]. In cooperative relay networks, the source broadcasts its information via one or a number of intermediate relay nodes along with, or without, direct transmission to the destination node. The relay nodes may either act as a repeater where it amplifies the received signals and this protocol is assumed in this thesis, or it may decode the received signals from the source node, thereby increasing complexity at the relays, before forwarding them to the receiver node. Whereas the destination node combines the multiple independent received copies of the signal which results in cooperative diversity. The maximum cooperative diversity gain can be achieved by using either a one-way scheme or a two-way scheme, and equals to the number of transmitting relay nodes. Generally, cooperative relay systems potentially offer the following main advantages for wireless communications [15] and [21]:

1. Reliability of services: A cooperative relay network can be extremely effective to cope with the fading phenomena of the wireless communications through cooperative diversity [21]. It also increases the reliability of services by ensuring the transmission even if the source to destination link is under severe fade.

2. Performance gains: Performance gains can be achieved due to capacity, diversity and path-loss gains. These gains can decrease power consumption due to transmitting over shorter links, provide higher capacity, higher transmission rate and improve the outage probability in a wireless network.

3. Extension of coverage: The cooperative relay network also expands the network coverage by increasing the source to destination travelling distance for the transmitted signal.

A cooperative relay network depicted in Figure 1.3 shows the increase in the service reliability and expansion of network coverage. In contrast, cooper-

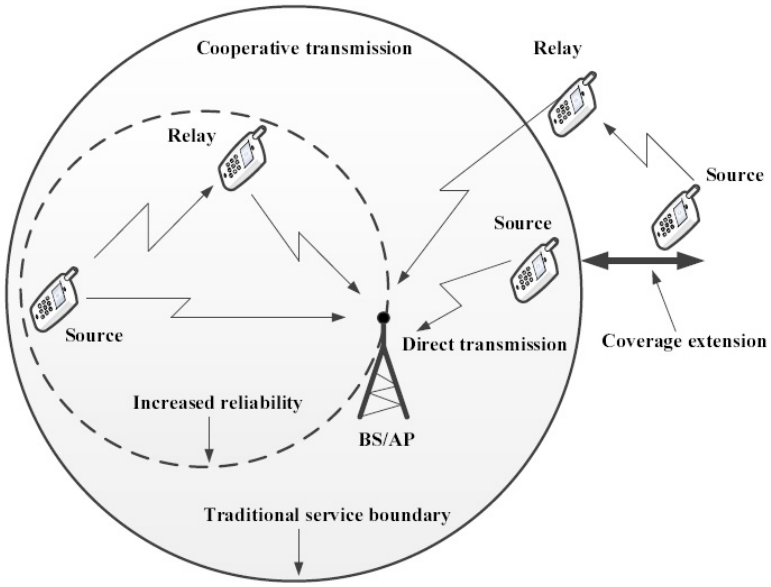

Figure 1.3. Coverage extension and service reliability proposed by cooperative relay network.

ative relay systems have some disadvantages which could affect the system performance such as synchronization. The synchronization issue is one of the most important challenges in wireless networks, since the cooperative wireless networks are asynchronous in nature, e.g., there may exist timing errors and multiple frequency offsets in the relay nodes forming the cooperative system. This will induce inter-symbol interference (ISI) between the relay nodes at the receiver node, which degrades the system performance and makes it impossible to exploit full cooperative diversity. This thesis considers asynchronous cooperative relay networks, and provides effective solutions to deal with the asynchronism in cooperative network. One of the potential solutions for mitigating asynchronism in cooperative wireless relay networks is by utilizing orthogonal frequency division multiplexing (OFDM) at the transmitter. A brief introduction to OFDM will be presented in the next section.

1.3 Orthogonal frequency division multiplexing

Orthogonal frequency division multiplexing (OFDM) is the optimal form of a multi-carrier modulation scheme [22] and [23] which forms the basis of many wireless standards such as the 802.11 Wi-Fi standard, the 802.16 WiMAX standard, the digital video broadcasting (DVB) standard and the asymmetric digital subscriber line (ADSL) standard [24]. It employs modern digital modulation techniques and both the inverse fast Fourier transform (IFFT) and fast Fourier transform (FFT), which in effect contain a bank of oscillators, demodulators and filters. In fact, IFFT and FFT algorithms are efficient methods to compute the inverse discrete Fourier transform (IDFT) at the modulator and a discrete Fourier transform (DFT) at the demodulator. In the OFDM technique the whole bandwidth is divided into many sub-carriers, which are orthogonal to each other with perfect synchronization between the transmitter and the receiver. It has the capability to reduce inter-symbol interference (ISI) because each subcarrier is modulated at a very low symbol rate which makes the symbols much longer than the channel impulse response, and as a result accurate data information can be extracted from each sub-carrier [25]. In addition, a cyclic prefix (CP) is

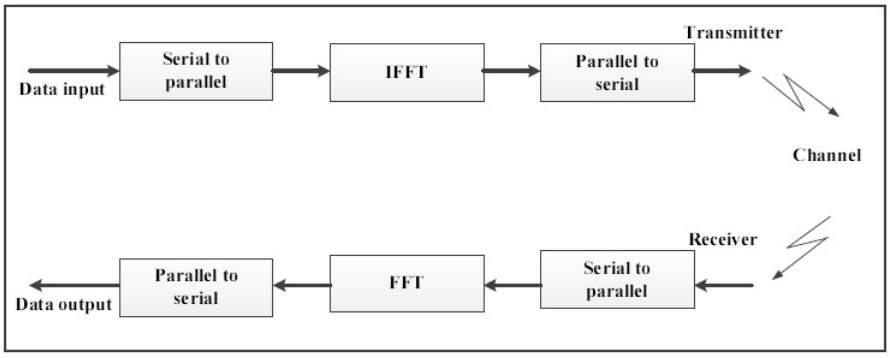

Figure 1.4. Basic block diagram of the conventional OFDM system, exploiting the IFFT and FFT..

inserted between consecutive OFDM symbols as a guard interval. Figure

1.4 illustrates a basic block diagram of the OFDM system. At the transmitter side, a sequence of data symbols in the frequency domain is converted into size M parallel streams, where each stream can be drawn from any signal constellations. The converted streams are then modulated onto M sub-carriers through a size M IFFT, which can be represented as follows

$$x(n) = \frac{1}{\sqrt{M}} \sum_{k=0}^{M-1} X(k) e^{\frac{j2\pi kn}{M}} \quad \text{for } n = 0, ..., M-1$$

where M denotes the duration of one OFDM symbol, k is the frequency index for the IFFT and n is the index for the sample of x. The M outputs of the IFFT are then converted to a serial data stream that can be modulated by a single carrier. At the receiver side, the received data streams are converted into M parallel streams that are processed by a size M FFT and can be represented as follows

$$X(k) = \frac{1}{\sqrt{M}} \sum_{n=0}^{M-1} x(n) e^{\frac{-j2\pi kn}{N}} \quad for\ k = 0, ..., M-1$$

This means the IFFT converts the input signal from the frequency-domain into a time-domain signal whilst maintaining the orthogonality, and the FFT converts the output signal time-domain into the frequency-domain to recover the information that was originally sent. Therefore, OFDM is an affective technique for cooperative wireless systems that suffer from imperfect synchronization, which will be discussed in Chapter 5. In the next section, a brief introduction to cognitive radio will be presented.

1.4 Cognitive radio

Cognitive radio is a wireless technology that can potentially be employed to sense, recognize and exploit the unutilized radio spectrum wisely at a given time [26]. The main characteristic of a cognitive radio is its intelligence that

allows sensing all possible radio spectra before it makes a decision on how and when to make use of a particular sector of the spectrum for communications. The use of radio spectrum is strictly managed by governments in most countries, and spectrum allocation is a legacy command-and-control regulation enforced by regulatory bodies, such as the federal communications commission (FCC) in the United States [27] and Ofcom in the United Kingdom [28]. Most of the existing wireless networks and devices follow fixed spectrum access (FSA) policies to use the radio spectrum, which means that radio spectral bands are licensed to dedicated users and services, such as TV, 3G networks, and vehicular ad hoc networks. Licensed users are referred to as the primary users (PUs) and the additional radio spectra users are named as cognitive users or secondary users (SUs) [29]. The standardization of the cognitive radio was carried out by the IEEE in parallel with the FCC. Several IEEE 802 standards for wireless systems have considered cognitive radio systems such as the IEEE 802.22 standard [30] and the IEEE 802.18 standard [31]. For example Sevension prepared a document in [31] which indicates that IEEE 802:18 supports the opportunistic use of the licensed spectrum bands on a non-interfering basis.

In general, in cognitive radio there are three main spectrum sharing approaches which can be classified as:

1. Overlay approach: The overlay approach (Figure 1.5) is also known as the interference free approach [32], in which once the spectrum hole is detected, the secondary users access part of the unoccupied spectrum to transmit their information with no interference to the primary users. The cognitive user (secondary user) can use part of their power for its communication and the remainder of the power to assist primary users' transmission. The advantage of this approach is that there is no interfering with the primary transmission, therefore this approach is assumed in this thesis. However, the major disadvantage of this

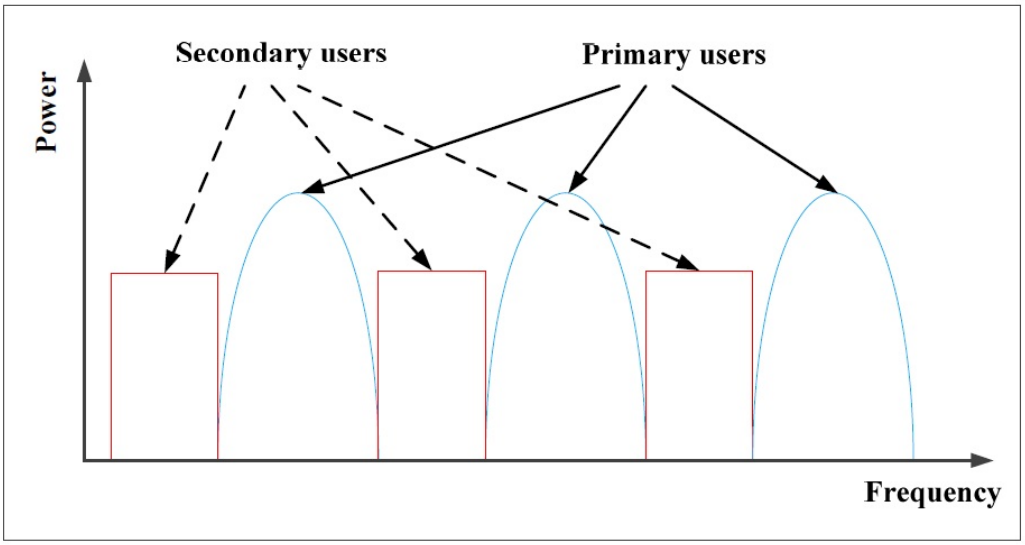

Figure 1.5. Overlay approach of cognitive radio.

approach is that the cognitive users need to be synchronized with the existing primary users' band. Also, cognitive users are required to continuously sense the spectrum before transmission.

2. Underlay approach: The underlay or interference tolerant approach (Figure 1.6) implements a wideband system [32]. The secondary users

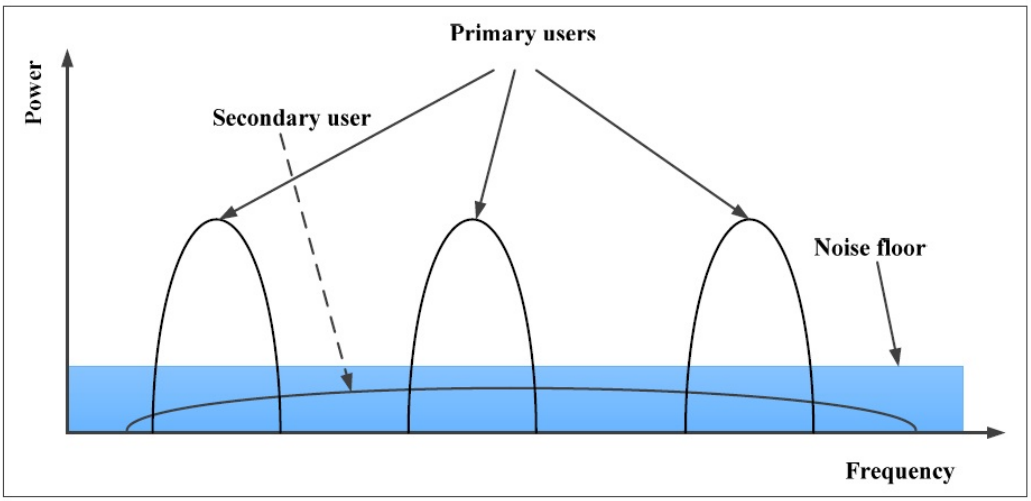

Figure 1.6. Underlay approach of cognitive radio.

use the radio spectrum at the same time with the primary users possi-

bly employing power allocation or frequency spreading techniques [33]. Hence, the secondary users must transmit with low transmit power to operate below the noise floor of the primary users ensuring a tolerable interference to the primary users. The underlay approach has the flexibility of transmission at any time and does not need to be synchronized with the primary users' band. However, the interference power constraints associated with this approach allow only short range communications.

3. Interweave approach: In this approach the secondary users are opportunistically accessing the spectrum holes without causing interference to the primary users [34]. These spectrum holes change with time and geographic location. In this technique, the secondary radio, therefore, is an intelligent wireless communication system that periodically monitors the radio spectrum, detects the presence/absence of primary users in the different frequency bands and then opportunistically interweaves the secondary signal through the holes that arise in frequency and time. However, in this technique, accurate detection of the presence of primary systems, especially in low signal-to-noise ratio scenarios, is critical to cognitive radio operation.

However, in cognitive radio there are two main challenges: the primary user detection and the transmission opportunity exploitation [35]. In fact detection of a primary user leads to the detection of a spectrum hole (spectrum sensing). A spectrum hole is an unoccupied spectrum band which is licensed to the primary user. The cooperative diversity, exploited by a relay network, has been investigated as an efficient solution to cope with the challenges of the cognitive radio [36] and [37]. In particular, the cooperative communications technique improves the ability of spectrum sensing by overcoming the problem of the hidden terminal and shadow effects, and helping in the

detection process of unoccupied spectrum which results in minimizing the probability of false alarms and increasing the opportunity to utilize the spectrum for transmission. In this thesis, the operation of a cooperative relay network has been investigated in a cognitive radio environment in Chapter 6. Next, the motivation for the research contribution of this thesis is given.

1.5 Motivation of the proposed research work

In the work presented in [38] by Alamouti, a transmit diversity scheme was presented and applied in cooperative relaying network in [39]. To improve the symbol transmission rate, a quasi orthogonal STBC (QO-STBC) scheme was proposed by Jafarkhani in [40], this QO-STBC achieves full code rate, but the orthogonality is relaxed. To achieve the full diversity in QO-STBC, a pairwise constellation rotation was proposed in [41] [42]. In order to further improve the QO-STBC performance, in this thesis, a modified QO-STBC (M-QO-STBC) has been considered, improved and then applied in cooperative relay networks. The M-QO-STBC has been inspired by the work in [43], to achieve full diversity and increase the code gain distance (CGD) between the codewords, where the CGD is further increased in this work by applying a genetic algorithm method. However, there are two main challenging problems related to cooperative systems. Firstly, end-to-end transmission rate can decrease due to the requirement of increasing the transmission stage, therefore, a two-way transmission scheme is considered in this thesis to increase the end-to-end transmission rate. The second challenge is, when designing high-performance cooperative networks, symbol-level synchronization among the relay nodes is required, however due to the nodes being in different locations and mismatch between their individual oscillators, this synchronisation is difficult to achieve. Therefore, in this thesis, this issue will be considered and an effective solution that can combat the timing error

problem by exploiting orthogonal frequency division multiplexing with cyclic prefix type of transmission is proposed. Moreover, due to the random nature of the wireless environment, the channel gains between the source node and destination node via relay nodes are different which results in poor channel quality between the source node and some intermediate relay nodes and destination node. This issue can affect the transmission quality to a certain extent. Therefore, in this thesis, a multi-relay selection scheme is considered to overcome this problem and decrease the outage probability of cooperative networks. However, cognitive radio is a recent wireless technology that can be employed to sense, recognize and exploit the unutilized radio spectrum wisely at a given time [26], therefore, a cognitive relay network with multi-relay selection will be provided to decrease the outage probability and also improve the spectrum efficiency.

On the basis of this foundation work the aims and objectives of this thesis are listed in the next section.

1.5.1 Aims and objectives

The aims of this thesis are:

1. Extend and transfer the advantage of M-QO-STBC in point-to-point transmission schemes to one-way and two-way cooperative communication; and thereby provide a framework in which the advantage of this codes is more likely to be practically realised due to its advantage, such as achieving full diversity, increasing data rate and increasing code gain distance.

2. Evaluate the improvement of one-way and two-way schemes over flat fading channels with relay selection through outage probability analysis.

3. Apply OFDM type of transmission on M-QO-STBC in cooperative

relay networks to mitigate timing errors.

4. Extend the M-QO-STBC to cognitive relay networks and then apply codeword error rate and outage probability as a performance measurement for the proposed system.

At the end of the study the objectives are to have

1. Demonstrated that M-QO-STBC for one-way and two-way schemes in cooperative relay systems, in various scenarios, can achieve full diversity and provide code gain distance.

2. Performed different types of outage probability analyses for one-way and two-way cooperative relaying communication system transmitting over flat fading channels.

3. Performed outage probability analysis for a cognitive AF network with multi-relay selection from the potential cooperative secondary relays based on the overlay approach with perfect and imperfect spectrum acquisition.

4. Published the research findings in international conferences and journals.

1.6 Organisation of the thesis

The structure of this thesis and its contributions, can be summarized as follows:

In Chapter 1, a quick introduction to conventional MIMO systems is given highlighting their main benefits and shortcomings. Furthermore, a general introduction to wireless communication systems including the basic concepts was provided together with brief background in STC and OFDM type transmission. In addition, a brief introduction to cognitive radio sys-

tems was provided highlighting the main functions of cognitive radio and the feature of the cooperative cognitive networks.

Chapter 2, introduces related background and literature survey for point-to-point STBC, distributed STBC and modified quasi-orthogonal space-time block codes. To evaluate the system performance of point-to-point STBC schemes, the Alamouti and the QO-STBC schemes are studied and discussed highlighting the advantage of each scheme. Then a brief introduction to distributed space-time block coding schemes with orthogonal, quasi-orthogonal and random orthogonal codes are presented. Finely, a method of set partitioning to be used in the modified QO-STBC is provided. The core research is presented in Chapters 3, 4, 5 and 6.

Chapter 3, investigates amplify-and-forward (AF) wireless relay networks for one-way and two-way communications through four relay nodes based on modified quasi-orthogonal space time block codes. This modified code is designed from set partitioning of two rotated quasi-orthogonal space-time codebooks then the subcodes are combined to be pruned to arrive at the modified codebook with the desired rate in order to increase the code gain distance.

In Chapter 4, outage probability analysis strategies for one-way and two-way cooperative AF relaying communication systems which transmits over flat channels with the best relay, the best four relay and the best N^{th} relay selection are presented. New exact analytical expressions for the probability density function, and cumulative density function of the received signal-to-noise ratio (SNR) are derived. These expressions are given in closed form for best relay selection and in integral form for N^{th} relay selection in the high SNR region for transmission over Rayleigh flat fading channel. Moreover, simulation results validate the accuracy of the derived closed-form expressions.

In Chapter 5, an OFDM-based modified space-time scheme for use in AF

one-way and two-way asynchronous cooperative relay networks with relay selection is proposed. The simulation results indicate that the OFDM-based scheme can significantly mitigate the delay and enhance the performance of the two systems under imperfect synchronization.

In Chapter 6, outage probability analysis strategies for a cognitive AF relay network with multi-relay selection from the potential cooperative secondary relays based on the overlay approach have been considered. Expressions for outage probability are determined for a frequency flat Rayleigh-fading environment from the received signal-to-noise ratio with perfect and imperfect spectrum acquisition in the proposed cognitive relay network based on D-QO-STBC.

Finely, in Chapter 7, the conclusions of the thesis are provided by summarizing contributions and also suggesting some future possible research directions.

Chapter 2

RELATED LITERATURE REVIEW

This chapter provides an overview of space-time block coding (STBC) design principles and performance, and discusses the STBC designed by Alamouti. It also considers the basic concepts of the conventional quasi-orthogonal STBC (QO-STBC) together with rotated and closed-loop QO-STBC. The design of STBCs amounts to finding code matrices that meet certain properties. The point-to-point STBC system codeword error rate performance is analyzed through simulation. Then the distributed space-time block coding concepts using N relay nodes which are relevant to this thesis are considered. Furthermore, the set partitioning method is used to increase the code gain distance to be used in a modified QO-STBC design.

2.1 Point-to-point space-time block coding

A wireless communication system with multiple transmitting and receiving antenna elements is called a MIMO system. MIMO systems provide a number of advantages over single-input single-output (SISO) systems. Sensitivity of fading is reduced by spatial diversity provided by multiple spatial paths leading to a significant improvement in the quality of the communication. MIMO communication generally operates by spreading the transmitted information across both space and time. Moreover, MIMO effectively takes

advantage of random fading [7], [12] and [44] and multipath delay spread when available [45] and [9] for improving the quality of wireless communications without any requirement for any extra spectrum.

Space time codes have been designed for such MIMO systems to achieve spatial diversity [8] [46], which provide improvement in system capacity and can be designed to achieve full rate, maximum diversity and the highest possible throughput, because of its low complexity encoding and maximum likelihood decoding. In addition, space time codes employ redundancy for the purpose of providing protection against channel fading, noise, and interference [47]. Moreover, a STBC can be considered as a modulation scheme for multiple antennas and includes block encoding of an incoming stream of data and simultaneously transmitting the symbols over N_t transmit antennas; this technique was first proposed by Alamouti in [38]. The Alamouti scheme includes a two transmit antenna STBC which utilizes full diversity and provides full code rate. It has also been shown in [48] that full diversity and full code rate block codes do not exist for complex valued symbols for more than two transmit antennas. However, quasi-orthogonal codes have been proposed by Jafarkhani [40] and Tirkkonen-Boariu-Hottinen (TBH) [49] that provide full code rate at the expense of loss in diversity. In both the Jafarkhani scheme and the TBH scheme, all information symbols are chosen in a single signal constellation therefore, after modulation, the modulated signals do not have full diversity, which results into degradation in performance. It was desired to have the quasi-orthogonal STBCs (QO-STBCs) with full diversity; to ensure good performance. In order to achieve that the authors in [50] proposed a QO-STBC with full diversity; the main idea of this scheme is to choose the signal constellations properly to ensure full diversity. However, the performance of the QO-STBC scheme was further improved by using closed-loop QO-STBC, which achieves full diversity with simple decoding at the receiver [51] where two phase feedback is used

at the third and fourth antennas. Brief outline of the Alamouti scheme and QO-STBCs schemes will be next prsented and their associated performance will be compared.

2.1.1 Alamouti scheme

The Alamouti space-time algorithm [38] is a simple transmit diversity scheme which provides full diversity, full data rate and improves the quality of the received signal by spreading the information across two antennas at the transmitter with different time symbol periods . The simple structure and linear detection of this code makes it very attractive; it has been adopted for both wideband code division multiple access (W-CDMA) and code division multiple access (CDMA) 2000 standards. Figure 2.1 shows the Alamouti STBC transmitter with two antennas. The input symbols to the space-time

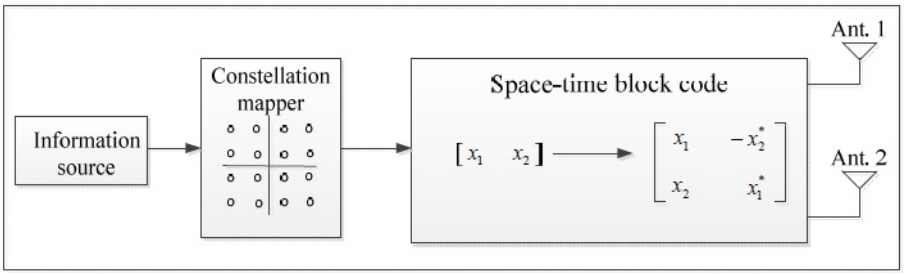

Figure 2.1. Transmitter diversity for Alamouti space-time block coding.

block encoder are divided into groups of two symbols each. At a given symbol period, the two symbols in each group x_1, x_2 are transmitted simultaneously from the two antennas. The signal transmitted from the first antenna is x_1 and the signal transmitted from the second antenna is x_2. In the next symbol period, the first and second antennas transmit $-x_2^*$ and x_1^* respectively where $(.)^*$ is the complex conjugate. Firstly, it is assumed that there is a single antenna at the receiver, and the receiver has perfect channel information h_1 and h_2, where h_1 and h_2 denote the generally complex channel gains from the first and the second transmit antennas to the receive antenna respectively.

It is also assumed that the channel gains are constant over two consecutive symbol transmission periods. The received signals can be expressed as

$$r_1 = h_1 x_1 + h_2 x_2 + n_1 \tag{2.1.1}$$

$$r_2 = -h_1 x_2^* + h_2 x_1^* + n_2 \tag{2.1.2}$$

where r_1 and r_2 are the received signals over two consecutive symbol periods and n_1 and n_2 represent additive Gaussian noise at the receiver. Define the code symbol vector $\mathbf{x} = [x_1 \quad x_2]^T$, the received signal vector $\mathbf{r} = [r_1 \quad r_2^*]^T$ and the noise vector $\mathbf{n} = [n_1 \quad n_2^*]^T$ where T denotes the transpose operator. Then (2.1.1) and (2.1.2) can be written in a matrix form as

$$\mathbf{r} = \mathbf{H}\mathbf{x} + \mathbf{n} \tag{2.1.3}$$

where

$$\mathbf{H} = \begin{bmatrix} h_1 & h_2 \\ h_2^* & -h_1^* \end{bmatrix} \tag{2.1.4}$$

which represents the equivalent channel matrix in the Alamouti code with a single receive antenna. The vector $\mathbf{n}$ is a complex Gaussian random vector with zero mean and covariance matrix $N_o I_2$ where I_2 is a 2×2 identity matrix. Define $\mathbf{X}$ as the set of all possible symbol pairs $\mathbf{x} = \{x_1, x_2\}$. Assuming that all the symbol pairs have the same probability and since the elements of the noise vector $\mathbf{n}$ are assumed to be additive white Gaussian noise (AWGN), therefore, the maximum likehood (ML) decoder is

$$\hat{\mathbf{x}} = \arg \min_{\hat{x} \in \mathbf{X}} ||\mathbf{r} - \mathbf{H}\hat{\mathbf{x}}||^2 \tag{2.1.5}$$

Since the channel matrix $\mathbf{H}$ is always orthogonal regardless of the channel coefficients, thus $\mathbf{H}^H\mathbf{H} = \lambda \, \mathrm{I}_2$ where $(.)^H$ is the conjugate transpose operator

and $\lambda = |h_1|^2 + |h_2|^2$. Consider multiplying both sides of (2.1.3) by $\mathbf{H}^H$ then

$$\hat{\mathbf{r}} = \mathbf{H}^H \mathbf{r} = \lambda \mathbf{x} + \hat{\mathbf{n}} \tag{2.1.6}$$

where $\hat{\mathbf{n}} = \mathbf{H}^H \mathbf{n}$. Therefore the decoding becomes

$$\hat{\mathbf{x}} = \arg \min_{\hat{x} \in \mathbf{X}} ||\hat{\mathbf{r}} - \lambda \hat{\mathbf{x}}||^2 \tag{2.1.7}$$

Since $\mathbf{H}$ is orthogonal, therefore the noise vector $\hat{\mathbf{n}}$ will have a zero mean and covariance matrix $\lambda N_o \mathrm{I}_2$, i.e., the elements of $\hat{\mathbf{n}}$ are i.i.d. Then by using this simple linear combining, the decoding rule in (2.1.7) reduces to two separate, and much simpler decoding rules for x_1 and x_2 as established in [38]. Figure 2.2 shows an Alamouti receiver with two antennas and when the receiver has

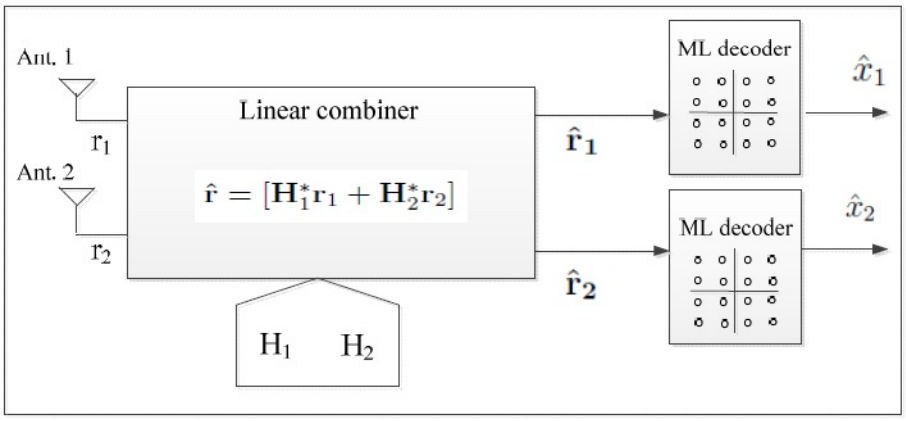

Figure 2.2. Receiver with two antennas for Alamouti space-time block coding.

N_r receive antennas, then the received signal vector at the n-th antenna is

$$\mathbf{r}_n = \mathbf{H}_n \mathbf{x} + \mathbf{n}_n \tag{2.1.8}$$

where $\mathbf{H}_n$ is the channel matrix and $\mathbf{n}_n$ is the noise vector at the two time instants from the two transmit antennas to the n-th receive antenna. In this

case, the ML decoding rule is

$$\hat{\mathbf{x}} = \arg \min_{\hat{x} \in \mathbf{X}} \sum_{n=1}^{N_r} ||\mathbf{r}_n - \mathbf{H}_n \hat{\mathbf{x}}||^2 \tag{2.1.9}$$

As before the decoding rule can be further simplified by multiplying the received signal vector $\mathbf{r}_n$ by $\mathbf{H}_n^H$. In this case, the diversity order provided by this scheme is $2N_r$. Note that for the above 2×2 STBC, the transmission rate is one symbol/transmission, and it achieves the maximum diversity order of 4 that is possible with a 2×2 frequency flat system.

The method of Alamouti can be generalized to more than two transmit antennas [48], [52] and [53]. The resulting orthogonal codes are still simply decoded with a linear receiver [38]. In addition, only a few codes with a rate of one symbol/transmission are available, and for general complex-valued signals, there is no orthogonal full rate code beyond the Alamouti code [48]. However, it is possible to design codes for more than two transmit antennas by relaxing the diversity and increasing the transmission rate, this will be considered in the next section.

2.1.2 Quasi-orthogonal space-time block codes

To improve the symbol transmission rate, the quasi-orthogonal STBC (QO-STBC) scheme was proposed by Jafarkhani in [40], a similar scheme was also proposed by Papadias in [54]. A quasi-orthogonal STBC with full code rate, but where the orthogonality is relaxed was constructed from the Alamouti scheme as follows:

$$X = \begin{bmatrix} A_{12} & A_{34} \\ -A_{34}^* & A_{12}^* \end{bmatrix} = \begin{bmatrix} x_1 & x_2 & x_3 & x_4 \\ -x_2^* & x_1^* & -x_4^* & x_3^* \\ -x_3^* & -x_4^* & x_1^* & x_2^* \\ x_4 & -x_3 & -x_2 & x_1 \end{bmatrix} \tag{2.1.10}$$

where

$$A_{12} = \begin{bmatrix} x_1 & x_2 \\ -x_2^* & x_1^* \end{bmatrix} \quad \text{and} \quad A_{34} = \begin{bmatrix} x_3 & x_4 \\ -x_4^* & x_3^* \end{bmatrix} \tag{2.1.11}$$

$$\begin{bmatrix} r_1 \\ r_2 \\ r_3 \\ r_4 \end{bmatrix} = \begin{bmatrix} x_1 & x_2 & x_3 & x_4 \\ -x_2^* & x_1^* & -x_4^* & x_3^* \\ -x_3^* & -x_4^* & x_1^* & x_2^* \\ x_4 & -x_3 & -x_2 & x_1 \end{bmatrix} \begin{bmatrix} h_1 \\ h_2 \\ h_3 \\ h_4 \end{bmatrix} + \begin{bmatrix} v_1 \\ v_2 \\ v_3 \\ v_4 \end{bmatrix} \tag{2.1.12}$$

A scheme with four transmit antennas and one receiver as shown in Figure

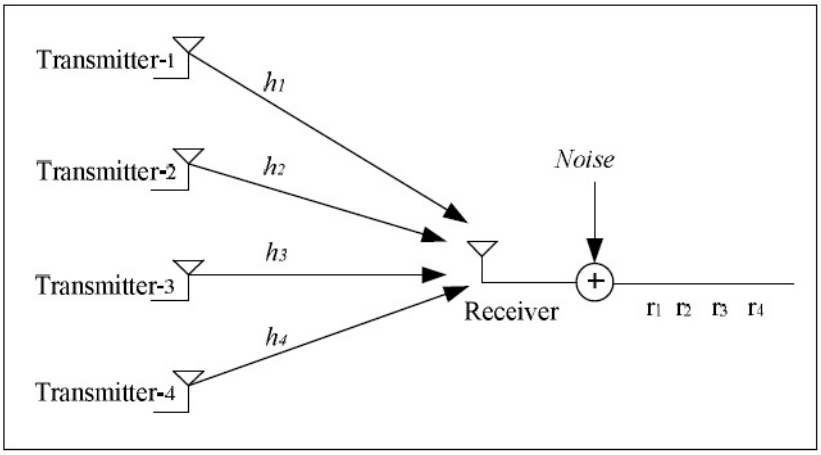

Figure 2.3. Four transmit and one receive antenna system.

(2.3) is considered. It is assumed that the channels are flat fading and they are denoted as h_i where $i = 1, ..., 4$. In terms of the transmitted symbols the received signal vector can be presented as

$$\begin{bmatrix} r_1 \\ r_2^* \\ r_3^* \\ r_4 \end{bmatrix} = \begin{bmatrix} h_1 & h_2 & h_3 & h_4 \\ -h_2^* & h_1^* & -h_4^* & h_3^* \\ -h_3^* & -h_4^* & h_1^* & h_2^* \\ h_4 & -h_3 & -h_2 & h_1 \end{bmatrix} \begin{bmatrix} x_1 \\ x_2 \\ x_3 \\ x_4 \end{bmatrix} + \begin{bmatrix} v_1 \\ v_2^* \\ v_3^* \\ v_4 \end{bmatrix} \tag{2.1.13}$$

or an scalar equation form as

$$\begin{aligned} r_1 &= h_1x_1 + h_2x_2 + h_3x_3 + h_4x_4 + v_1 \\ r_2^* &= h_2^*x_1 - h_1^*x_2 + h_4^*x_3 - h_3^*x_4 + v_2^* \\ r_3^* &= h_3^*x_1 + h_4^*x_2 - h_1^*x_3 - h_2^*x_4 + v_3^* \\ r_1 &= h_4x_1 - h_3x_2 - h_2x_3 + h_1x_4 + v_4 \end{aligned} \tag{2.1.14}$$

Thus (2.1.14) can be rewritten in general term as

$$\mathbf{r} = \mathbf{H}\mathbf{x} + \mathbf{v} \tag{2.1.15}$$

Matched filtering is performed by multiplying (2.1.15) by H^H, therefore

$$H^H r = H^H x + H^H v \tag{2.1.16}$$

$$\tilde{r} = \Delta x + \tilde{n} \tag{2.1.17}$$

where $(.)^H$ represents conjugate transpose, and Δ is the Grammian matrix and can be represented as

$$\Delta = \begin{bmatrix} \beta_d & 0 & 0 & \beta \\ 0 & \beta_d & -\beta & 0 \\ 0 & -\beta & \beta_d & 0 \\ \beta & 0 & 0 & \beta_d \end{bmatrix} \tag{2.1.18}$$

where $\beta_d = |h_1|^2 + |h_2|^2 + |h_3|^2 + |h_4|^2$, $\beta = \mathrm{R}_e\{h_1^*h_4 - h_2^*h_3\}$ and R_e denotes the real part operator. Some non-zero off diagonal terms appear at the receiver after matched filtering of the signal which reduces the diversity gain of the code. It also makes the decoding process slightly more complex than for the Alamouti code where pairs of the transmitted symbols need to be decoded separately as will be explained in the next section.

2.1.2.1 Pairwise decoding

If the i-th column of (2.1.10) is denoted by ν_i where $i = 1, 2, 3, 4$ therefore, for any variables x_1, x_2, x_3, x_4,

$$\langle \nu_1, \nu_2 \rangle = \langle \nu_1, \nu_3 \rangle = \langle \nu_2, \nu_4 \rangle = \langle \nu_3, \nu_4 \rangle = 0 \tag{2.1.19}$$

where $\langle \nu_i, \nu_j \rangle$ is the inner product of vectors ν_i and ν_j. Thus, the subspace created by ν_1 and ν_4 is orthogonal to the subspace created ν_2 and ν_3. From this orthogonality, the maximum-likelihood can be calculated as the sum of two terms $f_{14}(x_1, x_4) + f_{23}(x_2, x_3)$, where f_{14} is independent of x_2 and x_3 and f_{23} is independent of x_1 and x_4. Therefore, the decoding in pairs can be given by [8]:

$$f_{14}(x_1, x_4) + f_{23}(x_2, x_3) \tag{2.1.20}$$

where

$$\begin{aligned} f_{14}(x_1, x_4) = \sum_{i=1}^{4} [|h_i|^2(|x_1|^2 + |x_4|^2) + 2\mathrm{R}_e\{x_1(-r_1^* h_1 - r_2 h_2^* - r_3 h_2^* - r_4^* h_4) \\ + x_4(-r_1^* h_4 + r_2 h_3^* + r_3 h_3^* - r_4^* h_1)\} + 4\mathrm{R}_e\{x_1 x_4^*\}\mathrm{R}_e\{h_1 h_4^* - h_2^* h_3\}] \end{aligned}$$

and

$$\begin{aligned} f_{23}(x_2, x_3) = \sum_{i=1}^{4} [|h_i|^2(|x_2|^2 + |x_3|^2) + 2\mathrm{R}_e\{x_2(-r_1^* h_2 + r_2 h_1^* - r_3 h_4^* + r_4^* h_3) \\ + x_3(-r_1^* h_3 - r_2 h_4^* + r_3 h_1^* + r_4^* h_2)\} + 4\mathrm{R}_e\{x_2 x_3^*\}\mathrm{R}_e\{h_2 h_3^* - h_1^* h_4\}] \end{aligned}$$

In fact, full rate orthogonal designs with complex elements in its transmission matrix are impossible for more than two antennas [55] and as the rank of the QO-STBC matrix in (2.1.10) is two, therefore, for N_r receive antennas, a diversity order of $2N_r$ is achieved. In order to achieve the full diversity, rotated QO-STBCs will be considered in the next section.

2.1.2.2 Rotated quasi-orthogonal space-time block coding

It is possible to modify quasi-orthogonal codes to give them full diversity [56], [41], [42] and [57]. The main idea is to use different constellations for the two components of the quasi-orthogonal code by rotating symbols before transmission. The idea in this section is to choose signal constellations properly which provide codes which achieve full diversity. The asymptotic slope of the signal-to-noise ratio (SNR) performance curve depends on the diversity [40] [49]. In the Jafarkhani scheme [40], TBH scheme [49] and Papadias-Foschini scheme [58], the signal constellations are chosen arbitrarily, thus the resulting STBCs cannot guarantee full diversity. It is assumed that $G_q(x_1, x_2, ..., x_k)$ is a $q \times q$ orthogonal design and $x_1, x_2, ..., x_k$ are complex variables. A quasi-orthogonal design $Q_{2q}(x_1, x_2, ..., x_{2k})$ can be obtained as [50]

$$Q_{2q} = \begin{bmatrix} Y & Z \\ Z & Y \end{bmatrix} \tag{2.1.21}$$

where

$$Y = G_q(x_1, x_2, ..., x_k) \qquad \text{and} \qquad Z = G_q(x_{k+1}, x_{k+2}, ..., x_{2k})$$

Since Y and Z are orthogonal designs, thus

$$\begin{aligned} Q_{2q}^H Q_{2q} &= \begin{bmatrix} Y^H Y + Z^H Z & Y^H Z + Z^H Y \\ Z^H Y + Y^H Z & Z^H Z + Y^H Y \end{bmatrix} \\ &= \begin{bmatrix} a_1 I_q & a_2 I_q \\ a_2 I_q & a_1 I_q \end{bmatrix} \end{aligned} \tag{2.1.22}$$

where

$$a_1 = \sum_{i=1}^{2k} |x_i|^2 \qquad \text{and} \qquad a_2 = \sum_{i=1}^{k} (x_i x_{k+i}^* + x_{k+i} x_i^*)$$

The last quality in (2.1.22) follows from

$$Y^H Y + Z^H Z = (\sum_{i=1}^{k} |x_i|^2 I_q + \sum_{i=1}^{k} |x_{k+i}|^2 I_q)$$

and

$$\begin{aligned} Y^H Z + Z^H Y &= (Y+Z)^H (Y+Z) - Y^H Y - Z^H Z \\ &= (\sum_{i=1}^{k} |x_i + x_{k+i}|^2) I_q - (\sum_{i=1}^{k} |x_i|^2 I_q) - (\sum_{i=1}^{k} |x_{k+i}|^2) I_q \end{aligned} \tag{2.1.23}$$

The quasi-orthogonal design $Q_{2q}(x_1, x_2, ..., x_{2k})$ is applied to obtain STBCs with full diversity of $2q$ transmit antennas. For each i, $1 \leq i \leq k$, $\mathbb{S}_i$ denotes a signal constellation with unity average energy, and $\mathbb{S}_{k+i}$ denote the signal constellation generated by rotating $\mathbb{S}_i$ with angle of θ_i, $\mathbb{S}_{k+i} = \{e^{j\theta_i} s : s \epsilon \mathbb{S}_i\}$, denoted as $\mathbb{S}_i e^{j\theta}$. Moreover, $|\mathbb{S}_i|$ denotes the number of elements in $\mathbb{S}_i$. It is chosen as $2k$ symbols $s_1 \epsilon \mathbb{S}_1, s_2 \epsilon \mathbb{S}_2, ..., s_{2k} \epsilon \mathbb{S}_{2k}$, for any information sequence of length $\log_2(\Pi_{i=1}^{2k} |\mathbb{S}_i|)$. By replacing $x_1, x_2, ..., x_{2k}$ in $Q_{2q}(x_1, x_2, ..., x_{2k})$ by $s_1, s_2, ..., s_{2k}$, a new matrix $Q_{2q}(s_1, s_2, ..., s_{2k})$ is provided. At last STBC is transmitted as

$$C = \sqrt{\Gamma} Q_{2q}(s_1, s_2, ..., s_{2k}) \tag{2.1.24}$$

The factor $\sqrt{\Gamma}$ ensures that the transmitted signal in (2.1.24) obeys the energy constraint. The rate of this code is $\frac{1}{2q} \log_2(\Pi_{i=1}^{2k} |\mathbb{S}_i|)$ bits per channel use. From (2.1.22), the maximum likelihood (ML) decoding of (2.1.24) can be calculated separately on each pair of symbols s_i and s_{k+i}. The difference matrix between C and $\hat{C}$ is $\sqrt{\Gamma} Q_{2q}(s_1 - \hat{s}_1, s_2 - \hat{s}_2, ..., s_{2k} - \hat{s}_{2k})$. This difference matrix is denoted as ΔC, then, from (2.1.22)

$$(\Delta C)^H (\Delta C) = \Gamma \begin{bmatrix} (\Delta a_1) I_q & (\Delta a_2) I_q \\ (\Delta a_2) I_q & (\Delta a_1) I_q \end{bmatrix} \tag{2.1.25}$$

where

$$\Delta a_1 = \sum_{i=1}^{2k} |s_i - \hat{s}_i|^2$$

and

$$\Delta a_2 = \sum_{i=1}^{k} [(s_i - \hat{s}_i)(s_{k+i} - \hat{s}_{k+i})^*(s_{k+i} - \hat{s}_{k+i})(s_i - \hat{s}_i)^*]$$

Therefore, the determinant of (2.1.25) is calculated as

$$\det[(\Delta C)^H(\Delta C)] = \Gamma^{2q}[(\Delta a_1)^2 - (\Delta a_2)^2]^q. \tag{2.1.26}$$

It is clear that the determinant in (2.1.26) can be zero for $\theta = 0$ for all i, for example, when $s_i - \hat{s}_i = s_{k+i} - \hat{s}_{k+i}$, which means the space-time signals do not have full diversity. To solve this problem a proper rotation angle θ_i is required to make sure that the determinant in (2.1.26) is nonzero. For example, a simple case is considered, if all of $\mathbb{S}_i,\ 1 \leq i \leq k$, are binary phase-shift keying (BPSK), so $\mathbb{S}_i = \{1, -1\}$, the rotation angle is chosen as $\theta = \frac{\pi}{2}$, then the signal constellation $\mathbb{S}_{k+i} = e^{j\frac{\pi}{2}}$, $\mathbb{S}_i = \{j, -j\}$. Therefore, the difference $s_i - \hat{s}_i$ belongs to set $\{0, 2, -2\}$ and for any two symbols s_{k+1} and $\hat{s}_{k+1}$ in $\mathbb{S}_{k+i}$, the difference $s_{k+1} - \hat{s}_{k+1}$ belongs to set $\{0, 2j, -2j\}$. It can be seen that Δa_2 in (2.1.25) is zero. Therefore, the determinant of $(\Delta C)^H(\Delta C)$ is nonzero, which means that the space-time signals achieve full diversity. For BPSK and quadrature phase shift keying (QPSK) constellations $\theta = \frac{\pi}{2}$ and $\theta = \frac{\pi}{4}$ are the optimum rotation angles respectively to achieve the full diversity [50]. For example, in the Jafarkhani code, the third and fourth symbols are rotated before transmission to achieve the full diversity [50]. In the next section a closed-loop QO-STBC with full diversity will be considered.

2.1.2.3 Closed-loop quasi-orthogonal space-time block coding

The diversity gain is reduced by the non-zero off diagonal elements in matrix (2.1.18) which can be represented as

$$\beta = \mathrm{R}_e\{h_1^* h_4 - h_2^* h_3\} \tag{2.1.27}$$

therefore the transmitted signal can be modified by applying proper phase angles on the third and fourth antennas to make the two terms in (2.1.27) zeros. It is assumed that the signal from the third and fourth antennas are rotated by θ_1 and θ_2 respectively [51]. Therefore, (2.1.27) becomes

$$\beta = \mathrm{R}_e\{h_1^* h_4 e^{j\theta_1} - h_2^* h_3 e^{j\theta_2}\} \tag{2.1.28}$$

It is assumed that $\lambda_1 = h_1^* h_4^*$ and $\lambda_2 = h_2^* h_3$

$$\beta = |\lambda_1| cos(\theta_1 + \angle\lambda_1) - |\lambda_2| cos(\theta_2 + \angle\lambda_2) \tag{2.1.29}$$

where $|.|$ denotes the absolute value and $\angle$ denotes the angle ($arctan$) operators. Since $\beta = 0$ has infinite solutions for θ_1 and θ_2. By defining $\xi = arccos\frac{|\lambda_1|}{|\lambda_2|}$ the solutions can be represented as [51]

$$\theta_1 = arccos(\frac{|\lambda_2|}{|\lambda_1|} cos(\theta_2 + \angle\lambda_2)) - \angle\lambda_1 \tag{2.1.30}$$

where $\theta_2 \in [0, 2\pi]$ if $|\lambda_2| < |\lambda_1|$, or otherwise $\theta_2 \in [(\pi - \xi - \angle\lambda_2, \xi - \angle\lambda_2) \cup (2\pi - \xi - \angle\lambda_2, \pi + \xi - \angle\lambda_2)]$. Applying the exact phase as feedback, makes β and α in the matrix in (2.1.18) become $\beta = 0$ and $\alpha = |h_1^2| + |h_2^2| + |h_3^2 e^{\theta_1}| + |h_4^2 e^{\theta_2}|$ and it is evident that the closed-loop QO-STBC is orthogonal, which indicates that the information symbols can be detected separately with a simple ML decoder. Performance analysis of point-to-point STBCs will be simulated in the next section.

2.1.3 Simulations

In this section the performance of the Alamouti scheme is shown together with the QO-STBC schemes with and without feedback using quadrature phase shift keying (QPSK) modulation. It is assumed that the channels are uncorrelated Rayleigh fading and the receiver has perfect knowledge of each channel branch. Figure 2.4 shows the signal-to-noise ratio (SNR) versus

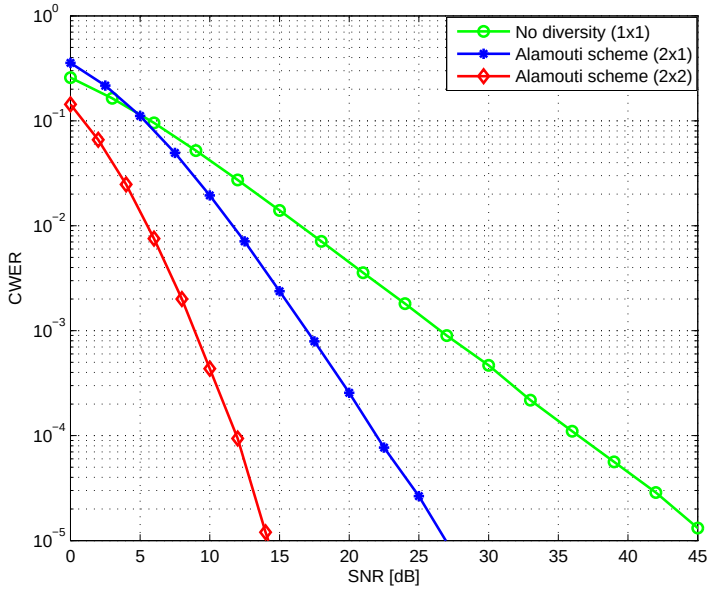

Figure 2.4. Performance of the Alamouti code using QPSK constellation.

codeword error rate (CWER) plot for the Alamouti system using one and two receive antennas. Note that using CWER in simulation gives worse performance than bit error rate (BER) for the same signal. However, the BER and CWER for the no diversity curve are the same; therefore, at the lowest SNR the no diversity curve is better than the Alamuiti curve corresponding to one receive antenna; but then the Alamouti curve crossed the no diversity curve due to its increased slope. As can be seen, the performance of the Alamouti code with two receive antennas is much better than the system without diversity and the Alamouti with one receive antenna. For example, at codeword error probability of 10^{-3}, Alamouti with two receive antennas

provides approximately 17 dB improvement compared to the no diversity system and approximately 8.5 dB improvement compared to the Alamouti with one receive antenna. More importantly, due to the higher diversity gain of the Alamouti code, the gap increases for higher SNR values. This is due to the fact that the degree of diversity dictates the slope of the CWER-SNR curve. Figure 2.5 show the comparison of average CWER performance of

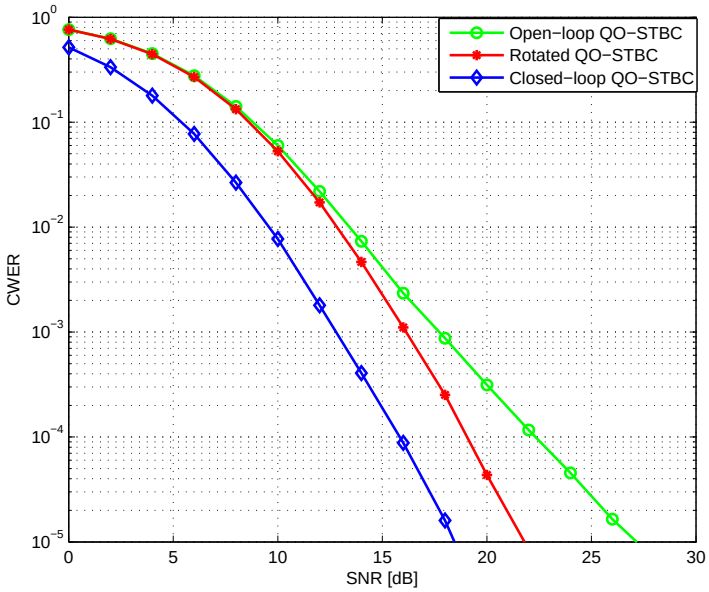

Figure 2.5. Performance of the non rotated, rotated and closed-loop QO-STBCs using QPSK constellation.

non rotated (conventional), rotated and closed-loop QO-STBC for a system with four transmit antennas and one receive antenna. It can be seen from the figure that at low SNRs (or high CWER) the curves of the non rotated and the rotated QO-STBC start from same point and they stay the same at low SNR. The reason for that is the code with full diversity benefits more from increasing the SNR. In other words, the diversity is very important at high SNR. Figure 2.5 also shows that the closed-loop QO-STBC has better performance over the non rotated and the rotated QO-STBC. For instance, at codeword error probability of 10^{-4}, the performance improvement of the closed-loop QO-STBC is approximately 6 dB compared to the non rotated

QO STBC scheme and about 3 dB compared to the rotated QO STBC with full diversity. The feedback method is successful in eliminating the off diagonal terms of the matrix in (2.1.18). In the next section, STBCs in cooperative networks will be considered.

2.2 Distributed space-time block coding

Multi-input multi-output (MIMO) wireless communication systems provide spatial diversity to improve link performance over single-input single-output communication systems. However, to obtain full diversity gain the spatial paths must be uncorrelated. In practice it is not always possible due to space limitation at the base station or at the mobile. In recent years, there has been increasing research in ad-hoc wireless networks looking for methods to exploit the spatial diversity provided by antennas of deferent users to improve the reliability and capacity of transmission [59] [60]. This improvement is called cooperative diversity and can be achieved by allowing single-antenna nodes to work together to achieve some of the benefits of point-to-point MIMO systems. The relay nodes in cooperative networks are generally sufficiently separated to ensure uncorrelated spatial paths between the source and destination nodes. In a cooperative communication system, there are two main cooperative methods: decode-and-forward (DF) and amplify-and-forward (AF) [15]. In the DF method, relay nodes decode the source information and then re-encode and re-transmit it to the destination. In the AF method, relay nodes only amplify and retransmit their received signals, including noise, to the destination. Therefore, AF type schemes have the advantage of simple implementation and low complexity in practical scenarios. In addition to complexity benefits, it has been shown in [61] that an AF scheme asymptotically, in terms of appropriate power control, approaches a DF one with respect to diversity. Therefore, in this

thesis, AF type methods will be considered.

Jing et al. [39] [62] proposed distributed space-time block coding (D-STBC) design in a wireless relay network based on a two-step amplify-and forward type protocol. It is known that orthogonal space-time codes have linear decoding complexity with full diversity and good performance. However, Tarokh et al. have already proved that complex orthogonal designs do not exist for four transmit antennas [48]. To solve this problem, Jafarkhani constructed a quasi-orthogonal design [40], in which pairs of transmitted symbols need be decoded separately. In the next section, a brief overview of cooperative wireless networks concepts relevant to this thesis will be presented.

2.2.1 Wireless relay network for distributed space-time block coding

The wireless communication relay network is shown in Figure 2.6, it consists of one transmitter node T_x, one receiver node R_x and R_i relay nodes where $i = 1, ..., N$. Each node in the system has a half-duplex antenna for either reception or transmission. It is assumed that the communication channels are quasi-static independent Rayleigh flat fading and there is no channel information at the relays, but the receiver has perfect channel information h_{s,r_i} and $h_{r_i,d}$, where h_{s,r_i} and $h_{r_i,d}$ represent the channels from the transmitter to the i-th relay and from the i-th relay to the receiver respectively. It is also assumed that there is no direct link between the source and the destination as path loss or shadowing is expected to render it unusable. The transmitter encodes the signal bits into symbols $\mathbf{x} = [x_1, ..., x_{T_s}]^T$ and $\mathbf{x}$ is normalized to be $E\{\mathbf{x}^H\mathbf{x}\} = 1$ where T_s and $E\{.\}$ denote the time slot and the expectation of a random variable, respectively [39]. The transmission operation has two stages, in stage one the transmitter sends signals $\sqrt{P_1 T_s}\mathbf{x}$

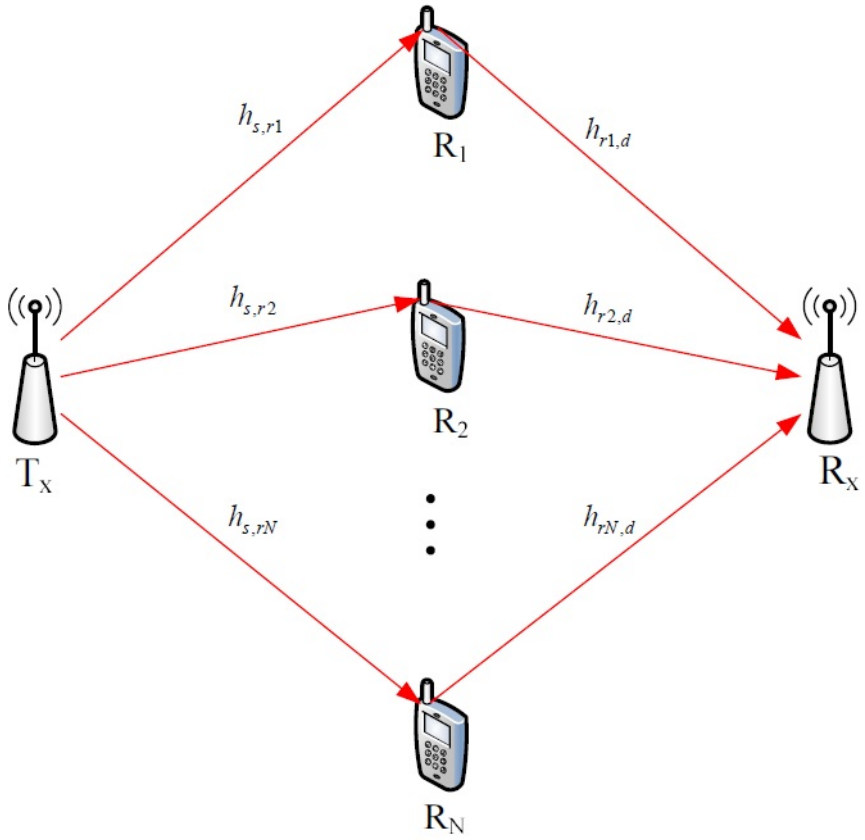

Figure 2.6. Wireless relay network with one transmitter node T_x, one receiver node R_x and R_N relay nodes.

to each relay where P_1 is the average power used at the transmitter for every transmission, whereas in stage two, the i-th relay sends its received signal t_i to the receiver. The noise vectors at the i-th relay $\mathbf{v}_i$ and at the receiver $\mathbf{w}_i$ have elements which are independent complex Gaussian random variables with zero-mean and unit-variance. Thus the distribution of the elements of $\mathbf{v}_i$ and $\mathbf{w}_i$ is $CN(0,1)$. The received signal at the i-th relay is corrupted by fading coefficient h_{s,r_i} and the noise vectors $\mathbf{v}_i$ given by

$$\mathbf{s}_i = \sqrt{P_1 T_s} h_{s,r_i} \mathbf{x} + \mathbf{v}_i \tag{2.2.1}$$

The i-th relay transmits the signal $\mathbf{t}_i$ which corresponds to the received signal $\mathbf{r}_i$ multiplied by a scaled unitary matrix. The transmitted signal from

the i-th relay node can be generated from

$$\begin{aligned}\mathbf{t}_i &= \sqrt{\frac{P_2}{P_1+1}}(A_i\mathbf{s}_i + B_i\mathbf{s}_i^*) \\ &= \sqrt{\frac{P_1P_2T_s}{P_1+1}}(h_{s,r_i}A_i\mathbf{x} + h_{s,r_i}^*B_i\mathbf{x}^*) + \sqrt{\frac{P_2}{P_1+1}}(A_i\mathbf{v}_i + B_i\mathbf{v}_i^*)\end{aligned} \tag{2.2.2}$$

The received signal vector $\mathbf{r}$ at the receiver is given by

$$\mathbf{r} = \sum_{i=1}^{N} h_{r_i,d}\mathbf{t}_i + \mathbf{w}_r \tag{2.2.3}$$

The special case that either $A_i = 0_{T_s}$, B_i is unitary or $B_i = 0_{T_s}$ and A_i is unitary is considered in this work. $A_i = 0_T$ means that the i-th relay column of the code matrix contains the conjugates $x_1^*, ..., x_{T_s}^*$ only and $B_i = 0_{T_s}$ means that the i-th relay column contains only the information symbols $x_1, ..., x_{T_s}$. Thus the following variables are defined as [39]

$$\hat{A}_i = A_i, \quad \hat{h}_{s,r_i} = h_{s,r_i}, \quad \hat{\mathbf{v}}_\mathbf{i} = \mathbf{v}_\mathbf{i}, \quad \mathbf{x}^{(i)} = \mathbf{x}, \qquad \text{if } B_i = 0$$

$$\hat{A}_i = B_i, \quad \hat{h}_{s,r_i} = h_{s,r_i}^*, \quad \hat{\mathbf{v}}_\mathbf{i} = \mathbf{v}_i^*, \quad \mathbf{x}^{(i)} = \mathbf{x}^*, \qquad \text{if } A_i = 0$$

From (2.2.2)

$$\mathbf{t_i} = \sqrt{\frac{P_1P_2T_s}{P_1+1}}\hat{h}_{s,r_i}\hat{A}\mathbf{x^{(i)}} + \sqrt{\frac{P_2}{P_1+1}}\hat{A}_i\hat{\mathbf{v}}_\mathbf{i}$$

The signal at the receiver can be calculated from (2.2.3) to be

$$\mathbf{r} = \sqrt{\frac{P_1P_2T_s}{P_1+1}}X\mathbf{h} + \mathbf{w} \tag{2.2.4}$$

where

$$\mathbf{h} = [\hat{h}_{s,r_1}h_{r_1,d} \ ... \ \hat{h}_{s,r_N}h_{r_N,d}]^T \tag{2.2.5}$$

and

$$X = [\hat{A}_1\mathbf{x}^{(1)} \ ... \ \hat{A}_N\mathbf{x}^{(N)}], \tag{2.2.6}$$

$$\mathbf{w} = \sqrt{\frac{P_2}{P_1 + 1}} \sum_{i=1}^{N} h_{r_i,d} \hat{A}_i \hat{\mathbf{v}}_i + \mathbf{w}_r \tag{2.2.7}$$

Therefore, without decoding, the relays generate a space-time codeword X distributively at the receiver. The vector $\mathbf{h}$ is the equivalent channel and $\mathbf{w}$ is the equivalent noise. The optimum power allocation to minimize end-to-end BER is when the transmitter uses half the total power and the relays share the other half [62]. Therefore, if the total power is P and the number of relays R then

$$P_1 = \frac{P}{2} \qquad \text{and} \qquad \mathrm{P}_2 = \frac{\mathrm{P}}{2\mathrm{R}} \tag{2.2.8}$$

Since the channel vector $\mathbf{h}$ is known at the receiver, the maximum-likelihood (ML) decoding is

$$\hat{\mathbf{x}} = \arg \min_{\mathbf{x}} \left\| \mathbf{r} - \sqrt{\frac{P_1 P_2 T_s}{P_1 + 1}} \; X \; \mathbf{h} \right\| \tag{2.2.9}$$

where $\|.\|$ represents Euclidean norm and *arg min* represents finding the smallest Euclidean norm from all possible X formed as in (2.2.6) from the source signal vectors $\mathbf{x}$ defined by the chosen source constellation.

2.2.1.1 Complex-orthogonal designs

A complex orthogonal design O_c of size n is an orthogonal matrix with entries $\pm x_1, \pm x_2, ..., \pm x_n$, and their conjugates $\pm x_1^*, \pm x_2^*, ..., \pm x_n^*$. The application of complex and Alamouti designs in relay networks is described in this section. For $T_s = \mathrm{R} = 2$ the matrices A_i and B_i which are used at the two relays are defined as [39]

$$A_1 = I_2, \; A_2 = B_1 = 0_2, \; B_2 = \begin{bmatrix} 0 & -1 \\ 1 & 0 \end{bmatrix} \tag{2.2.10}$$

The protocol of the distributed space-time coding described in (2.2.1), (2.2.2) and (2.2.3) is used. In the first step, at times 1 to T_s, the transmitter sends

the signal $\mathbf{x} = [x_1 \quad x_2]^T$ to the two relays. Therefore, according to (2.2.1), the received signals at the two relays are

$$r_1 = [r_{1,1} \quad r_{1,2}]^T \quad \text{and} \quad r_2 = [r_{2,1} \quad r_{2,2}]^T \tag{2.2.11}$$

In the second step, from times $T_s + 1$ to $2T_s$, the first and second relays send signals respectively as

$$t_1 \;=\; A_1 r_1 \;+\; B_1 r_1^* \;\text{ and }\; t_2 \;=\; A_2 r_2 \;+\; B_2 r_2^* \tag{2.2.12}$$

thus the signal at the receiver can be generated from (2.2.3) as

$$\begin{bmatrix} x_1 \\ x_2 \end{bmatrix} = h_{r_1,d} t_1 \;+\; h_{r_2,d} t_2 \;+\; \begin{bmatrix} w_1 \\ w_2 \end{bmatrix} \tag{2.2.13}$$

The space-time codeword formed at the two relays has the following form:

$$X = \begin{bmatrix} x_1 & -x_2^* \\ x_2 & x_1^* \end{bmatrix} \tag{2.2.14}$$

It is clear that, the space-time code in (2.2.14) is the transpose of the Alamouti structure. By defining $\mathbf{x} = [x_1 \quad -x_2^*]^T$, the Alamouti code is obtained which has the structure

$$X = \begin{bmatrix} x_1 & x_2 \\ -x_2^* & x_1^* \end{bmatrix} \tag{2.2.15}$$

2.2.1.2 Quasi-orthogonal designs

In relay networks with four relays, quasi-orthogonal designs can be used. For $T_s = R = 4$, the design matrices A_i and B_i at the relays are defined as [39]

$$A_1 = I_4,\ A_2 = 0_4,\ A_3 = 0_4,\ A_4 = \begin{bmatrix} 0 & 0 & 0 & 1 \\ 0 & 0 & -1 & 0 \\ 0 & -1 & 0 & 0 \\ 1 & 0 & 0 & 0 \end{bmatrix}$$

$$B_1 = 0_4,\ B_2 = \begin{bmatrix} 0 & -1 & 0 & 0 \\ 1 & 0 & 0 & 0 \\ 0 & 0 & 0 & -1 \\ 0 & 0 & 1 & 0 \end{bmatrix},\ B_3 = \begin{bmatrix} 0 & 0 & -1 & 0 \\ 0 & 0 & 0 & -1 \\ 1 & 0 & 0 & 0 \\ 0 & 1 & 0 & 0 \end{bmatrix},\ B_4 = 0_4$$

Thus, the space-time codeword generated by the relays has the following form:

$$X = \begin{bmatrix} x_1 & -x_2^* & -x_3^* & x_4 \\ x_2 & x_1^* & -x_4^* & -x_3 \\ x_3 & -x_4^* & x_1^* & -x_2 \\ x_4 & x_3^* & x_2^* & x_1 \end{bmatrix} \tag{2.2.16}$$

By defining $\mathbf{x} = [x_1 \quad -x_2^* \quad -x_3^* \quad x_4]^T$, the original form of the quasi-orthogonal codes in [6] can be designed, which has the structure

$$X = \begin{bmatrix} x_1 & x_2 & x_3 & x_4 \\ -x_2^* & x_1^* & -x_4^* & x_3^* \\ -x_3^* & -x_4^* & x_1^* & x_2^* \\ x_4 & -x_3 & -x_2 & x_1 \end{bmatrix}$$

2.2.1.3 The general distributed linear dispersion code

In this section, the general type of distributed linear dispersion space-time code is described [63]. At the i-th relay, the transmitted signal is designed

in (2.2.2) as

$$t_i = \sqrt{\frac{P_2}{P_1+1}}(A_i \mathbf{r}_i + B_i \mathbf{r}_i^*), \quad \text{where} \;\; i = 1, 2, ..., R \tag{2.2.17}$$

The real and imaginary parts in (2.2.17) are separated as

$$\begin{bmatrix} t_{i,\mathrm{R}_e} \\ t_{i,\mathrm{I}_m} \end{bmatrix} = \sqrt{\frac{P_2}{P_1+1}} \begin{bmatrix} A_{i,\mathrm{R}_e} + B_{i,\mathrm{R}_e} & -A_{i,\mathrm{I}_m} + B_{i,\mathrm{I}_m} \\ A_{i,\mathrm{I}_m} + B_{i,\mathrm{I}_m} & A_{i,\mathrm{R}_e} - B_{i,\mathrm{R}_e} \end{bmatrix} \begin{bmatrix} r_{i,\mathrm{R}_e} \\ r_{i,\mathrm{I}_m} \end{bmatrix} \tag{2.2.18}$$

where R_e and I_m denote the real and imaginary parts for a complex number respectively. It is assumed that the $2T_s \times 2T_s$ matrix,

$$\begin{bmatrix} A_{i,\mathrm{R}_e} + B_{i,\mathrm{R}_e} & -A_{i,\mathrm{I}_m} + B_{i,\mathrm{I}_m} \\ A_{i,\mathrm{I}_m} + B_{i,\mathrm{I}_m} & A_{i,\mathrm{R}_e} - B_{i,\mathrm{R}_e} \end{bmatrix}$$

is orthogonal. Thus at the relays, the transmit power per transmission is P_2. The equivalent equation for the system can be written as [62]:

$$\hat{\mathbf{x}} = \sqrt{\frac{P_1 P_2 T_s}{P_1+1}} \mathrm{H}\, \hat{\mathbf{s}} + \;\mathbf{w}, \tag{2.2.19}$$

where H and $\mathbf{w}$ denote the equivalent channel matrix and noise vector respectively and they can be generated from:

$$\mathrm{H} = \sum_{i=1}^{N} \begin{bmatrix} h_{r_i,d,\mathrm{R}_e} I_{T_s} & -h_{r_i,d,\mathrm{I}_m} I_{T_s} \\ h_{r_i,d,\mathrm{I}_m} I_{T_s} & h_{r_i,d,\mathrm{R}_e} I_{T_s} \end{bmatrix} \begin{bmatrix} A_{i,\mathrm{R}_e} + B_{i,\mathrm{R}_e} & -A_{i,\mathrm{I}_m} + B_{i,\mathrm{I}_m} \\ A_{i,\mathrm{I}_m} + B_{i,\mathrm{I}_m} & A_{i,\mathrm{R}_e} - B_{i,\mathrm{R}_e} \end{bmatrix} \begin{bmatrix} h_{s,r_i,\mathrm{R}_e} I_{T_s} & -h_{s,r_i,\mathrm{I}_m} I_{T_s} \\ h_{s,r_i,\mathrm{I}_m} I_T & h_{s,r_i,\mathrm{R}_e} I_{T_s} \end{bmatrix}$$

$$\mathbf{w} = \begin{bmatrix} \mathbf{w}_{\mathrm{R}_e} \\ \mathbf{w}_{\mathrm{I}_m} \end{bmatrix} + \sqrt{\frac{P_2}{P_1+1}} \sum_{i=1}^{R} \begin{bmatrix} h_{r_i,d,\mathrm{R}_e} I_{T_s} & -h_{r_i,d,\mathrm{I}_m} I_{T_s} \\ h_{r_i,d,\mathrm{I}_m} I_{T_s} & h_{r_i,d,\mathrm{R}_e} I_{T_s} \end{bmatrix} \begin{bmatrix} A_{i,\mathrm{R}_e} + B_{i,\mathrm{R}_e} & -A_{i,\mathrm{I}_m} + B_{i,\mathrm{I}_m} \\ A_{i,\mathrm{I}_m} + B_{i,\mathrm{I}_m} & A_{i,\mathrm{R}_e} - B_{i,\mathrm{R}_e} \end{bmatrix} \begin{bmatrix} \mathbf{v}_{\mathrm{R}_e} \\ \mathbf{v}_{\mathrm{I}_m} \end{bmatrix}$$

and $\hat{\mathbf{x}}$ is defined as

$$\begin{bmatrix} \mathbf{x}_{\mathrm{R}_e} \\ \mathbf{x}_{\mathrm{I}_m} \end{bmatrix}$$

2.2.1.4 Random orthogonal designs

To generate random orthogonal designs generate A_i and B_i such that the matrix [4]

$$\begin{bmatrix} \mathrm{R}_e(A_i + B_i) & -\mathrm{I}_m(A_i - B_i) \\ \mathrm{I}_m(A_i + B_i) & \mathrm{R}_e(A_i - B_i) \end{bmatrix} \tag{2.2.20}$$

is uniform in the space of orthogonal matrices, a Gaussian matrix of size $2T_s$ by $2T_s$ is firstly generated. Then use a QR decomposition of the matrix to obtain the orthogonal matrix Q, which is uniform on the space of orthogonal matrices. Then A and B are calculated from this $2T_s$ by $2T_s$ matrix using the formula given in (2.2.20). For example, the real part of A is the first block plus the 4-th block of the matrix and the imaginary part is built from the other two parts of the matrices. For each iteration, a new set of A and B is generated. Thus if

$$Q = \begin{bmatrix} Z_1 & Z_2 \\ Z_3 & Z_4 \end{bmatrix} \tag{2.2.21}$$

Then

$$Z_1 = \mathrm{R}_e(A_i + B_i) = \frac{(A_i + B_i) + (A_i + B_i)^*}{2}$$

$$Z_4 = \mathrm{R}_e(A_i - B_i) = \frac{(A_i - B_i) + (A_i - B_i)^*}{2}$$

Therefore

$$Z_1 + Z_4 = A_i + A_i^* = 2\mathrm{R}_e(A_i) \tag{2.2.22}$$

and

$$Z_1 - Z_4 = -2\mathrm{R}_e(B_i) \tag{2.2.23}$$

Now generating Z_2 and Z_3

$$Z_2 = -\mathrm{I}_m(A_i - B_i) = -\left[\frac{(A_i + B_i) - (A_i - B_i)^*}{2j}\right]$$

$$Z_3 = \mathrm{I}_m(A_i + B_i) = \frac{(A_i + B_i) - (A_i + B_i)^*}{2j}$$

Therefore

$$Z_2 + Z_3 = \frac{2B_i - 2B_i^*}{2j}$$

$$Z_2 + Z_3 = 2\ \mathrm{I}_m(B_i) \tag{2.2.24}$$

and

$$Z_2 - Z_3 = -2\ \mathrm{I}_m(A_i) \tag{2.2.25}$$

Thus A_i and B_i for random orthogonal designs can be generated from

$$A_i = A_{i,\mathrm{R}_e} + jA_{i,\mathrm{I}_m} \tag{2.2.26}$$

where

$$A_{i,\mathrm{R}_e} = \frac{Z_1 + Z_4}{2} \quad \text{and} \quad A_{i,\mathrm{I}_m} = \frac{Z_2 - Z_3}{-2}$$

and

$$B_i = B_{i,\mathrm{R}_e} + jB_{i,\mathrm{I}_m} \tag{2.2.27}$$

where

$$B_{i,\mathrm{R}_e} = \frac{Z_1 - Z_4}{2} \quad \text{and} \quad B_{i,\mathrm{I}_m} = \frac{Z_2 + Z_3}{-2}$$

In the next section, the codeword error rate performance of the distributed space-time block coding using two and four relays will be simulated.

2.2.2 Simulations

This section shows the simulated performance of the distributed space-time codes for different number of relays R, and the total transmit power P. It is assumed that the fading coefficients between the transmitter and the relays and between the relays and the receiver are independent complex Gaussian random variables with zero-mean and unit-variance. Figure 2.7 shows the

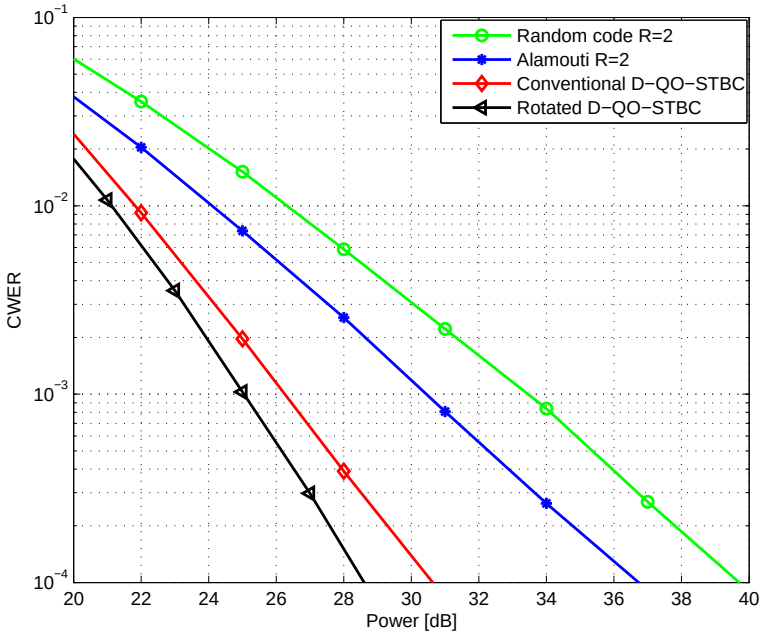

Figure 2.7. End-to-end CWER performance of relay networks with QPSK signal.

simulated codeword error rate (CWER) performance of orthogonal, quasi-orthogonal and random D-STBC using QPSK symbols. The figure indicates that the rotated quasi-orthogonal scheme with $R = 4$ has the best performance compared to others. For example, at codeword error probability of 10^{-3} the rotated D-QO-STBC is approximately 9 dB, 6 dB, and 1.5 dB better than the random, Alamouti D-STBC and contentional QO-D-STBC respectively. The figure also shows that the Alamouti D-STBC is approximately 3 dB better than the random D-STBC at high transmit powers at codeword error probability of 10^{-3}. Furthermore, it can be seen that the

CWER curve of Alamouti and quasi-orthogonal D-STBC decreases faster than that of the random D-STBC.

2.3 Modified quasi-orthogonal space-time block codes

Quasi-orthogonal space-time codes (QO-STCs) [40] were designed to increase the symbol transmission rate. However, QO-STC could not achieve full diversity. To overcome this problem, a pairwise constellation rotation was proposed in [41] [42]. In [43] a new code was designed from modified quasi-orthogonal codes by applying appropriate signal rotations to either of the two parts of the quasi-orthogonal code and then by combining these modified quasi-orthogonal codes and pruning codewords from the combined code. These codewords were chosen from the union of two modified quasi-orthogonal codes and the pruning is achieved by a set partitioning algorithm applied to each of the constituent quasi-orthogonal codes. This set partitioning is inspired by the techniques first proposed in [56] and further enhanced by the authors in [64]. The first method is specifically for the QO space-time code and the second one is the general space-time code set partitioning method as will be considered in the next section.

2.3.1 Set partitioning

A set partitioning approach for BPSK and QPSK symbols for four transmit antennas is to be considered in this section. The purpose of the set partitioning is to design a code that maximizes the code gain distance (CGD). The complexity of the exhaustive search required to design the code varies with the fourth power of the constellation cardinality. The algorithm in [56] reduces the complexity by designing the set partitioning of L-PSK depending on $\frac{L}{2}$-PSK where L is even and the rotation is $\phi = \frac{L}{2}$. It is assumed that x_1, x_2, x_3 and x_4 are symbols from an L-PSK constellation and x_1 and

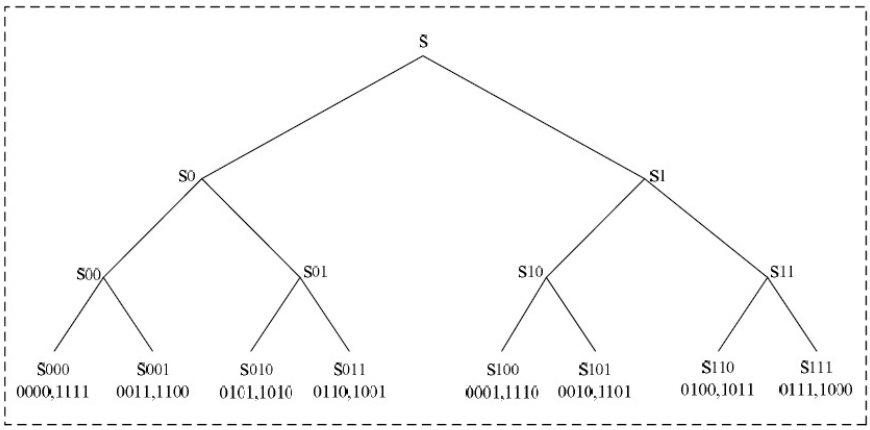

Figure 2.8. Set Partitioning Tree for BPSK.

x_2 are rotated by $\frac{\pi}{L}$ to derive $\hat{x_1}$ and $\hat{x_2}$ and it is the same if x_3 and x_4 are rotated instead of x_1 and x_2 to give a similar result [56]. Figure 2.8 shows the set partitioning tree for BPSK; the CGD between different codewords increases from the root to the leaves of the set-partitioning tree and it can be explained as

1. The codewords in branches s_1 and s_0 differ in one bit, for example the two codewords 0000 and 0001 differ in one symbol.

2. The codewords between s_{00}, s_{01} s_{10}, s_{11} differ in two symbols that belong to constellations with different rotations and it can be seen in x_2 and x_4 in the codewords 0000 and 0101.

3. The codewords between $s_{000}, s_{001}, s_{010}, s_{011}, s_{100}, s_{101}, s_{110}, s_{111}$ differ in two symbols from the same constellation, for example x_3 and x_4 in 0000 and 0011.

4. At the end, the codewords at the leaves differ in 4 symbols, which is clear in the codewords 0000 and 1111.

This gives the following 16 codewords for four antennas:

Table 2.1 shows an example for set partitioning for BPSK. The values 0,1

0000	0011	0101	0110	0001	0010	0100	0111
1111	1100	1010	1001	1110	1101	1011	1000

Table 2.1. Set Partitioning for BPSK.

represent 1, -1, respectively, the angle $\frac{\pi}{2}$ is the optimum rotation for quasi-orthogonal space-time block coding using BPSK, also 0, 1 represent $j, -j$ respectively after applying the rotation angle for the third and fourth symbols [56]. In the QPSK (where $L = 4$) constellation for four transmit antennas, all the combinations are found between 0 and $\frac{L}{2}$ as shown in Table 2.2, which is constructed from the leaves of the tree shown in Figure 2.9. Then every codeword in the original set partitioning of BPSK shown in

0000 2222	0020 2202
2200 0022	0002 2220
2020 0202	0200 2022
2002 0220	2000 0222

Table 2.2. The combinations between 0 and 2.

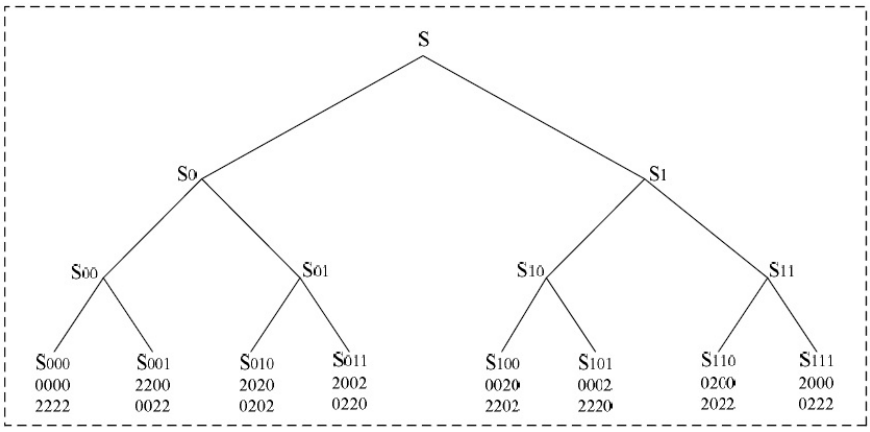

Figure 2.9. Subsets created by the combination of 0 and L/2.

Table 2.1 is added to the combinations in Table 2.2 to get $16 \times 16 = 256$

codewords for QPSK partitioning as shown in Table 2.3. The angle $\frac{\pi}{4}$ is picked for QPSK since it is the optimum rotation angle [56]. To maximize CGD, the subsets $S_{00\ 001}$ and $S_{00\ 010}$ which are derived from Figure 2.9 are switched, as shown in Table 2.3. Similarly, the other subsets are switched as $S_{00\ 101}$ with $S_{00\ 110}$, $S_{01\ 001}$ with $S_{01\ 010}$ and $S_{01\ 101}$ with $S_{01\ 110}$ to increase the CGD. Corresponding subsets rooted in set S_1 have been switched to achieve the set partitioning in Table 2.3. Figures 2.10 and 2.11 show

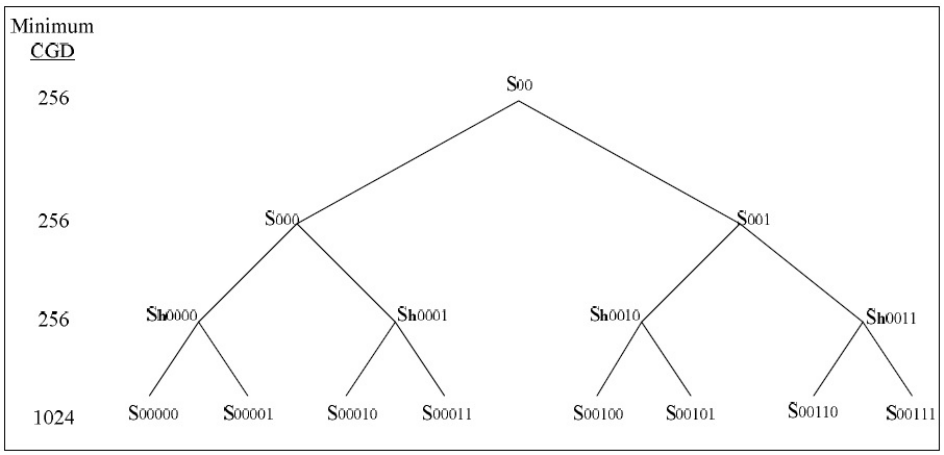

Figure 2.10. Subtree of set partitioning for QPSK based on Figure 2.9.

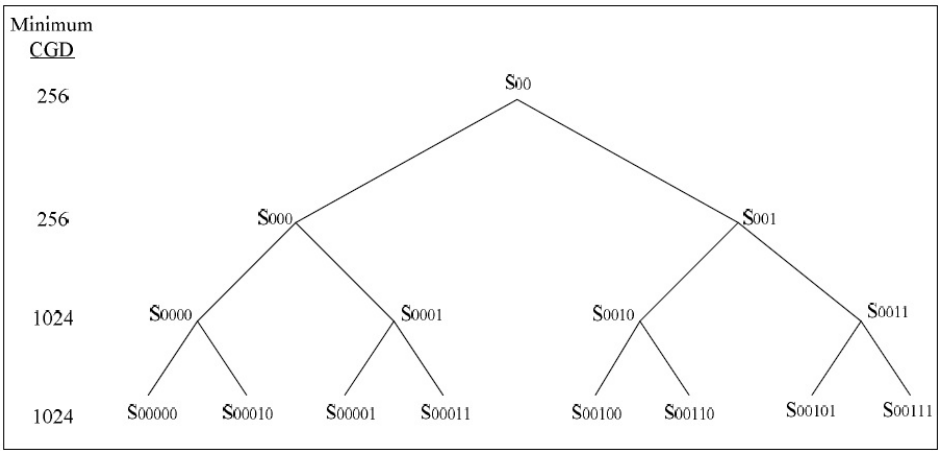

Figure 2.11. Subtree of set partitioning for QPSK after switching some of the subsets.

an example of such a switching. Using the splitting in Figure 2.9 for S_{00} results in the set partitioning in Figure 2.10. From this figure, it can be seen

Table 2.3. Set Partitioning for QPSK.

S															
S_0								S_1							
S_{00}				S_{01}				S_{10}				S_{11}			
S_{000}		S_{001}		S_{010}		S_{011}		S_{100}		S_{101}		S_{110}		S_{111}	
S_{0000}	S_{0001}	S_{0010}	S_{0011}	S_{0100}	S_{0101}	S_{0110}	S_{0111}	S_{1000}	S_{1001}	S_{1010}	S_{1011}	S_{1100}	S_{1101}	S_{1110}	S_{1111}
0000	0020	1100	1120	0101	0121	1001	1021	0001	0021	1101	1121	0100	0120	1000	1020
2222	2202	3322	3302	2323	2303	3223	3203	2223	2203	3323	3303	2322	2302	3222	3202
2200	0002	3300	1102	2301	0103	3201	1003	2201	0003	3301	1103	2300	0102	3200	1002
0022	2220	1122	3320	0123	2321	1023	3221	0023	2221	1123	3321	0122	2320	1022	3220
****	****	****	****	****	****	****	****	****	****	****	****	****	****	****	****
2020	0200	3120	1300	0321	2101	3021	1201	2021	0201	3121	1301	0320	2100	3020	1200
0202	2022	1302	3122	2103	0323	1203	3023	0203	2023	1303	3123	2102	0322	1202	3022
2002	2000	3102	3100	0303	0301	3003	3001	2003	2001	3103	3101	0302	0300	3002	3000
0220	0222	1320	1322	2121	2123	1221	1223	0221	0223	1321	1323	2120	2122	1220	1222
****	****	****	****	****	****	****	****	****	****	****	****	****	****	****	****
1111	1131	0011	0031	1010	1012	0110	0112	1110	1130	0010	0030	1011	1013	0111	0113
3333	3313	2233	2213	3232	3230	2332	2330	3332	3312	2232	2212	3233	3231	2333	2331
3311	1113	2211	0013	3210	1030	2310	0130	3310	1112	2210	0012	3211	1031	2311	0131
1133	3331	0033	2231	1032	3212	0132	2312	1132	3330	0032	2230	1033	3213	0133	2313
****	****	****	****	****	****	****	****	****	****	****	****	****	****	****	****
3131	1311	2031	0211	3012	1210	0312	2110	3130	1310	2030	0210	3013	1211	0313	2111
1313	3133	0213	2033	1230	3032	2130	0332	1312	3132	0212	2032	1231	3033	2131	0333
3113	3111	2013	2011	3030	3010	0330	0310	3112	3110	2012	2010	3031	3011	0331	0311
1331	1333	0231	0233	1212	1232	2112	2132	1330	1332	0230	0232	1213	1233	2113	2133

that the minimum CGD for subsets S_{h0000}, S_{h0001}, S_{h0010} and S_{h0011} is 256, by switching $S_{00\ 001}$ with $S_{00\ 010}$ and $S_{00\ 101}$ with $S_{00\ 110}$ as in Figure 2.11, the minimum CGD for subsets S_{0000}, S_{0001}, S_{0010} and S_{0011} is 1024, which is increased. Finally, this partitioning is going to be used in this thesis in terms of QO-STBC, all the codewords which are under S_0 are one set and the codewords which are under S_1 are the second set. The modified quasi-orthogonal STBC will be discussed in more details in Chapter 3. The next section will be the summary of the chapter.

2.4 Summary

In this chapter, orthogonal and quasi-orthogonal STBCs have been investigated, simulated and the performances of the Alamouti scheme with perfect channel evaluation has been considered as well as the non rotated, rotated and closed-loop quasi-orthogonal STBC. It was shown that the Alamouti code provides two important properties, firstly, the code provides the maximum possible diversity and secondly, the simple decoding where each symbol is decoded separately using a linear processing. It was also shown that QO-STBC was constructed to increase the symbol transmission rate but the diversity is relaxed. This QO-STBC could achieve the full diversity by using different constellations for the two components of the quasi-orthogonal code, by rotating two symbols before transmission. The resulting rotated QO code provided full diversity, rate of one symbol per transmission, and pairwise decoding with good performance. On the other hand, the closed-loop QO-STBC achieved full diversity, rate of one symbol per transmission together with simple decoding. Furthermore, the chapter discussed the expanding wireless network coverage with the use of cooperative relay networks and it gave a brief overview of cooperative wireless networks concepts relevant to this thesis. Finally, this chapter described the modified QO-STBC and showed that the set partitioning method could be used to increase the code gain distance. In the next chapter, the modified quasi-orthogonal STBC will be discussed in more detail and used in cooperative networks by increasing the code gain distance.

Chapter 3

MODIFIED DISTRIBUTED QUASI-ORTHOGONAL SPACE-TIME BLOCK CODES FOR ONE-WAY AND TWO-WAY TRANSMISSION

This chapter investigates wireless relay networks for one-way and two-way communications through four relay nodes based on modified quasi-orthogonal space time block codes (M-QO-STBCs). The relay nodes form a modified distributed quasi-orthogonal space time block code (M-D-QO-STBC) and assist the communication between source and destination nodes. Firstly, the proposed M-D-QO-STBC for one-way relay network is considered and compared with the proposed closed-loop D-QO-STBC and the rotated open loop D-QO-STBC. This is followed by a consideration of two-way communication over four relay nodes based on a M-QO-STBC to achieve full data rate. Finally, simulation results to demonstrate the performance of the schemes are presented.

3.1 Introduction

Recently, the concept of distributed MIMO has been proposed to exploit spatial diversity by allowing simple single antenna nodes to cooperate. Distributed space-time block coding (D-STBC), when designed for two relay nodes using the Alamouti code [38], achieves half data rate and full diversity. However, the authors in [49] and [40] proposed STBC from a quasi-orthogonal (QO) design where the orthogonality is relaxed to provide higher symbol transmission rate. With the QO design the rank of the QO-STBC matrix is two, therefore, for M_r receive antennas, a diversity of $2M_r$ is achieved [8]. The maximum diversity of $4M_r$ for a complex orthogonal code is impossible in this case if all symbols are chosen from the same constellation. Improved QO-STBCs can be achieved by using different constellations for different symbols. For example, in [39] the third and fourth symbols are rotated before transmission, and it is shown that it is possible to provide full diversity for distributed QO-STBCs (D-QO-STBCs). In this chapter the performance of D-QO-STBCs based on an amplify-and-forward (AF) type protocol for one-way transmission is further improved by using a modified code. This modified code is obtained by expanding the codebook of conventional QO-STBC then pruning is applied to maximize the distance property of the code [43]. The pruning is achieved by a set partitioning algorithm applied to each of the constituent quasi-orthogonal codes. This set partitioning is inspired by the techniques first proposed in [56] and further enhanced by the authors in [64].

Cooperative strategy type space-time coding for one-way wireless networks achieves only half transmission rate; in order to achieve full unity rate, a two-way (TW) communication for AF wireless relay networks scheme is considered in this chapter. In this scheme two parties transmit information to each other which was considered first by Shannon [65]. Recently, academic

and industrial communities have started considering the TW channel over a relay network due to its potential application to enable range and rate enhancements of future cellular systems [66], [67] and [68]. Distributed rotated open and closed-loop QO-STBC for two-way wireless relay networks were considered in [69] where full rate and full cooperative diversity were achieved. In this chapter the performance of the TW scheme is improved by implementing the proposed modified code in the system. In addition a genetic algorithm technique is used to search for the optimum rotation matrix to maximize the distance property for the codes to improve the performance of the modified code.

3.2 Modified distributed quasi-orthogonal space-time block codes for one-way wireless relay networks

In this section, a modified distributed quasi-orthogonal space-time block code (M-D-QO-STBC) for one-way transmission for quasi-static flat fading channels is proposed where the information is sent from the source to the destination assisted by four relay nodes. The simulation results show that the proposed scheme provides improved codeword-error rate (CWER) performance than the earlier scheme represented in [39].

3.2.1 System model

Figure 3.1 depicts a wireless relay network with one transmit node $\mathrm{T_x}$, one receive node $\mathrm{R_x}$ and all the other nodes operate as relays R_i where $i = 1, 2, 3, 4$. Each node has one antenna for either transmission or reception. The channel from the transmitter to the i-th relay and from the i-th relay to the receiver are denoted by h_{s,r_i} and $h_{r_i,d}$ respectively. It is assumed that these channels are quasi-static independent Rayleigh flat fading and there is no channel information at the relays, but the receiver has perfect

channel information h_{s,r_i} and $h_{r_i,d}$. At the transmitter, the information bits

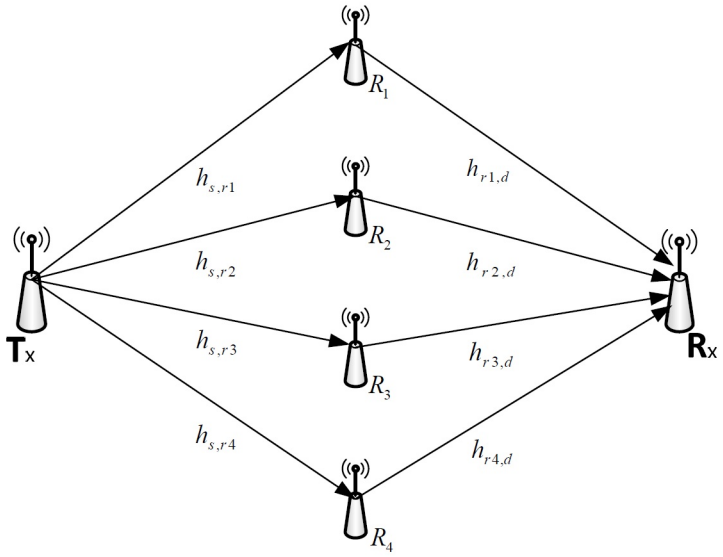

Figure 3.1. Two hop one-way wireless four relay network.

are encoded into symbols $\mathbf{x} = [x_1, ..., x_{T_s}]^T$ where $(.)^T$ denotes the transpose and T_s is the time slot length and $\mathbf{x}$ is normalized to be $E\{\mathbf{x}^H\mathbf{x}\} = 1$ [39] where $(.)^H$ and $E\{.\}$ denote the Hermitian operator and the expectation of a random variable respectively. The transmission operation involves a two-step protocol, in step one the transmitter sends signals $\sqrt{P_1 T_s}\mathbf{x}$ to each relay at time 1 to T_s where P_1 is the average power used at the transmitter for every transmission. Therefore, the received signal at the i-th relay is corrupted by fading h_{s,r_i} and the noise vector $\mathbf{v}_i$ and is given by

$$\mathbf{s}_i = \sqrt{P_1 T_s} h_{s,r_i}\mathbf{x} + \mathbf{v}_i \tag{3.2.1}$$

In step two each relay amplifies and transmits its received signal to the destination. The received signal at the destination is given by

$$\mathbf{r} = \sum_{i=1}^{4} h_{r_i,d}\mathbf{t}_i + \mathbf{w}_r \tag{3.2.2}$$

where $\mathbf{w}_r$ is the noise vector at the receiver and $\mathbf{t}_i$ is the transmitted signal from the i-th relay node which is generated from

$$\begin{aligned}\mathbf{t}_i &= \sqrt{\frac{P_2}{P_1+1}}(A_i\mathbf{s}_i + B_i\mathbf{s}_i^*) \\ &= \sqrt{\frac{P_1P_2T_s}{P_1+1}}(h_{s,r_i}A_i\mathbf{x} + h_{s,r_i}^*B_i\mathbf{x}^*) + \sqrt{\frac{P_2}{P_1+1}}(A_i\mathbf{v}_i + B_i\mathbf{v}_i^*)\end{aligned} \tag{3.2.3}$$

where A_i and B_i are the matrices used at the relays to distribute the signals and P_2 denotes the average transmission power at every relay node. The special case that either $A_i = 0$, B_i is unitary or $B_i = 0$ and A_i is unitary is considered in this work. Define as in [39]

$$\hat{A}_i = A_i, \quad \hat{h}_{s,r_i} = h_{s,r_i}, \quad \hat{\mathbf{v}}_\mathbf{i} = \mathbf{v}_\mathbf{i}, \quad \mathbf{x}^{(i)} = \mathbf{x}, \qquad \text{if } B_i = 0$$

$$\hat{A}_i = B_i, \quad \hat{h}_{s,r_i} = h_{s,r_i}^*, \quad \hat{\mathbf{v}}_\mathbf{i} = \mathbf{v}_i^*, \quad \mathbf{x}^{(i)} = \mathbf{x}^*, \qquad \text{if } A_i = 0$$

From (3.2.3)

$$\mathbf{t_i} = \sqrt{\frac{P_1P_2T_s}{P_1+1}}\hat{h}_{s,r_i}\hat{A}\mathbf{x^{(i)}} + \sqrt{\frac{P_2}{P_1+1}}\hat{A}_i\hat{\mathbf{v}}_\mathbf{i}$$

The signal at the receiver can be calculated from (3.2.2) following the approach in [39]

$$\mathbf{r} = \sqrt{\frac{P_1P_2T_s}{P_1+1}}X\mathbf{h} + \mathbf{w} \tag{3.2.4}$$

where

$$X = [\hat{A}_1\mathbf{x}^{(1)} \ ... \ \hat{A}_4\mathbf{x}^{(4)}], \tag{3.2.5}$$

$$\mathbf{h} = [\hat{h}_{s,r_1}h_{r_1,d} \ ... \ \hat{h}_{s,r_4}h_{r_4,d}]^T \tag{3.2.6}$$

and

$$\mathbf{w} = \sqrt{\frac{P_2}{P_1+1}}\sum_{i=1}^{4} h_{r_i,d}\hat{A}_i\hat{\mathbf{v}}_i + \mathbf{w}_r \tag{3.2.7}$$

Therefore, the relays calculate a space-time codeword X distributively at the receiver; $\mathbf{w}$ is the equivalent noise vector at the receiver and $\mathbf{h}$ is the

equivalent channel vector. The optimum power allocation to minimize end-to-end codeword-error rate CWER is when the transmitter uses half the total power and the relays share the other half [62]. Therefore, if the total power is P and the number of relays R then

$$P_1 = \frac{P}{2} \quad \text{and} \quad \mathrm{P}_2 = \frac{\mathrm{P}}{2\mathrm{R}} \tag{3.2.8}$$

If the channel vector $\mathbf{h}$ is known at the receiver, the maximum-likelihood (ML) decoding can be used to detect the received vector as

$$\arg \min_{\hat{S}\epsilon S} \left\| \mathbf{r} - \sqrt{\frac{P_1 P_2 T_s}{P_1 + 1}}\ \hat{S}\ \mathbf{h} \right\| \tag{3.2.9}$$

where $\|.\|$ represents Euclidean norm and $\hat{S}$ is the possible code matrices which depend on the particular constellation employed.

3.2.2 Modified code design for one-way transmission

The design of A_i and B_i which give the quasi-orthogonal code are

$$A_1 = I_4,\ A_2 = A_4 = 0_4,\ A_3 = \begin{bmatrix} 0 & 0 & 1 & 0 \\ 0 & 0 & 0 & 1 \\ 1 & 0 & 0 & 0 \\ 0 & 1 & 0 & 0 \end{bmatrix}$$

$$B_1 = B_3 = 0_4 \tag{3.2.10}$$

$$B_2 = \begin{bmatrix} 0 & -1 & 0 & 0 \\ 1 & 0 & 0 & 0 \\ 0 & 0 & 0 & -1 \\ 0 & 0 & 1 & 0 \end{bmatrix},\ B_4 = \begin{bmatrix} 0 & 0 & 0 & -1 \\ 0 & 0 & 1 & 0 \\ 0 & -1 & 0 & 0 \\ 1 & 0 & 0 & 0 \end{bmatrix}$$

The matrix 0_4 indicates a 4×4 matrix with all zero elements. The rotation using modified D-STBCs is applied either on the first pair or the second pair

of symbols [43], thus the codeword is:

$$X(\Phi_1,\Phi_2)=\begin{bmatrix} x_1e^{j\Phi_1} & x_2e^{j\Phi_1} & x_3e^{j\Phi_2} & x_4e^{j\Phi_2} \\ -x_2^*e^{-j\Phi_1} & x_1^*e^{-j\Phi_1} & -x_4^*e^{-j\Phi_2} & x_3^*e^{-j\Phi_2} \\ x_3e^{j\Phi_2} & x_4e^{j\Phi_2} & x_1e^{j\Phi_1} & x_2e^{j\Phi_1} \\ -x_4^*e^{-j\Phi_2} & x_3^*e^{-j\Phi_2} & -x_2^*e^{-j\Phi_1} & x_1^*e^{-j\Phi_1} \end{bmatrix} \tag{3.2.11}$$

where $x_1,\ x_2,\ x_3$, and x_4 are symbols from the constellation and Φ_1 and Φ_2 are the rotation angles. The matrices $X(\Phi_1, \Phi_2)$ consist of a whole quasi-orthogonal codebook. By changing (Φ_1, Φ_2) a family of codebooks can be generated, for BPSK modulation $\Phi_1 = \Phi_2 = \frac{\pi}{2}$ [43]. At the beginning, the union of two quasi-orthogonal codebooks, $\mathbb{T} \cup \mathbb{S}$ is taken, where $\mathbb{S} = X(\frac{\pi}{2}, 0)$ and $\mathbb{T} = X(0, \frac{\pi}{2})$. Given that $\mathbb{T} \cup \mathbb{S}$ has twice as many codewords the union is pruned down by one-half to get the new code $\mathbb{C}$, which has the original rate. The performance of the modified codebook $\mathbb{C}$ is bounded below by the performance of quasi-orthogonal codes $\mathbb{S}$ and $\mathbb{T}$, because each of them is one possible pruning of $\mathbb{S} \cup \mathbb{T}$. Therefore, the process can only improve the code. Firstly, the codebooks $\mathbb{S}$ and $\mathbb{T}$ are partitioned such that each partition has good distance properties, then $\mathbb{C}$ is constructed by combining these partitions [43]. For instance, for the BPSK case, firstly, $X(0, \frac{\pi}{2})$ is set to generate 16 possible matrices which is S, then all the 16 matrices are presented by their binary values. For the second set $\mathbb{T}$, $X(\frac{\pi}{2}, 0)$ is taken to generate another 16 matrices, so the total number of matrices which is generated in $\mathbb{T} \cup \mathbb{S}$ is 32 matrices. Since $\mathbb{T} \cup \mathbb{S}$ has twice as many codewords, the first 16 matrices are taken from the first set and divided as in [43] into:

$$\mathbb{S}_1 = \{0000, 0011, 0101, 0110, 1001, 1010, 1100, 1111\}$$

$$\mathbb{S}_2 = \{0001, 0010, 0100, 0111, 1000, 1011, 1101, 1110\}$$

now there is a new codeset $\mathbb{S}_1$, which is made from 8 codewords, each codeword is represented by its four binary symbols (x_1, x_2, x_3, x_4). The same steps are taken for the second set to obtain $\mathbb{T}_1$ and $\mathbb{T}_2$. The new codebook $\mathbb{C} = \mathbb{S}_1 \cup \mathbb{T}_2$.

3.2.3 Code gain distance

The inter-distance of the subcodes can be generated in a mannar similar to [70]. Thus for two possible codewords X and Y the code gain distance $\mathrm{CGD} = \det(\Pi)$ where as in [43]

$$\Pi = ((X - Y)(X - Y)^H).$$

The minimum CGD of the codebook $\mathbb{S}$ is defined as the minimum CGD of all non identical codeword pairs of $(\mathbb{S} \times \mathbb{S})$, therefore the distance between two codebooks $\mathbb{S}$ and $\mathbb{T}$ is given by

$$\mathrm{D}(\mathbb{S}, \mathbb{T}) = \det(\Pi(X, Y)) \tag{3.2.12}$$

The minimum CGD of $\mathbb{S}$ and $\mathbb{T}$ as given in [43] is

$$D(\mathbb{S}_1, \mathbb{S}_2) = D(\mathbb{T}_1, \mathbb{T}_2) = 256 \tag{3.2.13}$$

and for $\mathbb{S}_1$ and $\mathbb{T}_2$ is

$$D(\mathbb{S}_1, \mathbb{T}_2) = 2304 \tag{3.2.14}$$

It is clear that the distance of the new code is increased, in particular the new codebook is built from $\mathbb{S}_1 \cup \mathbb{T}_2$ which has higher distance and thereby yields better performance. For higher rate codes the distance properties of the code can be generated and for QPSK modulation as in [43]

$$itisD(\mathbb{S}_1, \mathbb{T}_2) = 2.22 \tag{3.2.15}$$

It seems to be that the distance properties of the code should be increased to give better performance. In order to achieve that a unitary matrix $\mathbf{U}$ has been used [43]. By multiplying the codeword $\mathbb{T}_2$ by the unitary matrix as in [43]

$$\max_{\mathbf{U}} D(\mathbb{S}_1, \mathbb{T}_2\mathbf{U}) \tag{3.2.16}$$

where $\mathbf{U}$ =diag$(e^{j\theta_1}, e^{j\theta_2}, e^{j\theta_3}, e^{j\theta_4})$ and diag(.) denotes diagonal matrix. For a QPSK constellation $\mathbf{U} = \text{diag}(e^{j0.9\pi}, e^{j1.1\pi}, e^{j1.6\pi}, e^{j0.4\pi})$ and $\Phi_1 = \Phi_2 = \frac{\pi}{4}$, thus, a new distance can be calculated as in [43]

$$tobe D(\mathbb{S}_1, \mathbb{T}_2) = 43.94 \tag{3.2.17}$$

and therefore the minimum distance of the code is increased which will give better performance. Therefore, the first part of the work in this chapter is implementing the M-D-QO-STBC scheme in the proposed wireless relay network for one-way transmission. A full maximum likelihood decoder (MLD) over the new codebook has been used in this work. For comparison purposes, distributed closed-loop QO-STBC is proposed.

3.3 Distributed closed-loop quasi-orthogonal STBC for one-way transmission

A distributed closed-loop QO-STBC for a wireless relay network is depicted in Figure 3.2. It is assumed that the source node is T_x, the destination node is R_x, the relay nodes are R_1, R_2, R_3 and R_4 and there are two feedback paths. The Grammian matrix of the codeword in (3.2.11) without rotation

can be presented as

$$\Delta = \mathbf{H}^H\mathbf{H} = \begin{bmatrix} \beta_d & 0 & \beta & 0 \\ 0 & \beta_d & 0 & \beta \\ \beta & 0 & \beta_d & 0 \\ 0 & \beta & 0 & \beta_d \end{bmatrix} \tag{3.3.1}$$

where

$$\beta = 2R_e(h_{s,r_1}h_{r_1,d}h^*_{s,r_3}h^*_{r_3,d} - h_{s,r_2}h_{r_2,d}h^*_{s,r_4}h^*_{r_4,d}) \tag{3.3.2}$$

where $R_e\{.\}$ denotes the real part of a complex number. The nonzero off-

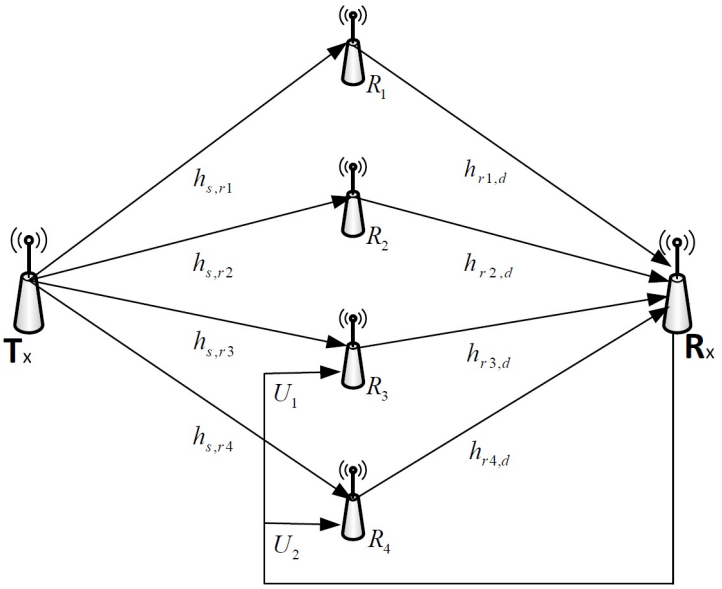

Figure 3.2. The proposed distributed one-way closed-loop QO-STBC system for four relay nodes with feedback to two nodes.

diagonal terms β_s which appear cause coupling between the estimated symbols, therefore, reducing the diversity gain of the code and the reason for using feedback to eliminate these off-diagonal elements. In this system, only partial channel information is fed back to two relays, each having different code processing, as it is enough to leverage the system gain to the maximum as shown in [51]. R_3 and R_4 are the two relays which are selected for

feedback in the system. The information t_{3j} and t_{4j} where $j = 1, ..., T_s$ are rotated by U_1 and U_2 before they are transmitted from the third and fourth relays [71], respectively, while the other two relays are kept unchanged. This is equivalent to multiplying the first term in (3.3.2) by U_1 and the second term by U_2 therefore

$$\beta = 2R_e(h_{s,r_1}h_{r_1,d}h^*_{s,r_3}h^*_{r_3,d}U_1 - h_{s,r_2}h_{r_2,d}h^*_{s,r_4}h^*_{r_4,d}U_2) \tag{3.3.3}$$

where $U_1 = e^{j\theta_1}$ and $U_2 = e^{j\theta_2}$. It is assumed that $\lambda_1 = h_{s,r_1}h_{r_1,d}h^*_{s,r_3}h^*_{r_3,d}$ and $\lambda_2 = h_{s,r_2}h_{r_2,d}h^*_{s,r_4}h^*_{r_4,d}$. Thus

$$\beta = |\lambda_1|cos(\theta_1 + \angle\lambda_1) - |\lambda_2|cos(\theta_2 + \angle\lambda_2) \tag{3.3.4}$$

where $|.|$ denotes the absolute value and $\angle$ denotes the angle ($arctan$) operators and by defining $\xi = arccos\frac{|\lambda_1|}{|\lambda_2|}$ the solutions can be represented as [51]

$$\theta_1 = arccos(\frac{|\lambda_2|}{|\lambda_1|}cos(\theta_2 + \angle\lambda_2)) - \angle\lambda_1 \tag{3.3.5}$$

where $\theta_2 \in [0, 2\pi]$ if $|\lambda_2| < |\lambda_1|$, or otherwise $\theta_2 \in [(\pi - \xi - \angle\lambda_2, \xi - \angle\lambda_2) \cup (2\pi - \xi - \angle\lambda_2, \pi + \xi - \angle\lambda_2)]$. The phase rotation on transmitted symbols is equivalent to rotating the phases of the corresponding channel coefficients. As a result, the received signals from the four relay nodes are

$$r_1 = t_{11}h_{r_1,d} + t_{21}h_{r_2,d} + t_{31}h_{r_3,d}U_1 + t_{41}h_{r_4,d}U_2 + w_1$$

$$r_2 = t_{12}h_{r_1,d} + t_{22}h_{r_2,d} + t_{32}h_{r_3,d}U_1 + t_{42}h_{r_4,d}U_2 + w_2$$

$$r_3 = t_{13}h_{r_1,d} + t_{23}h_{r_2,d} + t_{33}h_{r_3,d}U_1 + t_{43}h_{r_4,d}U_2 + w_3$$

$$r_4 = t_{14}h_{r_1,d} + t_{24}h_{r_2,d} + t_{34}h_{r_3,d}U_1 + t_{44}h_{r_4,d}U_2 + w_4$$

Therefore, the exact phase as feedback makes the channel matrix orthogonal and the matrix in (3.3.1) becomes

$$\Delta = \mathbf{H}^H\mathbf{H} = \begin{bmatrix} \beta_d & 0 & 0 & 0 \\ 0 & \beta_d & 0 & 0 \\ 0 & 0 & \beta_d & 0 \\ 0 & 0 & 0 & \beta_d \end{bmatrix} \tag{3.3.6}$$

where

$$\beta_d = |h_{s,r_1}h_{r_1,d}|^2 + |h_{s,r_2}h_{r_2,d}|^2 + |h_{s,r_3}h_{r_3,d}U_1|^2 + |h_{s,r_4}h_{r_4,d}U_2|^2$$

From the Grammian matrix in (3.3.6), it is evident that the closed-loop QO-STBC is orthogonal, which indicates that the information symbols can be detected separately with a simple ML decoder. Therefore, the detection vector $\mathbf{y} = [y_1 \;\; y_2 \;\; y_3 \;\; y_4]^T$ with the receive vector $\mathbf{r} = [r_1 \;\; r_2 \;\; r_3 \;\; r_4]^T$ can be calculated

Step 1: Linear transform

$$\begin{aligned} \mathbf{y} = [y_1 \;\; y_2 \;\; y_3 \;\; y_4]^T &= \mathbf{H}^H\mathbf{r} \\ &= (\sum_{i=1}^{2}|h_{s,r_i}h_{r_i,d}|^2 + \sum_{i=3}^{4}|U_{i-2}h_{s,r_i}h_{r_i,d}|^2)\ \mathbf{x} \\ &+ \mathbf{H}^H\mathbf{w} \end{aligned} \tag{3.3.7}$$

where

$$\mathbf{w} = \sum_{i=1}^{2}(\sqrt{\frac{P_2}{P_1+1}}h_{r_i,d}\hat{A}_i\hat{\mathbf{v}}_i) + \sum_{i=3}^{4}(\sqrt{\frac{P_2}{P_1+1}}h_{r_i,d}\hat{A}_i\hat{\mathbf{v}}_iU_{i-2}) + \mathbf{w}_r$$

Step 2: Least squares (LS) symbol wise detection

$$\hat{x_i} = arg\{\min_{x_i\in S_a}\left|y_i - \sqrt{\frac{P_1P_2T_s}{P_1+1}}\alpha x_i\right|^2\} \tag{3.3.8}$$

where S_a is the alphabet containing two symbols for BPSK. The performance of the scheme is next evaluated by simulation study.

3.4 Simulation results

MATLAB software is used in the simulations. All the schemes use BPSK and QPSK modulation, and have the same total transmit power. A comparison is made of the codeword error rate (CWER) performance of the proposed schemes with the earlier proposed schemes in D-QO-STBCs. It is assumed that four relay nodes are available in the proposed system, each relay node has a single antenna and there is no direct link between the transmitter and receiver. The channels are assumed to be Rayleigh flat fading and the real and imaginary parts of the channels and noise are generated by using the MATLAB function randn(). Figure 3.3 and Figure 3.4 illustrate the end-to-

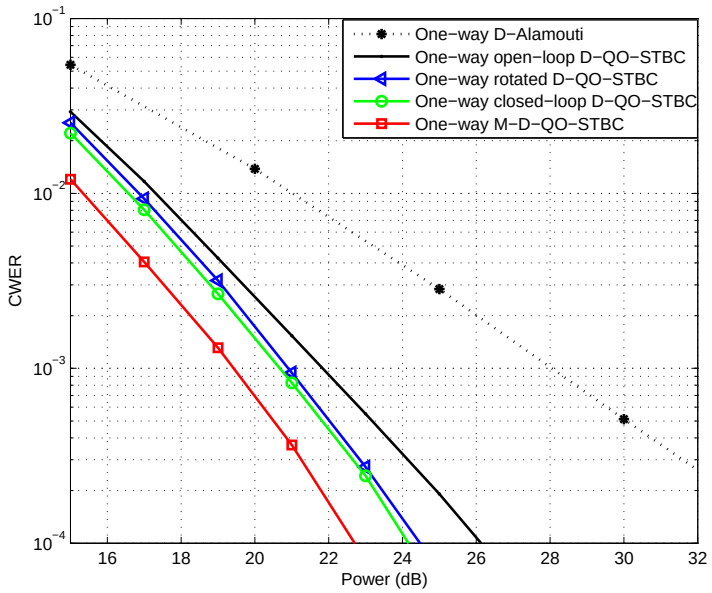

Figure 3.3. End-to-end CWER performance of relay networks with BPSK symbols

end CWER performance of the schemes versus the total transmitted power from the source node in dB. Due to the higher diversity gain of the QO-

STBCs, the gap between the D-QO codes and the distributed-Alamouti (D-Alamouti) increases for higher SNR values. This is due to the fact that the degree of diversity dictates the asymptotic slope of the CWER-SNR curve. The figures also show that the performance of both the proposed closed-loop D-STBC and the modified D-STBC is better than the performance of the rotated D-QO-STBC and D-Alamouti represented in [39]. This improvement of the two new proposed schemes is because both achieve the full cooperative diversity of order four, and the modified D-QO-STBCs provide an improved performance over all other schemes, due to the increase in the minimum distance properties of the original codebooks of the code. For example, in Figure 3.3, for the BPSK scheme, at a codeword error probability of 10^{-3}, the modified scheme provides a power saving of approximately 3.5 dB compared with open-loop D-QO-STBC in [40], approximately 2.5 dB compared with the rotated D-QO-STBC described in [39] and 1.5 dB compared with the proposed closed-loop D-STBC. On the other hand for the QPSK modulation the modified scheme provides a power saving of approximately 2.5 dB compared with open-loop D-QO-STBC in [40], approximately two dB compared with the one described in [39] and 1.5 dB compared with the proposed closed-loop D-QO-STBCs at a codeword error probability of 10^{-3}.

3.5 Modified distributed quasi-orthogonal space-time block coding for two-way wireless relay networks

In this section, a modified distributed quasi-orthogonal space-time block coding (M-D-QO-STBC) for two-way transmission for quasi-static flat fading channels is considered. In this scheme the information is exchanged between two terminals assisted by four relay nodes to achieve full data rate in every terminal at the same time. The simulation results show that the proposed scheme provides a significant CWER performance as compared to

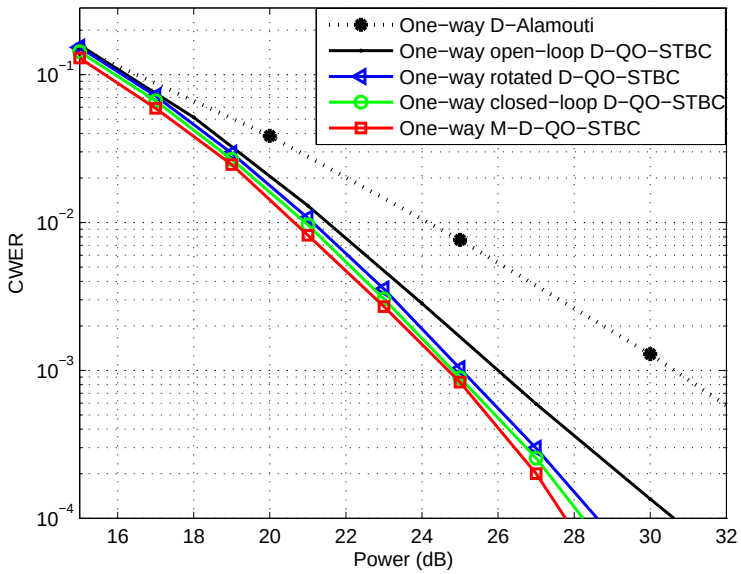

Figure 3.4. End-to-end CWER performance of relay networks with QPSK symbols

the distributed rotated open and closed-loop QO-STBC for two-way wireless relay networks considered in [69].

3.5.1 System model

The proposed wireless communication relay network is shown in Figure 3.5. It consists of two terminal nodes T_m, $m = 1, 2$ and four relay nodes R_i, $i = 1, ..., 4$. Each node has one half-duplex antenna for either transmission or reception. The channels from T_1 to R_i and from T_2 to R_i are denoted by f_i and g_i respectively and there is no direct link between T_1 and T_2 as path loss or shadowing is considered to render it unusable. It is assumed that the uplink channel gain from T_m to R_i is identical to the downlink channel gain from R_i to T_m and the communication channels and the noise are Rayleigh flat fading, f_i and g_i are independent and identical distributed (i.i.d.) with zero mean and unit variance $CN(0, 1)$. It is also assumed that there is no channel information at the relays but perfect channel information f_i and g_i is known at both terminals which in practice can be obtained by adapting

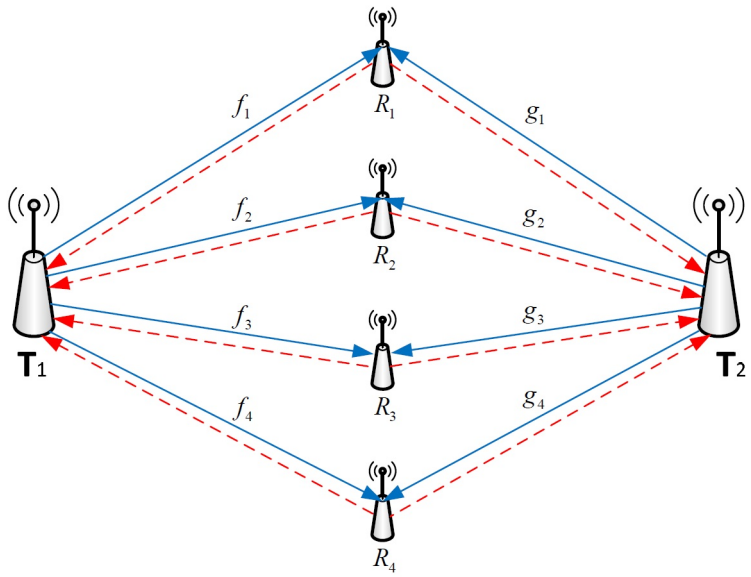

Figure 3.5. Basic structure of two-way wireless four-relay network where channels from the terminals to the relay nodes (solid) and from the relay nodes to the terminals (dashed).

the estimation algorithms in [72]. It is assumed that terminal T_m sends the signal $\mathbf{x}_m = [x_{m,1}, ..., x_{m,T_s}]^T$ to the other terminal, where $x_{m,t} \in \mathcal{C}_m$, $m = 1, 2$, $t = 1, ..., T_s$, $\mathcal{C}_m$ is a finite constellation with a unitary average power, and T_s is the length of the time slot. There is a two-step protocol for the transmission operation, in step one the two terminals T_m send the information $\sqrt{T_s P_{T_m}}\mathbf{x}$ where P_{T_m} is the average power used at the terminals at every transmission. If the total power is P then as defined in [39]

$$P_{T_1} = P_{T_2} = \frac{P}{4} \quad \text{and} \quad P_R = \frac{P}{2}$$

where P_R is the average power at the relay nodes. The received information at the i-th relay is corrupted by the fading f_i, g_i and the noise vector $\mathbf{v}_{r,i}$ and is given by

$$\mathbf{r}_i = \sqrt{T_s P_{T_1}} f_i \mathbf{x_1} + \sqrt{T_s P_{T_2}} g_i \mathbf{x_2} + \mathbf{v}_{r,i} \quad \text{for} \quad i = 1, ..., 4 \tag{3.5.1}$$

In step two, the i-th relay transmits its received signal to the terminals. An amplify-and-forward protocol is assumed in this system [39] therefore the signal at each relay is amplified before transmission. The transmit signal from the i-th relay is given by

$$\mathbf{t}_i = \digamma(A_i\mathbf{r}_i + B_i\mathbf{r}_i^*) \tag{3.5.2}$$

where A_i and B_i are unitary matrices that depend on the signal distributed at the relay nodes [39] and $\digamma$ is the amplification factor to maintain an average power P_R which can be calculated as [73]

$$\digamma = \sqrt{\frac{T_s P_R}{4(T_s P_{T_1} + T_s P_{T_2} + 1)}}$$

In this chapter, the special case when either $A_i = 0$ and B_i is unitary or A_i is unitary and $B_i = 0$ [39] is considered, therefore the conditions of the variables can be defined as

$$\hat{A}_i = A_i, \quad \hat{h}_{s,r_i} = h_{s,r_i}, \quad \hat{g}_i = h_{r_i,d}, \quad \hat{\mathbf{v}}_\mathbf{i} = \mathbf{v}_\mathbf{i}, \quad \mathbf{x}^{(\mathbf{i})} = \mathbf{x}, \qquad \text{if } B_i = 0$$

$$\hat{A}_i = B_i, \quad \hat{h}_{s,r_i} = h_{s,r_i}^*, \quad \hat{g}_i = h_{r_i,d}^*, \quad \hat{\mathbf{v}}_\mathbf{i} = \mathbf{v}_i^*, \quad \mathbf{x}^{(\mathbf{i})} = \mathbf{x}^*, \qquad \text{if } A_i = 0$$

If the noise terms at both terminals are denoted by $\mathbf{w}_{T_m}$, then the received signals at the terminals are given by

$$\mathbf{x}_{T_1} = \sum_{i=1}^{4} f_i\mathbf{t}_i + \mathbf{w}_{T_1} \tag{3.5.3}$$

$$\mathbf{x}_{T_2} = \sum_{i=1}^{4} g_i\mathbf{t}_i + \mathbf{w}_{T_2} \tag{3.5.4}$$

The noise vector terms $\mathbf{v}_i$ at the i-th relay and $\mathbf{w}_{T_m}$ at the terminals are assumed to have elements which are independent complex Gaussian random variables with zero-mean and unit-variance. Equations (3.5.3) and (3.5.4)

can be rewritten as

$$\mathbf{x}_{T_1} = F(\sqrt{T_s P_{T_2}} X_{T_2} \mathbf{h}_{T_2} + \sqrt{T_s P_{T_1}} X_{T_1} \mathbf{h}_m) + \mathbf{W}_{T_1} \tag{3.5.5}$$

$$\mathbf{x}_{T_2} = F(\sqrt{T_s P_{T_1}} X_{T_1} \mathbf{h}_{T_1} + \sqrt{T_s P_{T_2}} X_{T_2} \mathbf{h}_m) + \mathbf{W}_{T_2} \tag{3.5.6}$$

where

$$\mathbf{h}_{T_m} = [\hat{f}_1 \hat{g}_1 \ ... \ \hat{f}_4 \hat{g}_4]^T$$

$$\mathbf{h}_m = [\hat{h}_1^2 \ ... \ \hat{h}_4^2]^T$$

for

$$h_i = \begin{cases} g_i & \text{if} \quad m = 1 \\ f_i & \text{if} \quad m = 2 \end{cases}$$

$$X_{T_m} = [\hat{A}_1 \hat{x}_m^i \ ... \ \hat{A}_4 \hat{x}_m^4] \ \text{ for } m = 1, 2$$

and

$$\mathbf{W}_{T_m} = F \sum_{i=1}^{4} h_i \hat{A}_i \hat{\mathbf{v}}_i + \mathbf{w}_{T_m}$$

The maximum-likelihood (ML) decoding is used to detect the received vector and it is given by

$$\arg \min_{\hat{S} \epsilon S} ||\mathbf{x}_{T_m} - F(\sqrt{T_s P_{T_m}} \ \hat{S} \ \mathbf{h}_{T_m} + \sqrt{T_s P_{T_m}} \ S_m \ \mathbf{h}_m)|| \tag{3.5.7}$$

where $\hat{S}$ is the possible code matrices which depends on the constellation used and $||.||$ again represents the Euclidean norm.

3.5.2 Modified code design for two-way design

The design of the code is similar to (3.2.11), however, for the QPSK constellation which is used for higher rate, the rotations Φ_1 and Φ_2 of the symbols are $\Phi_1 = \Phi_2 = \frac{\pi}{4}$ [43] therefore the CGD for the modified codebook is

calculated as

$$D(\mathbb{S}_1, \mathbb{T}_2) = 2.22$$

It is clear that the modified code has a small distance thus the distance property of the code is not improved greatly which affects the performance of the system. In order to increase the distance of the modified code a unitary rotation matrix $\mathbf{U}$ is used. The codewords in $\mathbb{T}_2$ are multiplied by the matrix $\mathbf{U}$ as

$$\max_{\mathbf{U}} D(\mathbb{S}_1, \mathbb{T}_2\mathbf{U})$$

where

$$\mathbf{U} = \text{diag}(e^{j\theta_1}, e^{j\theta_2}, e^{j\theta_3}, e^{j\theta_4}) \tag{3.5.8}$$

and diag(.) denotes a diagonal matrix. The rotations within the unitary rotation matrix $\mathbf{U}$ were calculated in [43] to increase the CGD to 43.94. However, in this work a genetic algorithm is used to search for the optimum rotation matrix to maximize the distance property between the codes. The MATLAB fitness function reference of the genetic algorithm has four parameters for the rotation matrix the lower bound for each parameter is -2π and the upper bound is 2π. The size of populations which is used is 50000 with 100 generations. It is found that the optimum rotation which gives the maximum distance is

$$\mathbf{U} = \text{diag}(e^{j1.5832\pi}, e^{j.4165\pi}, e^{j.9165\pi}, e^{j1.0832\pi}), \tag{3.5.9}$$

and the maximum distance from the optimum rotation is

$$D(\mathbb{S}_1, \mathbb{T}_2\mathbf{U}) \approx 64$$

therefore the distance is maximized because of the optimum rotation matrix which improves the performance of the modified code.

3.6 Simulation results

In this section, simulation results of the modified D-QO-STBC compared with open and closed-loop D-QO-STBC for a two-way wireless relay network are shown using MATLAB software. The comparisons of average codeword error rate (CWER) of the schemes are simulated using BPSK and QPSK modulation. It is assumed that, four relay nodes are available in the proposed system, each node in the proposed system has a single antenna and there is no direct link between the two terminals. The channels are assumed to be Rayleigh flat fading and the real and imaginary parts of the channels and noise are generated by using the MATLAB function randn(). The simulation results are shown in Figure 3.6 and Figure 3.7. Due to the higher

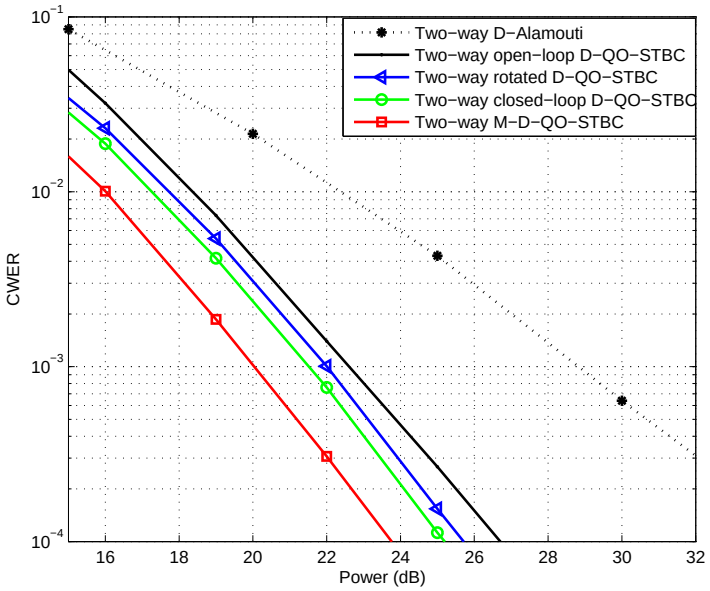

Figure 3.6. Performance comparison of two-way wireless four relay network with BPSK modulation.

diversity gain of the QO-STBCs, the gap between the D-QO codes and the D-Alamouti increases for higher SNR values. This is due to the fact that the degree of diversity dictates the asymptotic slope of the CWER-SNR curve. The figures also show that the modified D-QO-STBC for two-way transmis-

sion provides an improved performance over all other schemes in [69] due to the maximization in the distance properties of the original codebooks of the modified code. For example, in Figure 3.6, for the BPSK modulation, at a codeword error probability of 10^{-4}, the modified code provides a power saving of approximately 3.4 dB compared with the D-QO-STBC open-loop scheme, approximately 2.5 dB compared with the rotated D-QO-STBC open-loop scheme and 1.5 dB compared with the D-QO-STBC closed-loop scheme. For the QPSK modulation as shown in 3.7, the modified scheme provides a power saving of approximately 3 dB compared with the D-QO-STBC open-loop scheme, approximately 1.2 dB compared with the rotated D-QO-STBC open-loop scheme and 1 dB compared with the D-QO-STBC closed-loop scheme.

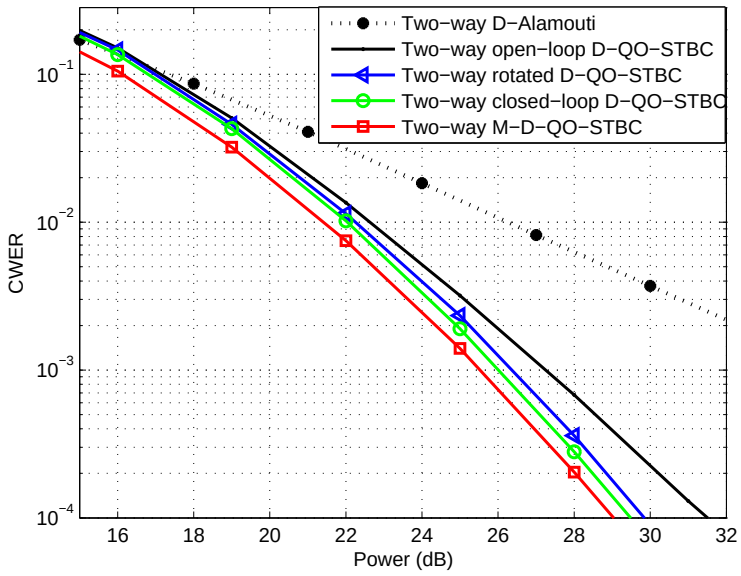

Figure 3.7. Performance comparison of two-way wireless four relay network with QPSK modulation.

3.7 Summary

In this chapter a modified D-QO-STBC with maximum distance for one-way and two-way AF wireless relay networks was proposed. This modified code was designed from set partitioning of two rotated quasi-orthogonal space-time codebooks then the subcodes were combined to be pruned to arrive at the modified codebook with the desired rate in order to increase the code gain distance. For higher rate codes the code distance was maximized by using a genetic algorithm to search for the optimum rotation matrix. Simulations for the modified D-STBC confirmed the advantages of this code compared to other open and closed-loop codes operating at the same CWER and total power. In particular, the modified D-QO-STBC scheme has the best performance over all the other schemes due to the gain from increasing the code distance and achieving the full diversity. In the next chapter, a relay selection technique will be used to increase the performance of the system, assuming a large number of available relays.

Chapter 4

OUTAGE PROBABILITY AND RELAY SELECTION ANALYSIS IN ONE-WAY AND TWO-WAY RELAY NETWORKS

In this chapter, outage probability and relay selection analysis of one-way and two-way cooperative relaying communication systems which transmit over Rayleigh flat fading channels are presented. In the one-way cooperative relay networks, analysis of outage probability for relay selection of four relay nodes is presented. Then, the outage probability analysis for the best and the best N^{th} relay selection schemes from a set of N available relays in two-way system is presented. Finally, the presented simulation results validate the accuracy of the derived closed-form expressions in the two proposed systems.

4.1 Introduction

Space time codes have been designed for multi-input multi-output (MIMO) systems to achieve spatial diversity to improve link performance [8] and [46].

Distributed MIMO has been recently proposed to exploit spatial diversity by allowing single antenna nodes to cooperate. In cooperative networks the relay nodes are generally sufficiently separated to ensure uncorrelated spatial paths between the source and destination [39] and [62]. Sometimes some relays have a poor channel quality which can provide limited signal quality to be received at the destination [74], therefore, relay selection (RS) techniques are often used to preserve the potential diversity gains in the networks and thereby provide a good transmission quality. Relay selection techniques can be used for both amplify-and-forward (AF) and decode-and-forward (DF) relaying schemes but an AF transmission protocol is assumed in this work due to the reduced complexity at the relays. Furthermore, the authors in [75], [76] and [77] showed that a full diversity order can be obtained with a relay selection technique in one-way cooperative networks. The performance of the one-way relaying scheme can be improved by maximizing the end-to-end SNR, whereas there are two terminals in the two-way relaying scheme, and hence the end-to-end SNR for both links should be considered. In this work, however the assumed relay selection policy is based on the local measurements of the instantaneous channel gain [75] between source and destination nodes through the relay nodes. This chapter will be divided into three sections, firstly, the outage probability for the best four relays for one-way relay networks will be calculated. Secondly, the outage probability analysis for best relay and best N^{th} relay selection in two-way relay networks, and finally the chapter summary will be given.

4.2 Outage probability for four relay selection in one-way relay networks

The recent developments in selection relaying for one-way transmission have largely focused on information theoretic analysis such as outage perfor-

mance [78], [79], [75] and [80]. The authors in [78] proposed a scheme to achieve DA opportunistic relaying with a direct link which is termed as fixed selective decode-and-forward (FSDF) relaying. However, this method requires high complexity at the relay nodes and destination node. In [79] the authors provide exact outage and diversity performance expressions for selection relaying and tight approximation over a sufficiently wide range of SNR regimes in the context of the AF transmission protocol. The work in [75] is based on local measurements of the instantaneous end-to-end wireless channel conditions to choose the best relay with which to cooperate. The work in [75] was extended in [80] to obtain outage-optimal opportunistic relaying in the context of selecting a single relay from a set of N available relays. Most of the previous work in relay selection considered the selection of a single best relay for cooperation. In this work the measurements of the instantaneous wireless channel condition are assumed to select the best four relays from a set of N available relays and then the selected relays are used for cooperation between the source and the destination nodes. The expression of the outage probability over Rayleigh flat fading channels is derived by using theoretical analysis of the PDF and CDF functions.

4.2.1 System model for a one-way cooperative relay network

Figure 4.1 depicts a wireless relay network with $R_N + 2$ nodes, one sender node, one destination node and all the other R_N nodes work as relays. Each node has one half-duplex antenna for either transmission or reception. The channel from the transmitter to the i-th relay is denoted by h_{s,r_i}, and from the i-th relay to the receiver is $h_{r_i,d}$, and there is no direct link between the source and the destination due to path loss and shadowing. It is assumed that the communication channels are Rayleigh flat fading and there is no channel information at the relays, but the receiver has perfect channel information. The transmission operation involves a two-step protocol; in step

one the transmitter node sends information x to each relay; the received

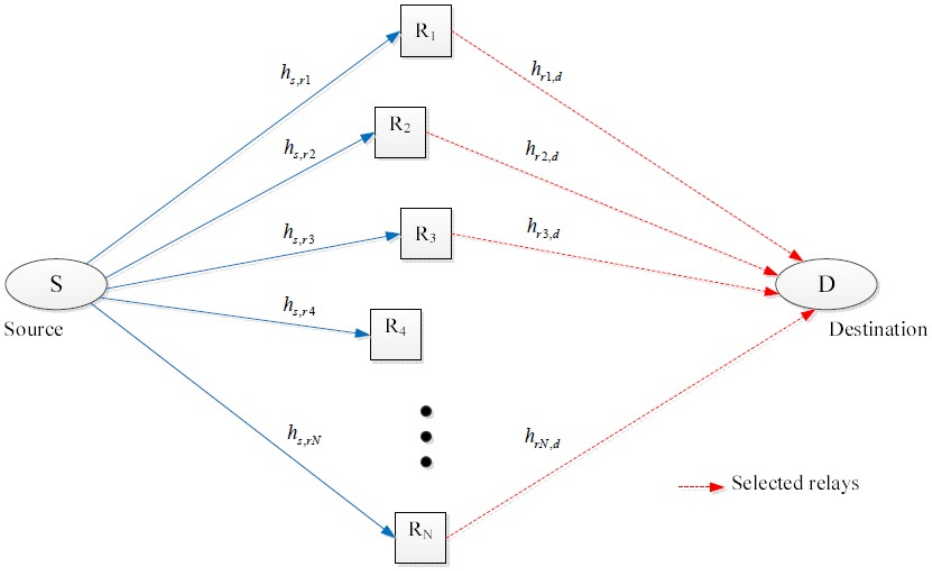

Figure 4.1. Two-hop one-way wireless relay network with N available relays and four selected relays for end-to-end transmission.

information at the i-th relay is corrupted by fading and noise and is given by

$$s_i = \sqrt{E_s} h_{s,r_i} x + n_{r_i} \tag{4.2.1}$$

where E_s is the average energy per symbol and n_{r_i} is complex additive white Gaussian random noise with zero-mean and unit-variance at the i-th relay. In step two, the i-th relay transmits its received information to the destination. An amplify-and-forward protocol is assumed in this work thus the signal at each relay is amplified before retransmission. The received information at the destination from the i-th relay is given by

$$r_i = \sqrt{P_i} h_{r_i,d} s_i + n_d \tag{4.2.2}$$

where n_d is the complex additive white Gaussian noise received at the destination and P_i is the i-th relay gain which is calculated as [76] $P_i =$

$\frac{E_s}{E_s|h_{s,r_i}|^2+N_0}$ where N_0 is the noise variance. The maximum ratio combining (MRC) technique is implemented at the destination, thus the instantaneous end-to-end SNR can be given by [81]

$$\gamma_D = \sum_{i=1}^{N} \frac{\gamma_{s,r_i}\gamma_{r_i,d}}{1+\gamma_{s,r_i}+\gamma_{r_i,d}} \tag{4.2.3}$$

where γ_{s,r_i} and $\gamma_{r_i,d}$ are the instantaneous SNRs of the links from the source to the i-th relay and from the i-relay to the destination respectively and given as $\gamma_{s,r_i} = |h_{s,r_i}|^2 \frac{E_s}{N_0}$ and $\gamma_{r_i,d} = |h_{r_i,d}|^2 \frac{E_s}{N_0}$. As the channels are modeled as Rayleigh fading channels therefore the SNRs are modeled as exponential random variables. Thus the PDF and the CDF of the SNR of the $u \in (s, r_i, r_i, d)$ links are given by

$$f_{\gamma_u}(\gamma) = \frac{1}{\bar{\gamma}_u} e^{\frac{-\gamma}{\bar{\gamma}_u}} \tag{4.2.4}$$

$$F_{\gamma_u}(\gamma) = 1 - e^{\frac{-\gamma}{\bar{\gamma}_u}} \tag{4.2.5}$$

where $\bar{\gamma}_u$ is the mean SNR for all links. To analyze the medium and high SNR regimes it is important to have simple closed form bounds, therefore the upper and lower bounds on γ_D are considered. From γ_D in (4.2.3) for $\gamma_{s,r_i} > 0$ and $\gamma_{r_i,d} > 0$ the lower and upper bound for equivalent SNR can be calculated as [82]

$$\gamma_D \geq \gamma_{low} \quad \text{where} \quad \gamma_{low} = \frac{1}{2}\sum_{i=1}^{N} min(\gamma_{s,r_i}, \gamma_{r_i,d}) \tag{4.2.6}$$

and

$$\gamma_D \leq \gamma_{up} \quad \text{where} \quad \gamma_{up} = \sum_{i=1}^{N} min(\gamma_{s,r_i}, \gamma_{r_i,d}) \tag{4.2.7}$$

The upper bound will be taken for the analysis in this work, then the CDF of $\gamma_i = min(\gamma_{s,r_i}, \gamma_{r_i,d})$ can be obtained as [83]

$$\begin{aligned} F_{\gamma_i}(\gamma) &= 1 - Pr(\gamma_{s,r_i} > \gamma) Pr(\gamma_{r_i,d} > \gamma) \\ &= 1 - [1 - F_{\gamma_{s,r_i}}(\gamma)][1 - F_{\gamma_{r_i,d}}(\gamma)] \end{aligned} \tag{4.2.8}$$

Substituting (4.2.5) into (4.2.8) with the appropriate index yields

$$F_{\gamma_i}(\gamma) = 1 - e^{\frac{-\gamma}{\bar{\gamma}_c}} \tag{4.2.9}$$

where $\bar{\gamma}_c = \frac{\bar{\gamma}_{s,r}\bar{\gamma}_{r,d}}{\bar{\gamma}_{s,r}+\bar{\gamma}_{r,d}}$. The channel parameters are assumed to be independent and identically distributed (i.i.d.) random variables and that $\bar{\gamma}_{s,r} = \bar{\gamma}_{r,d}$. Then the derivative of the CDF in (4.2.9) is taken to obtain the PDF of γ_i as

$$F_{\gamma_i}(\gamma) = \frac{1}{\bar{\gamma}_c} e^{\frac{-\gamma}{\bar{\gamma}_c}} \tag{4.2.10}$$

Next, the outage probability analysis for selecting the best four relays from a set of N relays will be considered.

4.2.2 Four relay selection and outage probability analysis in one-way relay networks

The conventional relay selection technique in [75] is assumed in this work. It requires the instantaneous SNR to be known from the source to relay node and relay node to the destination node, and then the best relay is selected to maximize the minimum SNR between them which can be represented as [75]

$$\hat{i} = \arg \max_i \min \{\gamma_{s,r}, \gamma_{r,d}\} \tag{4.2.11}$$

and this relay selection scheme is as shown in [84] equivalent to

$$\hat{i} = \arg\max_{i} \min\{|h_{s,r}|^2, |h_{r,d}|^2\} \tag{4.2.12}$$

Selecting four relays from a set of N available relays is based on the selection of γ_{max}, γ_{max-1}, γ_{max-2} and γ_{max-3} from the relays instantaneous SNR. As the selection will not be from an independent set and it is assumed that $\gamma_{max} = x_1$, $\gamma_{max-1} = x_2$, $\gamma_{max-2} = x_3$ and $\gamma_{max-3} = x_4$. Therefore, by using the theory of order statistics [85], then the joint distribution of the four most maximum values from N values is obtained as

$$f(x_1, x_2, x_3, x_4) = N(N-1)(N-2)(N-3)F(x_4)^{N-4} f(x_1) \\ f(x_2) f(x_3) f(x_4).$$

where

$$f(x_1) = \frac{1}{\bar{\gamma}_c} e^{\frac{-x_1}{\bar{\gamma}_c}}, \quad f(x_2) = \frac{1}{\bar{\gamma}_c} e^{\frac{-x_2}{\bar{\gamma}_c}}, \quad f(x_3) = \frac{1}{\bar{\gamma}_c} e^{\frac{-x_3}{\bar{\gamma}_c}}$$
$$f(x_4) = \frac{1}{\bar{\gamma}_c} e^{\frac{-x_4}{\bar{\gamma}_c}} \quad \text{and} \quad F(x_4) = 1 - e^{\frac{-x_4}{\bar{\gamma}_c}}$$

Therefore,

$$f(x_1, x_2, x_3, x_4) = \frac{N(N-1)(N-2)(N-3)}{\bar{\gamma}_C^4} F[1 - e^{\frac{-x_4}{\gamma}}]^{N-4} \\ e^{\frac{-x_1}{\gamma}} e^{\frac{-x_2}{\gamma}} e^{\frac{-x_3}{\gamma}} e^{\frac{-x_4}{\gamma}}. \tag{4.2.13}$$

The CDF of γ_{up} can be obtained as the sum of the random variables x_1, x_2, x_3 and x_4 therefore it can be obtained as

$$F_{\gamma_{up}}(\gamma_{up}) = Pr\{x_1 + x_2 + x_3 + x_4 \leq \gamma_{up}\} \tag{4.2.14}$$

Now $F_{\gamma_{up}}(\gamma)$ can be calculated as

$$F_{\gamma_{up}}(\gamma) = \int_0^{\frac{\gamma}{4}} \int_{x_4}^{\frac{\gamma-x_4}{3}} \int_{x_3}^{\frac{\gamma-x_4-x_3}{2}} \int_{x_2}^{\gamma-x_4-x_3-x_2} f(x_1, x_2, x_3, x_4) dx_1 dx_2 dx_3 dx_4 \tag{4.2.15}$$

Substituting the value of the PDF in (4.2.13) in (4.2.15) which gives

$$F_{\gamma_{up}}(\gamma) = \frac{N(N-1)(N-2)(N-3)}{\bar{\gamma}_C^4} \sum_{n=0}^{N-4} (-1)^n \int_0^{\frac{\gamma}{4}} \int_{x_4}^{\frac{\gamma-x_4}{3}} \int_{x_3}^{\frac{\gamma-x_4-x_3}{2}} \int_{x_2}^{\gamma-x_4-x_3-x_2} e^{\frac{-x_1}{\gamma}} e^{\frac{-x_2}{\gamma}} e^{\frac{-x_3}{\gamma}} e^{\frac{-x_4}{\gamma}} dx_1 dx_2 dx_3 dx_4$$

After some manipulations the $F_{\gamma_{up}}(\gamma)$ is obtained when $n = 0$ and $n \neq 0$, therefore

$$F_{\gamma_{up}}^{n=0}(\gamma) = \frac{N(N-1)(N-2)(N-3)}{\bar{\gamma}_c^3} \left[\frac{\bar{\gamma}_c^3}{24} - \frac{\bar{\gamma}_c^3}{24} e^{\frac{-\gamma}{\bar{\gamma}_c}} - \frac{\bar{\gamma}_c^2 \gamma}{24} e^{\frac{-\gamma}{\bar{\gamma}_c}} - \frac{\bar{\gamma}_c \gamma^2}{24} e^{\frac{-\gamma}{\bar{\gamma}_c}} + \frac{\bar{\gamma}_c \gamma^2}{48} e^{\frac{-\gamma}{\bar{\gamma}_c}} - \frac{\gamma^3}{144} e^{\frac{-\gamma}{\bar{\gamma}_c}} \right] \tag{4.2.16}$$

and

$$\begin{aligned} F_{\gamma_{up}}^{n\neq 0}(\gamma) = \frac{N(N-1)(N-2)(N-3)}{\bar{\gamma}_c^3} \sum_{n=1}^{N-4} \binom{N-4}{n} (-1)^n \\ \left[\frac{2\bar{\gamma}_c \gamma}{3(n+4)} + \left(\frac{-\bar{\gamma}_c^3}{6n} - \frac{\bar{\gamma}_c^2 \gamma}{6n} - \frac{\bar{\gamma}_c \gamma^2}{12} + \frac{2\bar{\gamma}_c^2 \gamma}{3n^2} + \frac{2\bar{\gamma}_c^3}{3n^2} \right. \right. \\ \left. - \frac{8\bar{\gamma}_c^3}{3n^3} \right) e^{\frac{-\gamma}{\bar{\gamma}_c}} + \left(\frac{-2\bar{\gamma}_c \gamma}{3(n+4)} + \frac{\bar{\gamma}_c^3}{6n} + \frac{\bar{\gamma}_c^2 \gamma}{6n} + \frac{\bar{\gamma}_c \gamma^2}{12} \right. \\ \left. \left. - \frac{\bar{\gamma}_c \gamma^2}{6n} - \frac{2\bar{\gamma}_c^3}{3n^2} - \frac{\bar{\gamma}_c^2 \gamma}{6n} + \frac{8\bar{\gamma}_c^3}{3n^3} + \frac{\bar{\gamma}_c \gamma^2}{12n} \right) e^{\frac{-(n+4)\gamma}{4\bar{\gamma}_c}} \right] \end{aligned} \tag{4.2.17}$$

The total CDF of γ_{up} can be expressed from (4.2.16) and (4.2.17) as

$$\begin{aligned}
F_{\gamma_{up}}(\gamma) &= F_{\gamma_{up}}^{n=0}(\gamma) + F_{\gamma_{up}}^{n\neq 0}(\gamma) \\
&= \frac{N(N-1)(N-2)(N-3)}{\bar{\gamma}_c^3}\Bigg\{\Bigg[\frac{\bar{\gamma}_c^3}{24} - \frac{\bar{\gamma}_c^3}{24}e^{\frac{-\gamma}{\bar{\gamma}_c}} \\
&- \frac{\bar{\gamma}_c^2\gamma}{24}e^{\frac{-\gamma}{\bar{\gamma}_c}} - \frac{\bar{\gamma}_c\gamma^2}{24}e^{\frac{-\gamma}{\bar{\gamma}_c}} + \frac{\bar{\gamma}_c\gamma^2}{48}e^{\frac{-\gamma}{\bar{\gamma}_c}} - \frac{\gamma^3}{144}e^{\frac{-\gamma}{\bar{\gamma}_c}}\Bigg] \\
&+ \sum_{n=1}^{N-4}\binom{N-4}{n}(-1)^n\Bigg[\frac{2\bar{\gamma}_c\gamma}{3(n+4)} + (\frac{-\bar{\gamma}_c^3}{6n} - \frac{\bar{\gamma}_c^2\gamma}{6n} - \frac{\bar{\gamma}_c\gamma^2}{12} \\
&+ \frac{2\bar{\gamma}_c^2\gamma}{3n^2} + \frac{2\bar{\gamma}_c^3}{3n^2} - \frac{8\bar{\gamma}_c^3}{3n^3})e^{\frac{-\gamma}{\bar{\gamma}_c}} + (\frac{-2\bar{\gamma}_c\gamma}{3(n+4)} + \frac{\bar{\gamma}_c^3}{6n} + \frac{\bar{\gamma}_c^2\gamma}{6n} + \frac{\bar{\gamma}_c\gamma^2}{12} \\
&- \frac{\bar{\gamma}_c\gamma^2}{6n} - \frac{2\bar{\gamma}_c^3}{3n^2} - \frac{\bar{\gamma}_c^2\gamma}{6n} + \frac{8\bar{\gamma}_c^3}{3n^3} + \frac{\bar{\gamma}_c\gamma^2}{12n})e^{\frac{-(n+4)\gamma}{4\bar{\gamma}_c}}\Bigg]\Bigg\}
\end{aligned} \tag{4.2.18}$$

Now the target outage probability of the four relay selection can be evaluated from (4.2.18). As the outage probability is when the average end-to-end SNR falls below a certain predefined threshold value α the outage probability is expressed as

$$P_{out} = \int_0^{\alpha} f_{\gamma u}(\gamma) = F_{\gamma_{up}}(\alpha) \tag{4.2.19}$$

Therefore using the CDF expression in (4.2.18), the outage probability for the best four relay selection can be obtained as

$$\begin{aligned}
P_{out} &= \frac{N(N-1)(N-2)(N-3)}{\bar{\gamma}_c^3}\Bigg\{\Bigg[\frac{\bar{\gamma}_c^3}{24} - \frac{\bar{\gamma}_c^3}{24}e^{\frac{-\alpha}{\bar{\gamma}_c}} \\
&- \frac{\bar{\gamma}_c^2\alpha}{24}e^{\frac{-\alpha}{\bar{\gamma}_c}} - \frac{\bar{\gamma}_c\alpha^2}{24}e^{\frac{-\alpha}{\bar{\gamma}_c}} + \frac{\bar{\gamma}_c\alpha^2}{48}e^{\frac{-\alpha}{\bar{\gamma}_c}} - \frac{\alpha^3}{144}e^{\frac{-\alpha}{\bar{\gamma}_c}}\Bigg] \\
&+ \sum_{n=1}^{N-4}\binom{N-4}{n}(-1)^n\Bigg[\frac{2\bar{\gamma}_c\alpha}{3(n+4)} + (\frac{-\bar{\gamma}_c^3}{6n} - \frac{\bar{\gamma}_c^2\alpha}{6n} - \frac{\bar{\gamma}_c\alpha^2}{12} \\
&+ \frac{2\bar{\gamma}_c^2\alpha}{3n^2} + \frac{2\bar{\gamma}_c^3}{3n^2} - \frac{8\bar{\gamma}_c^3}{3n^3})e^{\frac{-\alpha}{\bar{\gamma}_c}} + (\frac{-2\bar{\gamma}_c\alpha}{3(n+4)} + \frac{\bar{\gamma}_c^3}{6n} + \frac{\bar{\gamma}_c^2\alpha}{6n} \\
&+ \frac{\bar{\gamma}_c\alpha^2}{12} - \frac{\bar{\gamma}_c\alpha^2}{6n} - \frac{2\bar{\gamma}_c^3}{3n^2} - \frac{\bar{\gamma}_c^2\alpha}{6n} + \frac{8\bar{\gamma}_c^3}{3n^3} + \frac{\bar{\gamma}_c\alpha^2}{12n})e^{\frac{-(n+4)\alpha}{4\bar{\gamma}_c}}\Bigg]\Bigg\}
\end{aligned} \tag{4.2.20}$$

This expression can be used to study the performance of the best four relays selection scheme in one-way cooperative networks. In the next section the analytical results of the outage probability and the impact of the relay selection scheme on the system will be verified by numerical simulations.

4.2.3 Simulation results for the proposed one-way cooperative relay network

In this section, outage probability for the best relay selection from N available relay nodes is shown. In order to verify the results obtained from (4.2.20), all the relay node links have the same average SNR=5dB, there is no direct link between the transmitter and the receiver due to shadowing, or distance. All nodes are equipped with a single antenna and it is assumed that the channels are Rayleigh flat fading. The simulated values, as in Figures 4.2 are found

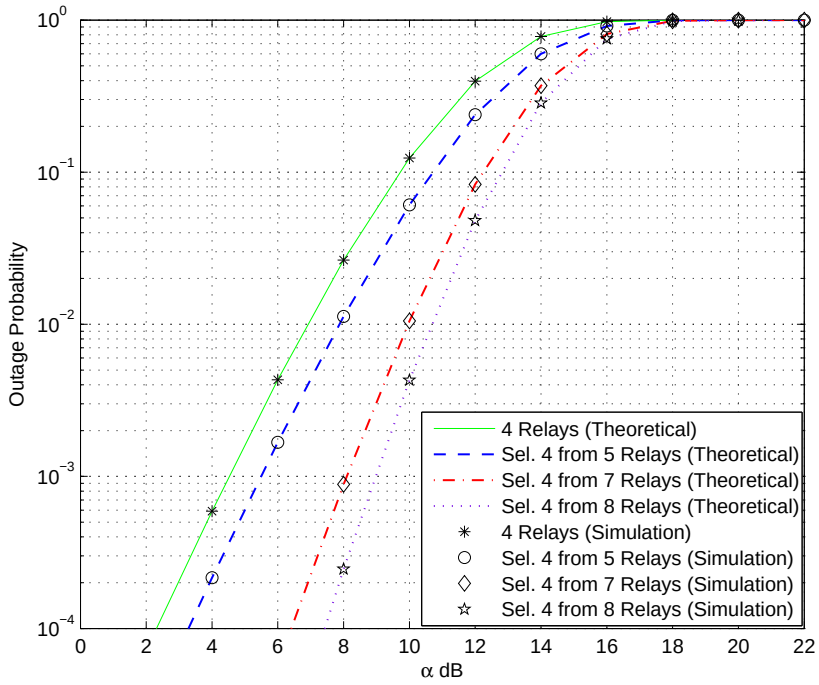

Figure 4.2. The theoretical and the simulation results of the outage probability performance of the best four relay selection; the simulation results are shown in points and the theoretical results as line style, where the SNR=5 dB.

by generating random variables with an exponential distribution using the MATLAB function exprnd() which represent the power gain of the channel. These values are then applied in the maxmin(.,.) operation and this process is repeated a sufficiently large number (for example, 10^6 values for this plot) of times to generate stable plots. This explains why it is expected that the simulated and theoretical expressions should be identical. Figure 4.2 shows the theoretical and the simulation results of the best four relay selection from N available relays where the theoretical results are shown in line style and the simulation results as points. To obtain the outage probability from the mathematical expression, it is assumed that all the links have the same average SNR which is 5dB. For different values of N, it can be seen that the theoretical results match well the simulation results and when the number of the available relays N increases the outage probability decreases and hence when the number of relays is large the outage event (no transmission) becomes less likely. For instance, when the number of the relays increases from four to eight, at the threshold value $\alpha = 8$dB the outage probability decreases significantly from approximately $2.6\text{x}10^{-2}$ to $2.5\text{x}10^{-4}$ and from $12.4\text{x}10^{-2}$ to $4.3\text{x}10^{-3}$ at the threshold value of $\alpha = 10$dB. In the next section the outage probability for relay selection in two-way relay networks will be considered.

4.3 Outage probability for relay selection in two-way relay networks

Recently, two-way relay selection has obtained much interest and has been studied in several works considering outage probability [86], [87], [88], [89] and [90]. The authors in [86] and [87] consider the outage probability of the two-way relaying paths as two parallel one-way paths and this means

the outage performance of the two terminals T_1 and T_2 are analyzing separately. In fact, in the two-way relaying scheme the two terminals exchange their information simultaneously between each other, therefore, the two-way scheme will be in outage whenever an outage occurs at either terminal T_1 or T_2. In [88] a closed form for the approximation and lower bound for the outage probability in two-way relaying were derived under distinct power interference environments. The authors in [89] and [90] investigated the outage probability for a two-way relaying scheme with asymmetric traffic and derived an expression for the outage probability considering interference at the relay nodes. The mentioned works have not investigated the unavailability of the selected relay, moreover, they considered the selection of one best relay for cooperation. However, if the best relay cannot be selected because it may be used by other terminals at the instant of time then the N^{th} best should be selected. In the next section, outage probability analysis of the best, the N^{th} best and the four best relays selection will be presented.

4.3.1 System model for two-way cooperative relay network

Figure 4.3 shows a cooperative multi-node network for two-way communications using two terminal nodes T_m, $m = 1, 2$ and relay nodes R_i, $i = 1...N$. The two terminals exchange their information between each other through the selected relay node. All the nodes have a single antenna and operate in half-duplex mode that cannot receive and transmit simultaneously. Denote the channel coefficient between T_1 and R_i and between T_2 and R_i as f_i and g_i respectively. It is assumed that the channel coefficients remain unchanged during the transmission of a signal code block (quasi-static Rayleigh fading) between any two nodes and they are known to the receiving node. The channel coefficients f_i and g_i are assumed to be independent and identical distributed (i.i.d.) with zero mean and unit variance $CN(0, 1)$. In step one, the two terminals T_m send the signal $\mathbf{x}_m = [x_{m,1}, ..., x_{m,T_s}]^T$ to the rely

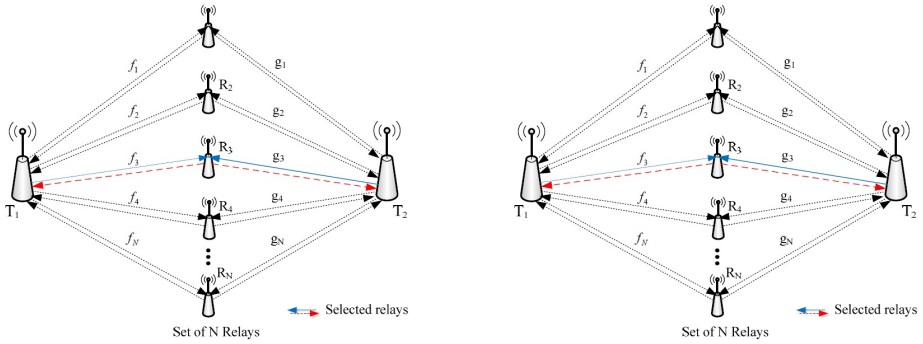

(a) (b)

Figure 4.3. (a) shows a system model of two-way wireless relay network selecting the best single relay whereas (b) shows a system model of two-way wireless relay network selecting the best four relays

nodes, where T denotes the transpose and T_s is the length of the time slot. The information vector $\mathbf{x}$ is normalized to be $E\{\mathbf{x}^H\mathbf{x}\} = 1$ [73] where $(.)^H$ and $E\{.\}$ denote the Hermitian operator and the expectation of a random variable respectively. The received information vector at the i-th relay is given by

$$\mathbf{r}_i = \sqrt{T_s P_{T_1}} f_i \mathbf{x_1} + \sqrt{T_s P_{T_2}} g_i \mathbf{x_2} + \mathbf{v}_{r_i} \quad \text{for} \quad i = 1, ..., N \tag{4.3.1}$$

where P_{T_m} is the average power used at the terminal T_m at every transmission and the elements of $\mathbf{v}_{r_i} \sim CN(0, \sigma^2)$ are additive white Gaussian noise (AWGN) terms at the relays. In the second step, the selected relay simplifies its received information and sends it to both terminals, therefore, the received information at both terminals after self-interference cancelation is

$$\begin{aligned} \mathbf{x}_{T_1} &= F f_i r_i + \mathbf{w}_{T_1} \\ &= F f_i (\sqrt{T_s P_{T_2}} g_i \mathbf{x_2} + \mathbf{v}_{r_i}) + \mathbf{w}_{T_1} \end{aligned} \tag{4.3.2}$$

$$\begin{aligned}\mathbf{x}_{T_2} &= \digamma g_i r_i + \mathbf{w}_{T_2} \\ &= \digamma g_i(\sqrt{T_s P_{T_1}} f_i \mathbf{x_1} + \mathbf{v}_{r_i}) + \mathbf{w}_{T_2} \end{aligned} \tag{4.3.3}$$

where the elements of $\mathbf{w}_{\mathrm{T}_m} \sim CN(0, \sigma_2^2)$ are AWGN at T_m and $\digamma = \sqrt{\frac{P_{r_i}}{P_{\mathrm{T}_1}|f_i|^2 + P_{\mathrm{T}_2}|g_i|^2 + \mathbf{v}_{r_i}}}$ is the amplification factor at the relay nodes as given in [73]. The instantaneous end-to-end SNR for the i-th relay are calculated as

$$\gamma_{\mathrm{T}_{1,i}} = \frac{\gamma_{i,1}\gamma_{i,2}}{2\ \gamma_{i,1} + \gamma_{i,2} + 1}, \qquad i = 1, \ldots, N \tag{4.3.4}$$

$$\gamma_{\mathrm{T}_{2,i}} = \frac{\gamma_{i,1}\gamma_{i,2}}{\gamma_{i,1} + 2\gamma_{i,2} + 1}, \qquad i = 1, \ldots, N \tag{4.3.5}$$

where $\gamma_{i,1} = \|f_i\|^2 \frac{P_{\mathrm{T}_1}}{N_0}$ and $\gamma_{i,2} = \|g_i\|^2 \frac{P_{\mathrm{T}_1}}{N_0}$ are the instantaneous SNRs of the links $\mathrm{T}_1 \leftrightarrow R_i$ and $\mathrm{T}_2 \leftrightarrow R_i$ respectively and N_0 is the noise variance [76].

4.3.2 Relay selection scheme in two-way wireless relay networks

Relay selection (RS) corresponds to finding a rule to select a cooperating relay on the basis of end-to-end SNR. For high decoding reliability at both terminals,T_1 and T_2, the max-min technique is a suitable scheme to choose the best i-th relay, as given in [84], is

$$\hat{i} = \arg\max_i \min\{\gamma_{\mathrm{T}_{1,i}}, \gamma_{\mathrm{T}_{2,i}}\} \tag{4.3.6}$$

This technique maximizes the worst case received SNR and minimizes the outage probability of the cooperative relay system. From end-to-end SNRs [91] and [84], it can be concluded that

$$\gamma_{\mathrm{T}_{1,i}} \gtreqless \gamma_{\mathrm{T}_{2,i}} \Leftrightarrow \|f_i\|^2 \gtreqless \|g_i\|^2$$

Therefore, the relay selection scheme in (4.3.6) is equivalent as shown in [84] to

$$\hat{i} = \arg\max_{i} \min\left\{\|f_i\|^2, \|g_i\|^2\right\} \tag{4.3.7}$$

This is exactly equivalent to the RS for one-way cooperative multi-node communication systems [84] [91] and [92]. The equivalence can hold if and only if the two terminals T_1 and T_2 are assumed to have the same transmit power. This is the fundamental assumption used in all the works reported in this thesis. It follows then, that one of the terminals can do the RS e.g. T_2, by using the following scheme [84]

$$\hat{i} = \arg\max_{i} \min\left\{\gamma_{\mathrm{T}_{1,i}}, \gamma_{\mathrm{T}_{2,i}}\right\} \tag{4.3.8}$$

Next, the outage probability analysis in two-way wireless relay networks will be considered

4.3.3 The outage probability analysis in two-way wireless relay networks

In wireless communication, outage performance is an important performance metric which indicates that the end-to-end SNR falls below a certain value. Since the outage event in two-way systems depends on both SNRs of the two terminals, the outage occurs when either the instantaneous rate of γ_{T_1} or γ_{T_2} falls below the threshold value γ, where $\gamma = 2^{2R} - 1$ and R is the target rate, therefore, the outage probability of the two-way systems can be written as [84]

$$\begin{aligned} P_{out} &= P_r(min(\gamma_{\mathrm{T}_1}, \gamma_{\mathrm{T}_2}) < \gamma) \\ &= 1 - P_r(\gamma_{\mathrm{T}_1} < \gamma, \gamma_{\mathrm{T}_2} < \gamma) \end{aligned} \tag{4.3.9}$$

Let $x = \gamma_{i,1}$ and $y = \gamma_{i,2}$, then

$$\begin{aligned} P_{out} &= 1 - P_r\left(\frac{xy}{2x+y+1} < \gamma, \frac{xy}{x+2y+1} < \gamma\right) \\ &= 1 - P_r\left(\frac{y\gamma+\gamma}{y-2\gamma} > x, \frac{2y\gamma+\gamma}{y-\gamma} > x\right) \end{aligned} \tag{4.3.10}$$

4.3.4 The CDF and PDF of the exact SNR in two-way wireless relay networks

As maintained before that the channels are modeled as Rayleigh fading channels therefore the PDF and CDF are modeled as exponential random variables, which is given as

$$f_{\gamma_{i,m}}(\gamma) = \frac{e^{-\frac{\gamma}{\overline{\gamma}}}}{\overline{\gamma}}, \tag{4.3.11}$$

where $\overline{\gamma}$ is called the scale parameter and is denoted as the average SNR. Then, for the new outage probability analysis for two-way relay selection the exact CDF and PDF of the end-to-end per hop SNR need to be obtained. Therefore, the PDF of the end-to-end per hop SNR becomes

$$f_{\gamma_{i,1}}(\gamma) = f_{\gamma_x}(x) = \frac{e^{-\frac{x}{\overline{\gamma}}}}{\overline{\gamma}} \qquad \text{and} \qquad f_{\gamma_{i,2}}(\gamma) = f_{\gamma_y}(y) = \frac{e^{-\frac{y}{\overline{\gamma}}}}{\overline{\gamma}}$$

By exploiting independence, then

$$f_{xy}(x,y) = f_{\gamma_x}(x)\ f_{\gamma_y}(y) \tag{4.3.12}$$

Then the CDF of the exact SNR γ_i^E can be obtained by integrating the region marked as shown in Figure 4.4 using Maple software

$$\begin{aligned} F_{\gamma_i^E}(\gamma) &= \int_0^{\gamma}\int_0^{\infty} f_{xy}(x,y)\ \ dxdy + \int_{\gamma}^{\infty}\int_0^{\frac{2y\gamma+\gamma}{y-\gamma}} f_{xy}(x,y)\ \ dxdy \\ &= 1 - 2\,e^{-3\,\frac{\gamma}{\overline{\gamma}}}\sqrt{2\,\gamma+1}\sqrt{\gamma}\,\mathrm{K}(1,\,2\,\frac{\sqrt{2\,\gamma+1}\sqrt{\gamma}}{\overline{\gamma}})\overline{\gamma}^{-1} \end{aligned} \tag{4.3.13}$$

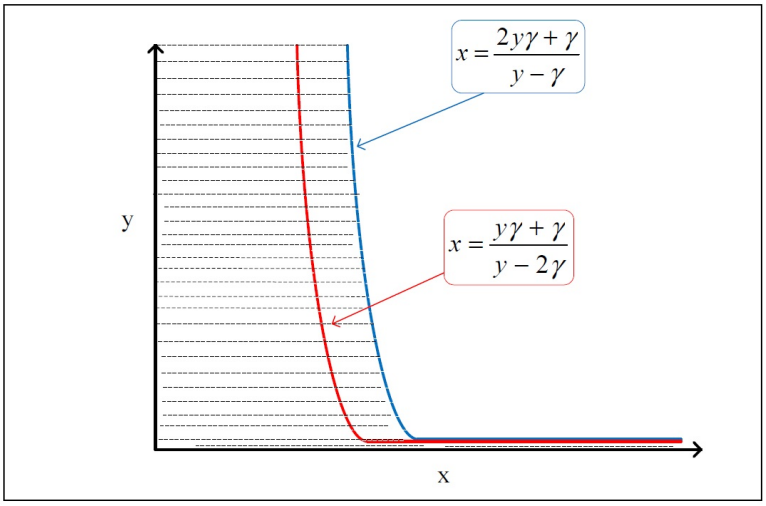

Figure 4.4. *Integration region to determine overall outage probability.*

The PDF of γ_i^E can be obtained by taking the derivative of the CDF (4.3.13)

$$
\begin{aligned}
f_{\gamma_i^E} \;=\; & \frac{d}{d\gamma}\left(F_{\gamma_i^E}(\gamma)\right) = 6\,\mathrm{e}^{-3\frac{\gamma}{\overline{\gamma}}}\sqrt{2\gamma+1}\sqrt{\gamma}\mathrm{K}\left(1,\,2\,\frac{\sqrt{2\gamma+1}\sqrt{\gamma}}{\overline{\gamma}}\right)\overline{\gamma}^{-2} \\
& -2\,\mathrm{e}^{-3\frac{\gamma}{\overline{\gamma}}}\sqrt{\gamma}\mathrm{K}\left(1,\,2\,\frac{\sqrt{2\gamma+1}\sqrt{\gamma}}{\overline{\gamma}}\right)\overline{\gamma}^{-1}\frac{1}{\sqrt{2\gamma+1}} - \mathrm{e}^{-3\frac{\gamma}{\overline{\gamma}}}\sqrt{2\gamma+1} \\
& \mathrm{K}\left(1,\,2\,\frac{\sqrt{2\gamma+1}\sqrt{\gamma}}{\overline{\gamma}}\right)\overline{\gamma}^{-1}\frac{1}{\sqrt{\gamma}} - 2\,\mathrm{e}^{-3\frac{\gamma}{\overline{\gamma}}}\sqrt{2\gamma+1}\sqrt{\gamma} \\
& \left(-\mathrm{K}\left(0,\,2\,\frac{\sqrt{2\gamma+1}\sqrt{\gamma}}{\overline{\gamma}}\right) - \frac{1}{2}\,\overline{\gamma}\mathrm{K}\left(1,\,2\,\frac{\sqrt{2\gamma+1}\sqrt{\gamma}}{\overline{\gamma}}\right)\frac{1}{\sqrt{2\gamma+1}}\frac{1}{\sqrt{\gamma}}\right) \\
& \left(2\,\frac{\sqrt{\gamma}}{\overline{\gamma}\sqrt{2\gamma+1}} + \frac{\sqrt{2\gamma+1}}{\overline{\gamma}\sqrt{\gamma}}\right)\overline{\gamma}^{-1}
\end{aligned}
\tag{4.3.14}
$$

where $\mathrm{K}(0,.)$ and $\mathrm{K}(1,.)$ are the modified Bessel function of the first and second order, respectively.

4.3.5 The best relay selection in two-way wireless relay networks

One best relay is selected from N available relays, namely, select the relay with highest instantaneous SNR from the N relays. According to the theory of order statistics in [93] and [85], the CDF of γ_i^E corresponds to the highest selected SNR from the N independent relays instantaneous SNRs as in

(4.3.8). Therefore, with the statistics obtained in (4.3.13), the outage probability is defined as when the average end-to-end SNR falls below a certain threshold value.

$$P_{out}^{E} = \int_{0}^{\alpha} f_{\gamma_i^E}(\gamma) d\gamma = F_{\gamma_i^E}(\gamma) = [F_{\gamma_i^E}(\gamma)]^N \tag{4.3.15}$$

Therefore, the outage probability can be expressed as

$$\begin{aligned} P_{out}^{E} &= \int_{0}^{\alpha} f_{\gamma_i^E}(\gamma) d\gamma = F_{\gamma_i^E}(\gamma) = [F_{\gamma_i^E}(\gamma)]^N \\ &= \left[1 - 2\, e^{-3\,\frac{\alpha}{\bar{\gamma}}} \sqrt{2\,\alpha + 1}\sqrt{\alpha}\, \mathrm{K}(1,\, 2\, \frac{\sqrt{2\,\alpha+1}\sqrt{\alpha}}{\bar{\gamma}}) \bar{\gamma}^{-1} \right]^N \end{aligned} \tag{4.3.16}$$

Sometimes the best relay is used by other terminals, therefore the N^{th} best relay will be considered in the next section.

4.3.6 The best N^{th} relay selection in two-way wireless relay networks

In the best relay selection scheme, the two terminals exchange their information between each other through the selected relay node from the set of N relays. The above study has only considered the perfect situation of relay selection. However, in some situations, the selected relay might be unavailable, the selected relay may be used by other terminals at the time the desired terminals request exchange information. Therefore, in order to avoid system outage, in the case when the relay is unavailable or used by others, the decision may be made to use the second, third or generally the N^{th} best relay. Considering the outage probability of the N^{th} best relay is an efficient way to evaluate the performance loss of the relay system. To evaluate the outage probability considering the effect of the situations that

are mentioned above, the PDF can be expressed as [94], [95] and [96]

$$f_{\gamma^E_{i_{th}}}(\gamma) = N\binom{N-1}{N^{th}-1} f_{\gamma^E_i}(\gamma)(F_{\gamma^E_i}(\gamma))^{N-N^{th}}(1-F_{\gamma^E_i}(\gamma))^{N^{th}-1} \quad (4.3.17)$$

where N is the number of available relays and N^{th} denotes the next maximum available relay. Then the CDF of the PDF in (4.3.17) can be obtained from

$$\begin{aligned} P^E_{out} &= F_{\gamma^E_{i_{th}}}(\gamma) = \int_0^\alpha f_{\gamma^E_{i_{th}}}(\gamma)d\gamma \\ &= \int_0^\alpha N\binom{N-1}{N^{th}-1} f_{\gamma^E_i}(\gamma)(F_{\gamma^E_i}(\gamma))^{N-N^{th}} \\ &\quad (1-F_{\gamma^E_i}(\gamma))^{N^{th}-1}d\gamma \end{aligned} \quad (4.3.18)$$

Therefore the CDF for the N^{th} relay selection can be obtained by substituting (4.3.13) and (4.3.14) into (4.3.18). Finally, (4.3.18) can be used to calculate the exact outage probability of the N^{th} relay selection. This result has been provided in Figure 4.6 by using the MATLAB software package and these integrals are evaluated with the quad function.

4.3.7 Simulation results for the proposed two-way wireless relay network

In this section, the outage probability performance of best single relay and N^{th} best relay selection from N available relays are shown. In order to verify the results obtained from mathematical expressions, (4.3.16) and (4.3.18), all the relay node links have the same average SNR, $\bar{\gamma} = 10$, and all noise variances are set to unity. There is no direct link between T_1 and T_2 as path loss or shadowing is assumed to render it unusable. All nodes are equipped with a single antenna and it is assumed that the channels are Rayleigh flat fading. The simulated values, as in Figures 4.5 and 4.6 are found by generating random variables with an exponential distribution using

the MATLAB function exprnd() which represents the power gain of the channel. These values are then applied in the maxmin(.,.) operation and this process is repeated a sufficiently large number of times to generate stable plots. This explains why it is expected that the simulated and theoretical expressions should be identical.

4.3.7.1 Simulation analysis for the best relay selection

Figure 4.5 shows the comparison of the outage probability of the best relay selection scheme from N available relays of two-hop wireless transmission using the formulae given in (4.3.16). Generally, increasing the number of relays

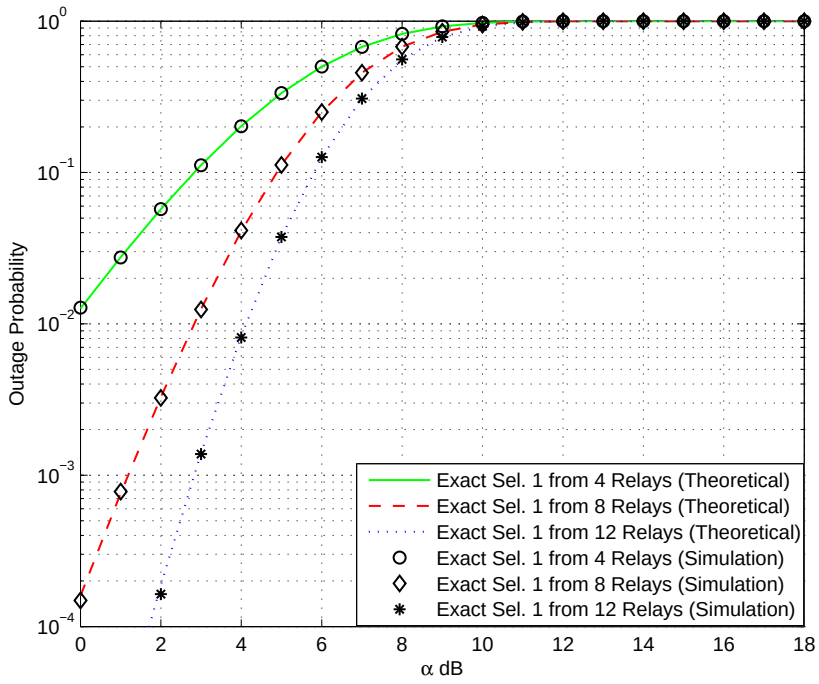

Figure 4.5. The theoretical and the simulation results of the outage probability performance of the best relay selection, the simulation results are shown in points and the theoretical results as line style, where the SNR=10 dB.

N, decreases the outage probability. For example, when the total number of available relays increases from 4 to 8 and the threshold value $\alpha = 8$, the outage probability of best relay selection is decreased from approximately 80% to 65%, and when the total number of available relays increases from

4 to 12 with the same threshold value, the outage probability of best relay selection is decreased from approximately 80% to 50%.

4.3.7.2 Simulation analysis for the N^{th} best relay selection

In this section, analysis of the impact of the unavailability of the selected relay is presented. The outage probability of the N^{th} relay selection from a set of N available relays, i.e. $N = 8$, is compared with the best single relay selection using the formulae given in (4.3.18). Figure 4.6 study the effect of

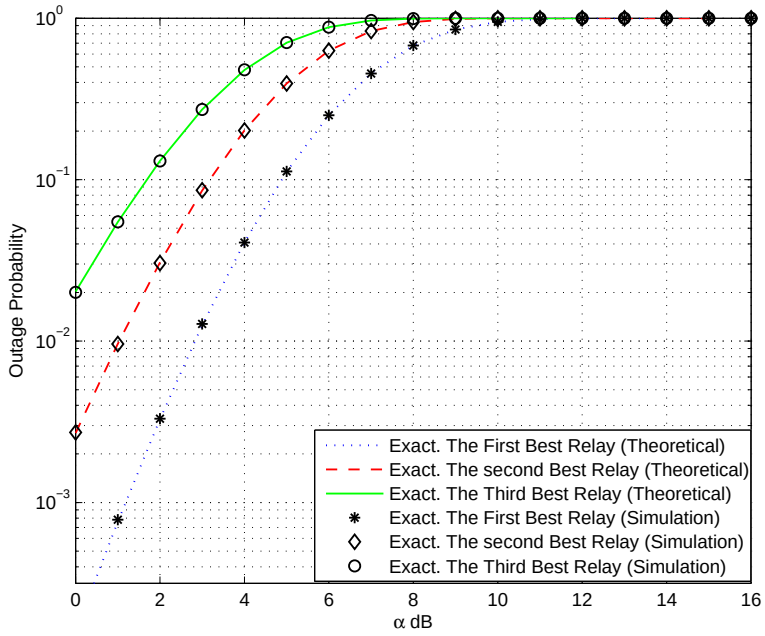

Figure 4.6. The theoretical and the simulation results of the outage probability performance of the best N^{th} relay selection, the simulation results are shown in points and the theoretical results as line style, where the SNR=10dB.

order of relay selection on the outage performance. It is clear from this figure that theoretical results perfectly fit with simulations results. Also it can be noticed that as the order of the selected N^{th} relay increases, the outage probability increases, thus the system performance is more degraded. For example, when the selected relay N^{th} increases from 1 to 2 and the threshold value $\alpha = 8$, the outage probability of best relay selection is increased from approximately 80% to 95%, and when the N^{th} increases from 1 to 3 with

the same threshold value, the outage probability of best relay selection is increased from approximately 80% to 99%.

4.4 Summary

This chapter has examined the outage probability analysis strategies with relay selection technique in a one-way and two-way AF relay networks. In the one-way relay network a closed form expression for the outage probability for four relay selection was derived by obtaining theoretic expression for PDF and CDF functions of end-to-end SNR over Ralyeigh flat fading channels. Whereas, in the two-way relay networks this chapter has presented the outage probability analysis for the best and the best N^{th} relay selection from a set of N available relays. New analytical expressions for the PDF, and CDF of end-to-end SNR were derived together with closed form expressions and integral form for outage probability over flat Rayleigh fading channels. Generally, numerical results were provided to show the advantage of the outage probability performance in one-way and two-way cooperative communication systems and has been confirmed that the theoretical values for the new outage probability match the simulated results. In practice, there is an effective problem of synchronization between the distributed relay nodes, therefore the next chapter will consider how to mitigate time misalignments among system nodes.

Chapter 5

OFDM-BASED MODIFIED QUASI-ORTHOGONAL SPACE-TIME SCHEME FOR USE IN ONE-WAY AND TWO-WAY ASYNCHRONOUS COOPERATIVE NETWORKS

One of the key challenges to design high-performance distributed space-time code systems is symbol-level synchronization among the relay nodes. Therefore, in this chapter, one-way and two-way asynchronous cooperative relay networks are considered. An orthogonal frequency-division multiplexing (OFDM) scheme with cyclic prefix (CP) is used in the proposed cooperative relay networks to mitigate the effects of time delays. Furthermore, when the number of available relays is more than two, a relay selection technique is used to select the best two relays. The OFDM scheme and the selection technique could improve the system performance as confirmed in the simulations.

5.1 Introduction

In wireless communication systems, the relay nodes within cooperative systems are spread over different locations which makes synchronization between these nodes difficult, and in most cases it is impossible to achieve perfect synchronization among distributed nodes. These imperfections provide a number of technical challenges for reliable wireless communication systems. In order to achieve full cooperative diversity gain, most previous authors made an assumption that perfect timing synchronisation between the cooperative relay nodes is required or propagation delays are identical e.g. [39], [73] and [69]. However, in a practical distributed MIMO system, this assumption is not a real representation of the transmission environment, since relay nodes are located at different places. Recently, there have been studies on space-time codes to achieve asynchronous cooperative spatial diversity, for example, in [97] the author proposed a new transmission scheme which employs distributed space-time block codes to achieve full diversity while tolerating imperfect synchronization. In [98], a space-frequency code to encode the information symbols across subcarriers at the relays to achieve full cooperative diversity and full multipath diversity for asynchronous communications was proposed. In [99], another scheme was proposed in which the OFDM pre-coding over relay nodes is avoided which results in reduced computational complexity. However, this scheme was proposed for a wireless system with only two relays and therefore the maximum achievable cooperative diversity is order two. Utilizing more than two relay nodes will result in improved diversity; hence, better mitigating the detrimental effects of fading channels. In this chapter, an asynchronous cooperative system is assumed for one-way and two-way relay networks using the M-D-QO-STBC scheme (explained in Chapter 3, Section 3.2). The effect of random delays is mitigated by implementing the orthogonal frequency-division multiplexing

(OFDM) technique and adding a cyclic prefix (CP) at the source. It is assumed that each relay has two antennas and at least two relays are available in each proposed network in this chapter. The system performance is further improved by using a relay selection technique when there are more than two relays available. The simulation results show the advantage of using the OFDM technique to mitigate the effect of random delays as well as the advantage of using a relay selection scheme. In the next section, a one-way asynchronous relay network is considered.

5.2 System model for one-way asynchronous cooperative relay network

Figure 5.1 shows the proposed asynchronous wireless cooperative network for one-way transmission. It consists of a source node T_x, a destination node R_x and relay nodes R_N where the source and destination nodes utilize one antenna while each relay node has two half-duplex antennas ($n = 1, 2$) for either reception or transmission. It is assumed that exact channel state information (CSI) is available at the destination and the distance between each pair of antennas on each relay is equal to at least half of the transmitted wavelength. The channel from the transmitter to the i-th relay and from the i-th relay to the receiver are denoted by $h_{s,r_{in}}$ and $h_{r_{in},d}$ respectively, where $i = 1, ..., N$. It is also assumed that the channels between any two nodes are modeled as quasi static Rayleigh flat fading channels. The asynchronism in the figure is modeled by the delays τ_{i1} and τ_{i2} for $i = 2, ..., N$ and the parameters τ_{i1} and τ_{i2} are assumed to be random integer variables in the range from 0 to 15 with uniform distribution. In order to achieve full diversity order over flat fading channels and without a synchronous transmission assumption among relay nodes, the system is designed to perform the following processes:

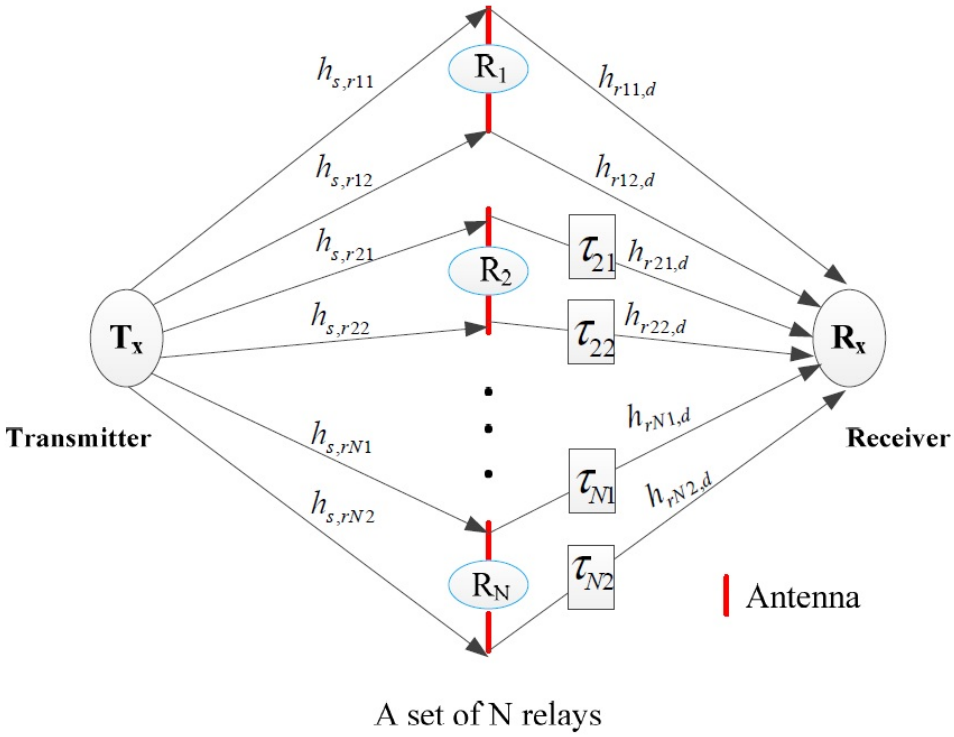

Figure 5.1. A one-way asynchronous cooperative relay network constituting of source, destination and N two-antenna relay nodes. Asynchronism is modeled by the delays τ_{i1}, τ_{i2} for $i = 2, ..., N$.

5.2.1 Source node processing

In this stage, information bits are mapped to complex symbols z_y^k as a first step of the process. At the next step each block of modulated symbols is used by an OFDM modulator of M subcarriers. Denote four consecutive OFDM blocks as $\mathbf{z}^k = [z_0^k \ , ..., \ z_{M-1}^k]^T$, where k is OFDM block index, $k = 1, 2, 3, 4$, and $(.)^T$ denotes the transpose operation. Moreover, the first block $\mathbf{z}^1$ and the third block $\mathbf{z}^3$ are modulated by an M-point inverse discrete Fourier transform (IDFT), and the second block $\mathbf{z}^2$ and the fourth block $\mathbf{z}^4$ are modulated by an M-point discrete Fourier transform (DFT). Then each OFDM block is preceded by a CP with length $l_{cp} = 16$, therefore, each OFDM symbol consists of $M + l_{cp}$ samples. Denote four consecutive time domain OFDM symbols as $\overline{\mathbf{z}}^1$, $\overline{\mathbf{z}}^2$, $\overline{\mathbf{z}}^3$ and $\overline{\mathbf{z}}^4$, where $\overline{\mathbf{z}}^1$ consists of the IDFT($\mathbf{z}^1$) and the corresponding CP, $\overline{\mathbf{z}}^2$ consists of the DFT($\mathbf{z}^2$) and

the corresponding CP, $\overline{\mathbf{z}}^3$ consists of the IDFT($\mathbf{z}^3$) and the corresponding CP and $\overline{\mathbf{z}}^4$ consists of the DFT($\mathbf{z}^4$) and the corresponding CP. Finally, the OFDM symbols are sent to the relay nodes

5.2.2 Relay nodes processing

In this stage, the received signals at the relay nodes are processed and forwarded to the destination. It is assumed that the channel coefficients are constant during four OFDM symbol intervals. The received signal at the n-th antenna in the i-th relay for four successive OFDM symbol durations can be written as

$$\mathbf{r}_{in}^{k} = \sqrt{P_1}\overline{\mathbf{z}}^{k}\ h_{s,r_{in}} + \mathbf{v}_{in}^{k} \tag{5.2.1}$$

where $\sqrt{P_1}$ is the transmission power at the source node and $\mathbf{v}_{in}^{k}$ is the corresponding additive white Gaussian noise (AWGN) at the antenna relay node with zero-mean and unity-variance elements in four successive OFDM symbol durations where $k = 1, 2, 3, 4$. The received noisy signal at the relay nodes is processed and transmitted to the destination according to the jth column of the relay block encoding matrix

$$\mathcal{B}\begin{bmatrix} \mathbf{r}_{11}^{1} & -(\mathbf{r}_{12}^{2})^{*} & \mathbf{r}_{21}^{3} & -(\mathbf{r}_{22}^{4})^{*} \\ \zeta(\mathbf{r}_{11}^{2}) & \zeta((\mathbf{r}_{12}^{1})^{*}) & \zeta(\mathbf{r}_{21}^{4}) & \zeta((\mathbf{r}_{22}^{3})^{*}) \\ \mathbf{r}_{11}^{3} & -(\mathbf{r}_{12}^{4})^{*} & \mathbf{r}_{21}^{1} & -(\mathbf{r}_{22}^{2})^{*} \\ \zeta(\mathbf{r}_{11}^{4}) & \zeta((\mathbf{r}_{12}^{3})^{*}) & \zeta(\mathbf{r}_{21}^{2}) & \zeta((\mathbf{r}_{22}^{1})^{*}) \end{bmatrix} \tag{5.2.2}$$

where $\zeta(.)$ denotes the modulo-M time-reversal of the signal, $\mathcal{B} = \sqrt{\frac{P_2}{P_1+1}}$ as defined in [39] and P_2 is the average transmission power at each relay. The optimum power allocation proposed in [62] is used therefore, $P_1 = \frac{\mathrm{P}}{2}$ and $P_2 = \frac{\mathrm{P}}{2\mathrm{R}_N}$ where P is the total transmission power in the whole system.

5.2.3 Destination node processing

At this node, timing synchronization is implemented for the path from the first relay node and the other relay nodes have timing error τ_{in}, where $\tau_{in} < l_{cp}$. To remove the impact of timing errors in the received OFDM symbols, two steps are implemented to process the data; step one: the CP is removed from each OFDM symbol block as in a conventional OFDM system and as is shown in Figure 5.2; the second step: as the time reversal $\zeta(.)$ operation is performed in (5.2.2) which causes misalignment in the second and the fourth frames, a reordering process is therefore needed to correct the misalignment in the frames. Since $\tau_{in} < l_{cp}$ the orthogonality between the subcarriers is obtained. Due to the asynchronism in the system the delay in the time domain is represented as a phase change in the frequency domain,

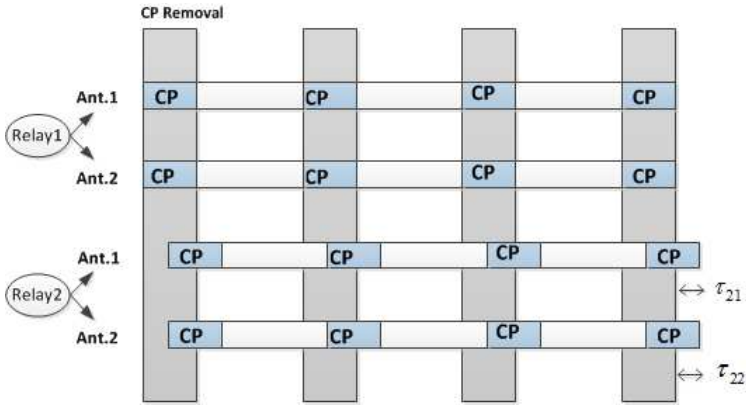

Figure 5.2. CP-removal based on relay one (two antennas) synchronization.

$$\mathbf{D}_y^{\tau_{in}} = [D_0^{\tau_{in}}, D_1^{\tau_{in}}, ..., D_{M-1}^{\tau_{in}}]^T \tag{5.2.3}$$

where $D_y^{\tau_{in}} = e^{\frac{-j2\pi y\tau_{in}}{M}}$ and $y = 0, 1, ..., M-1$, let

$$\mathbf{z}_{11} = [z_{1,0}, z_{1,1}, ..., z_{1,M-1}]^T, \qquad \mathbf{z}_{12} = [z_{2,0}, z_{2,1}, ..., z_{2,M-1}]^T$$

$$\mathbf{z}_{21} = [z_{3,0}, z_{3,1}, ..., z_{3,M-1}]^T \text{ and } \mathbf{z}_{22} = [z_{4,0}, z_{4,1}, ..., z_{4,M-1}]^T$$

be the received four successive OFDM blocks at the destination after removing the CP and taking the DFT transformations. If $\mathcal{B}_T = \sqrt{\frac{P_1 P_2}{P_1+1}}$ as in [39], then the received signals at the destination node are

$$\begin{aligned}\mathbf{z}_{11} = \mathcal{B}_T[&DFT(IDFT(\mathbf{z}^1))h_{s,r_{11}}h_{r_{11},d} + DFT(-(DFT(\mathbf{z}^2))^*)h^*_{s,r_{12}}h_{r_{12},d}\\ &+DFT(IDFT(\mathbf{z}^3))\mathrm{o}\mathbf{D}^{\tau_{21}}h_{s,r_{21}}h_{r_{21},d}+DFT(-(DFT(\mathbf{z}^4)))\mathrm{o}\mathbf{D}^{\tau_{22}}h^*_{s,r_{22}}\\ &h_{r_{22},d} + \tilde{\mathbf{v}}^1_{11}h_{r_{11},d} + \tilde{\mathbf{v}}^2_{11}h_{r_{12},d} + \tilde{\mathbf{v}}^3_{11}\mathrm{o}\mathbf{D}^{\tau_{21}}h_{r_{21},d} + \tilde{\mathbf{v}}^4_{11}\mathrm{o}\mathbf{D}^{\tau_{22}}h_{r_{22},d}] + \mathbf{d}_{11}\end{aligned} \tag{5.2.4}$$

$$\begin{aligned}\mathbf{z}_{12} =&\mathcal{B}_T[DFT(\zeta(IDFT(\mathbf{z}^2)))h_{s,r_{11}}h_{r_{11},d}+DFT(\zeta((DFT(\mathbf{z}^1)))^*)h^*_{s,r_{12}}h_{r_{12},d}\\ &+ DFT(\zeta(IDFT(\mathbf{z}^4)))\mathrm{o}D^{\tau_{21}}h_{s,r_{21}}h_{r_{21},d} + DFT(\zeta((DFT(\mathbf{z}^3))))\mathrm{o}D^{\tau_{22}}\\ &h^*_{s,r_{22}}h_{r_{22},d}+\tilde{\mathbf{v}}^1_{12}h_{r_{11},d}+\tilde{\mathbf{v}}^2_{12}h_{r_{12},d}+\tilde{\mathbf{v}}^3_{12}\mathrm{o}\mathbf{D}^{\tau_{21}}h_{r_{21},d}+\tilde{\mathbf{v}}^4_{12}\mathrm{o}\mathbf{D}^{\tau_{22}}h_{r_{22},d}]+\mathbf{d}_{12}\end{aligned} \tag{5.2.5}$$

$$\begin{aligned}\mathbf{z}_{21} = \mathcal{B}_T[&DFT(IDFT(\mathbf{z}^3))h_{s,r_{11}}h_{r_{11},d} + DFT(-(DFT(\mathbf{z}^4))^*)h^*_{s,r_{12}}h_{r_{12},d}\\ &+DFT(IDFT(\mathbf{z}^1))\mathrm{o}D^{\tau_{21}}h_{s,r_{21}}h_{r_{21},d}+DFT(-(DFT(\mathbf{z}^2)))\mathrm{o}D^{\tau_{22}}h^*_{s,r_{22}}\\ &h_{r_{22},d} + \tilde{\mathbf{v}}^1_{21}h_{r_{11},d} + \tilde{\mathbf{v}}^2_{21}h_{r_{12},d} + \tilde{\mathbf{v}}^3_{21}\mathrm{o}\mathbf{D}^{\tau_{21}}h_{r_{21},d} + \tilde{\mathbf{v}}^4_{21}\mathrm{o}\mathbf{D}^{\tau_{22}}h_{r_{22},d}] + \mathbf{d}_{21}\end{aligned} \tag{5.2.6}$$

$$\begin{aligned}\mathbf{z}_{22} =&\mathcal{B}_T[DFT(\zeta(IDFT(\mathbf{z}^4)))h_{s,r_{11}}h_{r_{11},d}+DFT(\zeta((DFT(\mathbf{z}^3)))^*)h^*_{s,r_{12}}h_{r_{12},d}\\ &+ DFT(\zeta(IDFT(\mathbf{z}^2)))\mathrm{o}D^{\tau_{21}}h_{s,r_{21}}h_{r_{21},d} + DFT(\zeta((DFT(\mathbf{z}^1))))\mathrm{o}D^{\tau_{22}}\\ &h^*_{s,r_{22}}h_{r_{22},d}+\tilde{\mathbf{v}}^1_{22}h_{r_{11},d}+\tilde{\mathbf{v}}^2_{22}h_{r_{12},d}+\tilde{\mathbf{v}}^3_{22}\mathrm{o}\mathbf{D}^{\tau_{21}}h_{r_{21},d}+\tilde{\mathbf{v}}^4_{22}\mathrm{o}\mathbf{D}^{\tau_{22}}h_{r_{22},d}] + \mathbf{d}_{22}\end{aligned} \tag{5.2.7}$$

where $\mathbf{d}_{in}$ is the noise vector with zero mean AWGN elements at the destination node, $\tilde{\mathbf{v}}^k_{in}$ is the DFT of $\mathbf{v}^k_{in}$ and o is the Hadamard product. By using

$$(IDFT(\mathbf{z}))^* = DFT(\mathbf{z}^*), \quad (DFT(\mathbf{z}))^* = IDFT(\mathbf{z}^*)$$
$$\text{and} \quad DFT(\zeta(DFT(\mathbf{z}))) = IDFT((DFT(\mathbf{z})))$$

then, the received data signals (5.2.4), (5.2.5), (5.2.6) and (5.2.7) at each subcarrier y where $y \in [0, ..., M-1]$ can be written as the following quasi-orthogonal design

$$\begin{bmatrix} z_{y,11} \\ z_{y,12} \\ z_{y,21} \\ z_{y,22} \end{bmatrix} = B_T \begin{bmatrix} z_{y,1} & -z^*_{y,2} & z_{y,3} & -z^*_{y,4} \\ z_{y,2} & z^*_{y,1} & z_{y,4} & z^*_{y,3} \\ z_{y,3} & -z^*_{y,4} & z_{y,1} & -z^*_{y,2} \\ z_{y,4} & z^*_{y,3} & z_{y,2} & z^*_{y,1} \end{bmatrix} \begin{bmatrix} h_{y,s,r_{11}} h_{y,r_{11},d} \\ h^*_{y,s,r_{12}} h_{y,r_{12},d} \\ D_y^{\tau_{21}} h_{y,s,r_{21}} h_{y,r_{21},d} \\ D_y^{\tau_{22}} h^*_{y,s,r_{22}} h_{y,r_{22},d} \end{bmatrix} + \begin{bmatrix} w_{y,11} \\ w_{y,12} \\ w_{y,21} \\ w_{y,22} \end{bmatrix} \tag{5.2.8}$$

where $w_{y,in} = \mathcal{B}(v^1_{y,11} h_{r_{11},d} + v^2_{y,12} h_{r_{12},d} + v^3_{y,21} D_y^{\tau_{21}} h_{r_{21},d} + v^4_{y,22} D_y^{\tau_{22}} h_{r_{22},d} + d_{y,11} + d_{y,12} + d_{y,21} + d_{y,22})$. The quasi orthogonal code in (5.2.8) requires pairwise decoding at the destination.

Modified distributed quasi-orthogonal STBC (M-D-QO-STBC) is also used in this proposed relay network, which was explained in detail in Chapter 3, Section 3.2. In the next section, the relay selection technique is considered.

5.2.4 Relay selection technique

When the number of available relays is more than two, then a relay selection method based on local measurements of the instantaneous end-to-end wireless channel conditions is used to select the best two relays from a set of N available relays [75]. Then the selected relays are used for cooperation between the source node and the destination node. According to the CSI, the maximum and minimum gains of each relay node can be determined at the destination. Therefore, the SNR at the destination node is given by

$$\gamma_D = \sum_{i \in R_R} \sum_{n \in 1,2} \frac{\gamma_{s,r_{in}} \gamma_{r_{in},d}}{1 + \gamma_{s,r_{in}} + \gamma_{r_{in},d}} \tag{5.2.9}$$

where R_R represents the set of relay indices for the relays selected in the multi-relay selection scheme; $\gamma_{s,r_{in}}$ and $\gamma_{r_{in},d}$ are the instantaneous SNR of the links from the source to the relay node antenna and from the relay node

antenna to the destination respectively and given as $\gamma_{s,r_{in}} = |h_{s,r_{in}}|^2 \frac{E_s}{N_0}$ and $\gamma_{r_{in},d} = |h_{r_{in},d}|^2 \frac{E_s}{N_0}$ where E_s is the average energy per symbol and N_0 is the noise variance. The relay selection procedure has two steps, firstly, a group of relays is selected according to the condition $\tau_{max} < l_c$ then the best two relays are selected from the selected group where $\tau = 0$ for the first relay node. The policy of selecting the single two antenna relay can be expressed as

$$\Upsilon_{i1} = \min\{\gamma_{s,r_{i1}}, \gamma_{r_{i1},d}\}, \text{ and } \Upsilon_{i2} = \min\{\gamma_{s,r_{i2}}, \gamma_{r_{i2},d}\}$$

Therefore, the best relay node can be selected as

$$\max_{i \in 1,\ldots,N} \{\min\{\Upsilon_{i1}, \Upsilon_{i2}\}\}.$$

In the next section, the performance of the proposed asynchronous one-way relay network with the relay selection technique will be assessed by simulation.

5.2.5 Simulation results

In this section, simulation results using MATLAB software show the performance of the proposed asynchronous one-way M-D-QO-STBC scheme using QPSK modulation. For all simulation comparisons, the average end-to-end codeword error rate (CWER) is calculated and OFDM coding with 64 subcarriers and a CP length of 16 is used. It is assumed that, at least two relay nodes are available in the proposed system, each relay node has two antennas and the transmitter and receiver nodes have one antenna. It is also assumed that there is no direct link between the transmitter and the receiver. It is assumed that the channels are Rayleigh flat fading and the real and imaginary parts of the channels and noise are generated by using the MATLAB function randn(). Figure 5.3 shows the results of detection at the destination node for the D-QO-STBC and M-D-QO-STBC schemes. It can be observed

from the figure that the detection does not achieve the available cooperative diversity gain and cannot deliver a good end-to-end performance under imperfect synchronization for both schemes. On the other hand, the figure shows that the OFDM-based scheme can significantly mitigate the delay when $\tau <$ CP which enhances the performance of the system under imperfect synchronization. In addition the simulations show that the OFDM-based M-D-QO-STBC scheme provides a better performance over the OFDM-based conventional D-QO-STBC [39] due to achieving full spatial diversity and

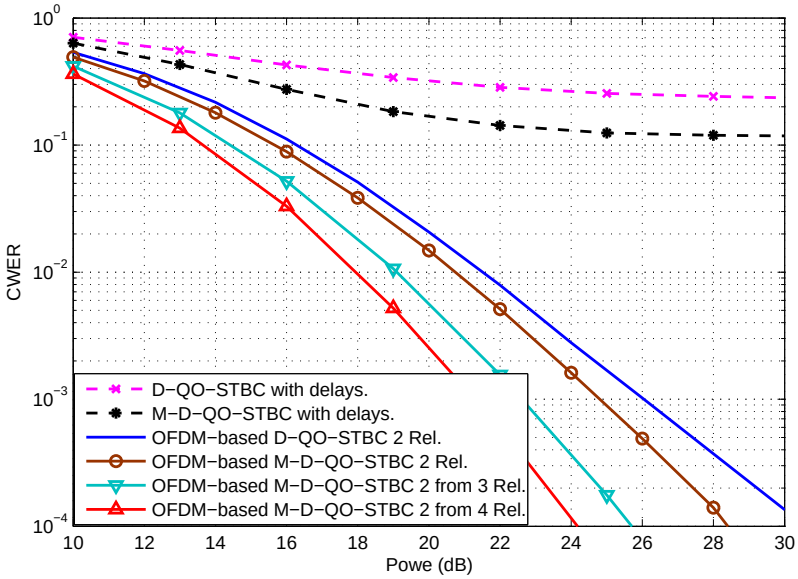

Figure 5.3. Performance of OFDM-based M-D-QO-STBC for one-way asynchronous cooperative relay network with relay selection technique using QPSK signal.

the improvement in the code gain distance (CGD) which was obtained from the maximization of the distance properties of the original codebooks of the modified code as shown in Chapter 3, Section 3.2.3. The figure also shows that, when the number of available relays, under the condition of $\tau <$ CP, is more than two the relay selection technique improves the system performance significantly. For example, when the number of available relays increases from two to three, the power saving provided is approximately 2.5

dB and 3.5 dB compared to the M-D-QO-STBC scheme with two relays and the conventional D-QO-STBC scheme respectively at a CWER probability of 10^{-3}. And when the number of available relays increases to four relays, the proposed system performance improves by approximately 4 dB compared to the proposed system with two relays, this improvement is due to the improvement in the diversity as the number of available relays increases. In the next section, OFDM-based for asynchronous two-way cooperative network will be considered.

5.3 Two-way asynchronous cooperative relay network using M-QO-STBC

In this section, a M-D-QO-STBC scheme using the OFDM method for a two-way asynchronous cooperative system is presented, where the OFDM method is implemented at both terminals, and simple operations i.e. time-reversion and complex conjugation are implemented at the relay nodes. The cyclic prefixes (CP) at both terminals are used for combating the timing errors introduced by the relay nodes.

5.3.1 System model

Consider a wireless network with relay nodes R_N, and two terminal nodes T_m where $m = 1, 2$ as shown in Figure 5.4. Each terminal node is equipped with one half-duplex antenna, whereas, each relay node has two half-duplex antennas ($n = 1, 2$). It is assumed that there is no direct path between the two terminals due to shadowing effects or path loss. The two terminals depend on the relay nodes, which exploit an amplify-and-foreword (AF) protocol, to exchange their information. The channel from T_1 to the i-th relay and from T_2 to the i-th relay are denoted f_{in} and g_{in} respectively where $i = 1, ..., N$. It is also assumed that the channel coefficients are unchanged

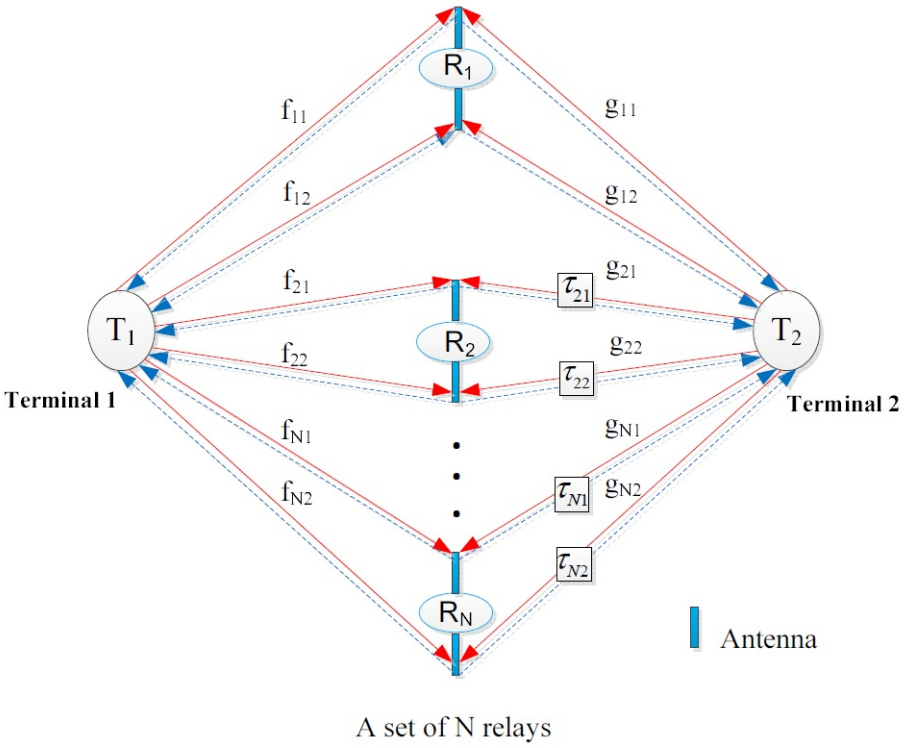

Figure 5.4. A two-way asynchronous cooperative relay network consisting of two terminal nodes and N relay nodes.

during the transmission of a signal code block (quasi-static frequency-flat Rayleigh fading) between any two nodes and they are known to the receiving terminals. In order to achieve full diversity over flat fading channels and without a synchronous transmission assumption among relay nodes, the two-way relay system is designed to perform the following processes:

5.3.2 Transmission process at terminals

In this stage, firstly, the information at the two terminals are mapped onto complex symbols and fed to an OFDM modulator with M subcarriers, then the terminals broadcast their information. Denote the four consecutive OFDM blocks at each terminal as $\mathbf{z}_m^k = [z_{0,m}^k, ..., z_{M-1,m}^k]^T$ where k represents OFDM block index, $k = 1, 2, 3, 4$, and m is the terminal number, $m = 1, 2$. At each terminal, the first block $\mathbf{z}_m^1$ and the third block $\mathbf{z}_m^3$ are modulated by an M-point inverse discrete Fourier transform (IDFT),

then these OFDM blocks are preceded by a CP with length $l_{cp_m} = 16$. In contrast, the second block $\mathbf{z}_m^2$ and the fourth block $\mathbf{z}_m^4$ are modulated by an M-point discrete Fourier transform (DFT), then these OFDM blocks are preceded by a CP with length $l_{cp_m} = 16$. Thus, each OFDM symbol consists of $M + l_{cp_m}$ samples. Therefore, denote the four consecutive time domain OFDM symbols at each terminal as $\overline{\mathbf{z}}_m^1$, $\overline{\mathbf{z}}_m^2$, $\overline{\mathbf{z}}_m^3$ and $\overline{\mathbf{z}}_m^4$ where $\overline{\mathbf{z}}_m^1$ consists of the IDFT($\mathbf{z}_m^1$) and the corresponding CP, $\overline{\mathbf{z}}_m^2$ consists of the DFT($\mathbf{z}_m^2$) and the corresponding CP, $\overline{\mathbf{z}}_m^3$ consists of the IDFT($\mathbf{z}_m^3$) and the corresponding CP and $\overline{\mathbf{z}}_m^4$ consists of the DFT($\mathbf{z}_m^4$) and the corresponding CP. Finally, each terminal T_m sends the OFDM symbols to the relay nodes.

5.3.3 Transmission process at relay nodes

In this stage, the received information at the relay nodes is processed and forwarded to the terminals. It is assumed that the channel coefficients are constant during four OFDM symbol intervals. The received four successive OFDM symbol durations at the n-th antenna in the i-th relay from the two terminals are given by

$$\mathbf{r}_{in}^k = \sqrt{T_s P_{\mathrm{T}_1}}\overline{\mathbf{z}}_1^k \; f_{in} + \sqrt{T_s P_{\mathrm{T}_2}}\overline{\mathbf{z}}_2^k \; g_{in} + \mathbf{v}_{in}^k \tag{5.3.1}$$

where P_{T_m} is power transmission at each terminal where $m = 1, 2$, T_s is the time slot and $\mathbf{v}_{in}^k$ represents a noise vector with elements of zero mean AWGN at the n-th antenna in the i-th relay node with unit variance and zero mean. The optimum power allocation proposed in [62] is used therefore, if P denotes the total transmission power in the whole system, and P_R is the total relay node power, then $P_{\mathrm{T}_1} = P_{\mathrm{T}_2} = \frac{P}{4}$ and $P_R = \frac{P}{2}$. Each relay node next pre-codes the received data packet from both terminals, and then transmits the data back to both terminals. Before the relay nodes transmit their information, simple operations such as time-reversion and

complex conjugation are implemented. Therefore, the encoding matrix at the relay nodes can be represented as

$$\mathbb{B}\begin{bmatrix} \mathbf{r}_{11}^{1} & -(\mathbf{r}_{12}^{2})^{*} & \mathbf{r}_{21}^{3} & -(\mathbf{r}_{22}^{4})^{*} \\ \zeta(\mathbf{r}_{11}^{2}) & \zeta((\mathbf{r}_{12}^{1})^{*}) & \zeta(\mathbf{r}_{21}^{4}) & \zeta((\mathbf{r}_{22}^{3})^{*}) \\ \mathbf{r}_{11}^{3} & -(\mathbf{r}_{12}^{4})^{*} & \mathbf{r}_{21}^{1} & -(\mathbf{r}_{22}^{2})^{*} \\ \zeta(\mathbf{r}_{11}^{4}) & \zeta((\mathbf{r}_{12}^{3})^{*}) & \zeta(\mathbf{r}_{21}^{2}) & \zeta((\mathbf{r}_{22}^{1})^{*}) \end{bmatrix} \tag{5.3.2}$$

where $\mathbb{B} = \sqrt{\frac{T_s P_R}{N(T_s P_{\mathrm{T}_1} + T_s P_{\mathrm{T}_2} + 1)}}$ as in [73] and $\zeta(.)$ denotes the modulo-M time-reversal of the signal.

5.3.4 Information extraction process at the terminal nodes

At the terminal nodes, timing synchronization is implemented for the path from T_1 to T_2 through the first relay node and other paths have delays of τ_{in}. Therefore, the relayed signals arrive at each terminal at different time instants. To remove the impact of timing errors, both terminals perform the following operations:

1. Remove the CP from each received OFDM symbol.
2. Perform the reordering process on the OFDM received frames to correct for the misalignment caused by the time reversal by shifting the last l_{cp_m} samples of the M-point vector as the first l_{cp_m} samples.
3. Each terminal subtracts its own signal.

Due to the asynchronism in the system the delay in the time domain is represented as a phase change in the frequency domain,

$$\mathbf{D}_y^{\tau_{in,m}} = [D_0^{\tau_{in,m}}, D_1^{\tau_{in,m}}, ..., D_{M-1}^{\tau_{in,m}}]^T \tag{5.3.3}$$

where $D_y^{\tau_{in,m}} = e^{\frac{-j2\pi y\tau_{in,m}}{M}}$ and $y = 0, 1, ..., M-1$, let

$$\mathbf{z}_{\mathrm{T}_m,11} = [z_{1,0}, z_{1,1}, ..., z_{1,M-1}]^T, \qquad \mathbf{z}_{\mathrm{T}_m,12} = [z_{2,0}, z_{2,1}, ..., z_{2,M-1}]^T$$
$$\mathbf{z}_{\mathrm{T}_m,21} = [z_{3,0}, z_{3,1}, ..., z_{3,M-1}]^T \text{ and } \mathbf{z}_{\mathrm{T}_m,22} = [z_{4,0}, z_{4,1}, ..., z_{4,M-1}]^T$$

be the received four successive OFDM blocks at the two terminals after removing the CP and taking the DFT transformations. If $\mathbb{B}_T = \sqrt{\frac{T_s P_R P_{\mathrm{T}_m}}{N(T_s P_{\mathrm{T}_1} + T_s P_{\mathrm{T}_2} + 1)}}$ [73], then the received signals at terminal T_1 can be written as

$$\begin{aligned}\mathbf{z}_{\mathrm{T}_1,11} =& \mathbb{B}_T[DFT(IDFT(\mathbf{z}_2^1))g_{11}f_{11} + DFT(-(DFT(\mathbf{z}_2^2))^*)g_{12}^*f_{12} + DFT \\ & (IDFT(\mathbf{z}_2^3))\mathrm{o}\mathbf{D}^{\tau_{21}}g_{21}f_{21} + DFT(-(DFT(\mathbf{z}_2^4)))\mathrm{o}\mathbf{D}^{\tau_{22}}g_{22}^*f_{22} + \tilde{\mathbf{v}}_{11}^1 f_{11} \\ & + \tilde{\mathbf{v}}_{11}^2 f_{12} + \tilde{\mathbf{v}}_{11}^3\mathrm{o}\mathbf{D}^{\tau_{21}}f_{21} + \tilde{\mathbf{v}}_{11}^4\mathrm{o}\mathbf{D}^{\tau_{22}}f_{22}] + \mathbf{d}_{\mathrm{T}_1,11}\end{aligned} \tag{5.3.4}$$

$$\begin{aligned}\mathbf{z}_{\mathrm{T}_1,12} =& \mathbb{B}_T[DFT(\zeta(IDFT(\mathbf{z}_2^2)))g_{11}f_{11} + DFT(\zeta((DFT(\mathbf{z}_2^1)))^*)g_{12}^*f_{12} + \\ & DFT(\zeta(IDFT(\mathbf{z}_2^4)))\mathrm{o}D^{\tau_{21}}g_{21}f_{21} + DFT(\zeta(((DFT(\mathbf{z}_2^3)))))\mathrm{o}D^{\tau_{22}}g_{22}^*f_{22} + \\ & \tilde{\mathbf{v}}_{12}^1 f_{11} + \tilde{\mathbf{v}}_{12}^2 f_{12} + \tilde{\mathbf{v}}_{12}^3\mathrm{o}\mathbf{D}^{\tau_{21}}f_{21} + \tilde{\mathbf{v}}_{12}^4\mathrm{o}\mathbf{D}^{\tau_{22}}f_{22}] + \mathbf{d}_{\mathrm{T}_1,12}\end{aligned} \tag{5.3.5}$$

$$\begin{aligned}\mathbf{z}_{\mathrm{T}_1,21} =& \mathbb{B}_T[DFT(IDFT(\mathbf{z}_2^3))g_{11}f_{11} + DFT(-(DFT(\mathbf{z}_2^4))^*)g_{12}^*f_{12} + DFT \\ & (IDFT(\mathbf{z}_2^1))\mathrm{o}D^{\tau_{21}}g_{21}f_{21} + DFT(-(DFT(\mathbf{z}_2^2)))\mathrm{o}D^{\tau_{22}}g_{22}^*f_{22} + \tilde{\mathbf{v}}_{21}^1 f_{11} \\ & + \tilde{\mathbf{v}}_{21}^2 f_{12} + \tilde{\mathbf{v}}_{21}^3\mathrm{o}\mathbf{D}^{\tau_{21}}f_{21} + \tilde{\mathbf{v}}_{21}^4\mathrm{o}\mathbf{D}^{\tau_{22}}f_{22}] + \mathbf{d}_{\mathrm{T}_1,21}\end{aligned} \tag{5.3.6}$$

$$\begin{aligned}\mathbf{z}_{\mathrm{T}_1,22} =& \mathbb{B}_T[DFT(\zeta(IDFT(\mathbf{z}_2^4)))g_{11}f_{11} + DFT(\zeta((DFT(\mathbf{z}_2^3)))^*)g_{12}^*f_{12} + \\ & DFT(\zeta(IDFT(\mathbf{z}_2^2)))\mathrm{o}D^{\tau_{21}}g_{21}f_{21} + DFT(\zeta(((DFT(\mathbf{z}_2^1)))))\mathrm{o}D^{\tau_{22}}g_{22}^*f_{22} + \\ & \tilde{\mathbf{v}}_{22}^1 f_{11} + \tilde{\mathbf{v}}_{22}^2 f_{12} + \tilde{\mathbf{v}}_{22}^3\mathrm{o}\mathbf{D}^{\tau_{21}}f_{21} + \tilde{\mathbf{v}}_{22}^4\mathrm{o}\mathbf{D}^{\tau_{22}}f_{22}] + \mathbf{d}_{\mathrm{T}_1,22}\end{aligned} \tag{5.3.7}$$

where $\mathbf{d}_{\mathrm{T}_1,in}$ is the noise vector at T_1 with elements of zero mean AWGN, $\tilde{\mathbf{v}}_{in}^{k}$ is the DFT of $\bar{\mathbf{v}}_{in}^{k}$ and o is the Hadamard product. By using

$$(IDFT(\mathbf{z}))^* = DFT(\mathbf{z}^*), \quad (DFT(\mathbf{z}))^* = IDFT(\mathbf{z}^*)$$
$$\text{and} \quad DFT(\zeta(DFT(\mathbf{z}))) = IDFT((DFT(\mathbf{z})))$$

then, the received data signals (5.3.4), (5.3.5), (5.3.6) and (5.3.7) at each subcarrier y where $y \in [0, ..., M-1]$ can be written as

$$\begin{bmatrix} z_{y,11}^{\mathrm{T}_1} \\ z_{y,12}^{\mathrm{T}_1} \\ z_{y,21}^{\mathrm{T}_1} \\ z_{y,22}^{\mathrm{T}_1} \end{bmatrix} = \mathbb{B}_T \begin{bmatrix} z_{y,1} & -z_{y,2}^* & z_{y,3} & -z_{y,4}^* \\ z_{y,2} & z_{y,1}^* & z_{y,4} & z_{y,3}^* \\ z_{y,3} & -z_{y,4}^* & z_{y,1} & -z_{y,2}^* \\ z_{y,4} & z_{y,3}^* & z_{y,2} & z_{y,1}^* \end{bmatrix} \begin{bmatrix} f_{y,11} & g_{y,11} \\ f_{y,12} & g_{y,12}^* \\ D_y^{\tau_{21}} f_{y,21} & g_{y,21} \\ D_y^{\tau_{22}} f_{y,22} & g_{y,22}^* \end{bmatrix} + \begin{bmatrix} w_{y,11}^{\mathrm{T}_1} \\ w_{y,12}^{\mathrm{T}_1} \\ w_{y,21}^{\mathrm{T}_1} \\ w_{y,22}^{\mathrm{T}_1} \end{bmatrix} \tag{5.3.8}$$

where $w_{y,in}^{\mathrm{T}_1} = \mathbb{B}(v_{y,11}^1 f_{11} + v_{y,12}^2 f_{12} + v_{y,21}^3 D_y^{\tau_{21}} f_{21} + v_{y,22}^4 D_y^{\tau_{22}} f_{22} + d_{\mathrm{T}_1,y,11} + d_{\mathrm{T}_1,y,12} + d_{\mathrm{T}_1,y,21} + d_{\mathrm{T}_1,y,22}$. From (5.3.8), it is clear that, the quasi orthogonal code at each subcarrier is obtained at terminal T_1. In a similar way the signals at terminal T_2 are calculated, and they can be expressed as

$$\begin{aligned} \mathbf{z}_{\mathrm{T}_2,11} = \mathbb{B}_T[&DFT(IDFT(\mathbf{z}_1^1))f_{11}g_{11} + DFT(-(DFT(\mathbf{z}_1^2))^*)f_{12}^* g_{12} + DFT \\ &(IDFT(\mathbf{z}_1^3))\mathrm{o}\mathbf{D}^{\tau_{21}} f_{21} g_{21} + DFT(-(DFT(\mathbf{z}_1^4)))\mathrm{o}\mathbf{D}^{\tau_{22}} f_{22}^* g_{22} + \tilde{\mathbf{v}}_{11}^1 g_{11} \\ &+ \tilde{\mathbf{v}}_{11}^2 g_{12} + \tilde{\mathbf{v}}_{11}^3 \mathrm{o}\mathbf{D}^{\tau_{21}} g_{21} + \tilde{\mathbf{v}}_{11}^4 \mathrm{o}\mathbf{D}^{\tau_{22}} g_{22}] + \mathbf{d}_{\mathrm{T}_2,11} \end{aligned} \tag{5.3.9}$$

$$\begin{aligned} \mathbf{z}_{\mathrm{T}_2,12} = \mathbb{B}_T[&DFT(\zeta(IDFT(\mathbf{z}_1^2)))f_{11}g_{11} + DFT(\zeta((DFT(\mathbf{z}_1^1)))^*)f_{12}^* g_{12} + \\ &DFT(\zeta(IDFT(\mathbf{z}_1^4)))\mathrm{o}D^{\tau_{21}} f_{21} g_{21} + DFT(\zeta((DFT(\mathbf{z}_1^3))))\mathrm{o}D^{\tau_{22}} f_{22}^* g_{22} + \\ &\tilde{\mathbf{v}}_{12}^1 g_{11} + \tilde{\mathbf{v}}_{12}^2 g_{12} + \tilde{\mathbf{v}}_{12}^3 \mathrm{o}\mathbf{D}^{\tau_{21}} g_{21} + \tilde{\mathbf{v}}_{12}^4 \mathrm{o}\mathbf{D}^{\tau_{22}} g_{22}] + \mathbf{d}_{\mathrm{T}_2,12} \end{aligned} \tag{5.3.10}$$

$$\begin{aligned}\mathbf{z}_{\mathrm{T}_2,21} =& \mathbb{B}_T[DFT(IDFT(\mathbf{z}_1^3))f_{11}g_{11} + DFT(-(DFT(\mathbf{z}_1^4))^*)f_{12}^*g_{12} + DFT \\ & (IDFT(\mathbf{z}_1^1))\mathrm{o}D^{\tau_{21}}f_{21}g_{21} + DFT(-(DFT(\mathbf{z}_1^2)))\mathrm{o}D^{\tau_{22}}f_{22}^*g_{22} + \tilde{\mathbf{v}}_{21}^1 g_{11} + \\ & \tilde{\mathbf{v}}_{21}^2 g_{12} + \tilde{\mathbf{v}}_{21}^3\mathrm{o}\mathbf{D}^{\tau_{21}}g_{21} + \tilde{\mathbf{v}}_{21}^4\mathrm{o}\mathbf{D}^{\tau_{22}}g_{22}] + \mathbf{d}_{\mathrm{T}_2,21}\end{aligned} \tag{5.3.11}$$

$$\begin{aligned}\mathbf{z}_{\mathrm{T}_2,22} =& \mathbb{B}_T[DFT(\zeta(IDFT(\mathbf{z}_1^4)))f_{11}g_{11} + DFT(\zeta((DFT(\mathbf{z}_1^3)))^*)f_{12}^*g_{12} + \\ & DFT(\zeta(IDFT(\mathbf{z}_1^2)))\mathrm{o}D^{\tau_{21}}f_{21}g_{21} + DFT(\zeta(((DFT(\mathbf{z}_1^1)))))\mathrm{o}D^{\tau_{22}}f_{22}^*g_{22} + \\ & \tilde{\mathbf{v}}_{22}^1 g_{11} + \tilde{\mathbf{v}}_{22}^2 g_{12} + \tilde{\mathbf{v}}_{22}^3\mathrm{o}\mathbf{D}^{\tau_{21}}g_{21} + \mathbf{v}_{22}^4\mathrm{o}\mathbf{D}^{\tau_{22}}g_{22}] + \mathbf{d}_{\mathrm{T}_2,22}\end{aligned} \tag{5.3.12}$$

where $\mathbf{d}_{\mathrm{T}_2,in}$ is the noise vector at T_2 with elements of zero mean AWGN, and $\tilde{\mathbf{v}}_{in}^k$ is the DFT of $\mathbf{v}_{in}^k$. The received data signals (5.3.9), (5.3.10), (5.3.11), and (5.3.12) can be written as the following quasi-orthogonal design at each subcarrier,

$$\begin{bmatrix} z_{y,11}^{\mathrm{T}_2} \\ z_{y,12}^{\mathrm{T}_2} \\ z_{y,21}^{\mathrm{T}_2} \\ z_{y,22}^{\mathrm{T}_2} \end{bmatrix} = \mathbb{B}_T \begin{bmatrix} z_{y,1} & -z_{y,2}^* & z_{y,3} & -z_{y,4}^* \\ z_{y,2} & z_{y,1}^* & z_{y,4} & z_{y,3}^* \\ z_{y,3} & -z_{y,4}^* & z_{y,1} & -z_{y,2}^* \\ z_{y,4} & z_{y,3}^* & z_{y,2} & z_{y,1}^* \end{bmatrix} \begin{bmatrix} f_{y,11}\ g_{y,11} \\ f_{y,12}^*\ g_{y,12} \\ D_y^{\tau_{21}}f_{y,21}\ g_{y,21} \\ D_y^{\tau_{22}}f_{y,22}^*\ g_{y,22} \end{bmatrix} + \begin{bmatrix} w_{y,11}^{\mathrm{T}_2} \\ w_{y,12}^{\mathrm{T}_2} \\ w_{y,21}^{\mathrm{T}_2} \\ w_{y,22}^{\mathrm{T}_2} \end{bmatrix} \tag{5.3.13}$$

where $w_{y,in}^{\mathrm{T}_2} = \mathbb{B}(v_{y,11}^1 g_{11} + v_{y,12}^2 g_{12} + v_{y,21}^3 D_{y\mathrm{T}_1}^{\tau_{21}} g_{21} + v_{y,22}^4 D_y^{\tau_{22}} g_{22} + d_{\mathrm{T}_2,y,11} + d_{\mathrm{T}_2,y,12} + d_{\mathrm{T}_2,y,21} + d_{\mathrm{T}_2,y,22}$. Equation (5.3.13), shows that, the quasi orthogonal code at each subcarrier is obtained at terminal T_2.

The modified distributed quasi-orthogonal STBC (M-D-QO-STBC) is again also used in this proposed two-way asynchronous relay network, which was explained in detail in Chapter 3 Section 3.5. In the next section, a relay selection technique in two-way relay networks will be considered.

5.3.5 Relay selection technique

When the number of available relays is more than two, then a relay selection technique is used to select the best two relays. In this work the relay selection method employed is based on local measurements of the instantaneous end-to-end wireless channel conditions to select the best two relays from a set of N available relays [75]. Then the selected relays are used for cooperation between the two terminals. According to the channel state information (CSI), the maximum and minimum gains of each relay node can be determined at one of the terminals. The instantaneous end-to-end SNR for the n-th relay antenna are calculated as [76]

$$\gamma_{\mathrm{T}_{1,in}} = \frac{\gamma_{in,1}\gamma_{in,2}}{2\ \gamma_{in,1} + \gamma_{in,2} + 1}, \quad i = 1, \ldots, N \ \text{ and } \ n = 1, 2 \tag{5.3.14}$$

$$\gamma_{\mathrm{T}_{2,in}} = \frac{\gamma_{in,1}\gamma_{in,2}}{\gamma_{in,1} + 2\gamma_{in,2} + 1}, \quad i = 1, \ldots, N \ \text{ and } \ n = 1, 2 \tag{5.3.15}$$

where $\gamma_{in,1} = |f_{in}|^2 \frac{P_{\mathrm{T}_1}}{N_0}$ and $\gamma_{i,2} = |g_{in}|^2 \frac{P_{\mathrm{T}_1}}{N_0}$ are the instantaneous SNRs of the links $\mathrm{T}_1 \leftrightarrow R_{in}$ and $\mathrm{T}_2 \leftrightarrow R_{in}$ respectively and N_0 is the noise variance [76]. Firstly, a group of relay nodes is selecting according to $\tau_{in} < l_{c_m}$, then the best two relay nodes are selected from this group. At both terminals T_1 and T_2, the max-min technique is a suitable scheme to select the single two antenna relay as

$$\Upsilon_{i1}^{\mathrm{T}_m} = \min\{|f_{i1}^{\mathrm{T}_m}|^2, |g_{i1}^{\mathrm{T}_m}|^2\} \text{ and } \Upsilon_{i2}^{\mathrm{T}_m} = \min\{|f_{i2}^{\mathrm{T}_m}|^2, |g_{i2}^{\mathrm{T}_m}|^2\}$$

Therefore, the best relay is selected as

$$\max_{i \in 1,\ldots,N} \{\min\{\Upsilon_{i1}^{\mathrm{T}_m}, \Upsilon_{i2}^{\mathrm{T}_m}\}.$$

This is similar to the relay selection for one-way cooperative multi-node wireless communication systems [84] and [92]. The equivalence can hold

if and only if the two terminals T_1 and T_2 are assumed to have the same transmit power. This selection scheme provides diversity gains on the order of the number of relay nodes in the network [91], and that could improve the proposed scheme performance as will be presented in the simulations in the next section.

5.3.6 Simulation results

In this section, simulation results using MATLAB software show the performance of the proposed asynchronous one-way M-D-QO-STBC scheme using QPSK modulation. For all simulation comparisons, the average end-to-end codeword error rate (CWER) is calculated and OFDM coding with 64 subcarriers and a CP length of 16 is used at each terminal. It is assumed that at least two relay nodes are available in the proposed system, each relay node has two antennas and each terminal node has one antenna. It is also assumed that there is no direct link between the two terminals. It is assumed that the channels are Rayleigh flat fading and the real and imaginary parts of the channels and noise are generated by using the MATLAB function randn(). The integer delays τ_{in} are chosen randomly from 0 to 15 with the uniform distribution. Figure 5.5 shows the results of the proposed M-D-QO-STBC and the impact of relay selection technique on the proposed scheme in two-way relay network. It can be observed from the figure that the detection does not achieve the available cooperative diversity gain and cannot deliver a good end-to-end performance under imperfect synchronization for the proposed scheme. On the other hand, the figure shows the ability of the OFDM method to cope with and mitigate the timing delays in the system, which improves the robustness of the proposed system links and makes the system achieve full diversity and gain the improvement in the code gain distance in the M-D-QO-STBC scheme. The figure also shows that when the number of available relays increases, the power saving of the system is improved due

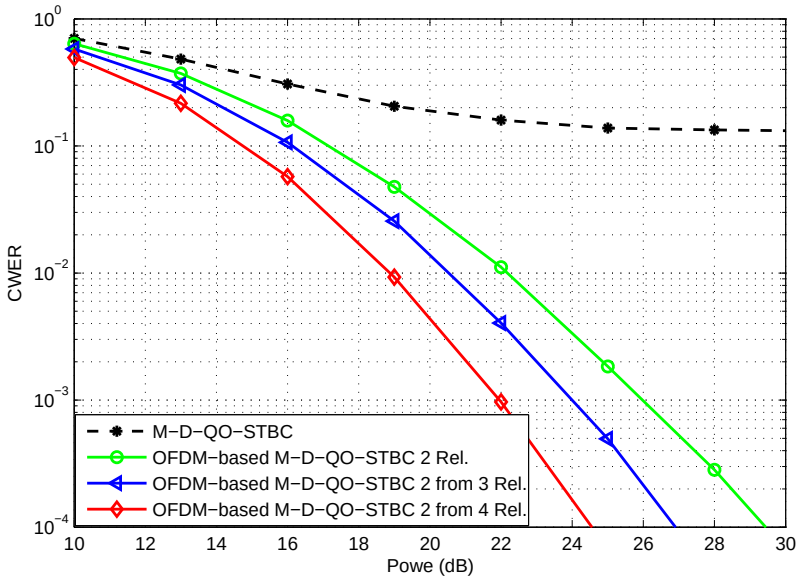

Figure 5.5. Performance of OFDM-based M-D-QO-STBC for two-way asynchronous cooperative relay network with relay selection technique using QPSK signal.

to the improvement in the diversity. For example, at codeword error probability 10^{-3}, when the number of the relays increases from two to three, a saving power of approximately 2 dB is provided, and approximately 4 dB when the number of the relays increases to four.

5.4 Summary

In this chapter, the M-D-QO-STBC scheme for one-way and two-way asynchronous cooperative relay networks was proposed. An OFDM data structure was employed with cyclic prefix (CP) insertion at the source in the one-way cooperative relay network and at the two terminal nodes in the two-way cooperative network to combat the effects of time asynchronicity at the relay nodes. The simulation results indicated that the OFDM-based scheme can significantly mitigate the delay when $\tau <$ CP which enhances the performance of the two systems under imperfect synchronization. It also shown that the performance of the proposed M-D-QO-STBC could be im-

proved by implementing the relay selection technique and that is because this selection scheme provides diversity gains on the order of the number of relay nodes in the network. In the next chapter, outage probability analysis for a cognitive amplify-and-forward relay network with multi-relay selection will be introduced.

Chapter 6

OUTAGE PROBABILITY ANALYSIS OF A COGNITIVE RELAY NETWORK WITH FOUR RELAY SELECTION

In this chapter, performance analysis and evaluation of an amplify-and-forward (AF) type relay cooperative network is investigated where the relays are equipped with cognitive radios. Expressions for outage probability are determined for a frequency flat Rayleigh-fading environment from the received signal-to-noise ratio with perfect and imperfect spectrum acquisition in a proposed cognitive relay network based on distritbuted quasi-orthogonal space-time block coding (D-QO-STBC). When the number of the available relays is more than four then a relay selection (RS) technique is used in order to select the best four cognitive relays from a set of M cognitive relay nodes for the cooperation. In addition a modified distributed quasi-orthogonal space-time block coding (M-D-QO-STBC) scheme with increased code gain distance is considered for use within the proposed cognitive relay network. To utilize the available spectrum opportunities with the modified quasi-orthogonal space-time block code, the code matrix can be adapted to the number of available cognitive relays. Simulation results show that the

four relay selection improves the system performance as is confirmed by the outage probability analysis and also show the modified code can significantly enhance the performance of the system and improve the reliability of the link as compared to conventional distributed quasi-orthogonal space-time block coding.

6.1 Introduction

The huge growth in wireless services has required more spectrum resources which are generally limited and administrated by special bodies [100]. However, cognitive radio (CR) is a key technology that can enhance spectrum utilization by allowing unlicensed secondary users (SUs) to share frequency bands with licensed primary users (PUs) without causing interference to the PUs [101] and [102]. There are two main challenges to the success of cognitive radio which are the primary user detection and the transmission opportunity utilization [35]. In general, CR networks can be divided into three different approaches interweave, underlay and overlay [102] and the overlay approach is assumed in this work. The overlay approach has the advantage of high interference temperature that can be tolerated and good detection of the primary signal. However, a disadvantage of this approach is that the cognitive users are required to sense the spectrum before transmission. Also, cognitive users need to be synchronized with the existing band of the PU. In contrast in the interweave scheme the SUs are only allowed to use the spectrum when PUs are inactive. The main difficulty in this scheme is that of sensing and predicting the activity of the PU in several radio channels. This task becomes more difficult if PUs are highly dynamic or the range of secondary transmissions increases, whereas the underlay approach is a more conservative choice. Rather than tracking the primary user activity and adapting to it, the cognitive users in the underlay approach must

transmit with low transmit power to operate below the noise floor of the PUs ensuring a tolerable interference to the PUs. This restricts underlay cognitive radio to low data rate applications or very short range applications. Cooperative communication technology is a novel technique that has the advantage to improve the signal quality and overcome the limitation of other wireless technologies such as equipment size, heavy shadowing, channel correlation and deep path loss [76]. It is also one of the key methods to enhance the development of CR networks. Recently, the number of studies in the field of cognitive radio capability in cooperative networks has grown considerably [100], [103], [35] and [104]. Generally, the inclusion of cognitive radio in cooperative communications implies equipping the intermediate relay nodes with cognitive radios to provide the capability of radio spectrum sharing among secondary and primary users, in addition to the advantages of cooperative communications. In contrast to the conventional cooperative technique, cognitive relays cooperate and transmit only if spectrum is available.

Exploiting cooperative diversity through relay selection (RS) has recently been considered in [75], [80] and [79] and information theoretic analysis, such as outage probability, has been used for performance evaluation [105], [106] and [107]. Many RS algorithms have been proposed which search over a number of candidate relays with different optimization criteria. Among these selection criteria the work in [75] is based on the method of selecting the best relay according to the local measurement of the instantaneous end-to-end channel gain to improve the system performance, and provide diversity gain on the order of the number of the available relay nodes in the network. This work was extended by the authors in [80] to obtain outage-optimal opportunistic relaying in the context of selecting a relay from a group of M available relays. The authors in [79] provide exact outage and diversity performance forms for selection cooperative relaying and closed form ap-

proximation over a wide range of signal-to-noise-ratio (SNR) regimes with a direct path. In [105] the authors investigated the outage performance and the achievable diversity order of opportunistic relaying used for cooperative cognitive secondary users. The outage performance analysis for cognitive cooperative networks using the best single relay has been proposed in [106], whereas in [107] the outage probability analysis for a wireless two cognitive relay network with perfect and imperfect spectrum acquisition has been considered. In [108] best relay selection in a multi-cell cognitive network with amplify-and-forward (AF) relays in the presence of interference at the secondary relays is studied.

Most RS approaches consider the selection of one or two best relays for cooperation. However, using one or two best relays is not always sufficient to satisfy the required outage probability at the destination. In this work, the outage probability of an amplify-and-forward (AF) cognitive relay network is considered. Furthermore, when there are more than four active relays the RS method is used to select the best four relays for cooperation which improves the system performance, as it is confirmed by outage probability analysis. Increasing the number of selected relays will incur practical overheads such as increased complexity in synchronization. In addition, in terms of distributed space-time coding (DSTC) most codes have been designed in the context of two or four relays, therefore this chapter focuses on four relay selection. To exploit the opportunity of the available spectrum, the code matrix is adapted to the number of active cognitive relay nodes where it is assumed that there are at least two active cognitive relays in each transmission. Also in this work a modified distributed quasi-orthogonal space-time code (M-D-QO-STBC) is generated to be used in the proposed cooperative cognitive network. This modified code is constructed by set partitioning a larger codebook which is built from two quasi-orthogonal space-time QO-STBCs with proper signal rotations, and then applying pruning to arrive at

the desired code rate in a way that increases the code distance [43]. The distance property for a QPSK signal is further increased by using an optimum rotation matrix which is obtained by using a genetic algorithm (GA) method [109].

6.2 Overview of the proposed system

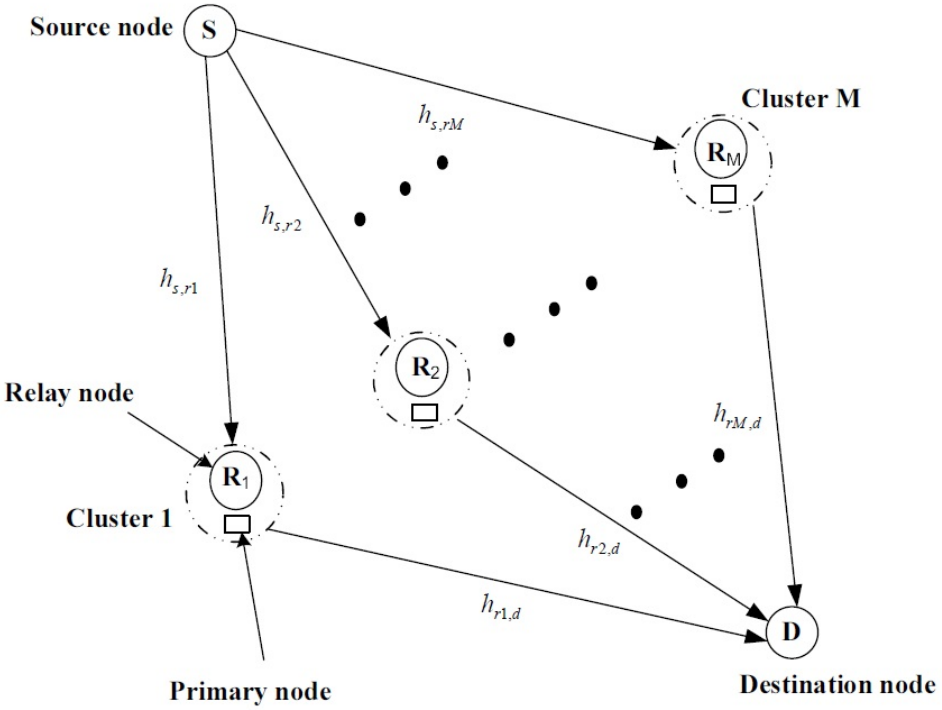

Figure 6.1. A half-duplex cognitive relay network with source node (S), a set of M clusters each consisting of a cognitive relay node (R_m) and a licensed node (shown inside broken circles) and a destination node (D).

A half-duplex cognitive relay network is considered which consists of a source node (S) that intends to communicate with a destination node (D) assisted by a group of clusters (M) of nodes. Each cluster consists of a licensed user node and cognitive relay node R_m where $m = 1, 2, ..., M$ and there is no direct link between the source and destination nodes as depicted in Figure 6.1. The channel between the transmitter and the m-th relay and

from the m-th relay to the receiver are denoted by h_{sr_m} and $h_{r_m d}$ respectively. The channels are assumed to be Rayleigh flat fading and the receiver to have perfect channel state information (CSI)[1]. The relay nodes are acting as CR$_s$ and it is assumed that every cognitive relay is within the transmission range of only one PU node. The cooperative transmission involves a two-step protocol to convey the data from the source to the destination. In step one, the transmitter broadcasts information y to all the cognitive relays, the received information at the m-th relay is given by

$$y_m = \sqrt{E_s} h_{sr_m}\ y + n_{r_m} \tag{6.2.1}$$

where E_s is the average transmit power and n_{r_m} represents the complex additive white Gaussian random noise (AWGN) variable with zero-mean and variance N_0 at the m-th relay. In step two, the m-th relay amplifies its received signal and forwards it to the destination. The received information from the m-th relay at the destination is represented by

$$z = g\ h_{r_m d}\ y_m + n_d \tag{6.2.2}$$

where n_d is the complex AWGN at the destination and g is the relaying gain which is defined as [81]

$$g = \sqrt{\frac{E_s}{|h_{sr_m}|^2 + N_0}} \tag{6.2.3}$$

It is assumed that γ_{sr_m} and $\gamma_{r_m d}$ are the instantaneous SNRs of the paths from the source node to the m-th relay node and from the m-th relay node to the destination node respectively and given as $\gamma_{sr_m} = |h_{sr_m}|^2 \frac{E_s}{N_0}$ and $\gamma_{r_m d} = |h_{r_m d}|^2 \frac{E_s}{N_0}$. Then the the equivalent SNR at the destination for one link

[1]The CSI is usually estimated through pilots and feedback [10] however the CSI estimation without feedback may also be applied [11]. Further study of the CSI estimation is beyond the scope of this work.

assuming $E_S = 1$ is [110]

$$\gamma_m = \frac{\frac{|h_{sr_m}|^2}{N_0}\frac{|h_{r_md}|^2}{N_0}}{\frac{|h_{r_md}|^2}{N_0} + \frac{1}{g^2 N_0}} = \frac{\gamma_{sr_m}\gamma_{r_md}}{1 + \gamma_{sr_m} + \gamma_{r_md}} \tag{6.2.4}$$

As multi-relay selection is used the maximum ratio combiner (MRC) is assumed at the destination [82]. If a time multiplexing approach was used for the transmission between the relays and the destination, the MRC would generate a capacity penalty. This could be mitigated by adopting a classical distributed space-time coding scheme as is applied in the simulations of this chapter. From (6.2.4), the choice of the relay gain defines the equivalent SNR at the destination and can be extending for M relays as

$$\gamma = \sum_{|Ms|} \gamma_m \tag{6.2.5}$$

where $|Ms|$ is the set of selected relays.

6.3 The outage probability analysis

The outage probability can be defined as when the average end-to-end SNR is below the required spectral efficiency threshold (α) and it can be expressed as in [111] as

$$P_{out} = P(\gamma < \alpha) \tag{6.3.1}$$

where $P(.)$ denotes probability. In the proposed system the channels are modeled as Rayleigh frequency flat fading channels therefore the SNRs are modeled as exponential random variables. Therefore the PDF and the CDF of the SNR in $u \in (sr_m, r_md)$ links are given by

$$f_{\gamma_u}(\gamma) = \frac{1}{\hat{\gamma}_u} e^{\frac{-\gamma}{\hat{\gamma}_u}} \tag{6.3.2}$$

$$F_{\gamma_u}(\gamma) = 1 - e^{\frac{-\gamma}{\hat{\gamma}_u}} \tag{6.3.3}$$

For the sake of simplicity the medium SNR regime is considered to obtain a closed form upper bound. From (6.2.5) for ($\gamma_{sr_i} > 0$) and ($\gamma_{r_id} > 0$) as equivalent SNRs the upper bound is [82]

$$\gamma \leq \sum_{|Ms|} \gamma_{up} \tag{6.3.4}$$

where $\gamma_{up} = min(\gamma_{sr_m}, \gamma_{r_md})$. When a single relay assists the source for transmission, the CDF of γ_{up} can be expressed as in [83] as

$$\begin{aligned} F_{\gamma_{up}}(\gamma) &= 1 - P(\gamma_{sr_m} > \gamma)P(\gamma_{r_md} > \gamma) \\ &= 1 - [1 - P(\gamma_{sr_m} \leq \gamma)][1 - P(\gamma_{r_md} \leq \gamma)] \\ &= 1 - [1 - F_{sr_m}(\gamma)][1 - F_{r_md}(\gamma)] \end{aligned} \tag{6.3.5}$$

Now the CDF is obtained by substituting (6.3.3) with the appropriate index into (6.3.5) which yields

$$F_{\gamma_{up}}(\gamma) = 1 - e^{\frac{-\gamma}{\gamma_c}} \tag{6.3.6}$$

where $\gamma_c = \frac{\hat{\gamma}_{sr_m}\hat{\gamma}_{r_md}}{\hat{\gamma}_{sr_m}+\hat{\gamma}_{r_md}}$. It is assumed that the channel parameters are represented by independent and identically distributed (i.i.d.) random variables and that $\hat{\gamma}_{sr_m} = \hat{\gamma}_{r_md}$. The PDF can be calculated by taking the derivative of the CDF in (6.3.6) as

$$f_{\gamma_{up}}(\gamma) = \frac{1}{\gamma c} e^{\frac{-\gamma}{\gamma_c}} \tag{6.3.7}$$

6.3.1 Outage probability analysis of the two-relay scheme

In this case, the number of available cognitive relays is two. It is assumed that $\gamma_1 = z_1$ and is greater than $\gamma_2 = z_2$, therefore the joint distribution of

these ordered values can be expressed [112] as

$$f(z_1, z_2) = M(M-1)F(z_2)^{M-2} f(z_1) f(z_2) \tag{6.3.8}$$

where $f(z_1) = \frac{1}{\gamma_c} e^{\frac{-z_1}{\gamma_c}}$, $f(z_2) = \frac{1}{\gamma_c} e^{\frac{-z_2}{\gamma_c}}$ and $M = 2$. Now the CDF is determined (See the Appendix) for the two-relay scheme as

$$F_{\gamma}^{(2)} = \int_0^{\frac{\gamma}{2}} \int_{z_2}^{\gamma - z_2} f(z_1, z_2)\, dz_1 dz_2 \tag{6.3.9}$$

After taking the integral the CDF for two relays is expressed as

$$F_{\gamma}^{(2)} = \frac{(\gamma_c\, e^{\frac{\gamma}{\gamma_c}} - \gamma_c - \gamma)\, e^{\frac{-\gamma}{\gamma_c}}}{\gamma_c} \tag{6.3.10}$$

Therefore the outage probability of the two-relay scheme can be evaluated using the CDF form in (6.3.10) as

$$P_{out} = \int_0^{\alpha} f_{\gamma}(\gamma) d\gamma = F_{\gamma}^{(2)}(\alpha) \tag{6.3.11}$$

6.3.2 Outage probability analysis of the three-relay scheme

In this case, it is assumed that the number of available cognitive relays to assist the transmission is three. It is also assumed that $\gamma_1 = z_1$, $\gamma_2 = z_2$ and $\gamma_3 = z_3$ where $z_1 > z_2 > z_3$, therefore the joint distribution can be expressed as

$$f(z_1, z_2, z_3) = M(M-1)(M-2)F(z_3)^{M-3} f(z_1) f(z_2) f(z_3) \tag{6.3.12}$$

where $f(z_1) = \frac{1}{\gamma_c} e^{\frac{-z_1}{\gamma_c}}$, $f(z_2) = \frac{1}{\gamma_c} e^{\frac{-z_2}{\gamma_c}}$, $f(z_3) = \frac{1}{\gamma_c} e^{\frac{-z_3}{\gamma_c}}$ and $M = 3$. Now the CDF for three relays can be calculated as

$$F_{\gamma}^{(3)} = \int_0^{\frac{\gamma}{3}} \int_{z_3}^{\frac{\gamma - z_3}{2}} \int_{z_2}^{\gamma - z_3 - z_2} f(z_1, z_2, z_3)\ dz_1 dz_2 dz_3 \tag{6.3.13}$$

after taking the integral then the CDF for three relays is obtained as

$$F_{\gamma}^{(3)} = \frac{(2{\gamma_c}^2\ e^{\frac{\gamma}{\gamma_c}} - 2{\gamma_c}^2 - 2\gamma\gamma_c - \gamma^2)\ e^{\frac{-\gamma}{\gamma_c}}}{2{\gamma_c}^2} \tag{6.3.14}$$

From (6.3.14) the outage probability of the three-relay scheme can be obtained as

$$P_{out} = \int_0^{\alpha} f_{\gamma}(\gamma) d\gamma = F_{\gamma}^{(3)}(\alpha) \tag{6.3.15}$$

6.3.3 Outage probability analysis of selecting four relays from M relays

When the number of available cognitive relays is more than four then a RS method is used which is based on local measurements of the instantaneous end-to-end wireless channel gains to select the best four relays from the available M relays [75] and [78]. According to (6.2.5) the maximum and minimum gains of each relay node can be determined; therefore, the policy of selecting the best four relays is based on selecting γ_{max}, γ_{max-1}, γ_{max-2} and γ_{max-3} from the instantaneous SNRs. As each selection will not be from an independent set and it is assumed that $\gamma_{max} = z_1$, $\gamma_{max-1} = z_2$, $\gamma_{max-2} = z_3$ and $\gamma_{max-3} = z_4$, therefore the joint distribution function of the four target values is generated [112] as

$$\begin{aligned} f(z_1, z_2, z_3, z_4) = M(M-1)(M-2)(M-3)F(z_4)^{M-4} \\ f(z_1)f(z_2)f(z_3)f(z_4). \end{aligned} \tag{6.3.16}$$

where

$$f(z_1) = \frac{1}{\gamma_c} e^{\frac{-z_1}{\gamma_c}}, \quad f(z_2) = \frac{1}{\gamma_c} e^{\frac{-z_2}{\gamma_c}}, \quad f(z_3) = \frac{1}{\gamma_c} e^{\frac{-z_3}{\gamma_c}} f(Z_4) = \frac{1}{\gamma_c} e^{\frac{-z_4}{\gamma_c}}$$
$$\text{and} \quad F(z_4) = 1 - e^{\frac{-z_4}{\gamma_c}} \tag{6.3.17}$$

Therefore,

$$f(z_1, z_2, z_3, z_4) = \frac{M(M-1)(M-2)(M-3)}{{\gamma_c}^4} F[1 - e^{\frac{-z_4}{\gamma_c}}]^{M-4} e^{\frac{-z_1}{\gamma_c}} e^{\frac{-z_2}{\gamma_c}} e^{\frac{-z_3}{\gamma_c}} e^{\frac{-z_4}{\gamma_c}} \tag{6.3.18}$$

and $F_\gamma^{(4)}(\gamma)$ is determined as

$$F_\gamma^{(4)} = \int_0^{\frac{\gamma}{4}} \int_{z_4}^{\frac{\gamma - z_4}{3}} \int_{z_3}^{\frac{\gamma - z_4 - z_3}{2}} \int_{z_2}^{\gamma - z_4 - z_3 - z_2} f(z_1, z_2, z_3, z_4)\, dz_1 dz_2 dz_3 dz_4 \tag{6.3.19}$$

by substituting the PDF values in (6.3.18) in (6.3.19) yields

$$F_\gamma^{(4)}(\gamma) = \frac{M(M-1)(M-2)(M-3)}{{\gamma_c}^4} \sum_{i=0}^{M-4} (-1)^i \int_0^{\frac{\gamma}{4}} \int_{z_4}^{\frac{\gamma - z_4}{3}} \int_{z_3}^{\frac{\gamma - z_4 - z_3}{2}} \int_{z_2}^{\gamma - z_4 - z_3 - z_2} e^{\frac{-z_1}{\gamma_c}} e^{\frac{-z_2}{\gamma_c}} e^{\frac{-z_3}{\gamma_c}} e^{\frac{-z_4}{\gamma_c}} dz_1 dz_2 dz_3 dz_4 \tag{6.3.20}$$

After some manipulations the $F_\gamma^{(4)}(\gamma)$ in the cases of $i = 0$ and $i \neq 0$ is determined, therefore

$$F_\gamma^{(4)i=0}(\gamma) = \frac{M(M-1)(M-2)(M-3)}{{\gamma_c}^3} \left[\frac{{\gamma_c}^3}{24} - \frac{{\gamma_c}^3}{24} e^{\frac{-\gamma}{\gamma_c}} - \frac{{\gamma_c}^2 \gamma}{24} e^{\frac{-\gamma}{\gamma_c}} - \frac{\gamma_c \gamma^2}{24} e^{\frac{-\gamma}{\gamma_c}} + \frac{\gamma_c \gamma^2}{48} e^{\frac{-\gamma}{\gamma_c}} - \frac{\gamma^3}{144} e^{\frac{-\gamma}{\gamma_c}} \right] \tag{6.3.21}$$

and

$$F_{\gamma}^{(4)i\neq 0}(\gamma) = \frac{M(M-1)(M-2)(M-3)}{{\gamma_c}^3}\sum_{i=1}^{M-4}\binom{M-4}{i}(-1)^i\left[\frac{2\gamma_c\gamma}{3(i+4)}\right.$$
$$+\left(\frac{-{\gamma_c}^3}{6i}-\frac{{\gamma_c}^2\gamma}{6i}-\frac{\gamma_c\gamma^2}{12}+\frac{2{\gamma_c}^2\gamma}{3i^2}+\frac{2{\gamma_c}^3}{3i^2}-\frac{8{\gamma_c}^3}{3i^3}\right)e^{\frac{-\gamma}{\gamma_c}}+$$
$$\left(\frac{-2\gamma_c\gamma}{3(i+4)}+\frac{{\gamma_c}^3}{6i}+\frac{{\gamma_c}^2\gamma}{6i}+\frac{\gamma_c\gamma^2}{12}-\frac{\gamma_c\gamma^2}{6i}-\frac{2{\gamma_c}^3}{3i^2}-\frac{{\gamma_c}^2\gamma}{6i}+\right.$$
$$\left.\left.\frac{8{\gamma_c}^3}{3i^3}+\frac{\gamma_c\gamma^2}{12i}\right)e^{\frac{-(i+4)\gamma}{4\gamma_c}}\right] \tag{6.3.22}$$

The complete CDF of $\gamma^{(4)}$ is determined from (6.3.21) and (6.3.22) as

$$F_{\gamma}^{(4)}(\gamma) = F_{\gamma}^{(4)i=0}(\gamma) + F_{\gamma}^{(4)i\neq 0}(\gamma)$$
$$= \frac{M(M-1)(M-2)(M-3)}{{\gamma_c}^3}\left\{\left[\frac{{\gamma_c}^3}{24}-\frac{{\gamma_c}^3}{24}e^{\frac{-\gamma}{\gamma_c}}-\frac{{\gamma_c}^2\gamma}{24}e^{\frac{-\gamma}{\gamma_c}}-\right.\right.$$
$$\left.\frac{\gamma_c\gamma^2}{24}e^{\frac{-\gamma}{\gamma_c}}+\frac{\gamma_c\gamma^2}{48}e^{\frac{-\gamma}{\gamma_c}}-\frac{\gamma^3}{144}e^{\frac{-\gamma}{\gamma_c}}\right]+\sum_{i=1}^{M-4}\binom{M-4}{i}(-1)^i\left[\frac{2\gamma_c\gamma}{3(i+4)}\right.$$
$$+\left(\frac{-{\gamma_c}^3}{6i}-\frac{{\gamma_c}^2\gamma}{6i}-\frac{\gamma_c\gamma^2}{12}+\frac{2{\gamma_c}^2\gamma}{3i^2}+\frac{2{\gamma_c}^3}{3i^2}-\frac{8{\gamma_c}^3}{3i^3}\right)e^{\frac{-\gamma}{\gamma_c}}+\left(\frac{-2\gamma_c\gamma}{3(i+4)}\right.$$
$$\left.+\frac{{\gamma_c}^3}{6i}+\frac{{\gamma_c}^2\gamma}{6i}+\frac{\gamma_c\gamma^2}{12}-\frac{\gamma_c\gamma^2}{6i}-\frac{2{\gamma_c}^3}{3i^2}-\frac{{\gamma_c}^2\gamma}{6i}+\frac{8{\gamma_c}^3}{3i^3}+\frac{\gamma_c\gamma^2}{12i}\right)$$
$$\left.\left.e^{\frac{-(i+4)\gamma}{4\gamma_c}}\right]\right\} \tag{6.3.23}$$

Therefore the outage probability of the four cognitive RS can be evaluated using the CDF form in (6.3.23) as

$$P_{out} = \int_0^{\alpha} f_{\gamma}(\gamma)d\gamma = F_{\gamma}^{(4)}(\alpha) \tag{6.3.24}$$

6.4 The outage probability analysis when spectrum acquisition is imperfect

In cognitive relay networks the relay nodes need to acquire the spectrum before they transmit; however, in a realistic condition, the spectrum may not always be available for transmission. Hence, the probability of sensing available spectrum must be considered. If k is the number of cognitive relays which successfully acquire spectrum opportunistically among M cognitive relay nodes, the probability of acquiring available spectrum is given by [111]

$$P(k) = \binom{M}{k} P_d^k (1 - P_d)^{M-k} \tag{6.4.1}$$

where P_d denotes the probability of detection and for Rayleigh fading distribution [113] is given by

$$P_d = e^{-\frac{\alpha}{2}} \sum_{n=0}^{\sigma-2} \frac{1}{n!} \left(\frac{\alpha}{2}\right)^n + \left(\frac{1+\gamma_c}{\gamma_c}\right)^{\sigma-1} \times \left[e^{-\frac{\alpha}{2(1+\gamma_c)}} - e^{-\frac{\alpha}{2}} \sum_{n=0}^{\sigma-2} \frac{1}{n!} \left(\frac{\alpha\gamma_c}{2(1+\gamma_c)}\right)^n\right] \tag{6.4.2}$$

where α denotes the threshold which is used for comparison to make a decision if the primary signal is present or not, σ represents the time-bandwidth product and (.)! is the factorial operation. Therefore, the outage probability of the cognitive relay network P_c is given as

$$P_c = \sum_{k=0}^{|Ms|} P_{out}\ P(k) \tag{6.4.3}$$

6.5 The quasi-orthogonal code structure for the availability of two, three and four cognitive relays

The received information over all channels is combined at the destination and can be represented as

$$\mathbf{z} = \mathbf{Y}\mathbf{h} + \mathbf{n}_d \tag{6.5.1}$$

where $\mathbf{h}$ is the equivalent channel vector and $\mathbf{Y}$ is a QO-ST codeword matrix which is generated distributively by the relays. When there are four available cognitive relays to cooperate then the QO-STBC has the structure of the conventional QO codeword as [50]

$$\mathbf{Y}=\begin{bmatrix} y_1 & y_2 & y_3 & y_4 \\ -y_2^* & y_1^* & -y_4^* & y_3^* \\ y_3 & y_4 & y_1 & y_2 \\ -y_4^* & y_3^* & -y_2^* & y_1^* \end{bmatrix} \tag{6.5.2}$$

where $(.)^*$ denotes the complex conjugate. The cognitive QO-STBC has a flexible code structure which can be adapted to the available cognitive relays after every sensing activity is implemented. Therefore, when there are only two active cognitive relays the code is designed as

$$\mathbf{Y}=\begin{bmatrix} 0 & y_2 & y_3 & 0 \\ 0 & y_1^* & -y_4^* & 0 \\ 0 & y_4 & y_1 & 0 \\ 0 & y_3^* & -y_2^* & 0 \end{bmatrix} \tag{6.5.3}$$

In the case of three active relays the code is of QO-STBC structure in (6.5.2) with only a single column with zero entries.

6.5.1 Modified distributed quasi-orthogonal STBC

To design the modified code, following the approach in [43], appropriate rotation angles Φ_1 and Φ_2 are applied on the first and second pairs of the symbols respectively within the QO-STBC in (6.5.2). Therefore, for the constellation symbols $y_1,\ y_2,\ y_3$ and y_4, the modified code is constructed as

$$\mathbf{Y}(\Phi_1,\Phi_2)=\begin{bmatrix} y_1e^{j\Phi_1} & y_2e^{j\Phi_1} & y_3e^{j\Phi_2} & y_4e^{j\Phi_2} \\ -y_2^*e^{-j\Phi_1} & y_1^*e^{-j\Phi_1} & -y_4^*e^{-j\Phi_2} & y_3^*e^{-j\Phi_2} \\ y_3e^{j\Phi_2} & y_4e^{j\Phi_2} & y_1e^{j\Phi_1} & y_2e^{j\Phi_1} \\ -y_4^*e^{-j\Phi_2} & y_3^*e^{-j\Phi_2} & -y_2^*e^{-j\Phi_1} & y_1^*e^{-j\Phi_1} \end{bmatrix} \tag{6.5.4}$$

where Φ_1 and Φ_2 are the rotation angles. A family of codebooks is generated by changing the rotations Φ_1 and Φ_2 to build a whole quasi-orthogonal codebook. In particular, the matrices of $\mathbb{S} = \mathbf{Y}(\Phi_1, 0)$ and $\mathbb{T} = \mathbf{Y}(0, \Phi_2)$ are generated, then the union of $\mathbb{S} \cup \mathbb{T}$ is taken to build a complete QO codebook. The union $\mathbb{S}\cup\mathbb{T}$ has twice as many codewords as needed, therefore, it is pruned to one-half size to reach the desired number of codewords in a manner that increases the minimum distance of the codebook. The pruning is achieved by applying a set partitioning algorithm to each of the generated QO codes. In addition, the set partitioning can be obtained by following the approach in [114] and [64]. In particular, to constitute the modified codebook Q, the set of the matrices from $\mathbb{S} = \mathbf{Y}(\Phi_1, 0)$ is partitioning into $\mathbb{S}_1$ and $\mathbb{S}_2$ whereas the set of the matrices from $\mathbb{T} = \mathbf{Y}(0, \Phi_2)$ is partitioning into $\mathbb{T}_1$ and $\mathbb{T}_2$ then the modified codebook is built as $Q = \mathbb{S}_1 \cup \mathbb{T}_2$.

The inter-distance between the subcodes can be calculated in a manner similar to in [43], for example, for two codewords Y_1 and Y_2 the code gain distance (GGD) CGD = det(Π) where

$$\Pi = ((Y_1 - Y_2)(Y_1 - Y_2)^H) \tag{6.5.5}$$

where $(.)^H$ represents the conjugate transpose. The minimum CGD of the codebook $\mathbb{S}$ is defined as the minimum CGD of all non identical codeword pairs of $(\mathbb{S} \times \mathbb{S})$, therefore the distance between two codebooks $\mathbb{S}$ and $\mathbb{T}$ is as described in [43] given by

$$\mathrm{D}(\mathbb{S}, \mathbb{T}) = \det(\Pi(Y_1, Y_2)) \tag{6.5.6}$$

For QPSK modulation the distance properties should be increased to give better performance. In order to achieve that, each subcode in $\mathbb{T}_2$ is rotated by using a unitary matrix $\mathbf{U}$ such as multiplying $\mathbb{T}_2$ by $\mathbf{U}$ as defined in [43] and found by

$$\max_{\mathbb{I}} D(\mathbb{S}_1, \mathbb{T}_2\mathbf{U}) \tag{6.5.7}$$

where D is the distance, $\mathbf{U} = \mathrm{diag}(e^{j\theta_1}, e^{j\theta_2}, e^{j\theta_3}, e^{j\theta_4})$ and diag(.) represents a diagonal matrix. A genetic algorithm is used to search for the optimum rotation matrix which increases the CGD of the modified code and it is found as

$$\mathbf{U} = \mathrm{diag}(e^{j1.5832\pi}, e^{j.4165\pi}, e^{j.9165\pi}, e^{j1.0832\pi}) \tag{6.5.8}$$

where the maximum distance from this rotation is

$$D(\mathbb{S}_1, \mathbb{T}_2\mathbf{U}) \approx 64 \tag{6.5.9}$$

therefore the distance of the code was increased because of the optimum rotation matrix $\mathbf{U}$ which gives better performance of the modified code. In this proposed scheme a full maximum likelihood decoder (MLD) over the modified code has been used.

6.6 Simulation results

In this section simulation results are firstly presented to verify the outage probability analysis and the codeword error rate for the proposed scheme in the proposed cognitive relay network. In order to verify the results obtained from mathematical expressions, (6.3.15), (6.3.15), (6.3.24) and (6.4.3), all the relay node links have the same average SNR = 10dB, and all noise variances are set to unity. There is no direct link between the transmitter and receiver as path loss or shadowing is assumed to render it unusable. All nodes are equipped with a single antenna and it is assumed that the channels are Rayleigh flat fading. The simulated values, as in Figures 6.2, 6.3, 6.4 and 6.5 are found by generating random variables with an exponential distribution using the MATLAB function exprnd() which represents the power gain of the channel. These values are then applied in the maxmin(.,.) operation and this process is repeated a sufficiently large number of times to generate stable plots. This explains why it is expected that the simulated and theoretical expressions should be identical. Figure 6.2 and Figure 6.3

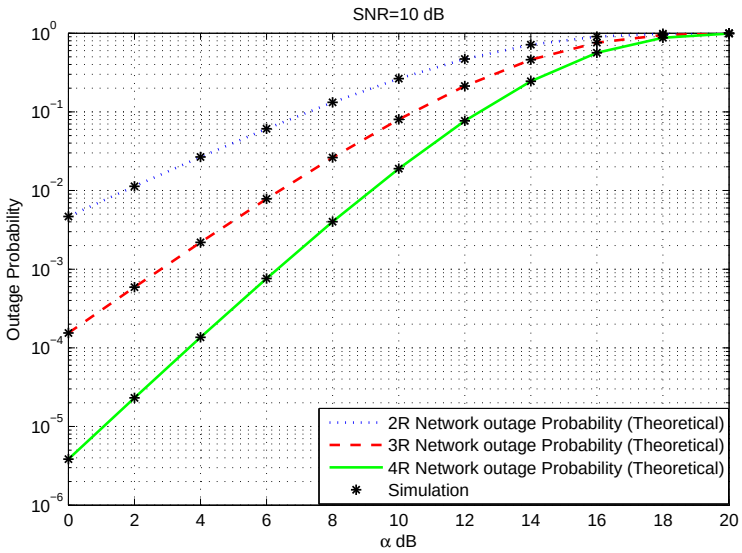

Figure 6.2. The theoretical and the simulation results of the outage probability performance of two, three and four relay network.

show the theoretical and the simulation results of the outage probability performance versus threshold α in dB for different numbers of active cognitive relays. The spectrum acquisition is considered to be both perfect and imperfect. Theoretical results are shown in line style and the simulation results as points. To obtain the outage probability from the mathematical expression, all the paths are assumed to have the same average SNR which is 10 dB. The figures also show that for different numbers of active cognitive relays the theoretical results match well the simulation results. Figure 6.2 shows that the outage performance of the system improves as the number of the active relays increases, for instance, at threshold value of $\alpha_{th} = 4$ dB the outage performance improves from approximately 4×10^{-2} to 1.5×10^{-4} when the number of cooperative relays increases from two to four respectively. In Fig-

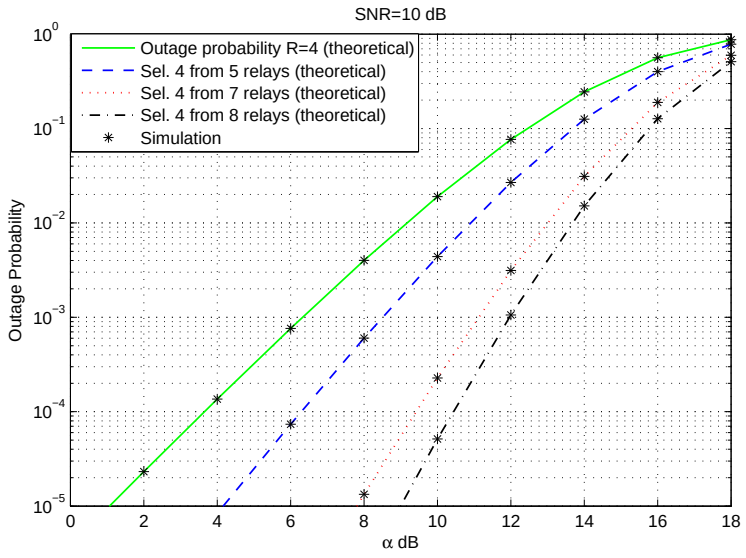

Figure 6.3. The theoretical and the simulation results of the outage probability performance based on selection cooperation versus SNR in dB.

ure 6.3 the outage probability performance based on selection cooperation is shown. It can be seen that when the number of the available relays M increases the outage probability decreases and hence when the number of the cognitive relays is large the outage event (no transmission) becomes less likely. For example, when the number of active cognitive relays increases

from five to eight, at the threshold value $\alpha_{th} = 4$ dB the outage probability decreases significantly from approximately 10^{-5} to 2×10^{-9} and from about 8×10^{-5} to 8×10^{-8} at threshold value of $\alpha_{th} = 6$ dB.

Figure 6.4 presents the comparison of outage probability performance for

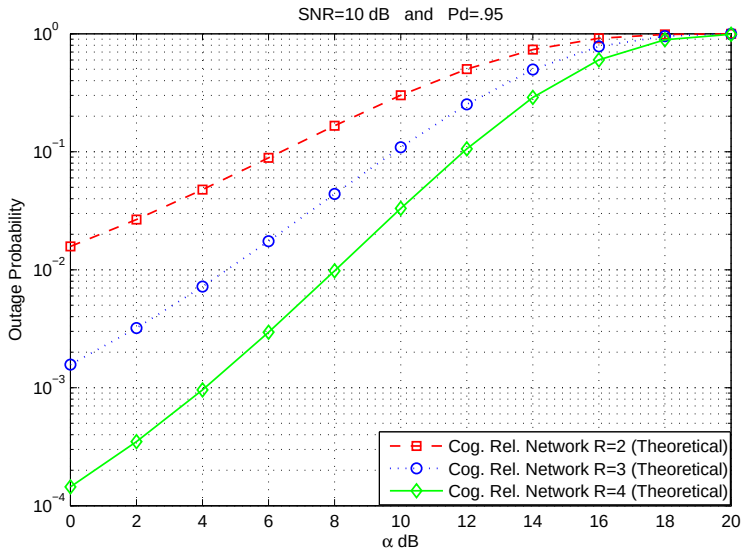

Figure 6.4. The theoretical results of the outage probability performance when spectrum acquisition is imperfect (Pd=.95) for two, three and four cognitive relay network.

the proposed cognitive relay network at a spectrum acquisition probability of $P_d = .95$ when two, three or four cognitive relays are active. It can be seen that there is a significant improvement in the outage performance when the number of cognitive relays increases due to the fact that increasing the number of cognitive relays leads to growth in the number of relays that are able to obtain spectrum. Figure 6.5 presents the comparison of outage probability performance for the proposed cognitive relay network at different values of spectrum acquisition probability when there are four active cognitive relays. At threshold value of $\alpha_{th} = 4$ dB when the spectrum acquisition probability changes from $P_d = .85$ to $P_d = .99$ the outage probability decreases significantly from approximately 8×10^{-3} to 3×10^{-4} and it reaches the minimum value of 1.5×10^{-4} when $P_d = 1$ (perfect spectrum acquisition).

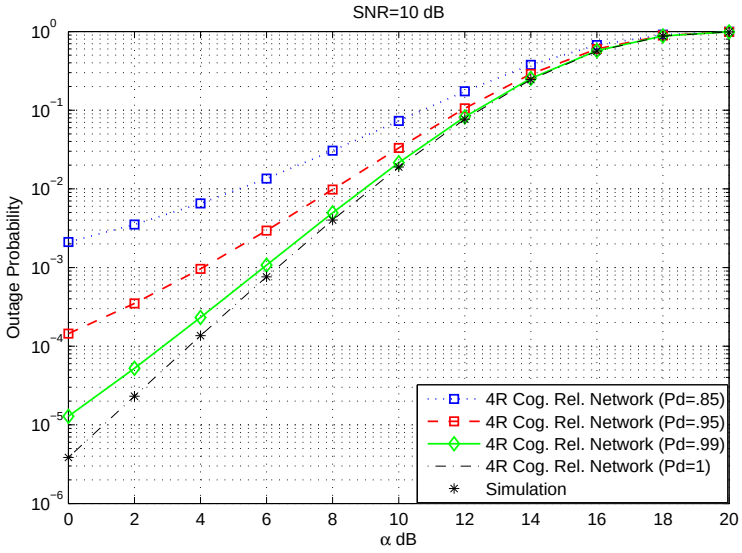

Figure 6.5. The theoretical and the simulation results of the outage probability performance for four relay cognitive network for different values of Pd.

In general, the higher outage probability is the indication of performance degradation due to the unavailability of the spectrum; as P_d decreases, the gain also decreases resulting in a higher outage probability. The outage probability improves if the spectrum can be acquired with a higher probability. Hence, the performance of the cognitive relay network depends entirely on the acquisition of the spectrum. Furthermore, Figure 6.6 shows the comparison between end-to-end codeword error rate (CWER) performance for the M-D-QO-STBC in three situations, that is: when two, three and four cognitive relay nodes are active. The graphs show a significant performance improvement as the number of active cognitive relays increases thereby attaining a more robust transmission of the QPSK signal. For instance, the four-relay cognitive system provides approximately 9 dB improvement more than the two-relay cognitive relay system in terms of SNR and approximately 4 dB more than the three-relay cognitive system at a codeword error probability of 10^{-3}. This is a result of the four-relay cognitive system benefitting from the full diversity and the CGD. On the other hand, Figure 6.7 shows the

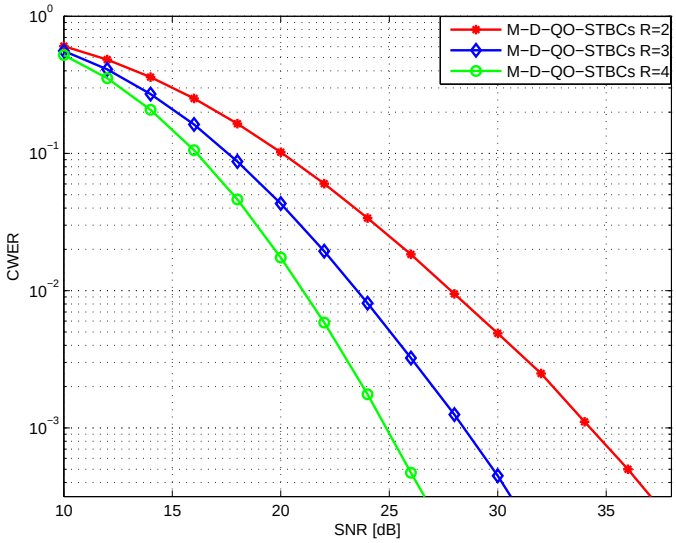

Figure 6.6. The CWER performance comparison of M-D-QO STBCs when there are two, three and four operational cognitive relays in the cognitive relay network for QPSK signal.

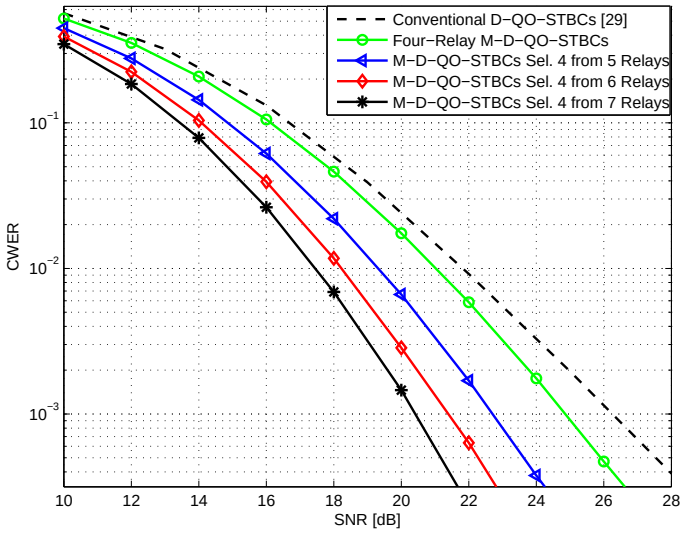

Figure 6.7. The performance comparison of M-D-QO STBCs and conventional D-QO STBCs in cognitive relay network and the performance of the system when the number of the active relays increases with QPSK modulation.

performance of the M-D-QO-STBC scheme as compared to the conventional D-QO STBC scheme [39], and the impact of the RS technique on the system

for QPSK signals when the number of available cognitive relays is four or more. It shows that the modified code provides an improved performance over the conventional D-QO-STBCs due to the maximization in the distance properties of the original codebooks within the modified code, in addition to achieving the full diversity. When the number of active cognitive relays increases the performance of the SNR of the system is improved. For example, at a codeword error probability of 10^{-3} the M-D-QO STBC provides approximately 2 dB improvement in the SNR over the conventional D-QO STBC, and when the number of active cognitive relays increases from four to five, seven and nine the performance of the SNR improves by approximately 2 dB, 3.5 dB and 4.5 dB respectively compared to the four relay M-D-QO STBC at the same codeword error probability.

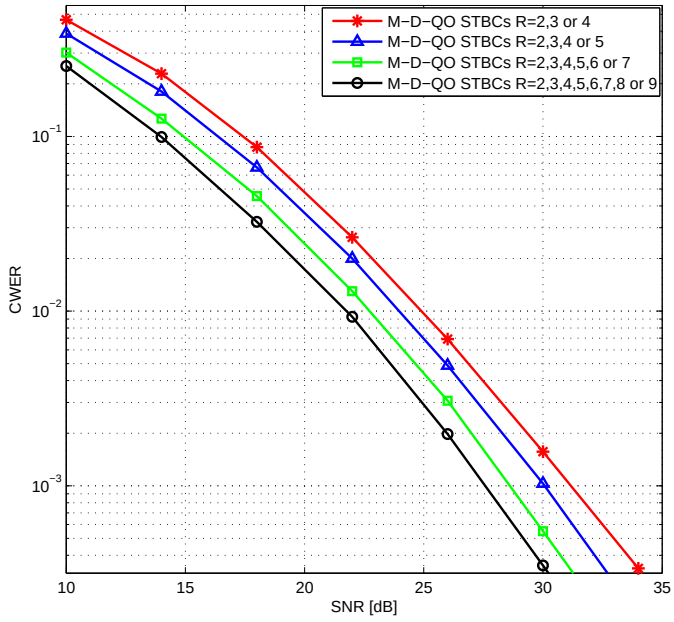

Figure 6.8. Performance comparison of cognitive relay network for the M-D-QO-STBCs when the availability of the cognitive relays changes randomly from two to four, two to five, two to seven and two to nine relays for QPSK signal.

Finally, the results in Figure 6.8 demonstrate the performance comparison of the proposed cognitive network when the number of operational cognitive

relays changes randomly after each codeword transmission from two to four, two to five, two to seven and two to nine relays for QPSK signal. The results confirm that when the number of the active relays increases the performance of the system improves.

6.7 Summary

In this chapter, the outage probability performance of a proposed cooperative cognitive relay network was evaluated. A closed form expression for the outage probability for RS cooperation over Rayleigh frequency flat fading channels was derived for perfect and imperfect spectrum acquisitions. The results showed the advantage in probability performance of the RS in cooperative cognitive systems when the spectrum acquisition is perfect. In contract, when the spectrum acquisition is imperfect the performance of the outage degrades significantly. A M-QO STBC for wireless cognitive relay networks was also proposed. This modified code is built by using a proper rotation and set partitioning of two QO codebooks. The cognitive relays exploit the spectrum opportunities without causing any interference to the licensed users, therefore the performance of the system depends on the spectrum acquisition and the number of operating relays. When the number of the available cognitive relays was more than four the RS technique was used to improve the performance of the system which was confirmed by simulation.

In the next chapter, the summary and conclusion to the thesis and future work will be provided.

Chapter 7

CONCLUSIONS AND FUTURE WORK

This thesis was devoted to one-way and two-way cooperative wireless systems using the modified distributed quasi-orthogonal space-time block coding (M-D-QO-STBC) scheme. The concept of space-time coding was explained in a systematic way. The new proposals of one-way and two-way M-D-QO-STBC schemes was shown to achieve worthwhile end-to-end performance gains in cooperative relay networks for different wireless challenges and scenarios. In this chapter, the contributions of this thesis are summarized and the performance gains are quantified. Also, some open issues are suggested, giving possible research directions for the future.

7.1 Conclusions

Modified distributed quasi-orthogonal space-time block coding (M-D-QO-STBC) schemes for one-way and two-way amplify-and-forward (AF) cooperative relay networks were proposed. These were shown to yield full diversity and achieve improved code gain distance which lead to enhanced system performance. Throughout this thesis, two-way relay networks have been investigated and effectively exploited to achieve full transmission rate. To further improve the system performance, an effective relay selection approach has been proposed. In addition, outage probability analysis was used for

one-way and two-way systems for performance assessment. Finally, outage probability analysis of multi-relay selection for an AF cooperative cognitive relay network has been introduced when the spectrum acquisition is perfect and imperfect. A review and conclusion for each chapter will be presented next:

In Chapter 1, the basic concept and characteristics of MIMO systems were provided together with a general introduction to cooperative networks. Then, a brief introduction to the main functions of the OFDM technique was also provided. Furthermore, a brief introduction to cognitive radio systems was provided highlighting the main functions of cognitive radio and the features of cooperative cognitive networks. Finally, the thesis outline was given together with the aims and objectives.

In Chapter 2, an overview of the various schemes in point-to-point and cooperative networks that were used in the thesis was presented and a brief introduction to distributed space-time coding schemes with orthogonal and quasi-orthogonal codes was given. To evaluate the system performance of point-to-point STBC schemes, the Alamouti and the QO-STBC schemes were studied and discussed highlighting the advantage of each scheme. It was shown that the Alamouti code provides the maximum possible diversity and has simple decoding at the receiver where each symbol is decoded separately using linear processing. It was also shown that QO-STBC was constructed to increase the symbol transmission rate but the diversity is relaxed. On the other hand, such a QO-STBC scheme could achieve full diversity by using different constellations for the two components of the quasi-orthogonal code or using a feedback method. Furthermore, expanding wireless network coverage with the use of cooperative relay networks is discussed in the chapter and a brief overview of cooperative wireless networks concepts relevant to this thesis is given. Finally, this chapter described the modified QO-STBC and showed that the set partitioning method could be used to increase the

code gain distance.

In Chapter 3, the M-D-QO-STBC scheme with increased code gain distance (CGD) for one-way and two-way AF wireless relay networks was proposed. This modified code was designed from set partitioning of two rotated quasi-orthogonal space-time codebooks then the subcodes were combined and pruned to arrive at the modified codebook with the desired rate in order to increase the CGD. For higher rate codes the code distance was maximized by using a genetic algorithm to search for the optimum rotation matrix and the code gain distance was increased from 43.94 to approximately 64. The resulting code has very good performance and significant coding gain over existing codes such as the open-loop D-QO-STBC scheme, rotated D-QO-STBC scheme and closed-loop D-QO-STBC scheme. Simulations for the M-D-STBC confirmed the advantages of this code compared to other open and closed-loop codes operating at the same CWER and total power. For example, for QPSK modulation at CWER 10^{-4}, the modified scheme provides a power saving of approximately 3 dB compared with the D-QO-STBC open-loop scheme, approximately 1.2 dB compared with the rotated D-QO-STBC open-loop scheme and 1 dB compared with the D-QO-STBC closed-loop scheme. In particular, the M-D-QO-STBC scheme has the best performance over all the other schemes due to the gain from increasing the code distance and achieving the full diversity.

In Chapter 4, new analytical expressions for the PDF, and CDF of end-to-end SNR were derived together with closed form expressions and integral forms for outage probability for one-way and two-way AF relay networks over flat Rayleigh fading channels. In the use of a one-way relay network a closed form expression for the outage probability for four relay selection was derived. In addition, the advantage of using the relay selection scheme in outage probability was confirmed by simulation. For instance, when the number of the relays increased from four to eight, at the threshold value

of 8 dB the outage probability decreased significantly from approximately $2.6\text{x}10^{-2}$ to $2.5\text{x}10^{-4}$. Whereas, for two-way relay networks, the outage probability analyses for the best, the best N^{th} and the best four relay selection from a set of N available relays were presented. The best relay selection from a group of N available relays was provided by using local measurements of the instantaneous channel conditions, and a selection scheme to maximize end-to-end SNR was adopted. Then the outage probability of the best N^{th} relay selection from a set of N available relays, i.e. $N = 8$ was compared with the best single relay selection. The effect of order of relay selection on the outage performance was also considered and it was noticed that as the order of the selected N^{th} relay increases, the outage probability increases, thus the system performance was more degraded. For example, at a threshold value of 8 dB when the selected N^{th} relay increased from 1 to 2, the outage probability of best relay selection was increased from approximately 80% to 95%. Furthermore, the exact outage probability for four relay selection was considered and then these best relays were used in the proposed scheme to decrease the outage probability, i.e. when target SNR = 4, the exact outage probability of the best four relay selection was decreased from almost 0.02 to 0.0003. Generally, the numerical results have shown the advantage in terms of the outage probability performance in one-way and two-way cooperative communication systems and have confirmed that the theoretical values for the new outage probability match the simulated results and when the number of available relays increases, the outage probability decreases.

Chapter 5 focused on the synchronization issue in wireless cooperative relay networks. In this chapter, robust schemes for cooperative relays based on the M-D-QO-STBC scheme for both one-way and two-way asynchronous cooperative relay networks were considered. These schemes exploited cooperative communication OFDM-based transmission to mitigate timing errors between relay nodes. In particular, an OFDM data structure was employed

with cyclic prefix (CP) insertion at the source in the one-way cooperative relay network and at the two terminal nodes in the two-way cooperative network to combat the effects of time asynchronism. In addition, a relay selection technique was proposed to further enhance the system performance of both proposed cooperative relay networks. The simulation results indicated that the OFDM-based scheme can significantly mitigate the delay when $\tau <$ CP which enhances the performance of the two systems under imperfect synchronization. It was also shown that the performance of the proposed M-D-QO-STBC was improved by implementing the relay selection technique. For example, at codeword error probability 10^{-3}, when the number of the relays (each relay has two antenna) increased from two to five, a power saving of approximately 5 dB was provided

In Chapter 6, outage probability performance of a proposed cooperative cognitive relay network was evaluated. A closed form expression for the outage probability for relay selection cooperation over Rayleigh frequency flat fading channels was derived for perfect and imperfect spectrum acquisitions. Furthermore, the M-QO-STBC scheme was also proposed for use in wireless cognitive relay networks. However, when the spectrum acquisition was perfect, the results showed the advantage in terms of outage probability performance of the relay selection in cooperative cognitive systems and confirmed that the system performance significantly improved as the number of available cognitive relays increased. In contract, when the spectrum acquisition was imperfect the outage performance degraded significantly. For example, when the spectrum acquisition probability changed from $P_d = .99$ to $P_d = .85$ the outage probability increased significantly from approximately 3×10^{-4} to 8×10^{-3}. Moreover, the comparison of outage probability performance was considered for the proposed cognitive relay network at a fixed spectrum acquisition probability, i.e. $P_d = .95$ and when the number of active relays increased from two to four and it was shown that the outage

probability decreased from approximately 0.088 to 0.0029 at the threshold value of 6 dB. It was also confirmed that a significant improvement in the outage performance when the number of cognitive relays increases due to the fact that expanding the number of cognitive relays leads to growth in the number of relays that are able to obtain spectrum. As cognitive relays exploit the spectrum opportunities without causing any interference to the licensed users, the performance of the system depends on the spectrum acquisition and the number of operating relays. When the number of available cognitive relays was more than four the relay selection technique was used to improve the performance of the system and simulations were used to confirm the advantage.

In summary, in this thesis, firstly, the M-D-QO-STBC scheme was used in one-way and two-way AF cooperative relay networks to achieve code gain distance and full diversity and use the OFDM type of transmission to mitigate timing error caused by asynchronism in relay networks. Then the outage probability of a multi-relay selection scheme in a one-way cooperative relay network and the best N^{th} and the best four relay selection in a two-way cooperative relay network have been investigated. Finally, the utilization of multi-relay selection has been examined in one-way AF cognitive relay networks, and a new outage probability analysis was confirmed.

A number of research problems that can be considered in the future will be presented in the next section.

7.2 Future work

This thesis opens up a number of research problems that can be considered. A few of the possible extensions of this work are as follows:

1. The work in this thesis assumed that perfect channel state information (CSI) was available at the destination node. In reality, CSI can only be

estimated which obviously will introduce errors. An interesting study would be examining the proposed schemes in this thesis with channel estimate imperfections in the CSI, and designing robust algorithms, to overcome this issue.

2. The relay networks presented in this thesis were based on a Rayleigh fading channel model. Future work could include other practical propagation models, such as Nakagami or Rician fading models. These distributions have gained much attention lately since they give better representation of practical environments such as land-mobile and indoor mobile multi-path propagation environments as well as scintillating ionospheric radio links [115].

3. Buffer-aided relaying is a new paradigm for wireless cooperative networks. In particular, buffers enable half-duplex relays in a cooperative network to adaptively choose whether to receive or transmit a packet in a given time slot based on the instantaneous quality of the receiving and transmitting channels [116]. Therefore, this technique can be used for relay selection scheme with power adaptation and inter-relay interference cancelation for cooperative diversity systems

4. The proposed schemes in this thesis considered only the case of a single source node wishing to communicate with a single destination node via asynchronous cooperative relay nodes. The issue can be extended and generalized to asynchronous multi-user environments which is a major potential research direction in practical wireless systems.

5. In Chapter 4, the outage probability of a relay selection scheme without interference in one-way and two-way cooperative networks has been studied. Extension to consider interference in one-way and two-way cooperative networks would be valuable.

6. In Chapter 6, an interesting extension of this work is to analyse cognitive relaying in an underlay environment dealing with power distribution to avoid or minimize the interference created to the primary user. Furthermore, the proposed work in this chapter can be extended to be considered in two-way cooperative cognitive relay networks.

Appendix

1-CDF integration

This appendix shows how to calculate the CDF of the random variable γ formed as the sum of the maximum and the second maximum random variables denoted Z_1 and Z_2 where $Z_1 + Z_2 \leq \gamma$. Therefore the CDF is given by

$$F_\gamma(\gamma) = P[Z_1 + Z_2 \leq \gamma] \tag{.0.1}$$

Figure A.1 shows the γ domain which should be calculated, therefore, for Z_1 and Z_2 are non-negative and $Z_1 \geq Z_2$ the CDF is calculated as

$$F_\gamma(\gamma) = \int_0^{\frac{\gamma}{2}} \int_{Z_2}^{\gamma - Z_2} f(Z_1, Z_2)\ dZ_1 dZ_2 \tag{.0.2}$$

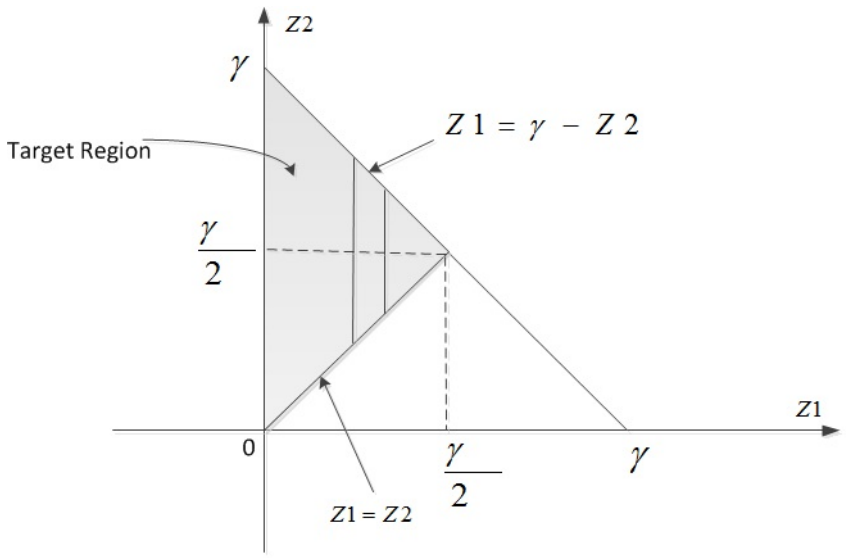

Figure A.1. The domain of γ.

2-Simulation Methodology

MATLAB^{TM} Release 2012a was used as a simulator tool in order to perform the simulator experiments.

Simulator

MATLAB^{TM} is a software package for high-performance in technical computing, integrating programming, visualization, and computation in a very user-friendly environment. Best of all, it also provides extensibility and flexibility with its own high-level programming language. Common uses of MATLAB^{TM} involve [reference here]:

(a) Mathematics (Arrays and matrices, linear algebra, etc.)

(b) Programming development (Function, data structures, etc.)

(c) Modeling and simulation (Signal Processing etc.)

(d) Data analysis (statistics etc.)

(e) Visualization (graphics, animation etc.)

All the simulations were performed by automation programs which were created by the author. The whole simulation program was divided in sub-functions which were built in M-files form.

Simulation Components

The following components were modeled, through the simulations:

1. Complex information symbols signals
2. Flat-fading channels (Rayleigh fading model)
3. Additive White Gaussian Noise
4. Delay spread
5. Fourier transforms and inverse Fourier transforms
6. Cyclic prefix (CP)
7. Signal reversal

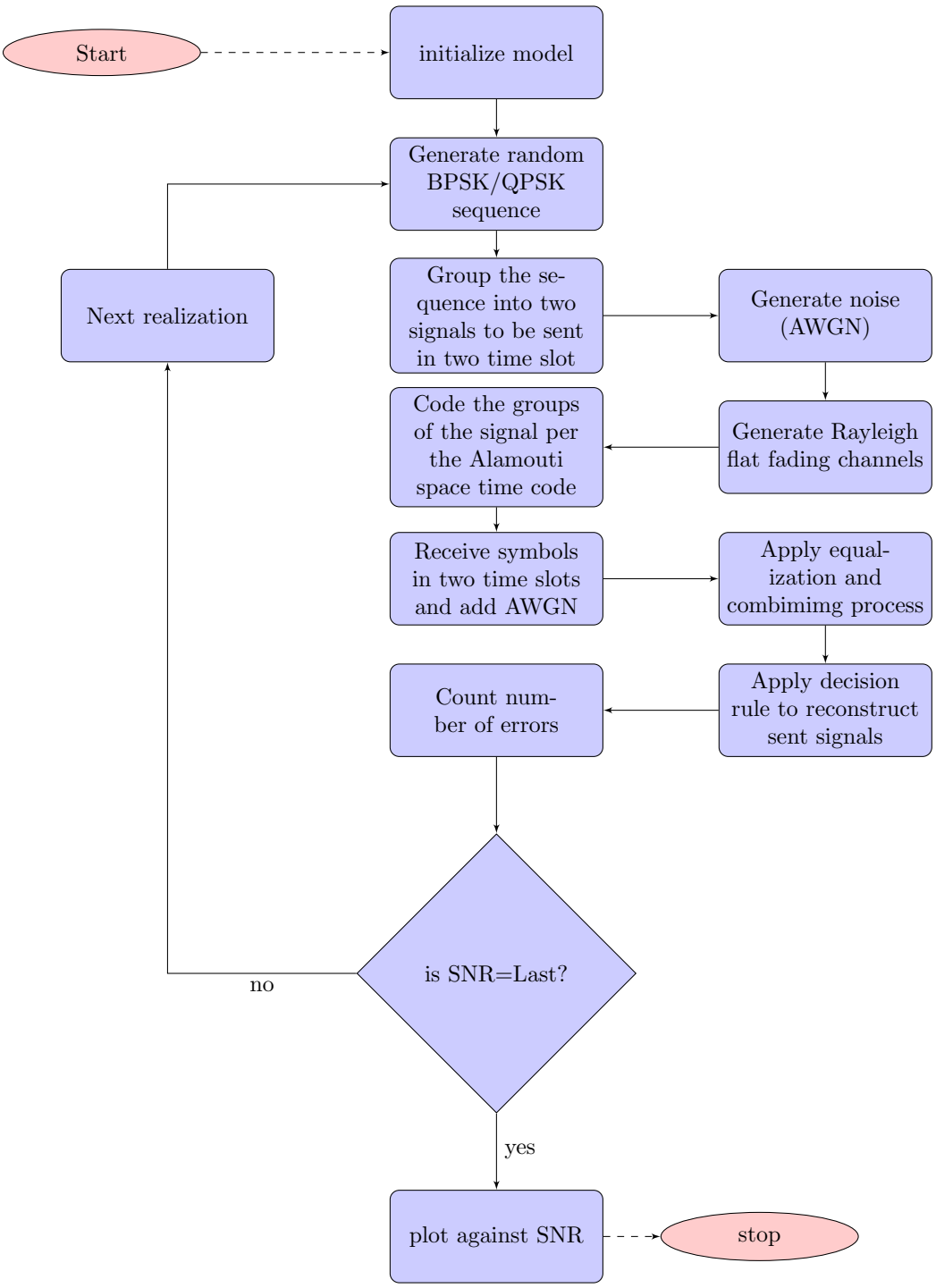

Figure 1: Flowchart for Alamouti STBC scheme

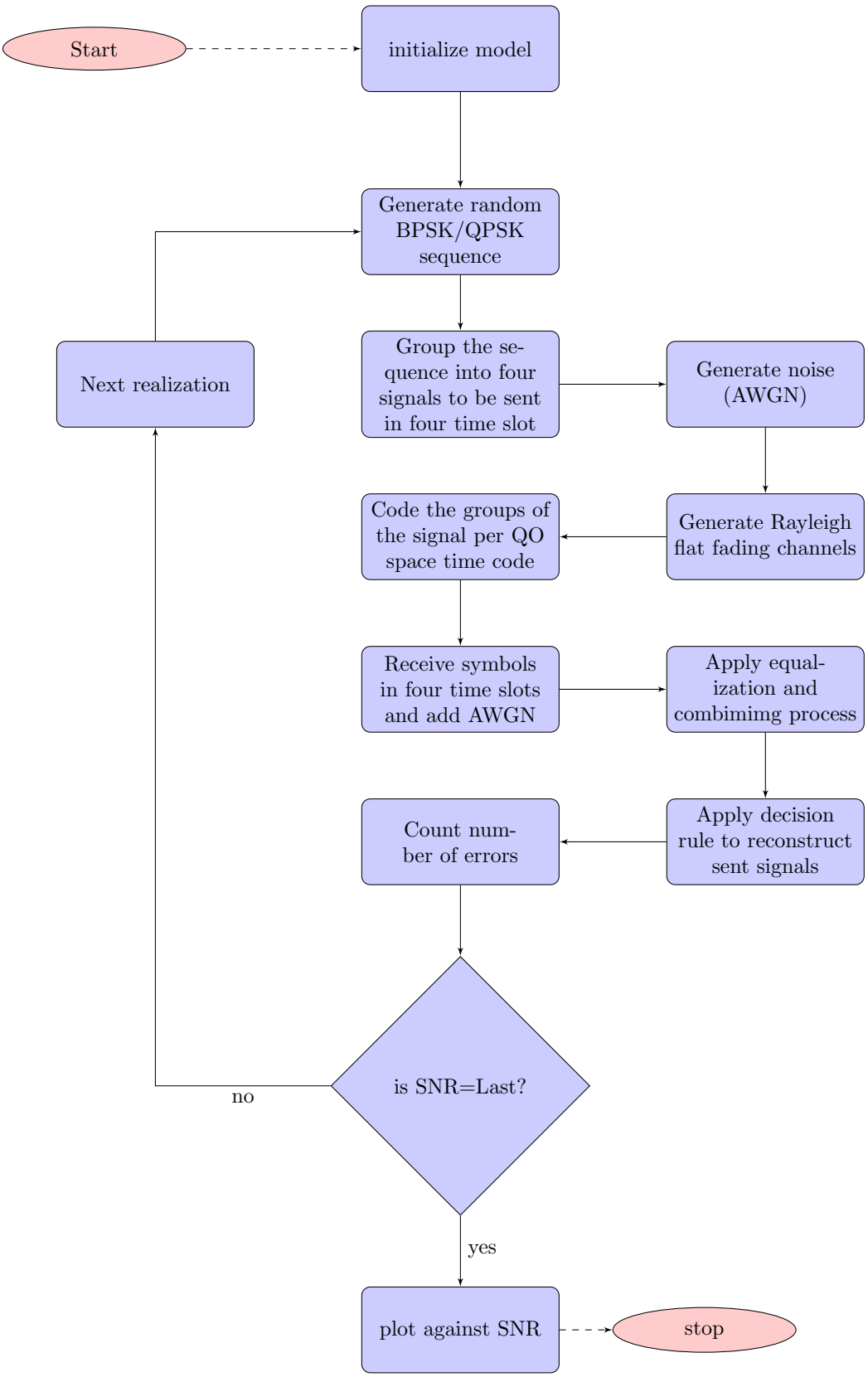

Figure 2: Flowchart for QO-STBC schemes.

1- In the rotated D-QO-STBC the 3^{th} and the 4^{th} signals are rotated by $\frac{pi}{2}$ for BPSK and by $\frac{pi}{4}$ for QPSK before transmission.

2- In the closed loop D-QO-STBC, the channel matrix is rotated see Section 2.1.2.3.

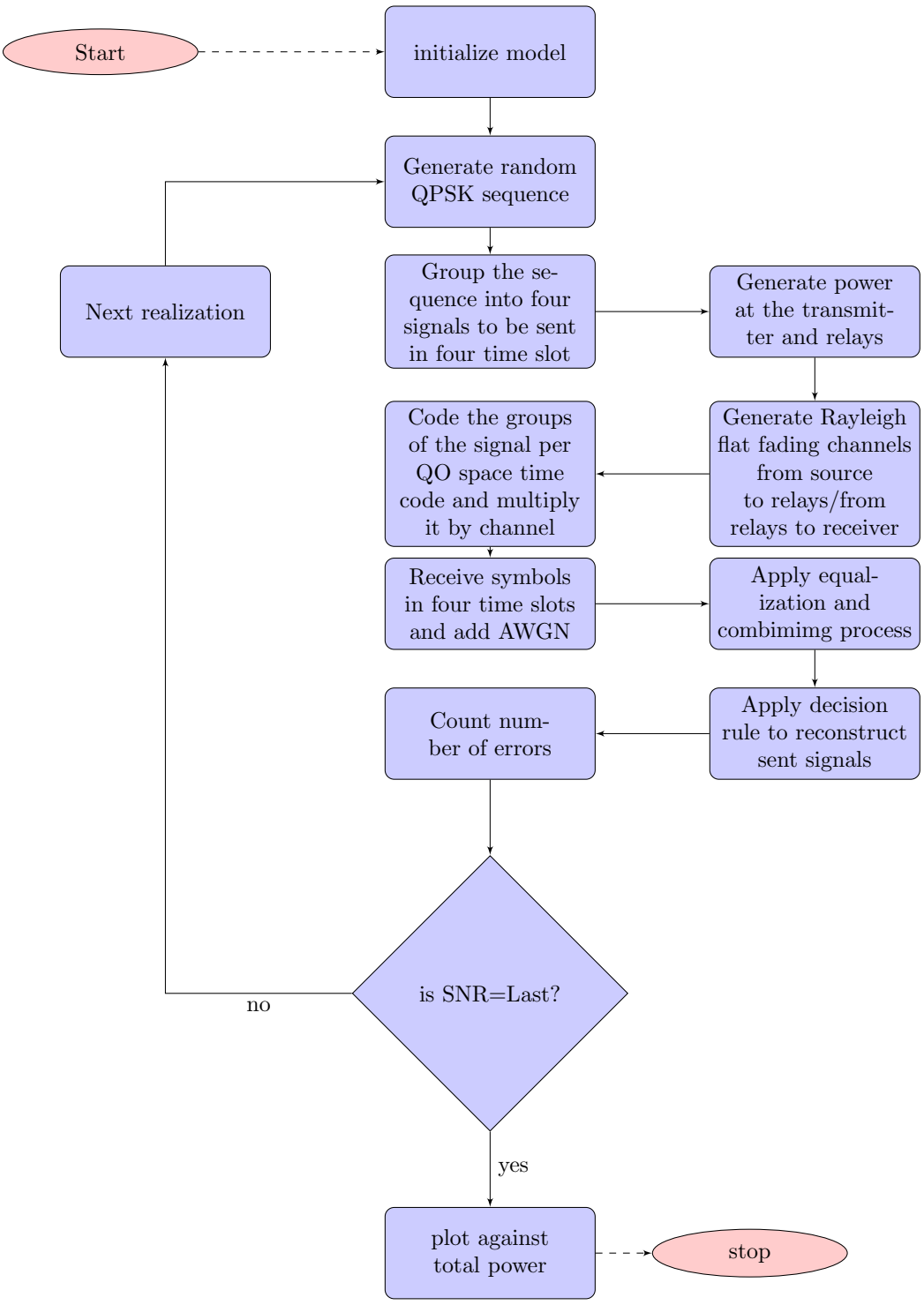

Figure 3: Flowchart for D-QO-STBC schemes for one-way transmission.
1- In the rotated D-QO-STBC the 3^{th} and the 4^{th} signals are rotated by $\frac{pi}{2}$ for BPSK and by $\frac{pi}{4}$ for QPSK before transmission.
2- In the closed loop D-QO-STBC, the channel matrix is rotated see Section 3.3.

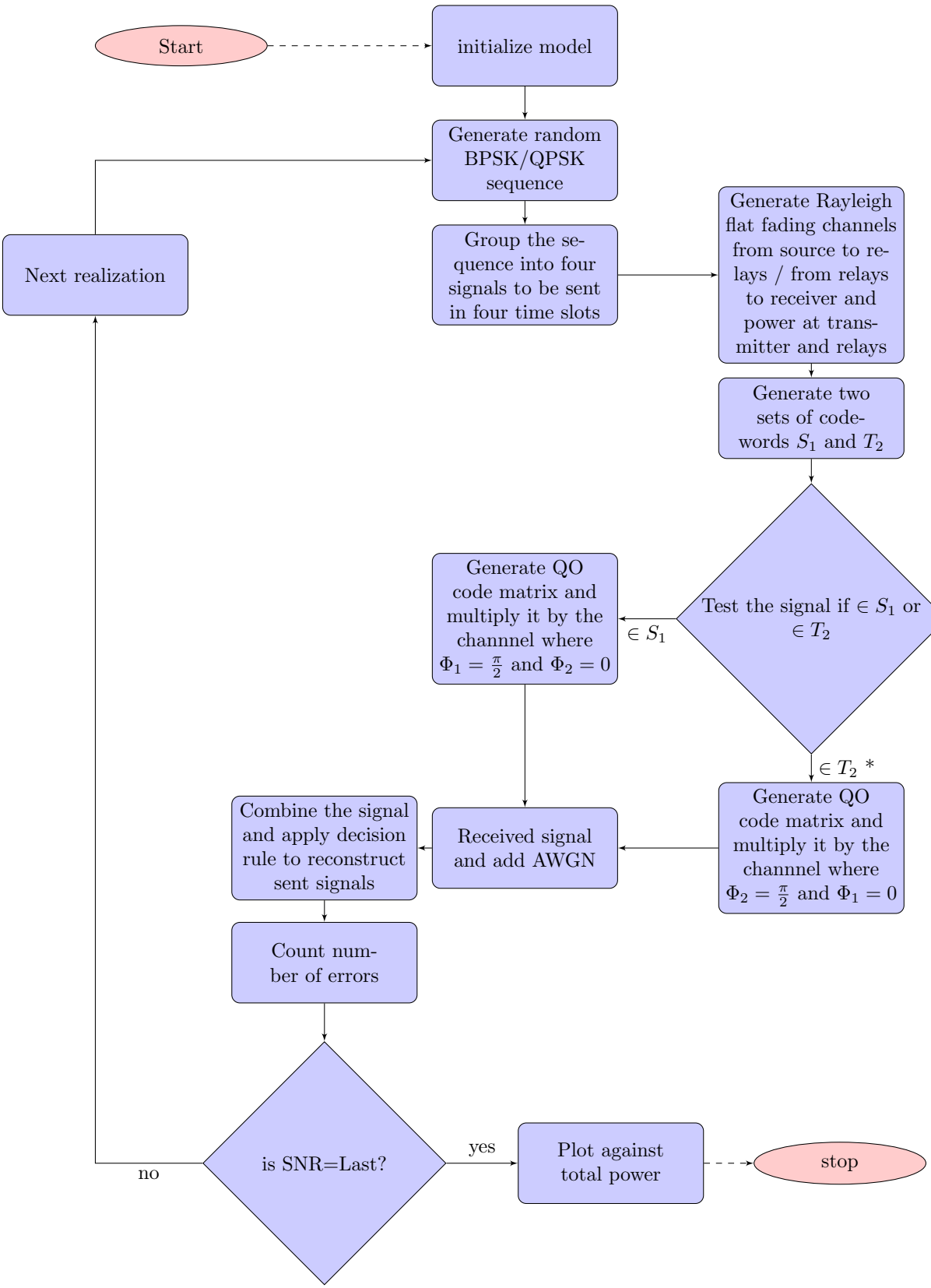

Figure 4: Flowchart for M-D-QO-STBC scheme for one-way transmission.
*In the QPSK signal the QO code matrix from T_2 is multiplied by unitary matrix U (explained in section 3.2.16).

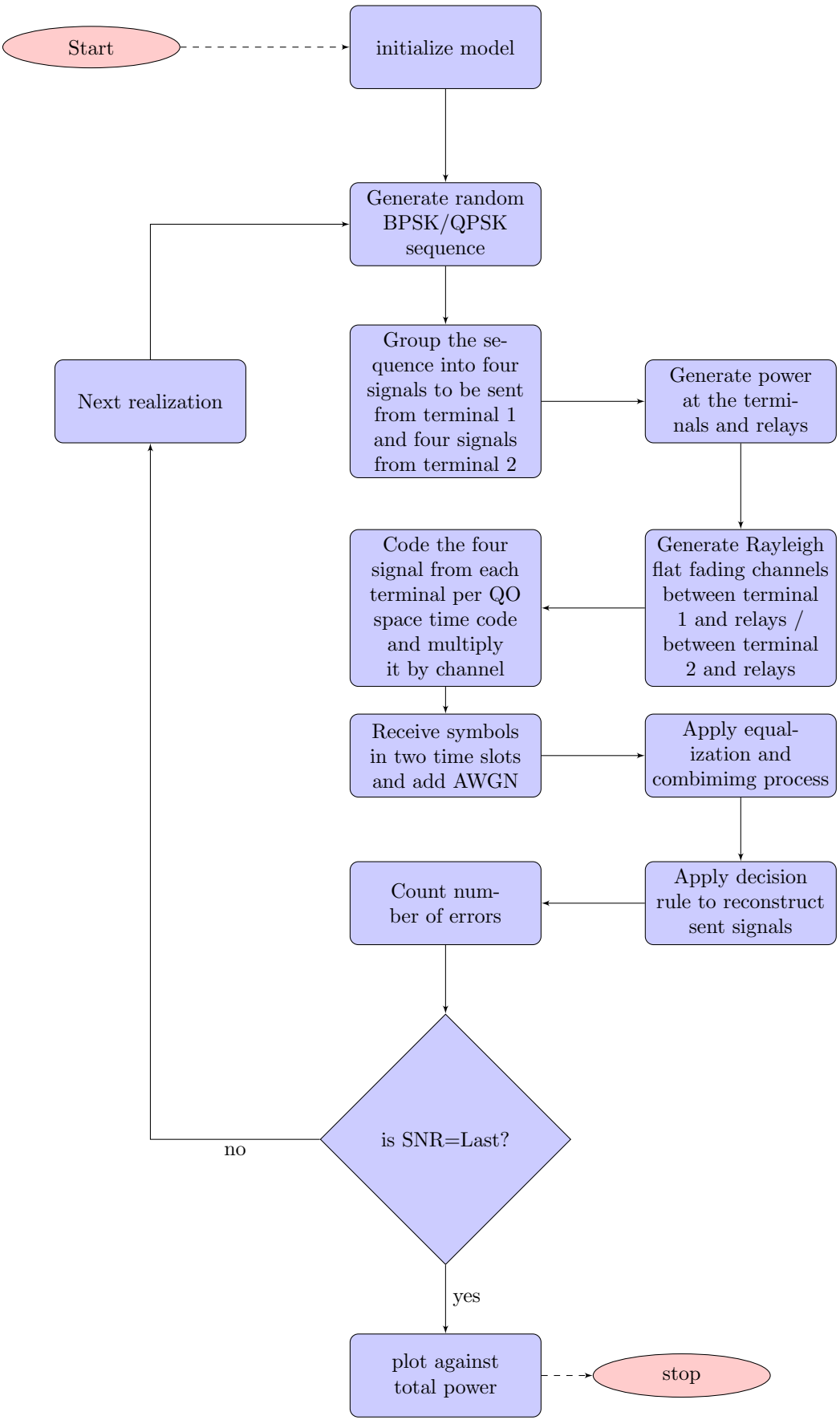

Figure 5: Flowchart for D-QO-STBC scheme for two-way transmission.

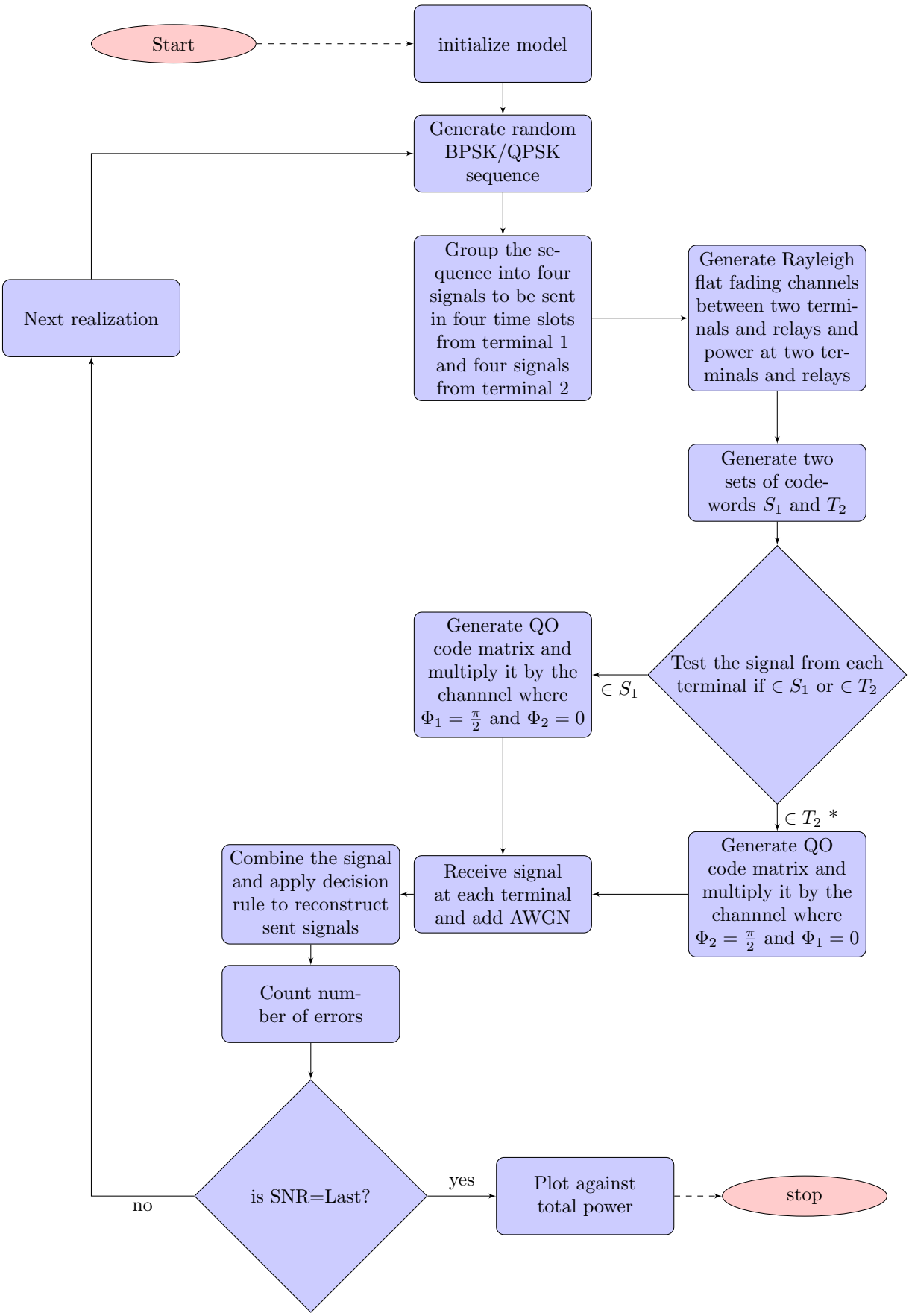

Figure 6: Flowchart for M-D-QO-STBC scheme for two-way transmission.
*In the QPSK signal the QO code matrix from T_2 is multiplied by unitary matrix U (explained in section 3.2.3 and 3.5.2).

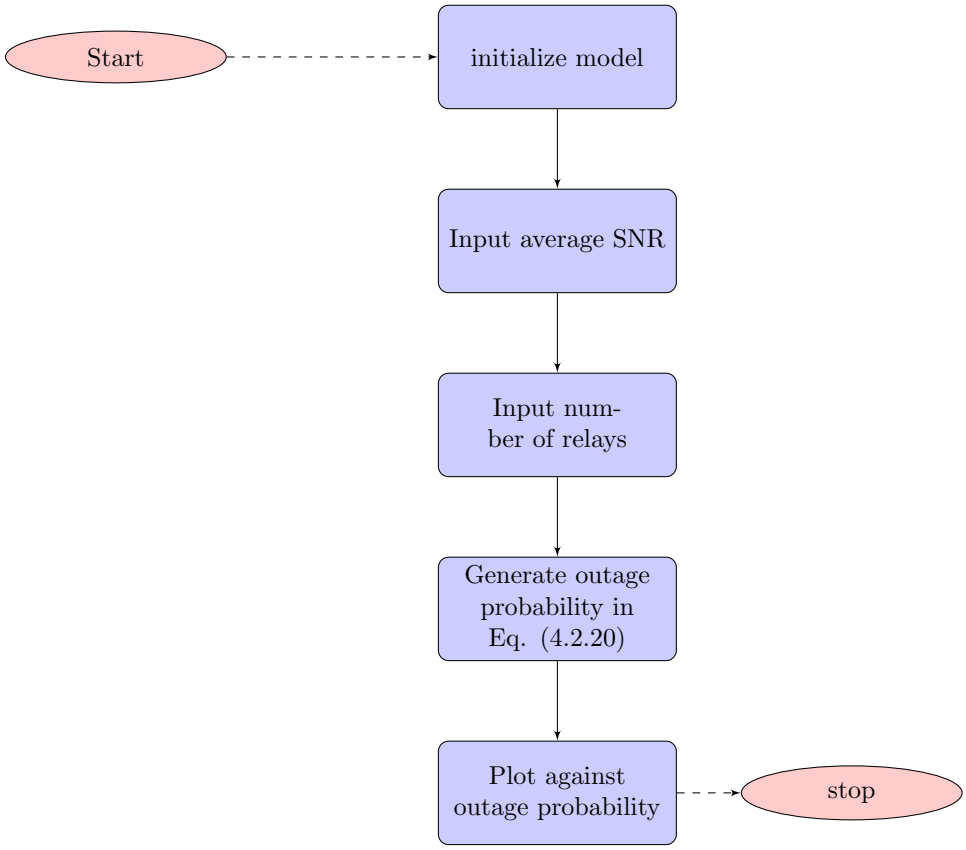

Figure 7: Flowchart for outage probability code for four relay selection for one-way relay network (theoretical).

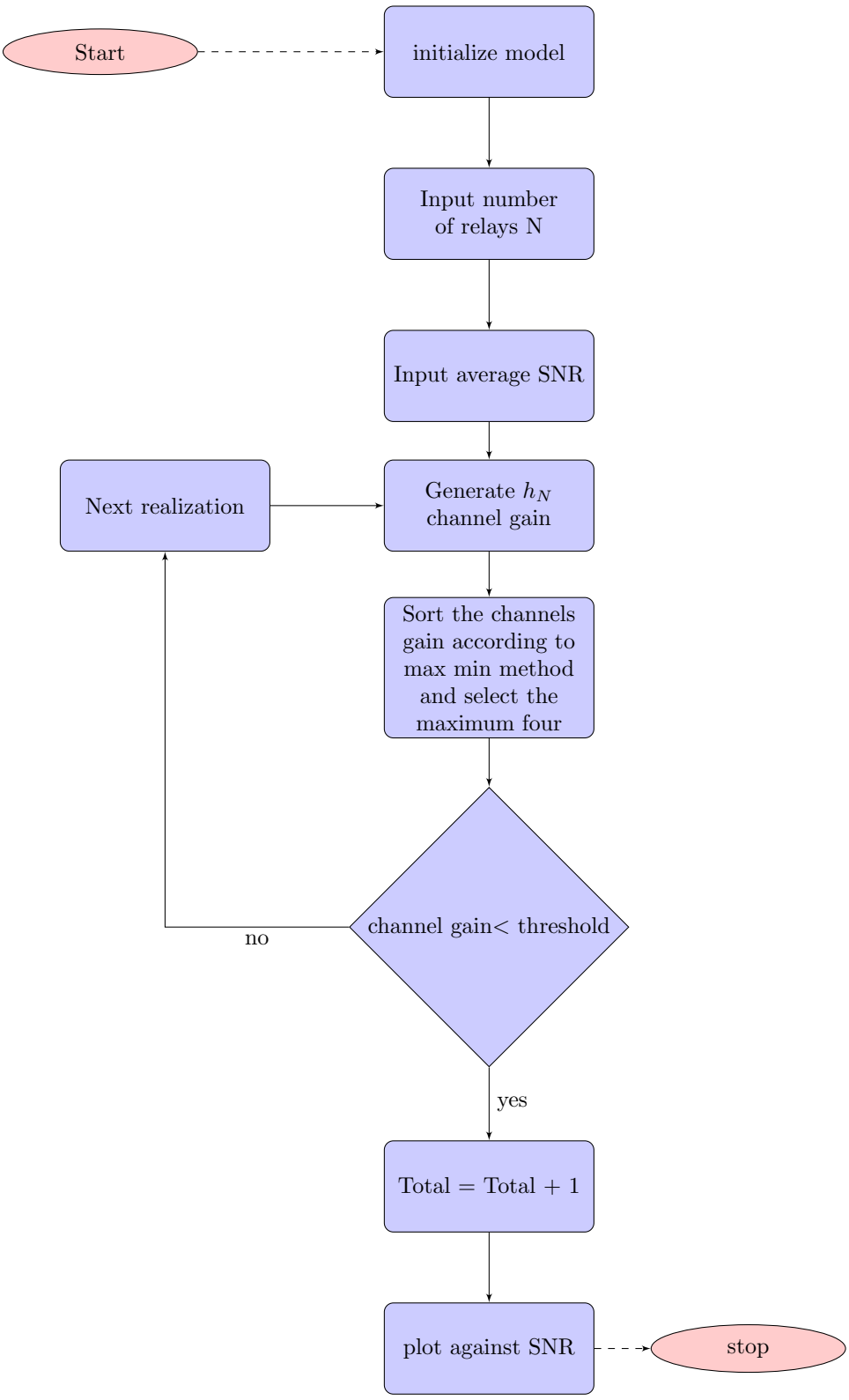

Figure 8: Flowchart for outage probability for four relay selection for one-way relay network (simulation)

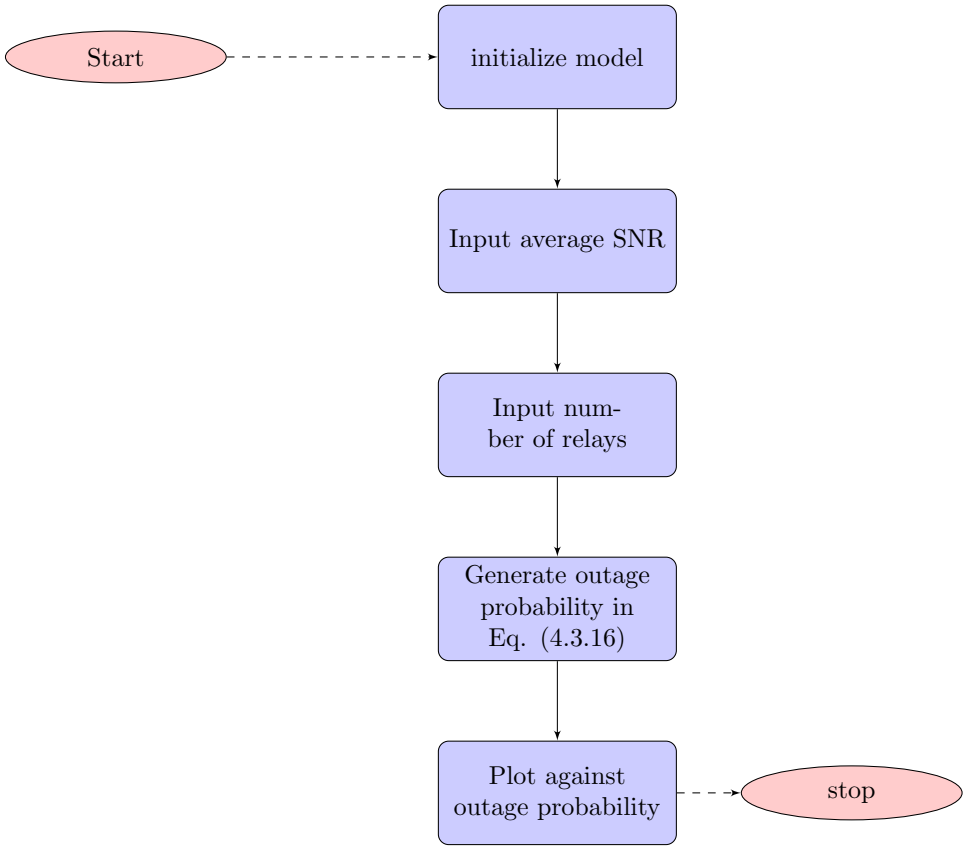

Figure 9: Flowchart for outage probability for the best relay selection for two-way relay network (theoretical).

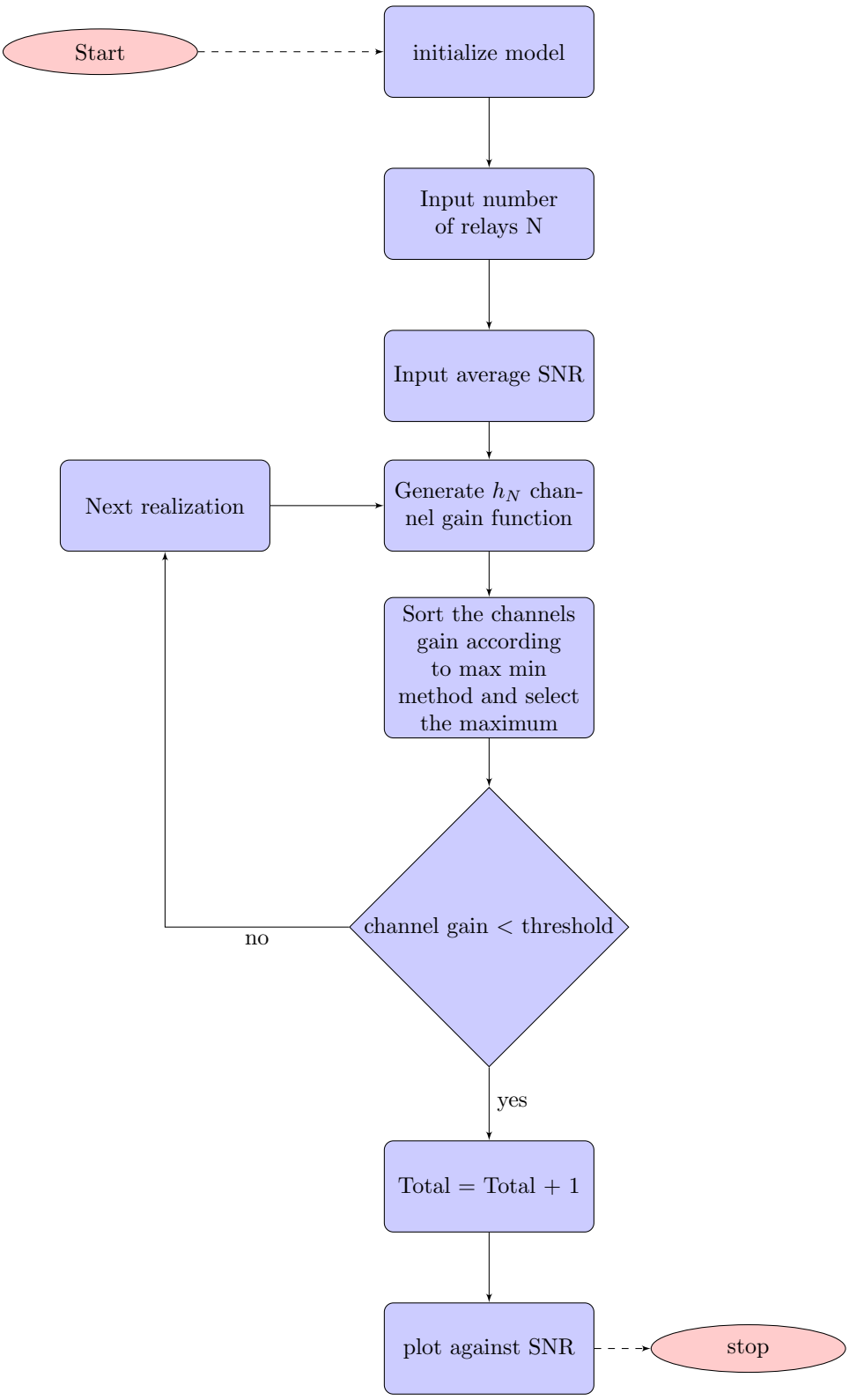

Figure 10: Flowchart for outage probability for best relay selection for two-way relay network (simulation)

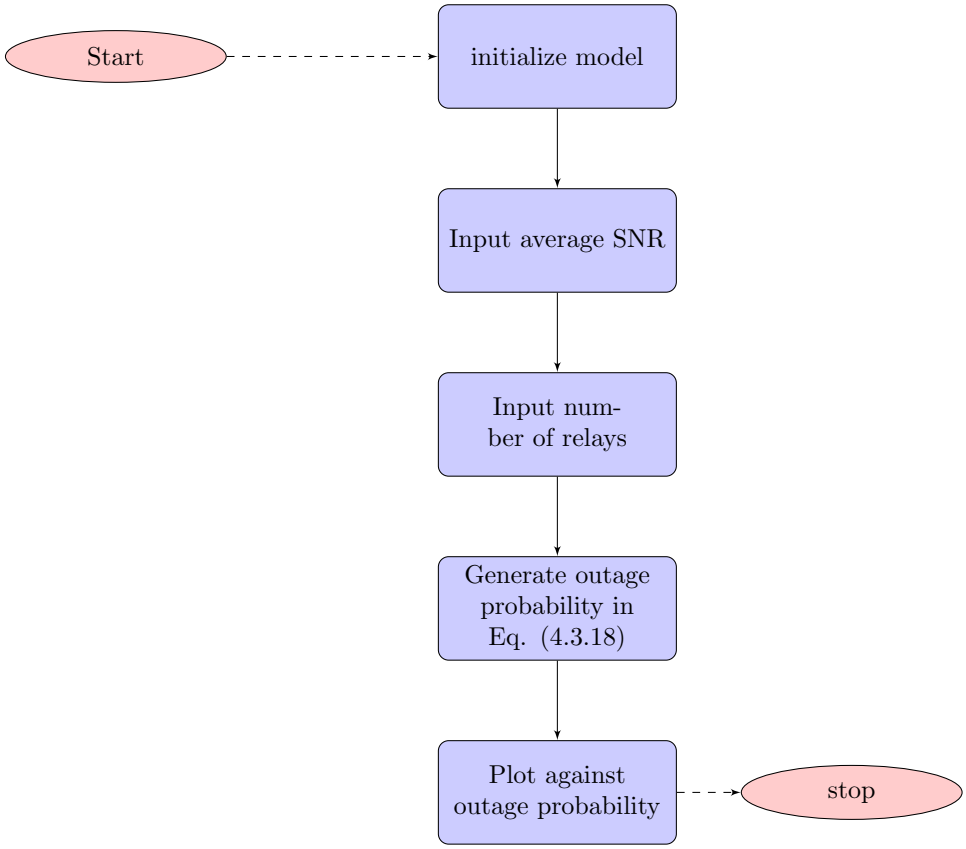

Figure 11: Flowchart for the N^{th} best relay selection for two-way relay network (theoretical).

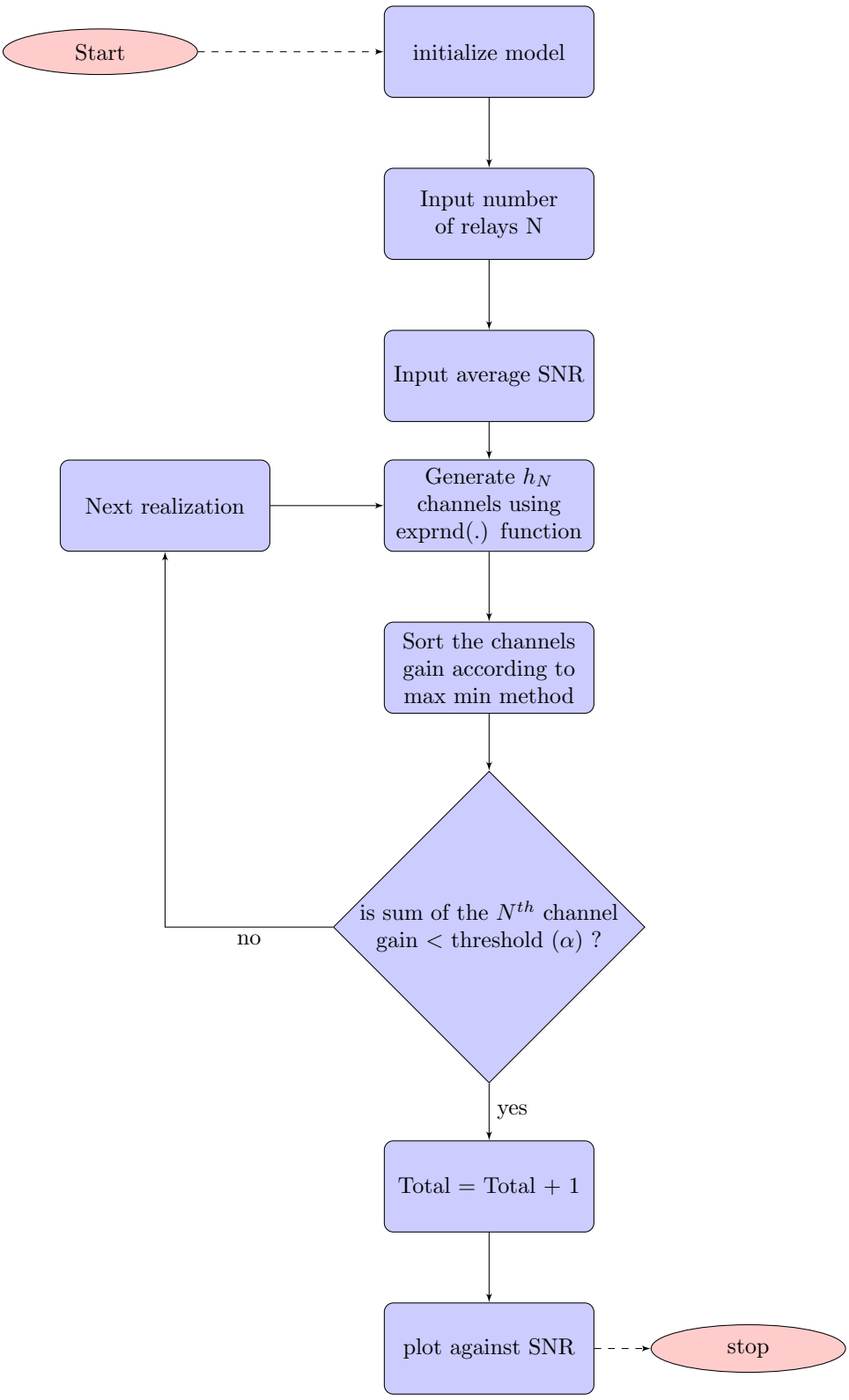

Figure 12: Flowchart for outage probability for N^{th} best relay selection for two-way relay network (simulation)

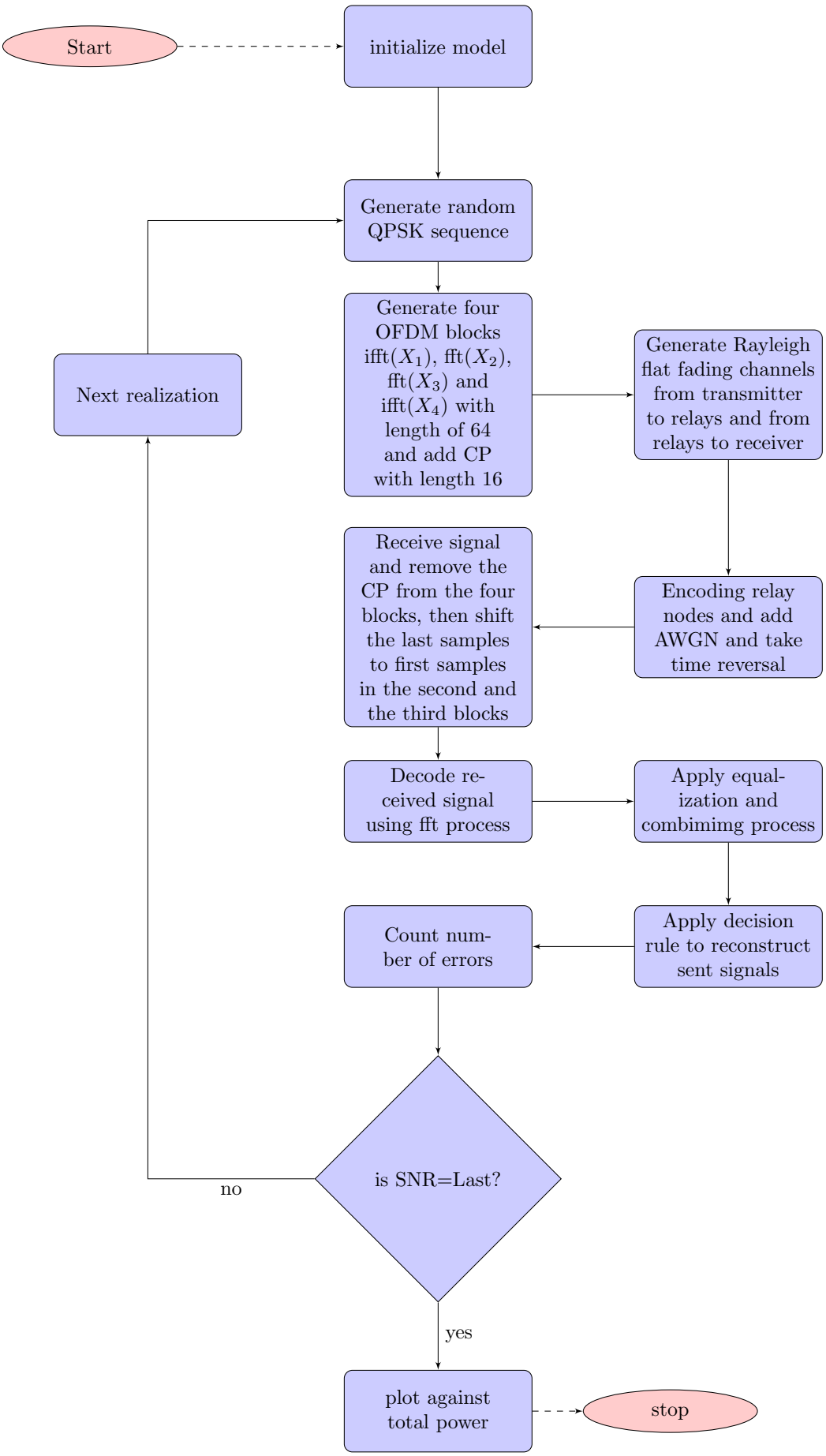

Figure 13: Flowchart for OFDM-based D-QO-STBC scheme.

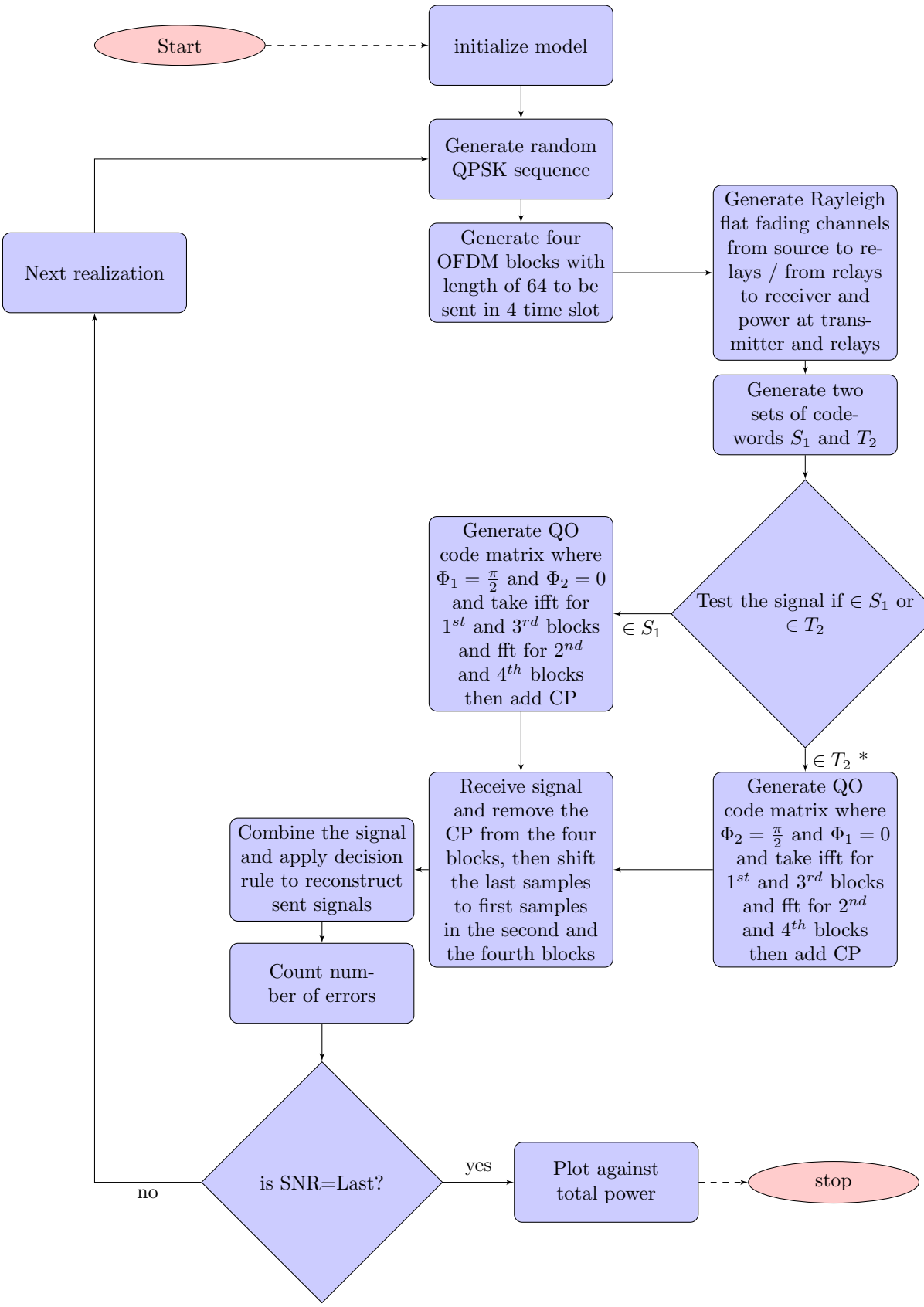

Figure 14: Flowchart for OFDM-based M-D-QO-STBC scheme for one-way transmission. *In the QPSK signal the QO code matrix from T_2 is multiplied by unitary matrix U (explained in section 3.2.16).

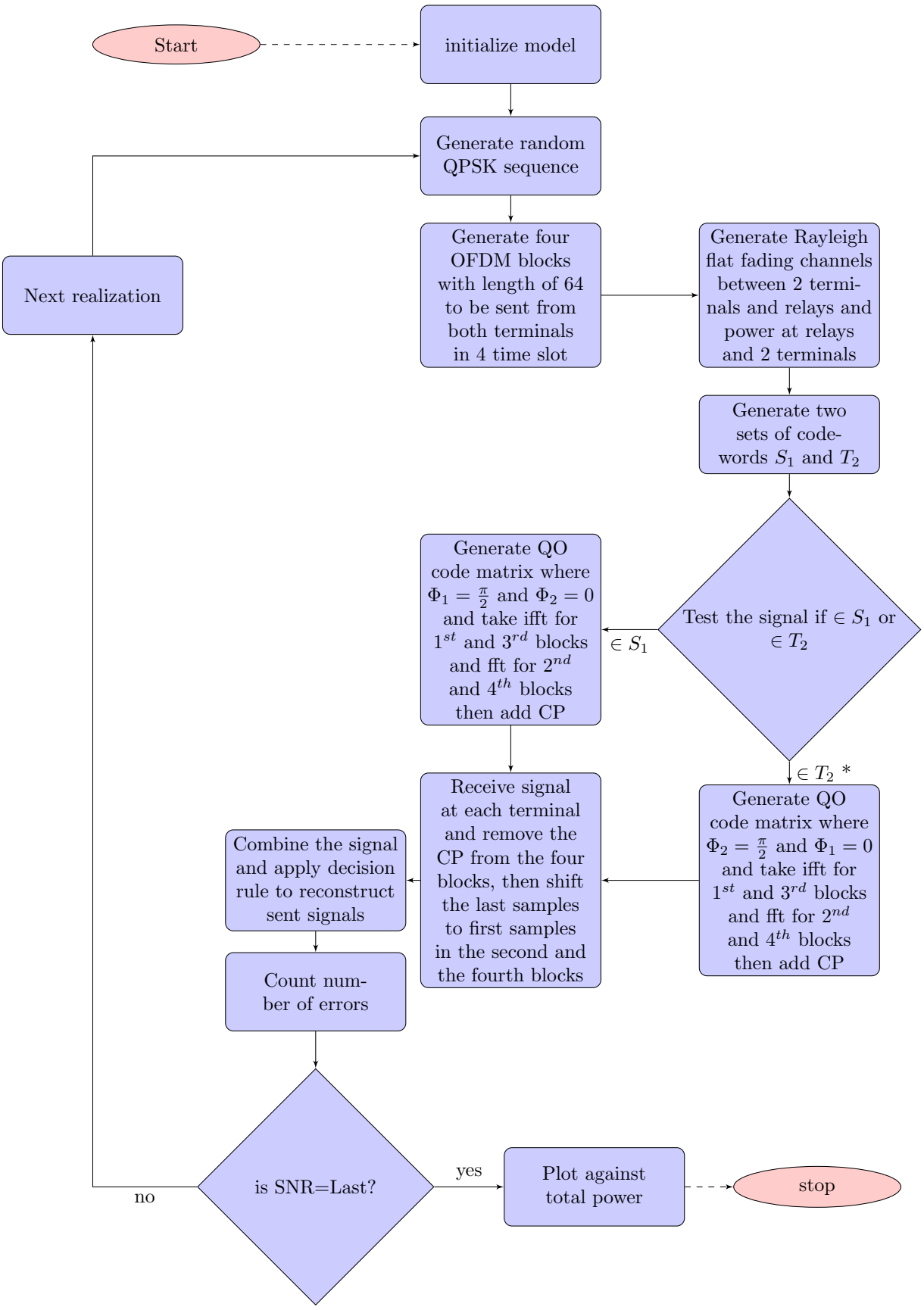

Figure 15: Flowchart for OFDM-based M-D-QO-STBC scheme for two-way transmission. *In the QPSK signal the QO code matrix from T_2 is multiplied by unitary matrix U (explained in section 3.2.16).

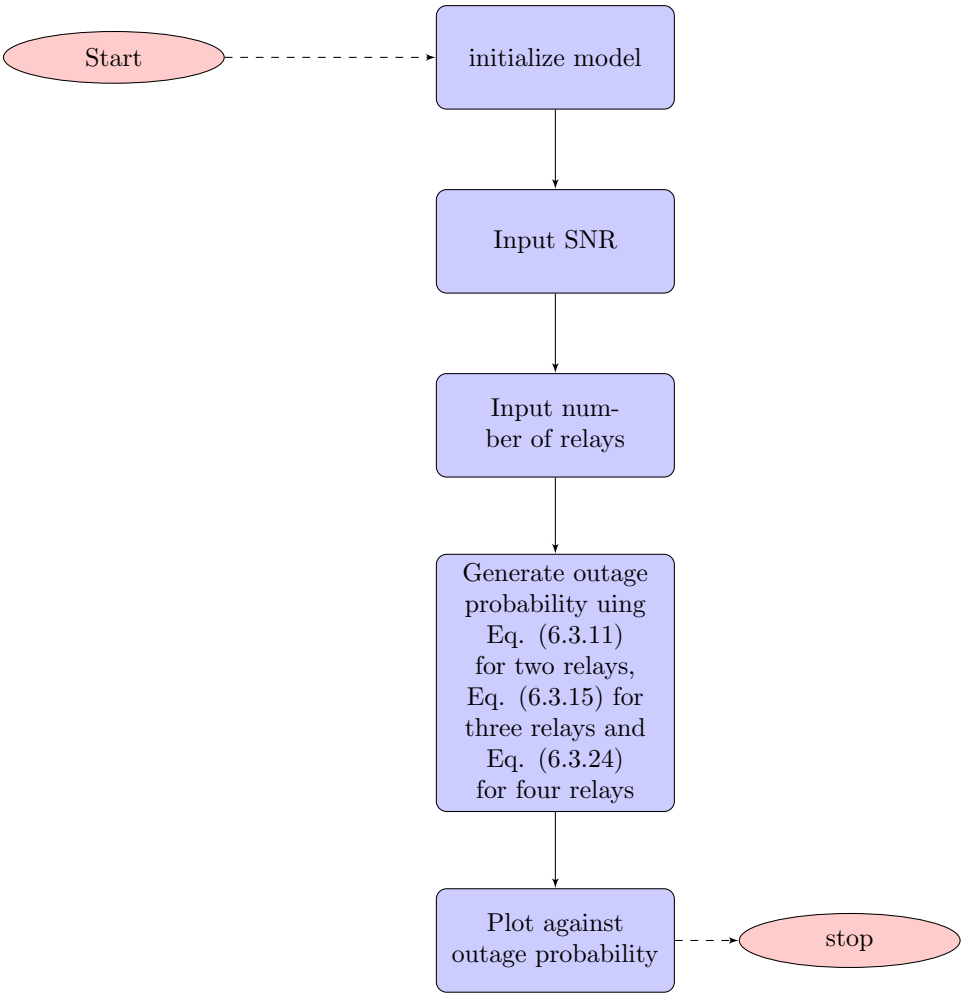

Figure 16: Flowchart for outage probability code for two, three and four one-way relay network (theoretical).

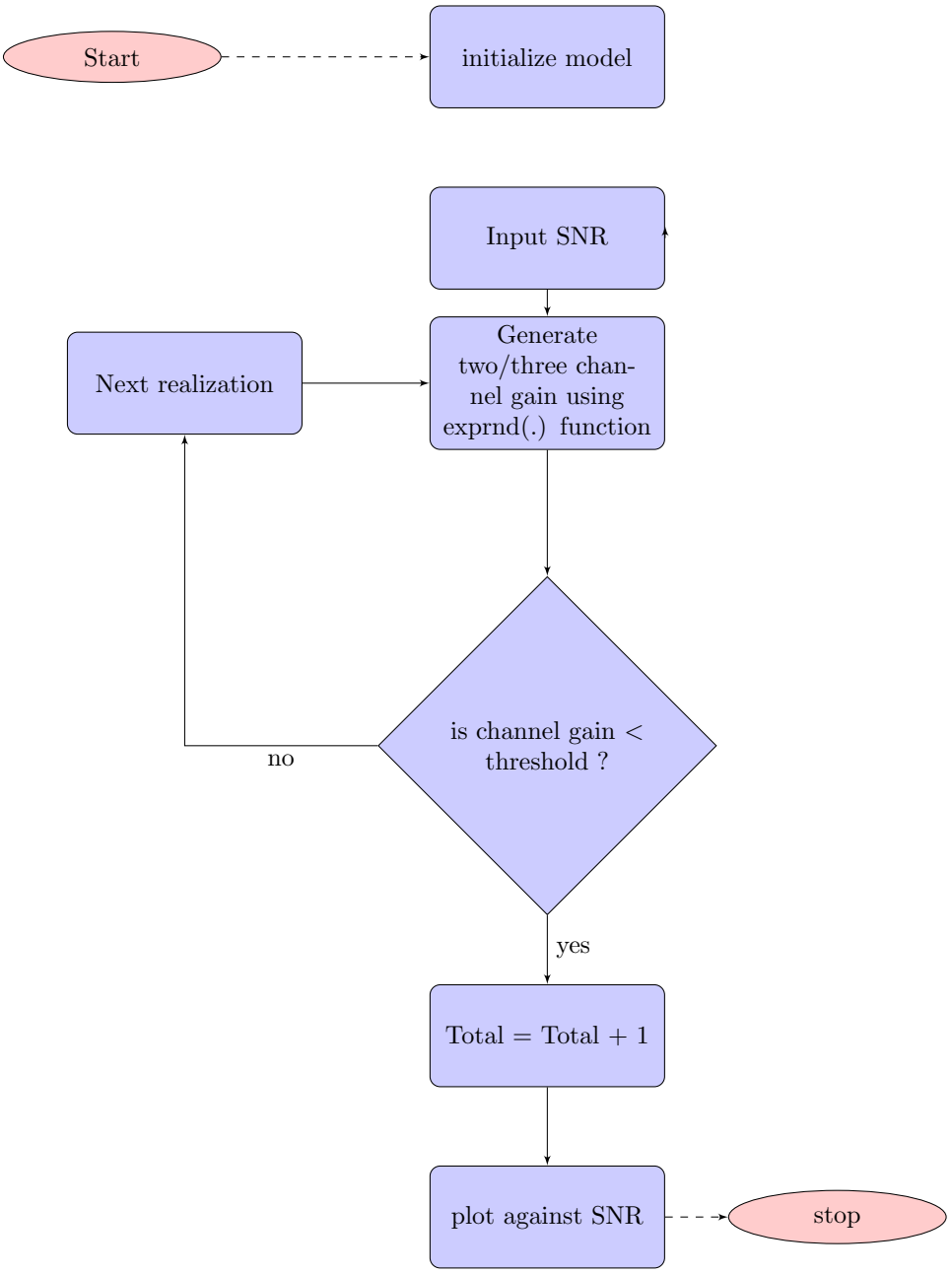

Figure 17: Flowchart for outage probability for two/three relay network (simulation)

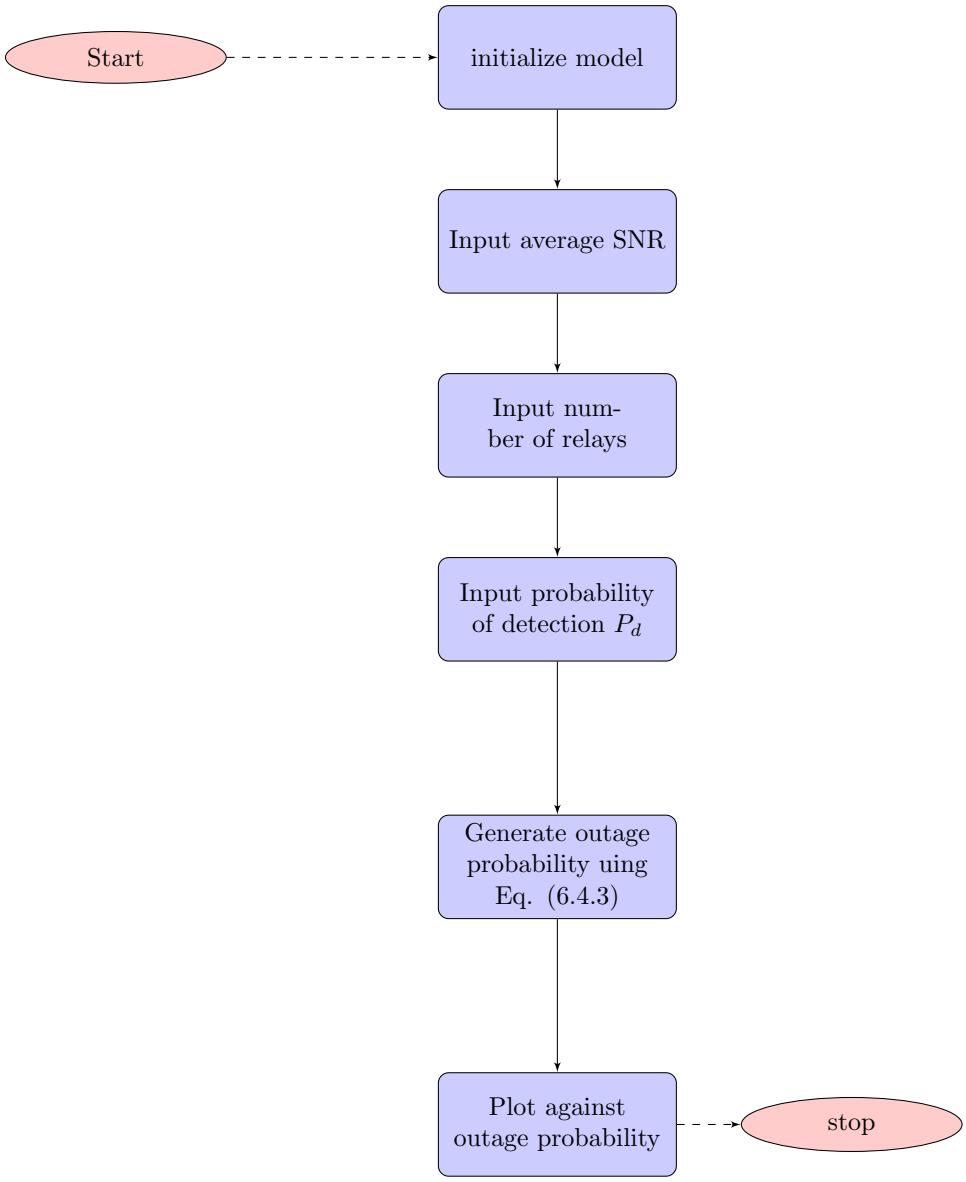

Figure 18: Flowchart for outage probability code when spectrum acquisition is imperfect (theoretical).

References

[1] D. Agrawal, V. Tarokh, A. Naguib, and N. Seshadri, "Space-time coded OFDM for high data-rate wireless communication over wideband channels," in *Vehicular Technology Conference, 1998. VTC 98. 48th IEEE*, vol. 3, pp. 2232–2236, 1998.

[2] L. J. Cimini and N. R. Sollenberger, "OFDM with diversity and coding for high bitrate mobile data applications," in *AT and T Technical Memorandum, HA6131000-961015-07TM*, 1997.

[3] Y. Gong and K. Letaief, "Performance evaluation and analysis of space-time coding for high data rate wireless personal communications," in *Vehicular Technology Conference, 1999. VTC 1999 - Fall. IEEE VTS 50th*, vol. 3, pp. 1331–1335, 1999.

[4] V. Tarokh, A. Naguib, N. Seshadri, and A. Calderbank, "Space-time codes for high data rate wireless communication: performance criteria in the presence of channel estimation errors, mobility, and multiple paths," *Communications, IEEE Transactions on*, vol. 47, no. 2, pp. 199–207, 1999.

[5] J. G. Proakis, *Digital Communications.* 4th Edition, McGrow-Hill, 2001.

[6] T. S. Rappaport, *Wireless Communications: Principles and Practice.* Prentice Hall, 1996.

[7] D. Gesbert, M. Shafi, D. S. Shiu, P. Smith, and A. Naguib, "From theory to practice: An overview of MIMO space-time coded wireless systems,"

Selected Areas in Communications, IEEE Journal on, vol. 21, no. 3, pp. 281–302, 2003.

[8] H. Jafarkhani, *Space-time coding: Theory and Practice*. Cambridge University Press, 1st ed., 2005.

[9] H. Bolcskei, D. Gesbert, and A. Paulraj, "On the capacity of OFDM-based spatial multiplexing systems," *Communications, IEEE Transactions on*, vol. 50, no. 2, pp. 225–234, 2002.

[10] A. Ghasemi and E. S. Sousa, "Fundamental limits of spectrum-sharing in fading environments," *IEEE Trans. Wireless Commun.*, vol. 6, no. 2, pp. 649–658, 2007.

[11] K. Hamdi, W. Zhang, and K. B. Lateief, "Power control in cognitive radio systems based on spectrum sensing side information," *IEEE International Conference on Communications ICC*, pp. 5161–5165, 2007.

[12] G. J. Foschini and M. J. Gans, "On limits of wireless communications in a fading environment when using multiple antennas," *Wireless Pres. Commun*, vol. 6, pp. 311–335, 1998.

[13] I. E. Telatar, "Capacity of multi-antenna Gaussian channels," *European Trans. Tel.*, vol. 10, no. 6, pp. 585–595, 1999.

[14] R. N. A. Paulraj and D. Gore, "MIMO: Wierless communication encyclopedia of wireless and mobile communication," in *Taylor Francis*, 2008.

[15] M. Dohler and Y. H. Li, *Cooperative communications hardware channel and PHY*. Mcgraw-Hill, 1991.

[16] A. Nosratinia, T. Hunter, and A. Hedayat, "Cooperative communication in wireless networks," *Communications Magazine, IEEE*, vol. 42, no. 10, pp. 74–80, 2004.

[17] Y. Jing and B. Hassibi, "Cooperative diversity in wireless relay networks with multiple-antenna nodes," in *Information Theory, 2005. ISIT 2005. Proceedings. International Symposium on*, pp. 815–819, 2005.

[18] D. Nguyen and M. Krunz, "Cooperative MIMO in wireless networks: recent developments and challenges," *Network, IEEE*, vol. 27, no. 4, pp. 48–54, 2013.

[19] Y. Yang, H. Hu, J. Xu, and G. Mao, "Relay technologies for wimax and lte-advanced mobile systems," *Communications Magazine, IEEE*, vol. 47, no. 10, pp. 100–105, 2009.

[20] S. Chieochan and E. Hossain, "Cooperative relaying in wi-fi networks with network coding," *Wireless Communications, IEEE*, vol. 19, no. 2, pp. 57–65, 2012.

[21] J. N. Laneman, "Cooperative diversity in wireless networks: Algorithms and architectures," in *Massachusetts Institute of Technology, Cambridge MA, USA: PhD dissertation*, 2002.

[22] M. Engels, "Wireless OFDM system: how to make them," in *USA: Springer Science*, 2004.

[23] G. Stuber, J. Barry, S. McLaughlin, Y. Li, M.-A. Ingram, and T. Pratt, "Broadband MIMO-OFDM wireless communications," *Proceedings of the IEEE*, vol. 92, no. 2, pp. 271–294, 2004.

[24] L. Hanzo, J. Akhtman, L. Wang, and M. Jiang, "MIMO-OFDM for LTE, Wi-Fi and WiMAX : coherent versus non-coherent and cooperative turbo-transceivers," *John Wiley and Sons Ltd*, 2011.

[25] K. Pietikainen, "Orthogonal frequency division multiplexing online available: http://vipnulled.com/doc/pdf/download/www_comlab_hut_fi–opetus–333–2004_2005_slides–ofdm_text.pdf,"

[26] J. Mitola, "Cognitive radio for flexible mobile multimedia communications," in *Mobile Multimedia Communications, 1999. (MoMuC '99) 1999 IEEE International Workshop on*, pp. 3–10, 1999.

[27] F. C. Commission, "Facilitating opportunities for flexible, efficient, and reliable spectrum use employing cognitive radio technologies," *ET Docket*, no. 03-108, 2005.

[28] Cognitive Radio Technology, "http://www.ofcom.org.uk/research/technology/overview/emertech/cograd/cogradmain.pdf,"

[29] S. Haykin, "Cognitive radio: brain-empowered wireless communications," *Selected Areas in Communications, IEEE Journal on*, vol. 23, no. 2, pp. 201–220, 2005.

[30] C. Cordeiro, K. Challapali, and D. Birru, "Ieee 802.22: An introduction to the first wireless standard based on cognitive radios," *J. Commun.*, vol. 1, p. 3847, 2006.

[31] C. R. Sevension, "In reply to comments of Ieee 802.18. 2004 [online] available: http://ieee802.org/18.,,"

[32] Q. Zhao and B. Sadler, "A survey of dynamic spectrum access," *Signal Processing Magazine, IEEE*, vol. 24, no. 3, pp. 79–89, 2007.

[33] J. Mietzner, L. Lampe, and R. Schober, "Distributed transmit power allocation for relay-assisted cognitive-radio systems," in *Signals, Systems and Computers, 2007. ACSSC 2007. Conference Record of the Forty-First Asilomar Conference on*, pp. 792–796, 2007.

[34] S. Srinivasa and S. Jafar, "The throughput potential of cognitive radio: A theoretical perspective," in *Signals, Systems and Computers, 2006. ACSSC '06. Fortieth Asilomar Conference on*, pp. 221–225, 2006.

[35] Z. Qian, J. Junchenge, and Z. Jin, "Cooperative relay to improve diversity in cognitive radio networks," *IEEE Commun. Mag*, vol. 47, no. 2, pp. 111–117, 2009.

[36] W. Zhang and K. B. Letaief, "Cooperative spectrum sensing with transmit and relay diversity in cognitive radio networks," *IEEE Transactions on Wireless Communications*, vol. 7, pp. 4761–4766, 2008.

[37] I. Krikidis, Z. Sun, J. N. Laneman, and J. Thompson, "Cognitive legacy networks via cooperative diversity," *IEEE Communications Letters*, vol. 13, no. 2, pp. 106–109, 2009.

[38] S. M. Alamouti, "A simple transmit diversity technique for wireless communications," *IEEE Journal on Select Areas in Communications*, vol. 16, no. 8, pp. 1451–1458, 1998.

[39] Y. Jing and H. Jafarkhani, "Using orthogonal and quasi-orthogonal designs in wireless relay networks," *IEEE Trans. Inf. Theory*, vol. 53, no. 11, pp. 4106–4118, 2007.

[40] H. Jafarkhani, "A quasi-orthogonal space-time block code," *IEEE Trans. Commun.*, vol. 49, no. 1, pp. 1–4, 2001.

[41] N. Sharma and C. B. Papadias, "Improved quasi-orthogonal codes through constellation rotation," *IEEE Trans. Commun.*, vol. 51, no. 3, pp. 563–571, 2003.

[42] W. Su and X. Xia, "Signal constellations for quasi-orthogonal space-time block codes with full diversity," *IEEE Transactions on Information Theory*, vol. 50, no. 10, pp. 2331–2347, 2004.

[43] M. Janani and A. Nosratinia, "Efficient space-time block codes derived from quasi-orthogonal structures," *IEEE Trans. Wireless Commun.*, vol. 6, no. 5, pp. 1643–1646, 2007.

[44] G. J. Foschini, "Layered space-time architecture for wireless communication in a fading environment when using multielement antennas," *Bell Labs. Tech. Journal*, vol. 2, pp. 41–59, 1996.

[45] G. Raleigh and J. M. Cioffi, "Spatial-temporal coding for wireless communications," *IEEE Transactions on Communications*, vol. 46, pp. 357–366, 1998.

[46] B. M. Hochwald and T. L. Marzetta, "Unitary space-time modulation for multiple-antenna communication in Rayleigh flat-fading," *IEEE Trans. Inf. Theory*, vol. 46, pp. 543–564, 2000.

[47] S. Haykin and M. Moher, *Modern Wireless Communications.* Pearson Prentice Hall, USA, 1st ed., 2005.

[48] V. Tarokh, H. Jafarkhani, and A. R. Calderbank, "Space-time block codes from orthogonal designs," *IEEE Trans. Inf. Theory*, vol. 45, no. 5, pp. 1456–1467, 1999.

[49] O. Tirkkonen, A. Boariu, and A. Hottinen, "Minimal non-orthogonality rate 1 space-time block code for 3+tx antennas," *in Proc. IEEE 6th ISSSTA Conf.*, vol. 2, pp. 429–432, 2000.

[50] W. Su and X. Xia, "Signal constellations for quasi-orthogonal spacetime block codes with full diversity," *IEEE Trans. Inf. Theory*, vol. 50, no. 10, pp. 2331–2347, 2004.

[51] S. L. C. Toker and J. A. Chambers, "Space-time block coding for four transmit antennas with closed loop feedback over frequency selective fading channels," *IEEE Information Theory Workshop*, vol. 2, pp. 195–198, 2003.

[52] V. Tarokh, N. Seshadri, and A. Calderbank, "Space-time codes for high data rate wireless communication: performance criterion and code construc-

tion," *Information Theory, IEEE Transactions on*, vol. 44, no. 2, pp. 744–765, 1998.

[53] G. Ganesan and P. Stoica, "Space-time diversity using orthogonal and amicable orthogonal designs," in *Acoustics, Speech, and Signal Processing, 2000. ICASSP '00. Proceedings. 2000 IEEE International Conference on*, vol. 5, pp. 2561–2564, 2000.

[54] C. B. Papadias and G. J. Foschini, "A space-time coding approach for systems employing four transmit antennas," *IEEE ICASSP*, vol. 4, no. 2, pp. 2481–2484, 2001.

[55] X.-B. Liang and X.-G. Xia, "On the nonexistence of rate-one generalized complex orthogonal designs," *Information Theory, IEEE Transactions on*, vol. 49, no. 11, pp. 2984–2988, 2003.

[56] H. Jafarkhani and N. Hassanpour, "Super-quasi-orthogonal space-time trellis codes for four transmit antennas," *IEEE Trans. Wireless Comun.*, vol. 4, no. 1, pp. 215–227, 2005.

[57] O. Tirkkonen, "Optimizing space-time block codes by constellation rotations," in *Finnish Wireless Communications Workshop (FWWC)*, 2001.

[58] C. B. Papadias and G. J. Foschini, "Capacity-approaching space-time codes for system employing four transmitter antennas," *IEEE Trans. Inf. Theory*, vol. 49, pp. 2481–2484, 2003.

[59] A. Sendonaris, E. Erkip, and B. Aazhang, "User cooperation diversity. part i. system description," *Communications, IEEE Transactions on*, vol. 51, no. 11, pp. 1927–1938, 2003.

[60] K. Azarian, H. El-Gamal, and P. Schniter, "On the achievable diversity-multiplexing tradeoff in half-duplex cooperative channels," *Information Theory, IEEE Transactions on*, vol. 51, no. 12, pp. 4152–4172, 2005.

[61] R. Nabar, H. Bolcskei, and F. Kneubuhler, "Fading relay channels: performance limits and space-time signal design," *Selected Areas in Communications, IEEE Journal on*, vol. 22, no. 6, pp. 1099–1109, 2004.

[62] Y. Jing and B. Hassibi, "Distributed space-time coding in wireless relay networks," *IEEE Trans. Wireless Commun.*, vol. 5, no. 12, pp. 3524–3536, 2006.

[63] B. Hassibi and B. Hochwald, "High-rate codes that are linear in space and time," *Information Theory, IEEE Transactions on*, vol. 48, no. 7, pp. 1804–1824, 2002.

[64] M. Janani and A. Nosratinia, "Generalized block space-time trellis codes: set parttioning and code design," *in Proc. IEEE WCNC New Orleans LA USA*, vol. 1, pp. 461–465, 2005.

[65] C. E. Shannon, "Two-way communication channels," *in Proc. 4th Berkeley Symp. on Math. and Stat. Prob.*, pp. 611–644, 1961.

[66] B. Rankov and A. Wittneben, "Spectral efficient signaling for half-duplex relay channels," in *Signals, Systems and Computers, 2005. Conference Record of the Thirty-Ninth Asilomar Conference on*, pp. 1066–1071, 2005.

[67] B. Rankov and A. Wittneben, "Achievable rate regions for the two-way relay channel," in *Information Theory, 2006 IEEE International Symposium on*, pp. 1668–1672, 2006.

[68] C. Hausl and J. Hagenauer, "Iterative network and channel decoding for the two-way relay channel," in *Communications, 2006. ICC '06. IEEE International Conference on*, vol. 4, pp. 1568–1573, 2006.

[69] F. Abdurahman, A. Elazreg, and J. Chambers, "Distributed quasi-orthogonal space-time coding for two-way wireless relay networks," in *Wire-*

less Communication Systems (ISWCS), 2010 7th International Symposium on, pp. 413–416, 2010.

[70] H. Jafarkhani and N. Seshadri, "Super-orthogonal space-time trellis codes," *IEEE Tran. on Inf. Theory*, vol. 49, no. 4, pp. 937–950, 2003.

[71] C. Toker, S. Lambotharan, and J. Chambers, "Closed-loop quasi-orthogonal STBCs and their performance in multipath fading environments and when combined with turbo codes," *Wireless Communications, IEEE Transactions on*, vol. 3, no. 6, pp. 1890–1896, 2004.

[72] T. Cui, F. Gao, and A. Nallanathan, "Optimal training design for channel estimation in amplify and forward relay networks," in *IEEE GLOBECOM conference on*, pp. 4015–4019, 2007.

[73] T. Cui, F. Gao, T. Ho, and A. Nallanathan, "Distributed space-time coding for two-way wireless relay networks," in *Communications, 2008. ICC '08. IEEE International Conference on*, pp. 3888–3892, 2008.

[74] Z. Bali, W. Ajib, and H. Boujemaa, "Distributed relay selection strategy based on source-relay channel," in *IEEE ICT Conference on*, pp. 138–142, 2010.

[75] A. Bletsas, A. Khisti, D. Reed, and A. Lippman, "A simple cooperative diversity method based on network path selection," *IEEE Jor. Sel. Areas in Commun.*, vol. 24, no. 3, pp. 659–672, 2006.

[76] J. N. Laneman, D. N. Tse, and G. W. Wornell, "Cooperative diversity in wireless networks: efficient protocols and outage behavior," *IEEE Trans. Inf. Theory*, vol. 50, no. 12, pp. 3062–3080, 2004.

[77] S. Ikki and M. H. Ahmed, "Performance analysis of dual-hop relaying communications over generalized gamma fading channels," *in Proc. of the IEEE Global Communications Conference, Washington*, 2007.

[78] E. Beres and R. S. Adve, "Outage probability of selection cooperation in the low to medium SNR regime," *IEEE Commun. Lett.*, vol. 11, no. 7, pp. 589–597, 2007.

[79] A. Adinoyi, Y. Fan, H. Yanikomeroglu, H. V. Poor, and F. Al-Shaalan, "Performance of selection relaying and cooperative diversity," *IEEE Trans. Wireless Commun.*, vol. 8, no. 12, pp. 5790–5795, 2009.

[80] A. Bletsas, H. Shin, and M. Z. Win, "Cooperative communications with outage-optimal opportunistic relaying,," *IEEE Trans.*, vol. 6, no. 9, pp. 3450–3460, 2007.

[81] J. N. Laneman and G. W. Wornell, "Energy efficient antenna sharing and relaying for wireless networks," *in Proc. IEEE WCNC Chicago, USA,*, no. 1, pp. 7–12, 2000.

[82] A. P. Anghel and M. Kaveh, "Exact symbol error probability of a cooperative network in Rayleigh-fading enviroment," *IEEE Trans. Wireless Commun.*, vol. 3, no. 5, pp. 1416–1421, 2004.

[83] A. Papoulis, *Probability, random variables, and stochastic processes.* McGraw-Hill, 1991.

[84] Y. Jing, "A relay selection scheme for two-way amplify-and-forward relay networks," in *IEEE International Conference on, Wireless Communications Signal Processing*, pp. 1–5, 2009.

[85] N. Balakrishnan and A. C. Cohen, *Order statistics and inference: estimation methods.* London : Academic Press, 1991.

[86] Q. Li, S. H. Ting, A. Pandharipande, and Y. Han, "Adaptive two-way relaying and outage analysis," *IEEE Transactions on, Wireless Communications*, vol. 8, no. 6, pp. 3288–3299, 2009.

[87] R. H. Y. Louie, Y. Li, and B. Vucetic, "Performance analysis of physical layer network coding in two-way relay channels," in *IEEE, Global Telecommunications Conference*, pp. 1–6, 2009.

[88] X. Liang, S. Jin, W. Wang, X. Gao, and K.-K. Wong, "Outage probability of amplify-and-forward two-way relay interference-limited systems," *IEEE Transactions on, Vehicular Technology*, vol. 61, no. 7, pp. 3038–3049, 2012.

[89] X. Ji, B. Zheng, and L. Zou, "Exact outage probability for decode-and-forward two-way relaying with asymmetric traffics," in *Information Science and Engineering (ICISE), 2010 2nd International Conference on*, pp. 2072–2075, 2010.

[90] J. Shen, N. Sha, Y. Cai, C. Cai, and W. Yang, "Outage probability of two-way amplify-and-forward relaying system with interference-limited relay," in *Wireless Communications and Signal Processing, International Conference on*, pp. 1–5, 2011.

[91] Y. Jing and H. Jafarkhani, "Single and multiple relay selection schemes and their achievable diversity orders," *IEEE Transactions on, Wireless Communications*, vol. 8, no. 3, pp. 1414–1423, 2009.

[92] D. Michalopoulos, G. Karagiannidis, T. Tsiftsis, and R. Mallik, "An optimized user selection method for cooperative diversity systems," in *IEEE GLOBECOM, Global Telecommunications Conference*, pp. 1–6, 2006.

[93] P. Po-Ning Chen, "Basic theories on order statistics." http://shannon.cm.nctu.edu.tw/prob/OR2s08.pdf.

[94] R. J. Vaughan and W. N. Venables, *Permanent Expressions for Order Statistic Densities*. Wiley for the Royal Statistical Society, 1972.

[95] A. Salhab, F. Al-Qahtani, S. Zummo, and H. Alnuweiri, "Outage analysis of Nth best DF relay systems in the presence of cci over Rayleigh fading channels," *IEEE, Communications Letters*, vol. 17, no. 4, pp. 697–700, 2013.

[96] S. Ikki and M. Ahmed, "On the performance of cooperative-diversity networks with the nth best-relay selection scheme," *IEEE Transactions on, Communications*, vol. 58, no. 11, pp. 3062–3069, 2010.

[97] X. Li, "Space-time coded multi-transmission among distributed transmitters without perfect synchronization," *Signal Processing Letters, IEEE*, vol. 11, no. 12, pp. 948–951, 2004.

[98] Y. Li, W. Zhang, and X.-G. Xia, "Distributive high-rate full-diversity space-frequency codes for asynchronous cooperative communications," in *Information Theory, 2006 IEEE International Symposium on*, pp. 2612–2616, 2006.

[99] Z. Li and X.-G. Xia, "A simple Alamouti space-time transmission scheme for asynchronous cooperative systems," *Signal Processing Letters, IEEE*, vol. 14, no. 11, pp. 804–807, 2007.

[100] K. B. Letaief and W. Zhang, "Cooperative communications for cognitive radio networks," *Proc. IEEE*, vol. 97, no. 5, pp. 878–893, 2009.

[101] J. Mitola and G. Q. Maguire, "Cognitive radio: Making software radios more personal," *IEEE Pers. Commun.*, vol. 6, no. 4, pp. 13–18, 1999.

[102] A. Goldsmith, S. A. Jafa, I. Maric, and S. Srinivasa, "Breaking spectrum gridlock withcognitive radios: an information theoretic perspective," *Proc. IEEE*, vol. 97, no. 5, pp. 894–914, 2009.

[103] O. Simeone, J. Gambini, U. Spagnolini, and Y. Bar-Ness, "Cooperation and cognitive radio," *in Proc. IEEE ICC, Glascow, UK*, pp. 6511–6515, 2009.

[104] Y.-C. Liang, K.-C. Chen, G. Y. Li, and P. Mahonen, "Cognitive Radio Networking and Communications: An Overview," *IEEE Trans. Vehicular Technology*, vol. 60, no. 7, pp. 689–694, 2011.

[105] J. B. Kim and D. Kim, "Outage Probability and Achievable Diversity Order of Opportunistic Relaying in Cognitive Secondary Radio Networks," *IEEE Trans. Wireless Commun.*, vol. 60, no. 9, pp. 2456–2466, 2012.

[106] H. A. Suraweera, P. J. Smith, and N. A. Surobhi, "Exact Outage Probability of Cooperative Diversity with Opportunistic Spectrum Access ," *in Proc IEEE ICC Workshops Beijing,*, pp. 79–84, 2008.

[107] N. A. Surobhi and M. Faulkner, "Outage probability analysis of a diamond relay network with opportunistic spectrum access," *in Proc IEEE ICSPCS Gold Coast, Australia,*, pp. 1–5, 2008.

[108] G. Chen and J. Chambers, "Study of relay selection in a multi-cell cognitive network," *Wireless Communications Letters, IEEE*, vol. 2, no. 4, pp. 435–438, 2013.

[109] M. A. Manna, F. Abdurahman, and J. A. Chambers, "Distributed quasi-orthogonal type space-time block coding with maximum distance property for two-way wireless relay networks," *IEEE IWCMC, Istanbul, Turkey*, pp. 1704–1707, 2011.

[110] M. O. Hasna and M. S. Alouini, "Performance analysis of two-hop relayed transmission over rayleigh fading channels," *IEEE 56th, Vehicular Technology Conference*, vol. 4, pp. 1992–1996, 2002.

[111] K. Lee and A. Yener, "Outage performance of cognitive wireless relay networks," *in Proc IEEE Globecom San Francisco, CA,*, pp. 1–5, 2006.

[112] N. Balakrishnan and A. C. Cohen, "Order statistics and inference: estimation methods," *London : Academic Press*, 2004.

[113] A. Ghasemi and E. S. Sousa, "Collaborative spectrum sensing for opportunistic access in fading environments," *in Proc. IEEE DySPAN, Baltimore, USA,*, pp. 131–136, 2005.

[114] H. Jafarkhani and N. Hassanpour, "Super-quasi-orthogonal space-time trellis codes for four transmit antennas," *IEEE Trans. Wireless Commun*, vol. 4, no. 1, pp. 215–227, 2005.

[115] M. K. Simon, J. K. Omura, R. A. Scholtz, and B. K. Levitt, *Spread Spectrum Communication Handbook.* The McGraw-Hill Companies, Inc., 1994.

[116] G. Chen, Z. Tian, Y. Gong, Z. Chen, and J. Chambers, "Max-ratio relay selection in secure buffer-aided cooperative wireless networks," *Information Forensics and Security, IEEE Transactions on*, vol. 9, no. 4, pp. 719–729, 2014.